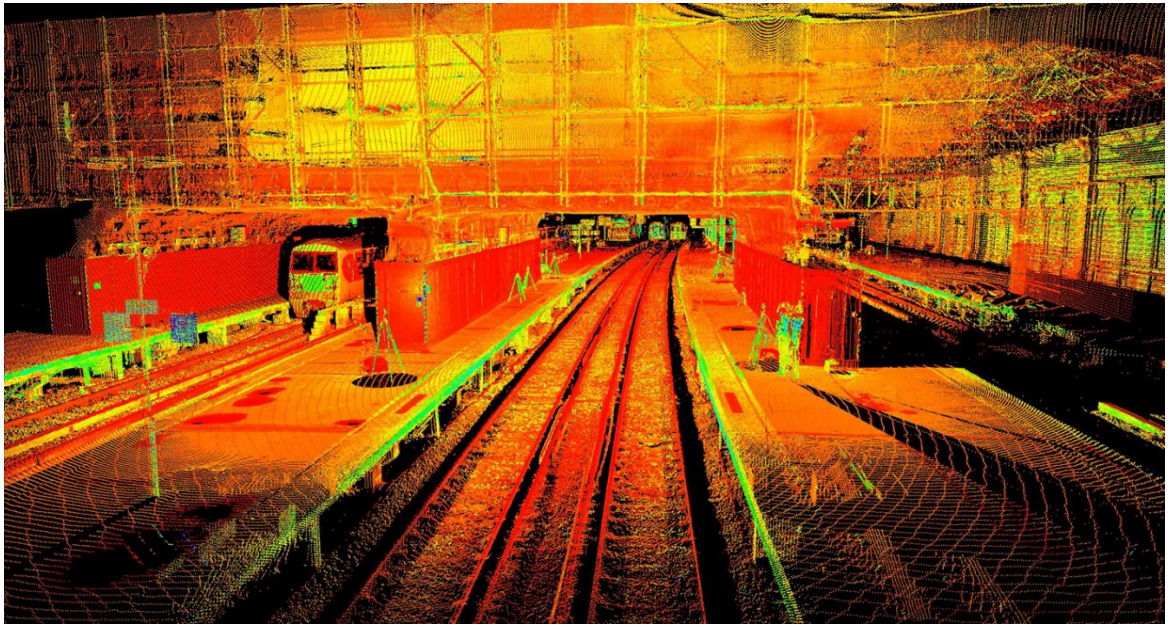


Non-contact monitoring of railway infrastructure with terrestrial laser scanning and photogrammetry at Network Rail



Anita Soni

Department of Civil, Environmental and Geomatic Engineering

University College London

Supervisors: Professor Stuart Robson, Mr Barry Gleeson

Thesis for the degree of Doctor of Engineering (EngD)

Virtual Environments, Imaging and Visualisation

2016

Declaration of Authorship

I, Anita Soni, confirm that the work presented in this thesis is my own. Where information has been derived from other sources, I confirm that this has been indicated in the thesis.

Signed

Date

Abstract

Current monitoring practices in the railway industry primarily rely on total station and prism based methods. This approach requires the installation and maintenance of prisms directly onto the structure being monitored which can be invasive and expensive. This thesis presents the outcomes of an industrial based doctorate, motivated by the Network Rail Thameslink Programme, to investigate the potential of terrestrial laser scanning and photogrammetry as an alternative non-contact and “target-less” solution to monitoring railway infrastructure. The contributions made by this thesis in the context of Network Rail requirements include: a laboratory based exploration of the state of the art in target and surface-based measurements; a validation of conventional, terrestrial laser scan and photogrammetric surveys of a deforming set of brick arches; and a novel prism-less method of track measurement using terrestrial laser scanner data. The complete project has been carried out as part of the highly complex and dynamic £900m London Bridge Redevelopment Project.

The thesis comprises of a review of existing monitoring system performance and highlights challenges in the adoption of this technology through interviews of leading professionals in the monitoring industry. Laboratory tests utilise network adjustment prediction and analysis to compare state of the art total station, terrestrial laser scanning and close-range photogrammetry instrumentation to both target and target-less deformation monitoring scenarios. The developed tests allow the performance of each technique to be assessed within the context of state of the art and Network Rail operational practice and are extensible to developments in each of these technologies. Results demonstrate performances to sub-millimetre level and are validated through the use of a Leica AT401 laser tracker. Each technique is then explored within the London Bridge Redevelopment Project through a series of live monitoring sites where their ability to either augment or replace existing survey techniques is evaluated. Results from the on-site monitoring of historic brick arch structures demonstrate surface measurements compatibility at the millimetre level, highlighting close agreement between instrument performance established in the laboratory.

A key use of prism-based techniques is in the determination of engineering track parameters where costly prism systems, both in terms of installation and subsequent maintenance, attached to the track are a key concern. Here laboratory validated track surface measurement, with terrestrial laser scanning, has been deployed on a 15 metre long dual track site and shown to be highly capable of replacing prism systems for the determination of accurate track geometry. This work has included a novel optical non-contact measurement process utilising individual rail cross section designs to automatically extract relevant track geometry parameters within 1mm of prism-based methods. The method offers excellent potential for incorporation into an automated track monitoring system. Outcomes from the thesis have been published in peer-reviewed journals and conferences.

Acknowledgements

Firstly, I would like to thank both my academic and industrial supervisors, Professor Stuart Robson and Barry Gleeson, for this opportunity. I feel very privileged to have been guided by leading professionals in both the academic and industrial world. Thank you both for your continuous support, invaluable insight and never-ending patience throughout.

A wide variety of surveying instrumentation was hired/borrowed for site and laboratory testing. Thanks go to Hexagon Metrology, Leica Geosystems, Plowman Craven Ltd and SCCS for providing these, often at short notice. Special thanks go to Dean Bain and Elspeth Backes for enabling access to London Bridge and Blackfriars stations for the site tests. I'd like to thank Michael Bachinski at MicroSurvey for providing a Star*Net license. Thanks go to Marcin Krzetowski and Matt Jenkinson at NR TLP for their support. Thanks also go to Sol Data Group for providing access to the LB monitoring database. Acknowledgements go to the interviewed monitoring specialists who generously gave their time and expertise to the study: Mike Black, Ian Harris, Frances McDonnell, Rory O'Rourke and John Richmond.

Thanks go to Ian Seaton and Les Irwin in CEGE for their support during the lab test work. I would like to give a huge thank you to my colleagues in 3DIMPact. Special thanks go to Hannah Corcoran, aka my partner in crime, who collaborated on the initial lab testing, has been a great listener for research ideas, has made me laugh throughout and has become one of my best friends during this study. I'd like to thank John Hindmarch for being my EngD buddy and providing moral support from the very beginning. I'm very grateful of my ex-colleagues for their expertise with technical issues: Mark Wakeling, Lieve Spincemaille and Joseph Severn.

I couldn't have got through the past few years without the love, support and laughter provided by my best friends: Em Graham, Sally El-Ghazali, Hannah Corcoran, Jayna Gadawala & Murs! Thank you for keeping me motivated by ensuring there was always something fun to do and never asking me about my research! I feel very lucky to have such loving friends.

Finally, I would like to dedicate this thesis to my family. Mum and Dad – there will never be enough words to express my gratitude for everything you've done for me and I wouldn't be here without your endless love and support (both emotional and financial). Nush – we did it! Thank you so much for your continuous motivation and support whilst living this experience in parallel with me. I particularly enjoyed our daily pep talks during the writing up stage! Kiyana and Miya – I love and thank you for always bringing lots of happiness to my life.

Table of contents

Abstract i

Acknowledgements iii

Table of contents iv

List of Figures viii

List of Tables..... xiv

List of abbreviations..... xvi

Glossary of hardware used xviii

Glossary of software used xx

Chapter 1 - Introduction 1

 1.1 Motivation for this of research 1

 1.2 Objectives of research 2

 1.3 Contributions to knowledge 3

 1.4 Thesis outline 4

 1.5 Publications from this work 6

Chapter 2 - Network Rail: an overview of monitoring practices 7

 2.1 Chapter Introduction 7

 2.2 Overview of Network Rail 8

 2.3 The Thameslink Programme 10

 2.3.1 Monitoring strategy and specification 12

 2.3.2 Monitoring implementation 14

 2.4 Monitoring industry context..... 16

 2.4.1 Lack of/limited monitoring standards/guidelines 17

 2.4.2 Access to railway infrastructure for monitoring 20

 2.4.3 Data handling 23

 2.4.4 Cost 23

 2.4.5 Lack of insight into monitoring data quality..... 24

 2.4.6 Lack of non-contact monitoring method..... 25

 2.5 Study Focus 25

 2.6 London Bridge Station Redevelopment Project: site test requirement for the study..... 27

 2.6.1 London Bridge Station track monitoring requirements 28

2.6.2	London Bridge Station arch monitoring requirements	32
2.7	Chapter Summary.....	34
Chapter 3 - A review of engineering surveying techniques used in deformation monitoring		36
3.1	Engineering deformation monitoring.....	36
3.2	Engineering surveying deformation measurement.....	38
3.2.1	Levelling	38
3.2.2	Total stations.....	40
3.2.3	Terrestrial laser scanning	48
3.2.4	Close-range photogrammetry	63
3.2.5	Laser trackers	69
3.2.6	Summary of engineering surveying measurement techniques	71
3.3	The role of network adjustment	72
3.3.1	Network design	72
3.3.2	Outlier detection and system calibration	76
3.3.3	Deformation analysis of networks with redundant measurements	79
3.3.4	Deformation analysis of networks with single measurements.....	87
3.4	Data information and communication.....	92
3.5	Chapter Summary.....	100
Chapter 4 - Instrumentation performance tests through point and surface-based measurements within a laboratory environment		102
4.1	Target-based instrumentation testing.....	102
4.1.1	Experiment 1: Network performance	103
4.1.2	Experiment 2: Target-based measurement capability.....	120
4.2	Surface-based instrumentation testing	133
4.2.1	Experiment 3: Surface-based measurement of laboratory rail.....	133
4.2.2	Experiment 4: Surface-based measurement and range translation performance of brick.....	143
4.3	Chapter Summary.....	151
4.4	Opportunities and challenges for Network Rail.....	153
4.4.1	Opportunities	153
4.4.2	Challenges.....	154
Chapter 5 – London Bridge Station site test: monitoring of railway track		155

5.1	Site Challenges	155
5.2	Data Capture.....	156
5.3	Importing Raw Scans	160
5.4	Point Cloud Registration	161
5.5	Track Extraction from Point Cloud.....	162
5.5.1	2D cross-section extraction.....	163
5.5.2	3D cross-section extraction.....	164
5.6	Data Cleaning.....	168
5.6.1	Edge Effects.....	169
5.6.2	Artefact Removal.....	171
5.7	Rail Track Fitting	175
5.7.1	Rail fitting inclusive of curvature	175
5.7.2	Rail fitting of planar sections.....	182
5.8	Measuring and validating track geometry against prism-based method ..	188
5.9	Chapter Summary.....	191
5.10	Opportunities and challenges for Network Rail.....	193
5.10.1	Opportunities.....	193
5.10.2	Challenges.....	194
Chapter 6 - London Bridge Station site test: monitoring of masonry arches.....		196
6.1	Site Challenges.....	197
6.2	Data capture.....	199
6.2.1	Total Station (TS) monitoring setup	199
6.2.2	TLS monitoring setup	204
6.2.3	CRP setup.....	205
6.3	Results and analysis	206
6.3.1	Comments on workflow.....	206
6.3.2	Manual monitoring results	208
6.3.3	TLS results	210
6.3.4	TS and TLS analysis	211
6.3.5	CRP vs TLS	215
6.4	Chapter Summary.....	218
6.5	Opportunities and challenges for Network Rail.....	220

6.5.1 Opportunities	220
6.5.2 Challenges.....	221
Chapter 7 - Conclusions and further work	223
7.1 Contributions to knowledge.....	223
7.2 Further work	228
References and bibliography.....	232
Appendices.....	243
Appendix A - Instrumentation specifications	243
Appendix B - Notes from railway industry monitoring interviews	246

List of Figures

Illustrations and photographs in this thesis are by the author unless otherwise stated.

Figure 2.1: GRIP Lifecycle – (taken from the Network Rail GRIP Policy Manual - Network Rail, 2010)..... 9

Figure 2.2: Scope of the Thameslink railway network through Central London (image taken from Inner Area Tour presentation - Network Rail Thameslink, 2010)..... 11

Figure 2.3: Monitoring outputs during the GRIP process 14

Figure 2.4: Organogram of monitoring implementation process at TLP 15

Figure 2.5: Network Rail Thameslink Programme Survey Process Map 19

Figure 2.6: Typical prism layout for track monitoring at Network Rail (image taken from the London Bridge Station Development Monitoring Specification) 22

Figure 2.7: Annotated image of London Bridge Station before redevelopment started 28

Figure 2.8: London Bridge Station undergoing major redevelopment (time-lapse images taken from the London Bridge Site-Eye camera) 29

Figure 2.9: Measuring track cant - image created based on UK Railway Group standards definition (1998)..... 30

Figure 2.10: Monitoring contractor approximation of track geometry parameters using prisms (image taken from Sol Data’s Geoscope Explorer (version 6.5) within the “Cant and Twist explanation” tab..... 31

Figure 2.11: Measuring track gauge (image taken from CEN, 2008)..... 32

Figure 2.12: Examples of London Bridge Station arches (top image taken from NR TLP published TruView) 33

Figure 2.13: London Bridge arches monitoring target arrangement 34

Figure 3.1: Example of automatic levelling: automatic level (left) to read levelling staff (right) at millimetre level 39

Figure 3.2: An example of a total station on a fixed pillar for deformation monitoring 40

Figure 3.3: Concept of a total station’s phase measurement phase taken from Kahlmann et al. (2006)..... 41

Figure 3.4: Examples of prism (top) and retroreflective targets (bottom) used with total stations..... 42

Figure 3.5: Typical automatic monitoring system configuration – image taken from Whitworth (2010)..... 44

Figure 3.6: Typical automatic monitoring setup using a total station 45

Figure 3.7: Example of large-scale automatic monitoring network on the CrossRail project including 52 total stations - image taken from Binder (2014)	47
Figure 3.8: Array of current TLS systems available starting on the left going clockwise: Reigl VZ-1000; Topcon GLS-2000; Faro Focus 3D X130 and X330; Leica ScanStation P20; Z+F 5010C.....	49
Figure 3.9: Time-of-flight distance measurement principle taken from Kahlmann et al. (2006)	50
Figure 3.10: Typical TLS targets - sphere and planar based (not to scale).....	53
Figure 3.11: Target centre extraction of sphere (top) and black and white (bottom) target.....	54
Figure 3.12: Example of point cloud registration in Leica Cyclone	55
Figure 3.13: Libraries available in PCL - taken from PCL documentation website..	57
Figure 3.14: Basic interface scheme for PCL code – image taken from Boehm et al. (2013).....	57
Figure 3.15: Example of handling large volumes of point cloud data at TLP using TruView	59
Figure 3.16: Configuration of Amberg Clearance GRP 5000 - image taken from Amberg (2015).....	60
Figure 3.17: Typical clearance analysis and track parameter output from kinematic TLS of railway	61
Figure 3.18: Principle of photogrammetric measurement – image taken from Luhmann et al. (2014)	64
Figure 3.19: Pinhole camera model - image taken from Luhmann et al. (2014).....	65
Figure 3.20: Retro-reflective photogrammetry targets.....	66
Figure 3.21: State of the art total station (left) and laser tracker (right)	70
Figure 3.22: Example of SMR target	71
Figure 3.23: An example of an error ellipse	75
Figure 3.24: Bespoke deformation detection tool developed by Setan and Ibrahim (2003) – image taken from this paper	85
Figure 3.25: Flow diagram of network design and adjustments for deformation monitoring – taken from Caspary and Rieger (2000)	87
Figure 3.26: Typical method of communicating monitoring data on TLP	94
Figure 3.27: Application of smoothing filters to monitoring observations.....	95
Figure 3.28: Example of presenting deformations with 95% confidence ellipses – image taken from Caspary and Rieger (2000)	96

Figure 3.29: Road pavement deformation measurement through 2D deformation vector field - image taken from Maas and Hampel (2006)	97
Figure 3.30: Deformation maps of different surface approximations using TLS – image taken from Alba et al (2006)	98
Figure 3.31: Different methods of displaying change in surface topography of a tunnel wall - image taken from Lemy et al (2006).....	99
Figure 4.1: Plan view of lab space and position of stations (S1-3) and Nests (N1-10)	104
Figure 4.2 a) 1.5" magnetic nest (left); b) 1.5" SMR target (centre); c) 1.5" target adapter (right).....	104
Figure 4.3: Schematic of relative error ellipse between two points	105
Figure 4.4: An example of a network adjustment plot using STAR*NET	106
Figure 4.5: Predicted relative error ellipses (semi-major axis) of prism and reflectorless target measurements based on instrument specification	108
Figure 4.6: Relative error ellipses (semi-major axis) - observed (circle) against predicted (triangle)	110
Figure 4.7: Length measurement errors and MPE boundary	112
Figure 4.8: TS30 relative error ellipse of network from different stations	113
Figure 4.9: Length error of network from different stations with the TS30	114
Figure 4.10: Relative error ellipses (semi-major axis) for angles only measurements from instruments	115
Figure 4.11: Length errors for angles only measurements from total stations.....	115
Figure 4.12: Standardised distance residuals of TS30 and TM30 from S1 and S2..	117
Figure 4.13: Standardised zenith residuals of TS30 and TMS30 from S1 and S2...	117
Figure 4.14: Standardised direction residuals of TS30 and TM30 from S1 and S2	118
Figure 4.15: Target array for range displacement measurements; HDS targets L1-L4 from left to right; tooling balls T1-T5 from left to right; precise prism MP (centre)	121
Figure 4.16: Target array testing setup.....	122
Figure 4.17: Histogram of residuals of tooling balls with and without T5	126
Figure 4.18: Point cloud of target array with target acquisition.....	129
Figure 4.19: Histogram of residuals of total station and TLS system measurements to TLS targets	132
Figure 4.20: CEN56E1 rail used for the laboratory tests	134
Figure 4.21: Expected height and distance of scanner to track (not to scale)	135

Figure 4.22: Cross-sections of lab rail through TLS and CRP in orthographic view	137
Figure 4.23: Planar based naming reference for rail	139
Figure 4.24: Histogram of time of flight scanners plane fitting residuals to web of rail	141
Figure 4.25: Histogram of phase based scanners plane fitting residuals to web of rail	141
Figure 4.26: Histogram of CRP plane fitting residuals to web of rail	142
Figure 4.27: Sample of brick wall used for laboratory tests	144
Figure 4.28: Point cloud from MS50, Focus 120 and CRP respectively from left to right	144
Figure 4.29: Brick wall translation test (white box) with the MS50	146
Figure 4.30: Colour surface displacement and histogram output from distance comparison in CloudCompare	147
Figure 4.31: Geomagic Qualify 2013 3D Deviation Comparison concept	148
Figure 4.32: Geomagic Qualify 2013 3D deviation output (in metres)	148
Figure 5.1 Image and point cloud of tamper proof and L-bar prisms typically used for total station monitoring, not to scale	156
Figure 5.2: Scan positions at platform level (image taken and adapted from London Bridge Monitoring Specification)	158
Figure 5.3: Scanner positions (top view) including cross-section locations and track labelling	159
Figure 5.4: Network plot from STAR*NET for scanner target positions	160
Figure 5.5: Segmented scan when importing .ZFS file into Cyclone 8.0	161
Figure 5.6: Tilt and turn target centre acquisition in Cyclone	162
Figure 5.7: 1mm cross-section of track from laboratory rail (left) and site rail (right)	163
Figure 5.8: Example of extracting cross-sections in Geomagic Qualify 2013	166
Figure 5.9: Spatial filtering settings in Microstation V8i	167
Figure 5.10: Automatic cross-section extraction using Cyclone (top view)	168
Figure 5.11: Coverage of track from Scan A and B - NOT TO SCALE	169
Figure 5.12: Random noise in extracted cross-section	169
Figure 5.13: Point traces directed back to scanner locations	170
Figure 5.14: Cross-section of rail from the design model, HDS7000 (green) and P20 (blue) laser scanner	170
Figure 5.15: Example of typical artefact associated with the track	171

Figure 5.16: Track weld artefact (top view).....	172
Figure 5.17: Colour coded histogram of plane fit of track weld artefact	172
Figure 5.18a) Histogram of residuals without data cleaning of weld artefact (left) and b) with data cleaning (right) in metres	173
Figure 5.19: Histogram of residuals of reference lab track from the HDS7000	173
Figure 5.20: Track cable connection artefact profile (left), corresponding face-on view (top right) and image of feature (bottom right)	174
Figure 5.21a) histogram of residuals without data cleaning of rivet artefact (left) and b) with data cleaning (right).....	174
Figure 5.22: Rail curvature based naming reference.....	175
Figure 5.23: CloudCompare example of fine registration of rail point cloud to design model.....	176
Figure 5.24: 3D Comparison results from the HDS7000 and P20.....	180
Figure 5.25: design rail geometry highlighting planar segments (in red)	183
Figure 5.26: RMS registration residuals of single and combined scan	187
Figure 5.27: 4-step methodology workflow for accurate rail fitting.....	188
Figure 5.28: Aerial view (top) and perspective view (bottom) of monitoring prism co- ordinates (blue vertices)	189
Figure 6.1 Image of London Bridge arches at street level with train shed visibly located overhead (image taken from NR TLP published TruView).....	197
Figure 6.2: Images from original arch test site inspection	198
Figure 6.3 : Typical site conditions of arches during data capture	199
Figure 6.4: General target arrangements of arch monitoring	200
Figure 6.5: Test area (white) with monitoring prism arrays (blue).....	202
Figure 6.6: Network plot of TS15 monitoring survey of test area with error ellipses (1σ).....	203
Figure 6.7: Graphical monitoring results from prism target RPE0057101- data taken from Sol Data Geoscope’s monitoring database	209
Figure 6.8: Deformation displacement map of a 5 x 12 metres area of local detail between epochs 1 and 4 (plan view, deflection in metres).....	211
Figure 6.9: Side (left) and perspective (right) view from point cloud of prism (circled in red) aligned to springing point of arch.....	212
Figure 6.10: Profile of arch from TLS data with movement vector dimensions (deflections shown in red).....	214
Figure 6.11: CRP point cloud of test area of masonry arches.....	215

Figure 6.12: Image of area used for Plane 1 highlighting wooden object	216
Figure 6.13: Front and side profile view of TLS (left) and CRP (right) point cloud for Plane 1	217
Figure 6.14: Comparison of arch profile between TLS and CRP data	218

List of Tables

Table 2.1: Network Rail GRIP stage aims and outputs (taken from the Network Rail GRIP Policy Manual - Network Rail, 2010)	10
Table 2.2: Summary of findings of monitoring issues from interviews.....	17
Table 2.3: Monitoring issues that this study allows to be addressed	26
Table 4.1: Measured translations from instruments to tooling balls	124
Table 4.2: Residuals of measurements to tooling balls from laser tracker and total station	125
Table 4.3: Measured translations from instruments to precise prism	127
Table 4.4: Residuals of measurements to precise prism from laser tracker and total station	128
Table 4.5: Measured translations from instruments to TLS targets	130
Table 4.6: Residuals of measurements to TLS targets from total station and TLS system.....	131
Table 4.7: RMS of local plane fit to PL2 using TLS and CRP	139
Table 4.8: RMS of plane fitting to brick wall	145
Table 4.9: RMS of plane fits to planar patch of a single brick	145
Table 4.10: Measured translations from TLS instrument to brick surface on translation stage.....	149
Table 4.11: Residuals of measurements from instrument to brick surface	149
Table 5.1: Epochs of TLS Data Acquisition at London Bridge Tracks	157
Table 5.2: Summary of RMS values of fitting point cloud to modelled rail.....	178
Table 5.3 : RMS of rail fitting procedure inclusive of rail curvature (L1,L2, L3) in laboratory	181
Table 5.4: Local plane fits from Scan A&B (left) and Scan C&D (right) at 9m chainage	183
Table 5.5: Track visibility of planar features	184
Table 5.6a) Registration RMS from Scan A&B (top) and b) Scan C&D (bottom)	185
Table 5.7 : RMS of rail fitting of planar sections using laboratory track	186
Table 5.8: Cant, twist, and gauge comparisons between total station and TLS results	190
Table 6.1 : Monitoring point co-ordinate standard deviations (1σ)	203
Table 6.2: Methodology workflow of TS, TLS and CRP for monitoring purposes	207

Table 6.3: Numerical manual monitoring results of arches including change in movement between epochs (mm).....	210
Table 6.4: Results from plane fitting using least squares estimation.....	215

List of abbreviations

ADM	Absolute Distance Meter
AMP	Asset Management Plan
ATR	Automatic Target Recognition
BTS	British Tunnelling Society
CDM	Construction Design and Management regulations
CIRIA	Construction Industry Research And Information Association
CRP	Close-Range Photogrammetry
EDM	Electromagnetic Distance Measurement
EPP	Emergency Preparedness Plan
EPSRC	Engineering and Physical Sciences Research Council
GMA	Ground Movement Assessment
GPRS	General Packet Radio Service
GPS/GNSS	Global Positioning System/ Global Navigation Satellite System
GRIP	Governance for Railway Investment Projects
HDR	High Dynamic Range imaging
ICP	Iterative Closest Point
LiDAR	Light Detection And Ranging
LSE	Least Squares Estimation
LVDT	Linear Variable Differential Transformer
MPE	Maximum Permissible Error
MVS	Multi-View Stereo
NR	Network Rail
PCL	Point Cloud Library
PPM	Parts Per Million

RMS	Root-mean square
SfM	Structure from Motion
SMR	Spherically Mounted Retro-reflector
TLP	Thameslink Programme
TLS	Terrestrial Laser Scanning
TS	Total Stations
WPP	Works Planning Package

Glossary of hardware used

Please refer to Appendix A for a summary of the manufacturer specifications of the instrumentation used.

Total Stations

Leica Nova MS50

Leica TM30

Leica TS30

Leica Viva TS15

Terrestrial Laser Scanners

Faro Focus 120 (also known as Faro Focus^{3D})

Leica HDS7000

Leica ScanStation 2

Leica ScanStation C10

Leica ScanStation P20

Laser Tracker

Hexagon Metrology Leica Absolute Tracker AT401

Camera

Nikon D3200 DSLR Camera + 16mm fish-eye lens

Targeting

Faro 5.7” standard reference sphere targets

Hexagon Metrology 1.5” spherically mounted retro-reflector (SMR) target

Hubbs 1.5” sphere mount nests

Hubbs 1.5” split bearing retro-reflective photogrammetry targets

Hubbs total station 1.5” spherical retro-reflector target

Leica Geosystems HDS 3” x 3” planar targets

Leica Geosystems HDS 6" black and white, tilt and turn targets

Leica GPHP1P precision prism reflector

Leica Hexagon Metrology 0.5" tooling ball reflectors

Glossary of software used

Software	Version	Purpose of software for this study	Open source (OS) or proprietary (P) software	“Black box processes”?*
Bentley Microstation	V8i (series 3)	Producing 2D and 3D CAD models of masonry arches and rail design model, calculating cant and twist of track	P	Yes
CloudCompare	2.5.5.2	Registration of track design model to acquired TLS point cloud	OS	No
Geomagic Qualify	2013.0.1	Producing deformation displacement maps from point cloud data	P	Yes
Geomagic Studio	2013.0.1	Producing 3D mesh from point cloud data	P	Yes
Leica Geosystems Cyclone	8.1.3	Importing and registering TLS data, automatically producing cross-sections of railway track	P	Yes
MathWorks MATLAB	R2012a	Producing histograms of the residuals from point cloud registration	P	No
MicroSurvey STAR*NET	8.1.2	Running least-squares network adjustment on survey measurements	P	No
n4ce	2.50c	Importing raw survey data and converting into STAR*NET format	P	Yes
UCL Geomatics Lens Distortion Correction (LDC),	1.2.1	Correcting images based on camera calibration using VMS	P	Yes
Vision Measurement System (VMS),	8.5	Camera calibration for CRP	P	No
VisualSFM	0.5.22	Running SfM process using CRP images to produce a dense 3D reconstruction	OS	No

* “Black box processes”: inability to access and audit key steps and outcomes. For example, statistical evidence on least squares fitting and adjustment or a log of changes made to input measurement data.

Chapter 1 - Introduction

This thesis has been submitted as part of an Engineering Doctorate (EngD) which is a collaborative research study between University College London (UCL) and Network Rail Thameslink Programme. It is a study partly funded by the Thameslink Programme and the Engineering and Physical Sciences Research Council (EPSRC), which has been hosted by the UCL doctoral training centre of Virtual Environments, Imaging and Visualisation (VEIV).

Network Rail (NR) are the owner and infrastructure manager of most of the rail network in England, Scotland and Wales. One of the projects at NR is the Thameslink Programme (TLP) which involves a £5billion upgrade of a major railway line through Central London. Some stations that have been upgraded include London St Pancras, Blackfriars and Farringdon Station. Currently London Bridge Station is going through redevelopment, which is due to be completed in 2018, will cost approximately £900m.

1.1 Motivation for this of research

The protection of existing infrastructure, e.g. structures, railway lines, stations etc. is essential for enabling these upgrades and redevelopments. Therefore structural monitoring is a fundamental requirement for safety, protection and operational efficiency. Railway monitoring usually consists of total stations measuring to glass prisms or targets directly attached to the structure being monitored, which can be invasive where drilling or gluing is required. This can result in safety and timing issues during installation as well as subsequent maintenance. It also provides discrete point information of the target and not necessarily the structure itself.

Currently the cost for monitoring a major station on the TLP, e.g. London Bridge Station, costs £1million per year. From an assurance point of view this seemed to be a substantial cost for monitoring alone. There was concern in the effectiveness of monitoring systems implemented. In particular there was uncertainty with the benefits of using prisms due to the multiple problems associated with their implementation during the lifetime of a project. For example, the prisms used for railway track monitoring often get kicked/turned during engineering hours, which results in a “null” reading from the total station.

Therefore, based on the advancement of technology in the surveying industry, NR TLP were seeking to investigate the potential of optical non-contact techniques such as terrestrial laser scanning and photogrammetry. It was thought that this could offer a change in the monitoring implementation process where prism installation and maintenance times and costs could be reduced, whilst capturing surface information of the structure as opposed to discrete point information of the target. When reviewing ongoing research and activities in the field the key issues in the application of these technologies are achieving the required accuracy and precision, as well as the analysis and communication of deformation monitoring results.

1.2 Objectives of research

Based on the motivation of this study, the objectives of this study from a Network Rail remit comprised of the following three concerns:

1. Do these prism issues at TLP, for example, the null readings and high maintenance costs, also appear across the railway monitoring industry?
2. Can prism-free monitoring technologies be applied at the London Bridge Station redevelopment project?
3. Can non-contact techniques replace prisms more widely across the railway monitoring industry?

As a result of these enquiries, the research has followed a two-stage process. Firstly laboratory comparisons and capability evaluation of both target and targetless systems in order to link performance with established engineering surveying network design. Experiments have been designed around leading edge instruments in current use but have included tools from engineering metrology, such as laser trackers and target nests, in order to challenge the engineering state of the art. These types of instrumentation, which are purpose-built for metrology applications, allow an order of magnitude better measurement capability to be used as a gold standard against engineering surveying techniques, which can be compared in a generic set of tests capable of accommodating future instrument developments.

Close working with NR, including assisting contractors with on-site surveys, was required to gain key access to active live railway monitoring sites in order to carry out practical evaluation of the techniques so that their fit for purpose to engineering need and ability to accommodate challenging site conditions can be included in the

experimental work. Out of six sites initially selected for evaluation, the work for this thesis has focused on the London Bridge Redevelopment Project and specifically around a set of actively deforming historic brick arches and the railway track above them. This enabled direct comparison between NR commissioned surveys along with a direct link into the NR engineering structure allowing detailed conversations centred on engineering need. For example the archway monitoring took place during a period of active change whilst changes in the track, expressed in the form of cant and twist could be compared with data from commissioned monitoring systems (see Chapter 2 for an explanation of terminology).

This combination has supported the development of and answers to the following key research questions which when brought together provide an academic rationale to the thesis with a clear novel contribution to the state of the art, whilst addressing the key points raised by NR at the outset of this study.

1. Can detection of change from surface-based measurements at a laboratory and site-based scale be applied independently to prism-based measurements to determine if these are fit for purpose and fulfil engineer's requirements?
2. Can non-contact instrumentation performance testing, such as TLS and CRP, be carried out to determine if similar levels of accuracy and precision as state of the art total stations can be achieved?
3. What are the advantage and disadvantages of replacing prisms on large scale monitoring projects?

1.3 Contributions to knowledge

This research makes the following contributions to knowledge:

1. A method for determining whether total station instrumentation is performing within the manufacturer's specification drawing upon established metrology standards and a laser tracker as a "gold standard" baseline. The method can be used for instruments of various stages of their lifetime given that 24/7 monitoring environments are extremely challenging. Since the method is founded on network analysis, a simulation mode can be used to ascertain the effect in any given monitoring network.
2. A method for testing state of the art instrumentation capability of point and surface-based measurements through laboratory testing. The developed

method can be applied to any instrument, target or surface type making it capable of testing future instruments which might be based on hybrid designs such as the combined scanning total station Leica MS50 and the portable laser tracker Leica AT402.

3. A novel rail fitting technique to allow railway track geometry, required for track monitoring, to be extracted has been validated in the laboratory and applied on site. This work has been presented at several peer-reviewed conferences and cited by other researchers. Extraction of a planar rail surface has been achieved to 0.6mm RMS whilst extraction of the complete rail cross-section has been achieved to better than 1.5mm RMS. This level of detection is commensurate with prism-based systems but offers the flexibility of extracting profiles and track parameters at user defined spacing within the post-process stage. The developed method is capable of full automation.
4. The validation of laboratory tests of measuring brick surfaces through a TLS monitoring survey on a site-based scale, independent of the prism based methods, to achieve a fit for purpose solution. TLS was able to deliver relative movements on a challenging live site environment through ad-hoc surveys. Despite an average uncertainty of 7mm between the registrations of epochs, the results validated the relative movements through 2D arch profiles as well as 3D deformation displacement maps at the millimetre level. This highlighted the issue of local vs global point cloud registration in order to detect small changes in the presence of very challenging engineering surveying connection networks.

These contributions are summarised in Chapter 7.

1.4 Thesis outline

Following the introduction provided in this chapter, the thesis is comprised of six main chapters.

To place the work in context, this thesis commences with a chapter written very much in an industry focused style. Chapter 2 provides a background to the Network Rail engineering need leading towards the requirements of implementing a monitoring scheme on a large-scale project such as TLP. A review of existing monitoring performance is presented through interviews of leading professionals in the monitoring industry. This overview is followed by a detailed background into the monitoring

requirements of the London Bridge Redevelopment Project, which provides the very active case studies for this research.

Chapter 3 reviews the current state of the art engineering surveying techniques used for deformation monitoring. It describes the well-established workflow carried out for analysing deformation monitoring using more traditional measurements such as total stations, including the communication of monitoring data to the relevant parties that is fit for purpose. The chapter also describes how emerging technologies such as TLS are beginning to be applied as a deformation monitoring tool and the current challenges associated with this.

Chapter 4 discusses the laboratory work carried out in this research to investigate instrument capability testing of point and surface-based monitoring using total stations, terrestrial laser scanners and close-range photogrammetry. Surface-based tests focus on typical surfaces encountered in the railway environment: railway track and masonry brick.

The findings from the laboratory experiments are used to apply surface-based monitoring techniques to two live monitoring sites on the London Bridge Redevelopment Project independently of the manual/automatic prism-based methods provided by the contractor. Chapter 5 shows TLS testing of a section of railway track required to be monitored throughout the project in order to accurately extract track geometry parameters.

Chapter 6 applies TLS and CRP to measure the movement of a set of historic brick arches which were deforming. The challenges with respect to gaining access to both of these sites in order to carry out these tests is discussed.

Chapters 4, 5 & 6 provide conclusions from the laboratory and site experiments carried out. These conclusions are then taken forward in an industry context by addressing the question “What does this mean for Network Rail?” in which a list of opportunities and challenges for Network Rail is provided.

Chapter 7 includes key contributions of the research project and opportunities of further work in an academic and rail industry context.

1.5 Publications from this work

The following papers and presentations relevant to the research topic have been written and presented at academic and industrial conferences and published in peer-reviewed academic journals and conference proceedings during the course of the research.

Journal publications

Soni, A., Robson, S., Gleeson, B. (2015) Structural monitoring for the rail industry using conventional survey, laser scanning and photogrammetry, *Applied Geomatics*, 7 (2), 123-138.

In submission: Soni, A., Corcoran, H., Robson, S., Testing the performance of current generation total stations for monitoring, *Survey Review*

Conference proceedings

Soni, A., Robson, S., Gleeson, B. (2015) Optical non-contact railway track measurement with static terrestrial laser scanning to better than 1.5mm RMS, *FIG Working Week 2015, Commission 6: Engineering Surveys*

Soni, A., Robson, S. & Gleeson, B. (2014) Extracting Rail Track Geometry from Static Terrestrial Laser Scans for Monitoring Purposes. *ISPRS-International Archives of the Photogrammetry, Remote Sensing and Spatial Information Sciences*, 1, 553-557.

Soni, A., Robson, S. & Gleeson, B. (2013) Comparison of conventional survey, laser scanning and photogrammetry for structural monitoring in the rail industry, *2nd Joint International Symposium on Deformation Monitoring*

Industrial conference presentations

“Emerging technologies in Monitoring”, Instrumentation and Monitoring Conference, London (2015)

“Instrumentation and Monitoring in the Railway Environment”, GeoBusiness, London (2014)

“The potential of laser scanning and photogrammetry for structural monitoring in the rail industry”, SPAR Europe, Amsterdam (2013)

Chapter 2 - Network Rail: an overview of monitoring practices

This Engineering Doctorate (EngD) required close working with Network Rail (NR) in order to understand the monitoring context and to gain access to key live sites through a complex possession based process. This chapter introduces that context including key questions from NR that initiated the funding for this work as an NR/EPSRC supported EngD. A significant period of the work was spent working as part of an NR team to gain an understanding of the very complex engineering requirements, communication chain, procurement, validation and relationship between different parties such as the client contractor relationship. Work carried out included interviews with key industry figures, presence at NR planning and decision making meetings and working on site with contractors. The London Bridge Redevelopment Project and its capability to provide two very active case studies, where movement was predicted, allowed the EngD to focus on particular key issues. The industrial focus of this study has necessitated a chapter written very much in an industry focused rather than an academic style. This thesis would not have been possible without the time and effort invested in this process. Acknowledgements go to Barry Gleeson at NR for facilitating this.

2.1 Chapter Introduction

As presented in Chapter 1 the motivation for this study arose from Network Rail Thameslink Programme (TLP). It was seen that the cost for monitoring a major station at TLP was £1 million per year. Also from a survey assurance point of view there was uncertainty in the effectiveness of the monitoring system implemented. In particular there was uncertainty of the benefit of using targets, such as glass prisms, due to multiple problems associated with their implementation during the lifetime of the project. Network Rail has a history of using target-based systems, especially prisms, for monitoring any type of structure. Due to this high cost of having a monitoring system and frequent issues with prisms, there was an incentive to answer the following questions:

1. Do these prism issues at TLP also appear across the railway monitoring industry?

2. Can prism-free monitoring technologies be applied at the London Bridge Station redevelopment project?
3. Can non-contact techniques replace prisms more widely across the railway monitoring industry?

The first question, which is associated with current monitoring industry practices, is addressed in this chapter by carrying out interviews with key figures in the industry to gain an insight into the monitoring practices on other projects at a similar or larger scale. After providing background information on Network Rail and the TLP below, a brief summary of the outcomes from these interviews is provided in section 2.4.

The second question is addressed in Chapters 5 and Chapter 6 where surface based measurements using TLS and CRP techniques, i.e. without the use of prisms or targets attached the surface, are applied. The techniques that are applied are based on the laboratory testing carried out in Chapter 4.

The third question is based on the potential use of these non-contact techniques. Based on the outcomes from the site testing in Chapter 5 and Chapter 6 this question is addressed in the conclusions of this thesis in Chapter 7.

2.2 Overview of Network Rail

Network Rail (NR) are the infrastructure maintainer of the UK's national rail network. They also undertake major infrastructure projects within specialist units under the umbrella of Investment Projects. The management of these investment projects is achieved through "Governance for Railway Investment Projects" (GRIP). This consists of 8 phases beginning with defining the output of the project through to the project close out (Network Rail, 2015). Figure 2.1 represents the lifecycle of GRIP. The Thameslink Programme is one of these investment projects.

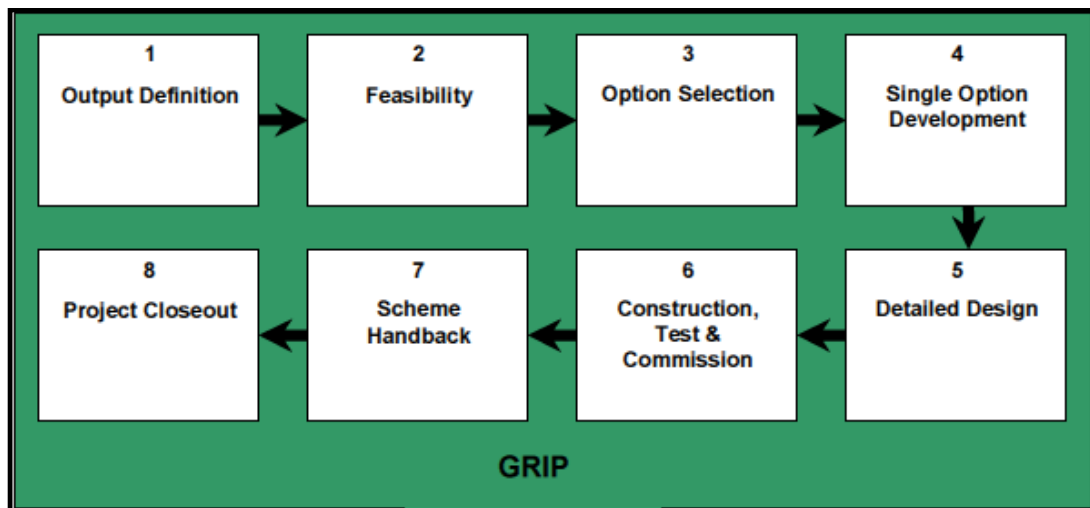


Figure 2.1: GRIP Lifecycle – (taken from the Network Rail GRIP Policy Manual - Network Rail, 2010)

GRIPs 1 and 2 involve strategic development of needs between the Department for Transport (DfT) in consultation with Network Rail Corporate. Once a major project is agreed, an Act of Parliament is generally required to give NR authority to move onto the next phase. In this case the TLP got its authority in 2006. Once this is approved, GRIP 3 (which is also known as “optioneering”) can commence. The primary outputs at GRIP stage gates are shown in Table 2.1.

GRIP Stage	Aim	Main output
1. Output Definition	To define the output for the project. For example, increase line capacity or reduce train delays.	Defining the needs and requirements – the problem or opportunity through stakeholder consultation.
2. Feasibility	Define the scope of investment and identify constraints. Confirm that the outputs can be economically delivered, and are aligned with organisational strategy.	Identifying solutions in response to the requirements.
3. Option Selection	Develops options for addressing constraints. Assesses and selects the most appropriate option that delivers the stakeholders requirements, together with confirmation that the outputs can be economically delivered.	Single option determined and stakeholder approval to option approved through Approval in Principle (AIP).
4. Single Option Development	Initiation of the development of the chosen single option.	Reference/Outline Design.
5. Detailed Design	Produces a complete, robust engineering design that underpins definitive cost/time/resource and risk estimates.	Full design to which the project will be built.
6. Construction, Test and Commission	Delivery to the specification and testing to confirm operation in accordance with design.	Project built, tested and commissioned into use.
7. Scheme Handback	Transfer asset responsibility from the project team to the operator and maintainer.	Project handed over to maintainer or operator.
8. Project Closeout	Closeout in an orderly manner. Contractual accounts are settled, and any contingencies and warranties are put into place. assessment of benefits carried out.	Project formally closed out and project support systems formally closed.

Table 2.1: Network Rail GRIP stage aims and outputs (taken from the Network Rail GRIP Policy Manual - Network Rail, 2010)

2.3 The Thameslink Programme

The Thameslink Programme (TLP) involves a £6 billion upgrade of the Thameslink railway network, which runs from Bedford to Brighton through Central London. The scope of the Thameslink railway network in Central London is shown in Figure 2.2.

Amongst the project's scope, one of the aims is to expand the network by increasing the number of car trains delivered between the "core" areas (from London St Pancras — London Bridge Station) as well as increasing the frequency of the number of trains per hour. This requires the development of major stations within the network over the project period which began in 2008 and is proposed to be completed by December 2018 through 3 main stages (Key Output 0, 1 and 2). Currently the programme is in Key Output 2 where the London Bridge Redevelopment Project is the main focus for

the phase. More information of the London Bridge Redevelopment Project and its use as a case study site for the EngD is provided in section 2.5.



Figure 2.2: Scope of the Thameslink railway network through Central London (image taken from Inner Area Tour presentation - Network Rail Thameslink, 2010)

The TLP project has been broken down into specific work packages: for example individual station upgrades have their own work scopes and GRIP stage deliverables (e.g. Farringdon, Blackfriars and London Bridge Station). For detailed outputs of each project within TLP, a “GRIP Product Matrix” is reviewed and clarified with the TLP individual project team. Amongst this detailed list includes outputs directly related to monitoring. The GRIP Product Matrix also identifies the required outputs of the GRIP stages.

At GRIP stage 4 the product deliverables can include a monitoring strategy and an outline monitoring specification along with the reference design for the single option determined from GRIP 3. An asset management plan (AMP), which may also have reference to monitoring assets, is also prepared at this stage. The AMP relates to NR operational assets which may be affected by works which include replacement, decommissioning or re-commissioning. The monitoring specification at GRIP 4 should include some details of potential impacts in relation to structural or ground

movement. The usual format for such impacts is a ground movement assessment. At GRIP 5 detailed design is produced, at which point structural calculations and potential movement impacts can be calculated more rigorously. It is also the stage when construction methods and sequencing can be used to inform the impact timing and therefore monitoring requirements from the outline developed at GRIP 4.

Generally there is a requirement to commence monitoring during GRIP 5 as most works require baseline period monitoring prior to commencement of works which have the potential for impact. For third parties, such as London Underground, this can be as long as 12 months of baseline monitoring. In some projects baseline monitoring studies can commence as early as GRIP 3 if circumstances dictate.

During GRIP 6 the construction activities actually commence and the monitoring system becomes live. NR and its contractors have an obligation for an Emergency preparedness plan (EPP) to be in place and operational during the works. The EPP is developed during GRIP 5 in consultation with affected parties and stakeholders. In the event that the monitoring systems report movement which exceeds a defined tolerance, the EPP outlines actions to be undertaken depending on the level of severity. This can include stopping train services and any works.

GRIP 7 involves the hand back stage. For monitoring there is usually a period of stabilisation post works, which may also be part of an agreement with third parties. There is also a requirement to archive data for a period of time (usually years) and produce a final report showing actual movement versus predicted movement during the works.

2.3.1 Monitoring strategy and specification

One of the key aims of most NR Infrastructure Programmes is to cause as little disruption as possible to retained assets belonging to Network Rail and its neighbours, including operational activities. Any works which have the potential to impact structural stability or asset performance require such impacts to be calculated and mitigated where possible. At GRIP 4 the purpose of the monitoring strategy is to identify the key areas that are the most sensitive, and to propose a strategy that will enable NR and its contractors to control and minimise such risks. The TLP aims to draw upon and use lessons learnt on previous projects when developing monitoring strategies and specifications. As well as defining the key areas to be monitored, the

strategy should also outline the asset owners and users, their likely requirements and any impacts this has on the programme or schedule of activities.

The initial monitoring strategy and specification are produced in GRIP 4 once the single option has been selected. These are generally produced by designers appointed to that stage. Both of these documents have to be reviewed and accepted by all TLP assurance engineers and to some extent other stakeholders and third parties. The detailed monitoring specification is produced by the designer (who can be a part of the design and build team, but not necessarily) during GRIP 5. This document provides more detail on the predicted movement impacts, the monitoring system, its accuracy and required frequency of measurement. It should also identify a zone of influence and the details of assets affected. Baseline survey requirements should also be identified and early commencement (prior to construction works) if required. The EPP and the AMP also need to be fully agreed during this GRIP stage. This involves liaison with third parties depending on the assets affected. It should also be noted that NR maintenance asset managers are considered a stakeholder distinct from the infrastructure project team itself. Figure 2.3 gives an overview of the standard monitoring outputs generally required through the different GRIP stages.

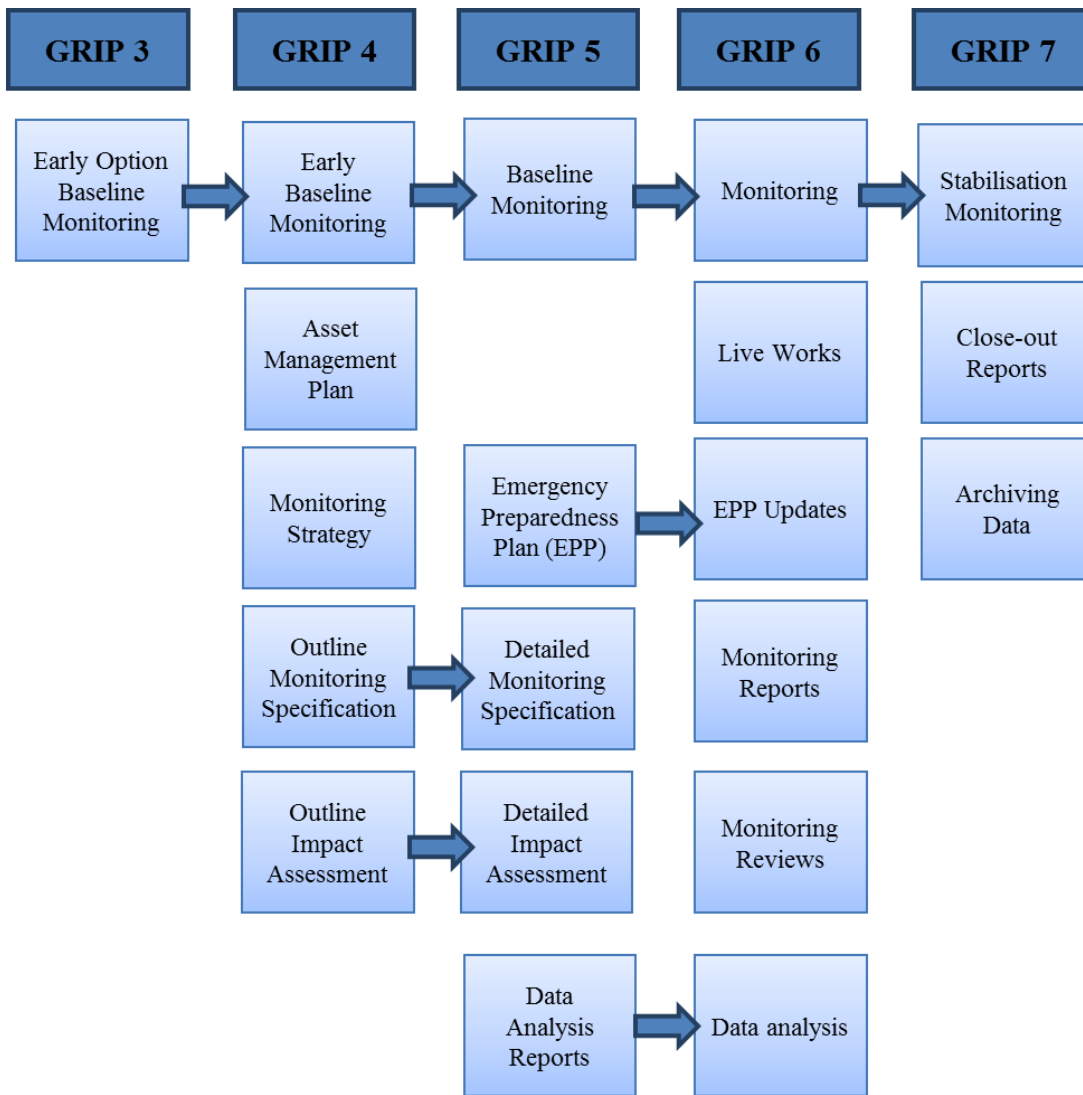


Figure 2.3: Monitoring outputs during the GRIP process

2.3.2 Monitoring implementation

Based on the time spent understanding monitoring processes during the beginning of the EngD, an organogram of the roles required for a monitoring implementation process on a large infrastructure project at NR TLP has been produced and is shown in Figure 2.4.

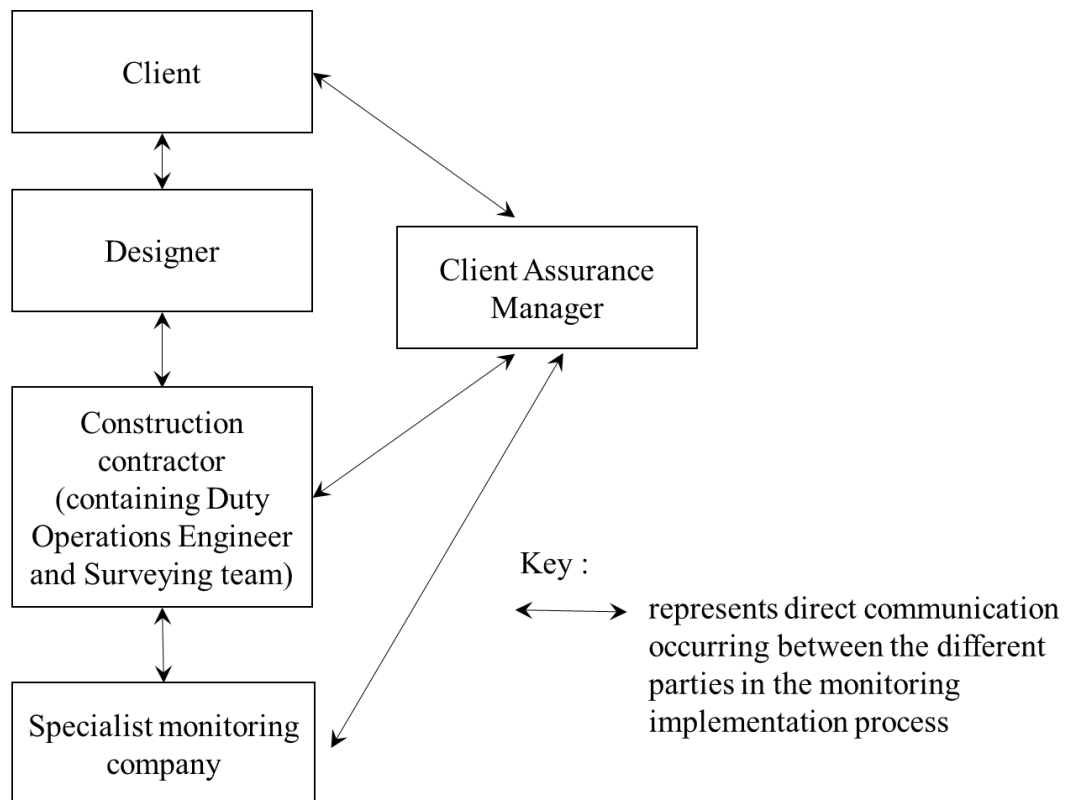


Figure 2.4: Organogram of monitoring implementation process at TLP

In this case the client is Network Rail, who are responsible for the project inception and scope through the GRIP process (discussed in section 2.2). A client assurance manager and additional asset/engineering assurance engineers (if required) is sourced from the client side and their responsibility is to oversee the implementation of monitoring through the supply chain and ensure the quality of the monitoring data is appropriate based on the requirements set by the designer. The construction contractor is responsible for implementation of all the monitoring works. In some cases additional monitoring can be undertaken independently for verification. Where the contractor lacks the technical expertise, in particular for automated monitoring systems, a significant amount of this work tends to be subcontracted out to specialist monitoring companies.

For the London Bridge Redevelopment Project, a lack of communication has led to a “disconnection” between the rail maintainer, designer, contractors and monitoring specialist company. This appears to have resulted in a slow development of the

monitoring specification and novel applications applied to the programme¹. There was also little evidence of alternative systems and their performance, including “post-monitoring” analysis being tested or discussed. All track and structural monitoring was dependent on direct contact methods of measurement (i.e. prisms) which appears to be prevalent throughout the UK rail industry. The logistics of accessing railways are such that installation and maintenance of these systems can be very time-consuming and costly. Coupled with the restrictions imposed by working in parallel to live operations, the overall implementation can be a very significant effort. Furthermore the volume of measurements and various end users and stakeholders presents additional technical and logistical challenges. As stated earlier a major station on NR infrastructure could cost up to £1 million per year to monitor for structural movement. The lack of qualitative or quantitative analysis makes it hard to determine whether the solutions used currently represent the optimum solution or meet the requirements intended. One of the reasons for this is the lack of a close-out report, which is a requirement of the monitoring specification, which would allow lessons of best practice to be learnt and applied to future monitoring projects.

Based on these findings during the research of the monitoring implementation processes at TLP, it was important to understand if these issues were prevalent throughout the railway monitoring industry. Therefore interviews were carried out with key members of the monitoring industry. The process and outcomes of these interviews is described in the next section.

2.4 Monitoring industry context

In order to gain a perspective of the monitoring issues observed at TLP, it was important to gain context from the monitoring industry to see if the issues arose on similar projects. Interviews were carried out on key monitoring specialists across the industry based on the organogram shown in Figure 2.4. This was to investigate whether these monitoring issues were project specific (e.g. Crossrail, Bond Street Station Upgrade, The Shard etc), relevant to someone within that particular role or whether it was a theme throughout the monitoring supply chain. Details of the interview process

¹ Based on my attendance at decision making meetings regarding the implementation of a monitoring scheme

and notes taken during the interviews can be found in Appendix B. Due to the varying roles of the interviewees within the monitoring supply chain, each person was fairly subjective and naturally had their own opinion on where the chain breaks down. However there were some common themes that arose from the interviews where improvements need to be made to the system as a whole but also throughout the monitoring supply chain. A list of these common issue areas are shown in Table 2.2 which is followed by a summary of each of the findings.

Common monitoring issue
Lack of/limited monitoring standards/guidelines
Access to railway infrastructure
Data handling
Cost
Lack of insight into monitoring data quality
Lack of non-contact monitoring method

Table 2.2: Summary of findings of monitoring issues from interviews

2.4.1 Lack of/limited monitoring standards/guidelines

Within the railway monitoring industry there appears to be a lack of standards to refer to when implementing a monitoring scheme on infrastructure typical to the railway environment. For example, if a tunnel or retaining wall is required to be monitored, there is no standard for setting up a scheme for that structure. There is a consensus in that a standard is required, however it can be seen that there could be difficulty in developing this type of standard because there are variations in the monitoring requirements from project to project. CIRIA (Construction Industry Research and Information Association), along with leading experts in their field, have produced best practice guides to provide guidance to asset owners, engineers and contractors for the maintenance and monitoring of various types of infrastructure, e.g. masonry arch bridges (McKibbins et al., 2006), concrete structures (Buenfield et al., 2008) and so on. The British Tunnelling Society (BTS) have also produced a best practice guide entitled *Monitoring Underground Construction: a best guide practice* (BTS, 2011). This document provides a guide for monitoring underground construction work but is not a standard or specification.

From the surveyors' and monitoring specialists' point of view, a lack of monitoring standards has often led to a poor specification. It is often the case that there is over

specification from the designer based on the uncertainty of the movement expected. Therefore it is important for future projects that a standard is met based on lessons learnt from previous projects to ensure there isn't any "overkill" in monitoring, which can lead to high costs. Brownjohn (2007) discusses a similar finding when reviewing monitoring of civil infrastructure. The author discusses the tendency to over-instrument where there is no incentive for a careful selection of sensors, mainly due to the background of the designer/engineer producing the specifications. During the extension of the Jubilee Line one of the interviewees expressed how precise levelling (see Chapter 3) was successfully used throughout the project and there was very limited manual prism monitoring, which was due to a "tight" monitoring specification. However, since the successful development of automatic prism based monitoring from manufacturers, it tends to be the default instrumentation specified by the engineer and is used on most large scale projects. A suggestion to resolve this is to provide a specification for that project in collaboration with all parties/members of the organogram (see Figure 2.4), especially the designer, engineer and surveyor. This could allow appropriate instrumentation to be selected.

A process map has been developed by the TLP Central Engineering Team to describe the processes required to carry out surveys that are compliant with NR's TLP requirements. As well as providing a workflow, the diagram highlights the roles and responsibilities of the client and contractor/supplier, including assurance requirements. An extract of this is shown in Figure 2.5. One of the outputs from a monitoring standard (which is project specific) could be to provide a similar type of process map to ensure all parties understand their roles within that particular monitoring implementation scheme.

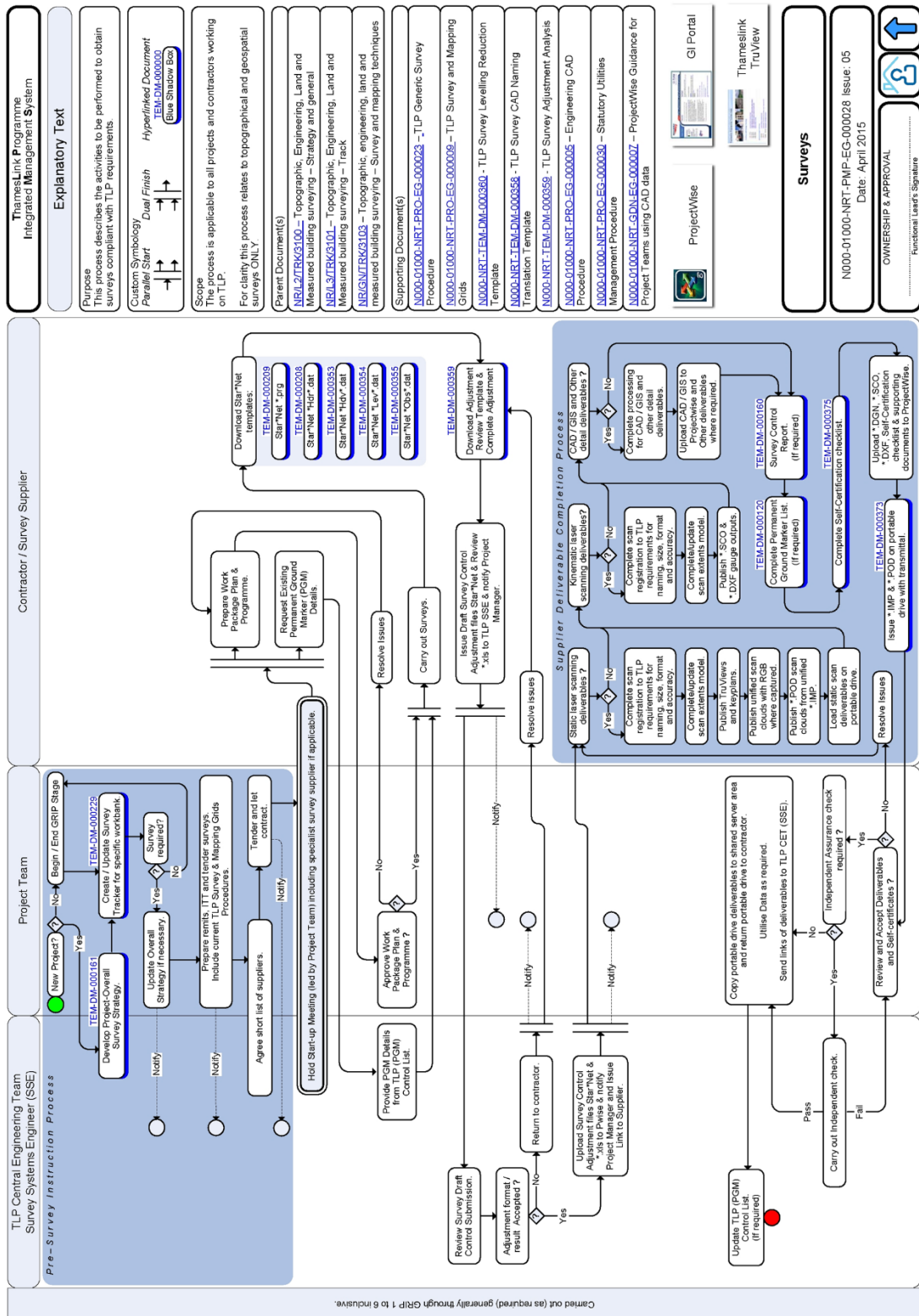


Figure 2.5: Network Rail Thameslink Programme Survey Process Map

At Network Rail there are standards in place for monitoring railway track adjacent to civil engineering works in order to monitor the geometry of the track and assess the

quality of it. The document contains trigger thresholds for changes in cant, twist and gauge of the track as well as any actions required if the thresholds are exceeded. The document considers the need for baseline monitoring, which is project dependent. It does advise the use of optical measurements.

With respect to structural monitoring at NR there is very little provision of a standard procedure to follow. Whilst some guidance is shown in NR survey standards documentation, it is generally stated that a specific remit is prepared. This is due to the unique monitoring situation each project has which requires its own specification and is very element specific. From NR's point of view it is key to assess the integrity of the surrounding structures with respect to the works. This assessment will be dependent upon the speed of the line that is undergoing work/being monitored. Movement would have a higher impact on the high speed lines compared to the slower commuter lines.

2.4.2 Access to railway infrastructure for monitoring

When interviewing specialists across the monitoring industry it could be seen that there were many similarities in the procedures set by clients in order to access railway infrastructure, for example Transport for London's London Underground. The process of gaining access to the railway infrastructure requires a lot of paper work, procedures to be followed and logistics to overcome. It's a time consuming and costly exercise, but must be taken into consideration when planning the time-scale for installation of a monitoring system, in particular the installation of prisms. The following focuses on the typical procedures required at NR. The same paperwork and procedures were required in order to gain access for the site work testing described in Chapter 5 and Chapter 6. Details of the access restrictions and limitations that needed to be overcome are described at the beginning of the respective chapters.

For any instrumentation to be installed for monitoring which may affect the operational railway environment, special permission for access to the area is required. Access which is required on or near the line involves significant advance planning and generally line closures to allow safe access. Closures of lines are termed "possessions" or "line blockages". The work carried out in Chapter 5 involved "piggybacking" onto a possession in order to gain access to the track safely.

For safety reasons worksites within possessions need to be booked 12 weeks in advance with a lock down of five weeks in advance to provide certainty of safety co-

ordination of activities. Work adjacent to equipment which can affect the operation of trains (such as signal boxes) can also require line closures. Due to the franchise system of train operation, failure to book in sufficient time can lead to costly compensation payments. Equally failure to “hand back” the space on time incurs immediate penalties per train minute of delay.

Along with significant notification and planning periods, a significant amount of paperwork and safety dedicated staff are required to support work activities. For any infrastructure works on the operational railway, a Works Package Planning (WPP) system is required which forms part of the compliance with Construction Design and Management Regulations (CDM). This document contains details of the work to be carried out, site details and briefing arrangements; the permits required, the risks of carrying the work out and what emergency arrangements are in place also need to be specified. For this study a WPP was produced for the site work carried out for the track monitoring testing in Chapter 5. This document can require many edits and changes to be approved which can be time consuming, potentially delaying the installation of a monitoring system which could be critical. There have been cases where access has not been approved in time, which has delayed the works more and has incurred unnecessary costs. The WPP must also cover the aspect of maintenance of the system if the site needs to be revisited to check or replace any of the targets or instruments.

2.4.2.1 Installation and maintenance of prism-based monitoring

Currently prism-based monitoring, using a total station and prism (see Chapter 3) is the default technique for any type of structural or track monitoring. The installation and maintenance of the system must be covered in the WPP. This type of monitoring setup is extremely high maintenance and expensive. Firstly on track, prisms can get covered in dirt quickly and require to be cleaned every 4-6 weeks. This requires logistics and access to be planned during engineering hours. Maintenance staff or workers can sometimes knock them out of position when walking over the track, causing them to face a different direction. This leads to a misreading or false trigger alarms being set off in the reporting system. If any alarm goes off, it is a requirement for the monitoring specialist or engineer to carry out a visual inspection to investigate the reality of the situation, which can be time consuming if special access is required.

For automated monitoring using Automatic Target Recognition ATR (see Chapter 3), prisms are typically installed as arrays across structures or track. An example of a track monitoring array is shown in Figure 2.6.

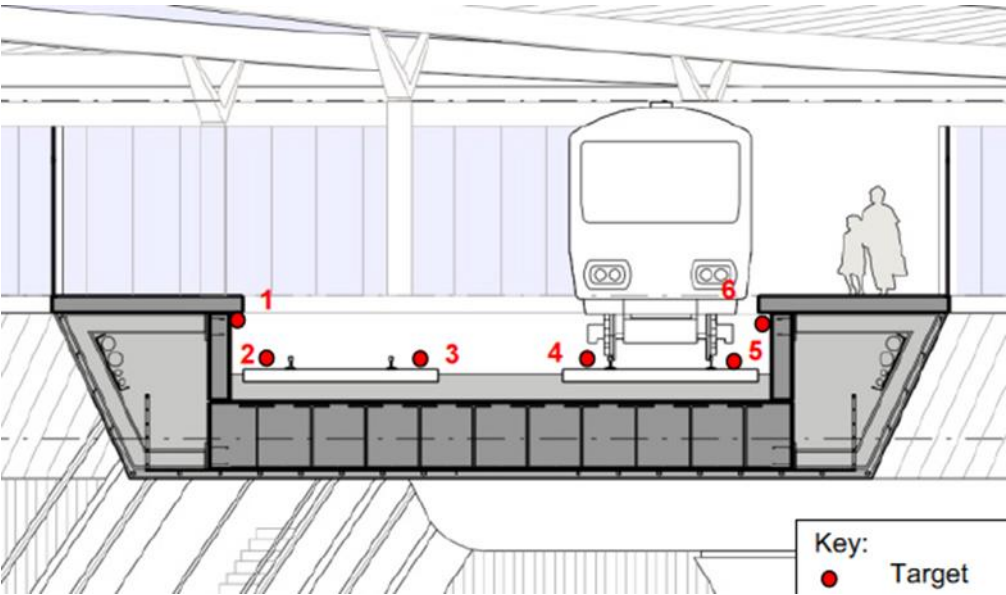


Figure 2.6: Typical prism layout for track monitoring at Network Rail (image taken from the London Bridge Station Development Monitoring Specification)

This in itself is expensive; if a single track needs to be monitored every 3 metres within 30m of the construction zone, this can lead up easily to hundreds of prisms. Each prism can cost from £60-£80 each depending on the manufacturer and quantities ordered. Using the example in Figure 2.6 a single array would cost £360-£480 alone. Based on the NR standards of monitoring, prism arrays are required every 3,6 or 9 metres depending on the movement expected. It is common for the arrays to be installed up to 100 metres or so outside the predicted zone of impact.

Each prism itself has to be installed precisely so that there is a direct line of sight to the instrument reading it. This can also be a time consuming and costly exercise, as well as adding to the safety risk of having someone on track during this process.

As well as maintaining the prisms, the total stations are required to be maintained by regular calibration. The highest performing instruments are currently designed to work continuously for approximately 8,000 hours, i.e. approximately 333 days, when a system calibration is required (Groom, 2009). As is normal with technology, a system may fail unexpectedly and need replacing immediately. Removing, temporarily replacing, fixing and re-installing an instrument can incur a large cost.

2.4.3 Data handling

Data that are collected from the monitoring instrumentation must be reported to the engineer to allow a remote inspection of the structure. It is typical for this to be delivered to the engineer via an online web interface (see Chapter 3) where alerts are delivered through email or SMS. The overall responsibility of delivering the monitoring data is the construction contractor. However the reporting system is usually developed and maintained by the monitoring contractor due to their expertise in this area. Across the industry it can be seen that there are many common issues with the data handling in terms of the volume, method of processing and communicating this back to the engineers.

One of the major issues for the automatic prism based monitoring system is the communication of data from the instrument to the internet database, which is typically through dial-up connection or GPRS. In areas of limited signal/connection, such as underground infrastructure, there is often a “traffic jam” of data being fed in which requires the system to be reset by physically going to the data-logging box. This box (which is in proximity to the total station) is a costly piece of equipment that may not be always directly accessible during working hours. This prolongs the time taken to re-instate the reporting system, which results in failure of the monitoring system, which is unacceptable to the stakeholders considering the reason for implementing monitoring.

The online reporting system provides a simple interface of the monitoring data in its raw format in table or graph form. As well as providing limited if any information on the quality of the monitoring data being reported, it can be a time consuming process for the engineer to examine each bit of data on a large scale project. It is sometimes the case that the raw data is presented directly to the engineer, which naturally runs the risk of containing errors (see Chapter 3), such as a misreading from the total station to the prism due to a passing train. Without this knowledge this could cause the engineer to deem this as some movement which would require further investigation. An alternative approach could report the data to the engineer in a much smarter way, e.g. applying data filtering to the raw data before presenting the results to the engineer.

2.4.4 Cost

The cost of structural monitoring implementation of any project can be significant. As can be seen above, the costs incurred are contributed from all aspects of the whole

strategy currently being used for monitoring: gaining access, installation, the instrumentation and technology itself and the maintenance of such equipment and reporting. The total estimated cost for monitoring during the entire London Bridge Redevelopment Project is £5million over 5 years. Monitoring along the Crossrail project, which is a much larger scale tunnelling project, is costing £100million. While these costs appear very high, the assurance it provides for asset protection and ultimately safe operations (e.g. passenger trains) whilst construction work takes place in the vicinity represent huge risks. By having an “improved” specification, which determines the sensors and systems that are required, this could allow a more efficient, reliable and flexible system, providing a better return on the investment.

2.4.5 Lack of insight into monitoring data quality

Deformation monitoring is a major aspect of engineering surveying where there are established workflows for processing observations, e.g. from total stations, and analysing these observations to determine if the monitoring network design is being achieved in reality. From a survey assurance point of view, there is little or no evidence of this type of observation analysis. Based on the experience from viewing monitoring reports, there is no evidence of reporting simple data quality measures of the observations, e.g. a standard deviation, which provides the level of uncertainty in the observations. This then needs to be compared back to the requirements of the original specification.

Engineers often demand a 1mm level of accuracy for structural monitoring. The basis for this value is unknown but is thought to be associated with the instrument accuracy levels stated by the manufacturer. However, these instrumentation specifications are only valid under test rather than site conditions, where the physical attachment of the target and interconnection between measurements made and the site co-ordinate system must be taken into account. The measurement network design is a vital part of understanding how the measurement capability matches the engineering requirement (see Chapter 3). In parallel, some monitoring specialists tend to have limited knowledge in engineering surveying and data quality checking, where their skills tend to lie in data management and communication. Based on the experience from attending monitoring implementation meetings at TLP, it can be seen that there is very little evidence of data quality checking. This is critical to the monitoring scheme as it's possible that observation errors could be misconstrued as movement.

2.4.6 Lack of non-contact monitoring method

One of the key and significant problems with prism based monitoring in the railway environment is the prisms themselves: they are attached to the structure being monitored - the actual surface of the structure isn't being monitored. As described earlier, if the target is knocked or moved, this doesn't represent the movement of the structure, it is purely alerting the user of the movement of the prism. It is an invasive and expensive monitoring technique that requires a substantial amount of maintenance. Based on the interviews it can be seen that there is a potential for applying non-contact surface monitoring in a railway environment, i.e. through terrestrial laser scanning and photogrammetry. However, there needs to be proof of concept for this to be considered as a method of monitoring if it is to be considered. All parties usually rely on the vendor to apply these technologies to demonstrate these potentials. The main hurdle is the transitioning from a traditional system to adopting a more novel approach. Therefore the consensus was that there needs to be a proof of concept in parallel with the current technologies on a site and answer questions such as:

- Is it accurate?
- Which assets could be used for this type of monitoring?
- What are its capabilities in terms of output?
- Can it replace manual and/or automatic monitoring?

In order to answer these kinds of questions, an ideal situation would be to have the proposed technique running in parallel with the current monitoring regime so that a comparison can be made. However in reality, based on the interview with the project designer it would require funding two monitoring methods which the client or the construction contractor aren't likely to fund.

2.5 Study Focus

Section 2.4 provided a very brief overview of some of common issues present across the monitoring industry, which are not only in existence at NR TLP. Addressing and resolving all of these issues is beyond the scope of this study. For example, an internal audit at NR would allow an in-depth assessment of each of the role's requirements within the monitoring supply chain. This could then be used to establish how a more collaborative approach can be achieved to produce an efficient and cost effective monitoring scheme along with a best practice guide. However, by looking at this

study’s requirement for investigating a non-contact monitoring technique, some of the issues from Table 2.2 can be addressed in this study. These are shown in Table 2.3 followed by a summary below.

Common monitoring issue	Can a study on non-contact surface monitoring improve this issue?
Lack of monitoring standards	No
Access to railway infrastructure	Yes
Data handling	No
Cost	Potentially* - see below
Lack of insight into monitoring data quality	Potentially* - see summary below
Lack of non-contact monitoring method	Yes

Table 2.3: Monitoring issues that this study allows to be addressed

As described in section 2.4.2, one of the main logistical issues associated with railway monitoring is gaining access to install prisms within the vicinity to track, so that continuous measurements can be made to protect the asset. This thesis will focus on removing that need for prisms or other targets attached on or near the track by investigating the potential of a non-contact and target-less approach. Ultimately, if this can be achieved, this would remove the need for installing and maintaining prisms, which would result in a reduction for gaining access to railway infrastructure. In turn this would hugely benefit the safety aspects associated by removing the need to put people on track to place and maintain the prism.

The cost of a non-contact surface monitoring solution may not reduce the total cost of a monitoring project with respect to instrumentation, but it could reduce the cost of accessing the track. The cost of a possession to access the track to install the prisms costs more than the prisms itself. Also, the removal for the need of prisms through having a non-contact and target-less solution will eliminate the costs associated with installing and maintaining prisms throughout a project. A full cost benefit analysis would be required to determine the return on investment in terms of reliability and flexibility of a monitoring system.

Even though this study does not directly address the issue of the lack of insight into the data quality aspect of a monitoring scheme, this thesis reiterates the importance of them for deformation monitoring. A comprehensive review of these well-established network analysis techniques is provided in Chapter 3. These techniques are then

applied in the laboratory and site test chapters - Chapters 4, 5 and 6 - when using total station observations.

This study directly addresses the common issue highlighted in the interviews relating to the lack of a non-contact and target-less monitoring method along railway infrastructure. Even though there is known to be a potential using state-of-the-art technology to measure and monitor surfaces, the methodology of applying it is not well-established. This study focuses on the potential of terrestrial laser scanning and photogrammetry. The site test work, which was a requirement of the EngD study, allows this thesis to focus on this issue. The next section describes the site test that was chosen for this thesis: London Bridge Station Redevelopment Project.

2.6 London Bridge Station Redevelopment Project: site test requirement for the study

When the EngD study was commissioned in 2010, the advanced works for Key Output 2 (see section 2.3) at London Bridge station was due to start in 2012, with the main redevelopment works planned to take place between 2013 and 2018.

London Bridge station was constructed on a series of masonry arches, built between 1836 and the end of the 19th century. The station's most recent remodelling, before the works began, comprised of six through tracks and nine terminating tracks, which can be seen in Figure 2.7.

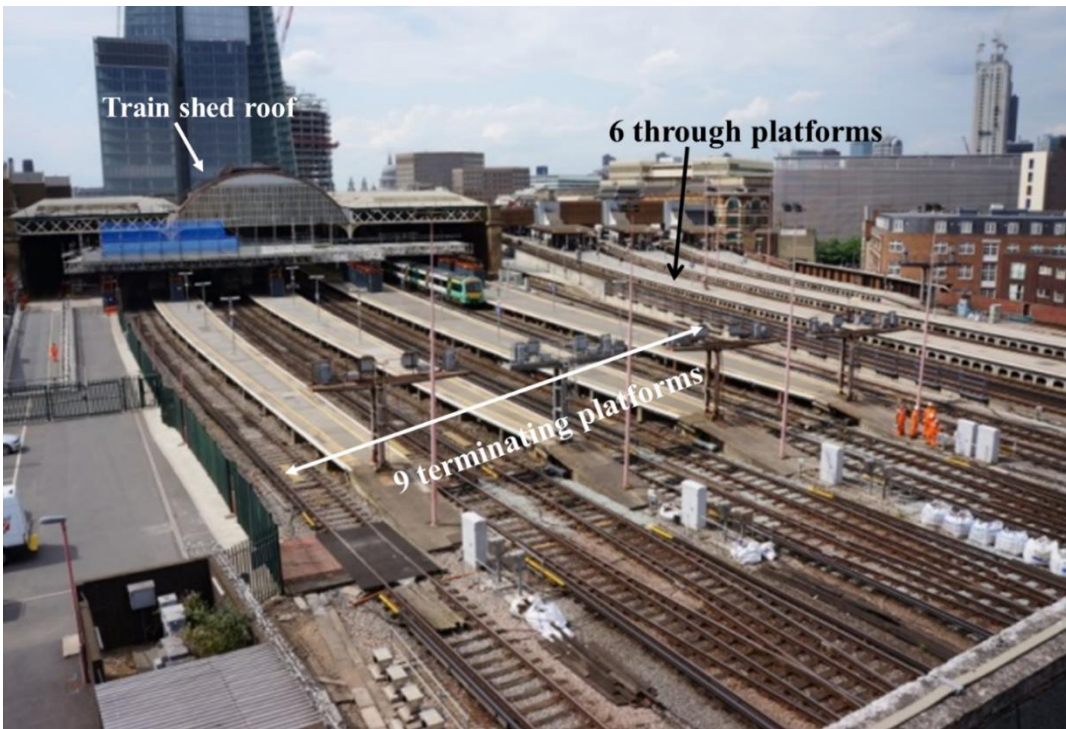


Figure 2.7: Annotated image of London Bridge Station before redevelopment started

The new development will comprise of 9 through and 6 terminating tracks as well as the train shed roof being removed. The station is required to remain operational during all stages of the refurbishment.

Because of the planned construction work, London Bridge Station provided an example of a large scale monitoring project where many typical railway infrastructures were required to be monitored continuously throughout the project, particularly the railway track and masonry brick arches. Therefore one of the EngD requirements was to use London Bridge station as a live site for testing the newer technologies for monitoring, with a focus on monitoring railway track and masonry brick arches. Detailed information of the engineer's monitoring requirements required of the railway track and masonry arches is provided here.

2.6.1 London Bridge Station track monitoring requirements

In order to determine the areas that are most sensitive to the demolition works, a ground movement assessment (GMA) was carried out to assess the heave adjacent to the demolition zone. Based on the works taking place below the track and at track level during various construction phases, Tracks 12 and 13 were required to be monitored during the EngD data capture phase. The outcome from this provides an advanced warning system of any potential dimensional changes in the track system which require closer inspection, whilst ensuring passengers have a safe and smooth journey from A

to B. Figure 2.8 provides a set of screenshots representing the construction work taking place in the vicinity of the track during the period of this study, including the removal of the train shed roof.

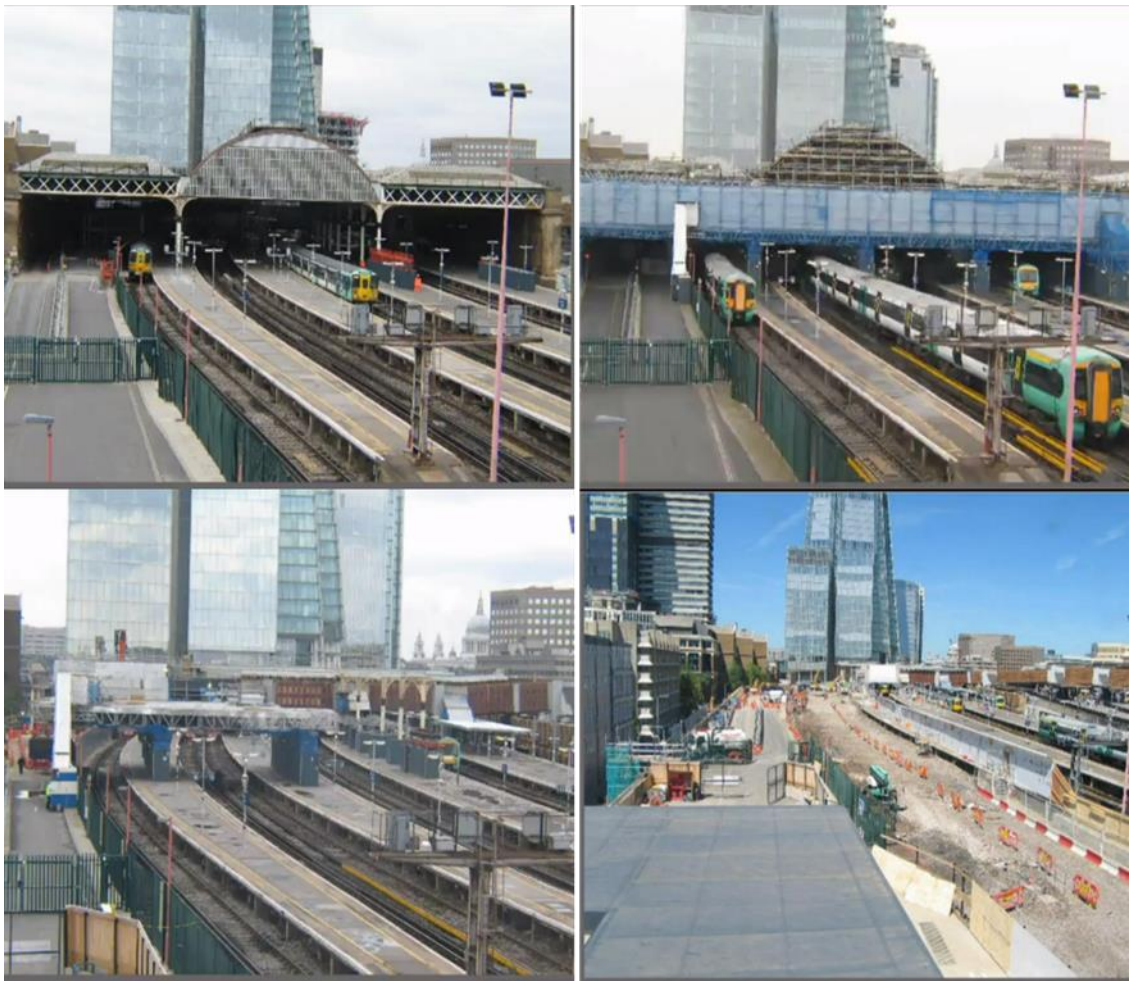


Figure 2.8: London Bridge Station undergoing major redevelopment (time-lapse images taken from the London Bridge Site-Eye camera)

According to the London Bridge Monitoring Specification, the following track geometry parameters are required to be monitored:

- Changes in track cant
- Changes in track twist
- Gauge

This thesis focuses on measuring the track cant, twist and gauge based on surface measurement of the track. Real-time monitoring is required for all the tracks within the demolition sphere of influence zone. Manual track monitoring is required when undertaking other constructions works that are likely to affect the track.

2.6.1.1 Track cant

According to the UK Railway Group standards, track cant is “the amount by which one running rail is raised above the other running rail” (Railway Group Standard, 1998). It can be measured at the centre of the rail head and expressed as a difference in height. The correct track cant allows trains to steer around curves whilst minimising friction and wear to the track, ensuring passengers don’t have a disruptive ride. The measurement of track cant is shown in Figure 2.9.

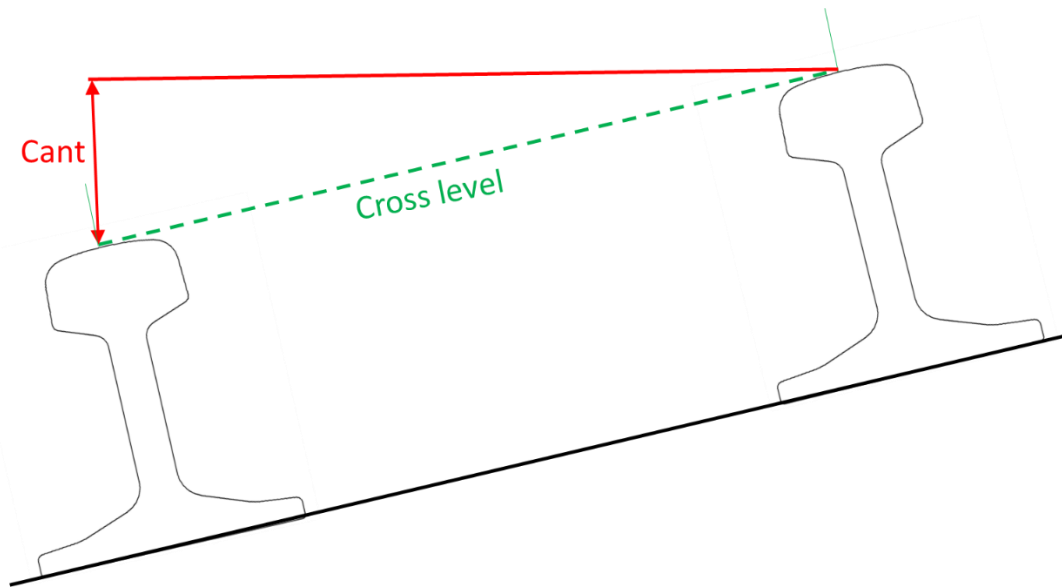


Figure 2.9: Measuring track cant - image created based on UK Railway Group standards definition, Railway Group Standard (1998)

Cant is positive when the outer rail on a curve is raised above the inner rail. Negative cant is when the inner rail is raised above the outer rail.

The engineering requirement of the prism location is shown in Figure 2.6. Currently SolData, who are the monitoring specialist contractor on this project, use the following approximations shown in Figure 2.10 to calculate track cant and twist based on these prism locations.

Essentially the cant is approximated by assuming the prism (which is attached to the sleeper) moves in sync with the track. Therefore any changes in height in the track will theoretically propagate through to the sleeper, which is bolted to the track. Other examples of track monitoring attach the prism to the web or foot of the track. In this case the change in height/vertical distance (in the Z direction) compared to the baseline measurement (in this case based on the track design cant) is calculated for each prism on both rails. This needs to be multiplied by an appropriate ratio to determine the actual

cant of the tracks. A multiplication ratio (1.432m/distance between the prisms in plan) is adopted here, where 1.432m is the UK standard gauge value. Cant is usually expressed in millimetres.

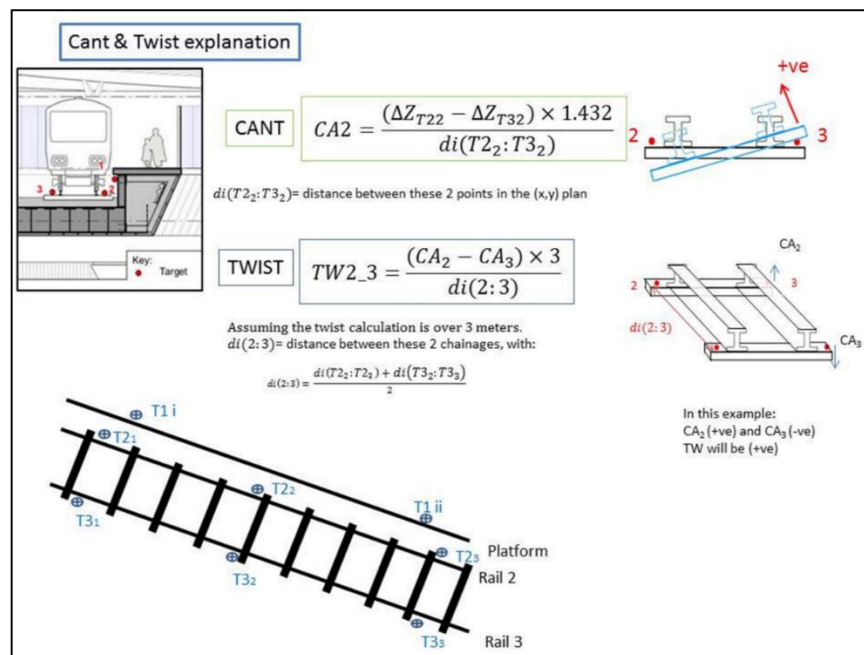


Figure 2.10: Monitoring contractor approximation of track geometry parameters using prisms (image taken from Sol Data’s Geoscope Explorer (version 6.5) within the “Cant and Twist explanation” tab)

2.6.1.2 Track twist

Track twist is the “variation in cross level over a given distance along the track” (Railway Group Standard, 1998). In other words this is the difference in track cant over a given distance. It can be expressed as a ratio or in millimetres. Based on the NR track monitoring requirements, these distances, also known as a chainage, are at 3, 6, 9 or 12 metre intervals depending on the level of movement expected in the vicinity of that particular bit of track during construction work. During the data acquisition phase of the site work there was a mixture of interval measurements required depending on the phase of the project and works taking place below or next to the track. Based on Figure 2.10 the track twist is estimated from the prisms by applying an appropriate ratio based on the interval required and the distance between prisms on the same track.

The monitoring specification for the London Bridge Redevelopment Project requires a baseline period of 1 week, from which the mean values of these are used as the zero baseline starting values for the track parameter calculations. The document also

specifies that the monitoring contractor is responsible for implementing a “robust backup manual monitoring plan” in case of disruptions in lines of sight due to passing trains. The document specifies that the accuracy of the monitoring “shall be at least $\pm 1\text{mm}$ ”. The reasoning behind this is not specified despite an expected change in cant of approximately 2mm.

2.6.1.3 Gauge

Based on the European standards of characterisation track geometry, the gauge of the track, G , is “the smallest distance between lines perpendicular to the running surface intersecting each rail head profile at point P ” (refer to Figure 2.11).

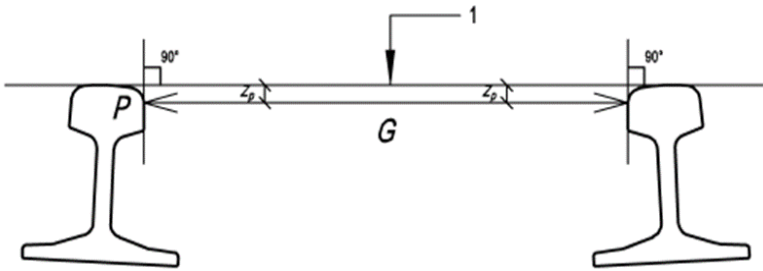


Figure 2.11: Measuring track gauge (image taken from CEN, 2008)

The change of gauge is another indicator that track movement has taken place, given a certain tolerance. Because monitoring prisms are fixed to the sleepers, the actual gauge of the track cannot be determined using this particular method. Therefore most NR monitoring specifications require periodic manual surveys to be carried out by the NR track maintenance engineers to confirm the gauge is at acceptable levels. Based on the surface measurement approaches explored in this study, it is thought that the gauge can be extracted from the point cloud of the track.

Chapter 5 presents a case study of applying non-contact optical techniques in order to measure the track cant, twist and gauge at London Bridge Station in a location where track monitoring was required.

2.6.2 London Bridge Station arch monitoring requirements

The arches are required to be monitored during the demolition and construction stages of the project. Figure 2.12 shows the arches at street level directly below the track (top image) as well as typical examples of the interiors of the arches (bottom left and right images).



Figure 2.12: Examples of London Bridge Station arches (top image taken from NR TLP published TruView)

During the advanced works, monitoring in the arches was required to ensure the structures beneath the tracks were not significantly affected by the increased load from the construction of the protection deck, which was installed during the advanced works to aid with the removal of the train shed roof. The arches were also required to be monitored during the main station development and therefore the monitoring requirements vary depending on the stage of the works.

The arches require the crown and springing points to be monitored so that the horizontal strain and angular distortion can be calculated along the transversal and longitudinal axes of the arch. Relative movement of the arches was also required to be calculated in order to record any rotation of the arches relative to each other. This thesis focused on the capability of measuring relative movements using non-contact techniques. Figure 2.13 represents the general target arrangement for the arches in order to carry out suitable monitoring.

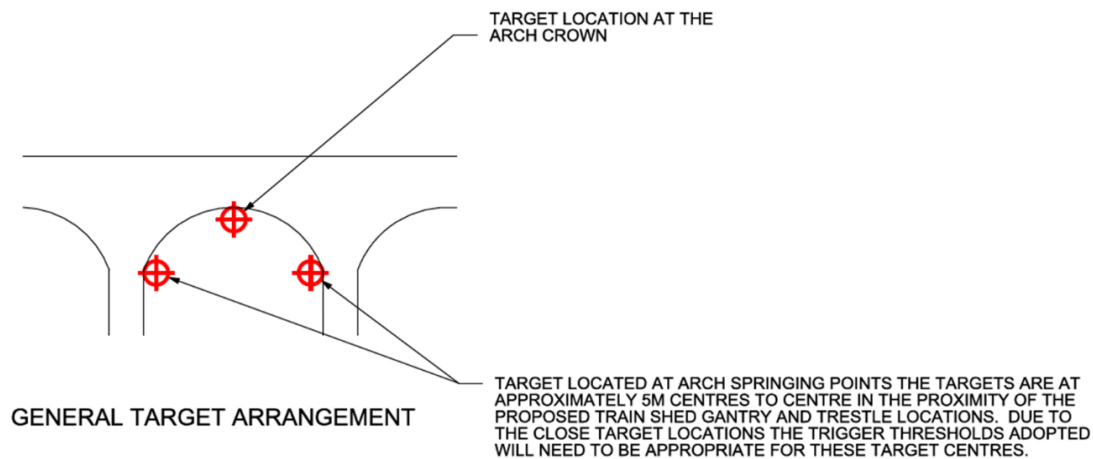


Figure 2.13: London Bridge arches monitoring target arrangement

Even though the arches required to be monitored during different phases of the construction, the general frequency required was weekly using manual monitoring. This is usually carried out by a surveyor within the survey team from the construction contractor. On average 4 weeks of arches monitoring post-construction is required.. The data are required to be imported into the monitoring system within 24 hours of completion of the survey. An accuracy of at least $\pm 3\text{mm}$ was required.

Chapter 6 presents a case study of using TLS and CRP for measuring relative movement of a set of arches at London Bridge station that required to be monitored whilst construction work was taking place.

2.7 Chapter Summary

This chapter provides the context of this industrial based EngD study, which is sponsored by Network Rail Thameslink Programme (TLP). It can be seen that there are significant costs associated with monitoring infrastructure on a project like the TLP, based on the significant risks to be managed for asset and operational protection. In relation to cost it is unclear if the investment delivers best value, particularly in terms of the purchase, installation and maintenance of prism target based systems. It is also clear that there is a lot of uncertainty in the quality of this type of data.

Based on interviews with key figures in the monitoring industry, it can be seen that some of these issues are prevalent across the rail monitoring industry. There appears to be a disconnection between the rail maintainer, designer, contractors and monitoring specialist companies. This has resulted in a slow development of both monitoring specifications and innovative solutions being applied within the monitoring industry.

One of the reasons for this is because of a lack of collaboration between the members of the monitoring supply chain. This aspect goes beyond the scope of this study. However, it is thought that by fully understanding the requirements from the engineer and allowing a more collaborative decision making process on the performance specification requirements, appropriate and innovative instrumentation can result in a more cost effective and efficient monitoring scheme being implemented.

This study focuses on removing the need for prism-based monitoring by investigating the potential of applying TLS and CRP as a tool for surface based measurements for monitoring. This would allow the impact of safety, logistical and reliability issues associated with prism monitoring to be improved whilst benefitting from the application of innovative technologies.

One of the requirements for this study is to carry out testing on a live monitoring project. Due to the fact construction works were taking place throughout the duration of the EngD study and it had multiple monitoring scenarios, the London Bridge Station Redevelopment Project was chosen.

In order to gain an understanding of the capabilities of TLS and CRP with respect to the current prism based monitoring methods, laboratory testing has been carried out. This is presented in Chapter 4 followed by site testing at London Bridge tracks in Chapter 5 and the arches in Chapter 6. The next chapter provides an overview of the current state of the art of engineering surveying techniques used in deformation monitoring.

Chapter 3 - A review of engineering surveying techniques used in deformation monitoring

Chapter 2 set the context for this study with regards to the monitoring requirement of typical railway infrastructure, for example track, arches and tunnels, at Network Rail. This chapter considers the technologies and research of the use of techniques applied to the railway industry as well as generally in the field of deformation monitoring.

There are many different types of instrumentation available for deformation monitoring such as levelling, total stations, laser scanning and photogrammetry which are categorised as geodetic terrestrial-based methods. This study particularly excludes geodetic aerial-based methods such as GPS (Global Positioning System)/GNSS (Global Navigation Satellite System) and aerial LiDAR systems (Light Detection and Ranging) based on the monitoring accuracy requirements at NR as well as the practical limitations of the technique when working in a tunnelled and underground environment.

This chapter describes some background information of deformation monitoring techniques typically used (section 3.1) and how these measurement systems are deployed in surveying and monitoring, particularly in the railway industry (section 3.2). Traditional methods use network design (section 3.3.1) as a method to compare the expected performance of the instrument to the observations carried out in reality. Once the measurements have been made, a rigorous analysis procedure (section 3.3) of the observations is required to determine whether deformation has taken place or not. This information is then required to be communicated to the engineer in a suitable and timely manner. These methods of communication is described in section 3.4.

3.1 Engineering deformation monitoring

An important function of engineering surveying is the monitoring of man-made structures, e.g. dams, bridges, viaducts and high-rise buildings, as well as naturally occurring movements, e.g. tectonic, seismic and glacial movements and landslides for deformation. The purpose of monitoring these man-made structures and natural movements is to assess the safety and performance of a structure brought about by loading and ground settlement, verify the expected movements from geological studies and most importantly to protect the safety of humans from the potential hazards caused

by movement of the structures (Casparly and Rüeiger, 2000). Network Rail's key objective is to get passengers from A to B safely and therefore monitoring railway track and any infrastructure posing risks to the journey is critical, particularly when any construction work is taking place in the vicinity of its railway infrastructure. Deformation monitoring is usually applied over a period of time at certain time intervals, also known as an epoch.

Depending on the structure and movements expected, different types of measurement techniques are applied for deformation monitoring. These are traditionally divided into two groups: geotechnical and geodetic monitoring (Richardus, 1977; Setan, 1995; Casparly and Rüeiger, 2000)

Geotechnical deformation monitoring directly measures the change in height (settlement gauge), length (extensometer), water pressure (piezometer), tilt (inclinometer) and velocity (accelerometer) of a structure or natural feature. These instruments usually provide relative movement of the structure in one dimension (Setan, 1995) and require direct contact to the structure/asset being monitored. More information of geotechnical instrumentation for monitoring can be found in "*Geotechnical instrumentation for monitoring field performance*" by John Dunnycliff (Dunnycliff, 1993).

Geodetic deformation monitoring techniques can produce one, two or three dimensional measurements based on two types of network: absolute and relative. Absolute monitoring networks consists of points or stations outside of deformable areas or zones of impact which are expected to remain stable throughout the monitoring process. These stations can then be used when defining the datum and provide absolute displacements of the points within the zones of impact/deformable areas. Relative monitoring networks are implemented when no stable points can be identified and all of the points in the area of interest are likely to undergo deformation (Cooper, 1987; Casparly and Rüeiger, 2000; Setan and Singh, 2001).

Geodetic measurements can be divided into aerial and terrestrial based methods. Aerial based techniques include SLR (Satellite Laser Ranging), SAR (Sythetic Aperture Radar) and also GNSS (Global Navigation Satellite System), whereas terrestrial based methods include digital levelling, robotic total stations (TS), TLS (terrestrial laser scanning), laser trackers and photogrammetry. This thesis focuses on terrestrial based

geodetic methods for measuring deformation and a brief overview of each technique is provided in section 3.2.

The first known applications of geodetic methods for deformation monitoring date back to the early twentieth century (Caspary and Rieger, 2000). Since then authors have presented different versions and combinations of the workflow process required for determining deformation (Richardus, 1977; Cooper, 1987; Setan, 1995; Bird, 2009). Overall it can be seen that there are four main stages that are critical in the deformation monitoring process. This consists of network design, the selection of deformation measurement techniques, deformation analysis followed by data information and communication. The remainder of this chapter is structured based on these four stages of the monitoring process. The next section provides an overview of the measurement systems and how they are deployed within a surveying and monitoring environment.

The deformation network design, measurement, analysis and communication processes described focus on observations from traditional and more modern terrestrial based geodetic techniques mentioned above.

3.2 Engineering surveying deformation measurement

As stated at the beginning of this chapter, this thesis focuses on deformation measurements using terrestrial based geodetic techniques, which are deployed within engineering surveying. This section provides a brief overview of each of the techniques, which are also used in the laboratory and site testing in this thesis: levelling, total stations, terrestrial laser scanning, close-range photogrammetry and laser trackers. Within each measurement type, the target types and initial data processing methods are described. Examples of their deployment within surveying and more specifically within deformation monitoring is also provided.

3.2.1 Levelling

In surveying, levelling is used to find the change in height, or vertical distance, between two points in relation to a horizontal plane or surface, e.g. a datum (Uren and Price, 2010). By using either an automatic or digital level along with a levelling staff, the vertical distance from the horizontal plane can be established where the heights of points are required. An example of using an automatic level and levelling staff is shown in Figure 3.1. Automatic levels require the user to manually read, write and

calculate the height information, whereas digital levels carry out all reading and data processing automatically by using an on-board computer by reading to a bar-coded levelling staff.



Image courtesy of Marc Usher, CEGE

Figure 3.1: Example of automatic levelling: automatic level (left) to read levelling staff (right) at millimetre level

3.2.1.1 Levelling & deformation monitoring

With respect to deformation monitoring, levelling provides 1D information of any changes in height of a set of points over time. The use of digital levels allows measurements to be made to a sub-millimetre level of precision automatically. It is common for digital levelling to be carried out on the outer boundaries of a construction site where the level of movements, based on the expected zone of impact map, are at the millimetre level. It provides an accurate, efficient and simple way of checking for this level of movement. This is the current practice for many construction sites. Based on the interviews carried out (see section 2.4), during the construction of the Jubilee Line Extension, a majority of the monitoring was done through manual precise levelling where there was hardly any automatic monitoring and very few prisms for manual monitoring. Monitoring specialists thought that the implementation of prism-based manual/automatic monitoring on projects had on occasion been “overkill”, where precise levelling could have easily been implemented as an accurate and cheaper alternative.

Due to the basic level of skills required for digital levelling, it is not vital for a qualified surveyor to carry out this work. For example at some of the Crossrail Project sites such as Farringdon and Paddington Station, banksmen are often trained to assist the

monitoring team on the levelling monitoring requirements. Any type of levelling does always require two people to carry out the work and the only automation available is the reading of the staff and on-board processing to calculate the changes in height. Also, the procedure involves setting the levelling staff up over a point to measure deformation and therefore cannot be used where points are inaccessible.

Precise digital levelling is often used to validate or complement another measurement technique to improve the integrity of the height information. For example Erol et al. (2004) used precise levelling to validate the height data from GPS when monitoring a viaduct, which is known to have weaknesses when deriving the height component of a position. It can be seen in Chapter 6 that precise levelling was incorporated into the monitoring scheme to validate the total station monitoring when a set of masonry arches appeared to be settling in the Z (height) direction unexpectedly.

3.2.2 Total stations

Total stations (TS) are used in surveying to measure angles and distances simultaneously to a high precision. Based on the measurements, 2D and 3D coordinates can be derived in an arbitrary grid or an established co-ordinate system. In land surveying TS are used to produce maps, topographic and detail surveys in 2D and 3D. Within engineering surveying, total stations are a key tool for setting out and deformation monitoring. Figure 3.2 shows a Leica TS15 total station being used to monitor the Llyn Brianne dam in Wales as part of the surveying fieldtrip at UCL.



Figure 3.2: An example of a total station on a fixed pillar for deformation monitoring

Current state of the art technology provides total stations, e.g. a Leica TS30, with an angle accuracy of $\pm 0.5''$ and distance accuracies of $\pm 1 \text{ mm} + 1 \text{ ppm}$ (parts per million). Angle measurements are made in the same way as an electronic theodolite, which uses a built-in angle encoder. The distance measurements are derived using an electromagnetic distance measurement (EDM). An electromagnetic wave or pulse is propagated from the instrument through the atmosphere to the glass prism or target and back again. There are two way of measuring distances: phase measurement and time pulsed. The specifications from the total stations typically used for surveying/monitoring and also for this thesis use the phase measurement method. An overview of manufacturer's specifications of the total stations used in this study can be found in the Appendix A. Essentially the distance is determined by measuring the difference in phase angle between the emitted and reflected signal. The difference is typically expressed as a fraction of a cycle, which can be converted into a distance if the frequency and velocity of the wave is known (Uren and Price, 2010). The process is extremely complex but the concept of the phase measurement process can be represented more simplistically in Figure 3.3.

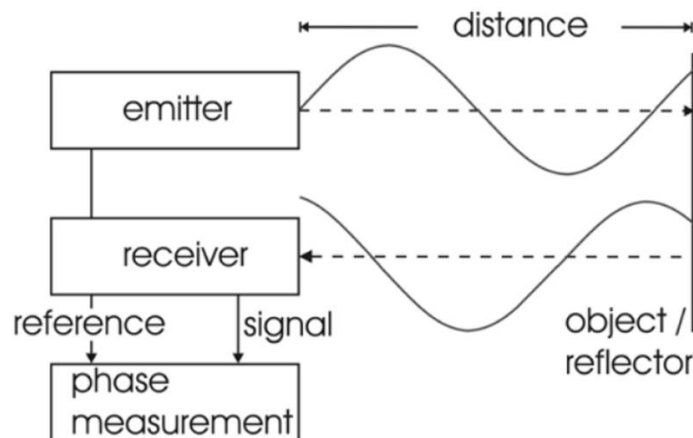


Figure 3.3: Concept of a total station's phase measurement phase taken from Kahlmann et al. (2006)

3.2.2.1 Total station targeting

In order to get a strong return signal, the distance measurement must be made to a highly reflective target such as a glass prism or target. Total station targets come in different shapes and sizes. A sample of these is shown in Figure 3.4 where different types of prisms are on the top row and retroreflective targets are shown on the bottom row.

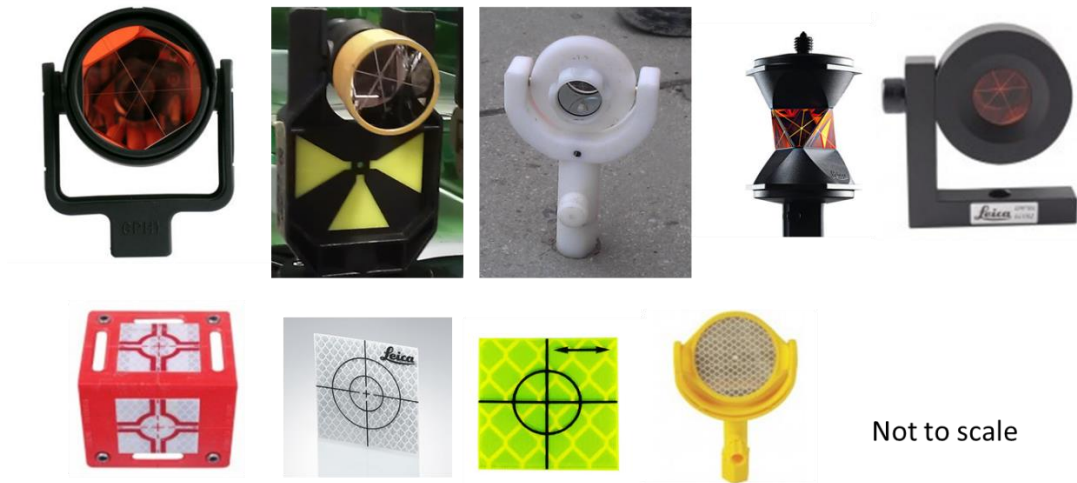


Figure 3.4: Examples of prism (top) and retroreflective targets (bottom) used with total stations

According to the Leica total station TS30 specification, a distance measurement of up to 3.5 kilometres can be made to a prism (see Appendix A). At TLP and other railway monitoring projects it is typical to use L-bar prisms (top row, right) for track monitoring due to their small size and ability to attach the L-bar to the sleeper of the track. However, these require significant maintenance as they often get knocked/kicked by workers during engineering hours. Particularly for track monitoring, prisms get covered by dirt from passing trains very quickly and require frequent cleaning, which can only be done when there is a possession during engineering hours.

A reflectorless distance measurement can also be taken where it's not possible to measure to a reflector, for example if the area is inaccessible or hazardous. Based on the manufacturer's specification the allowable range of measuring in reflectorless mode using the same instrument is reduced to approximately 1km. However this value is dependent on the atmosphere and visibility as well as the surface being measured. For example a white surface would reflect quite easily providing a strong return signal, whereas a black surface would not provide an efficient return signal. There is also a large laser footprint when using reflectorless mode, particularly at long ranges, and the signal strength is reduced which could result in an inaccurate or no measurement (Uren and Price, 2010). Experiments on the atmospheric effects of EDM measurements was carried out by Garrido-Villén et al. (2015) who concluded that when carrying out engineering surveying projects, the range of the instrument must be tested and that

manufacturers' specifications were not always accurate. It was also found that weather conditions had an adverse effect on the range of the EDM.

Over time the capability of TS has improved for the surveying industry. TS, such as the Leica TPS1200+, have been fitted with servo-motors to control their horizontal and vertical movement, commonly known as robotic total stations. With this built-in motor and the Automatic Target Recognition (ATR) function, this allows measurements to prisms or targets to be made quickly without the need of manual aiming through the telescope. More recently the "motorisation" process was improved using piezo-technology which allows the telescope to move very quickly with very little noise compared to the older models, as well as improving the ATR function and allowing real-time tracking of a moving prism. Other improvements include having built-in GPS/GNSS capabilities and an image capture function which has allowed low resolution images (~5 megapixel resolution) to be taken from the total station, mainly for documentation purposes. A more detailed review of the development of TS from various manufacturers from the 1960s onwards can be found in Scherer and Lerma (2009).

3.2.2.2 Total stations & deformation monitoring applications

Since the introduction of the ATR functionality, literature and industry practices have shown an increase in the uptake of TS for deformation monitoring of a wide variety of man-made and natural structures.

Deformation monitoring using TS can either be manual or automatic depending on the monitoring frequency requirements. For example, at London Bridge Station the masonry brick arches are required to be monitored manually by a surveyor weekly by measuring to the prisms on the arches to observe relative movement. This process allows quick measurements to be made through the ATR functionality, however it is a very traditional method and still requires a surveyor to be physically present with the total station which involves manually inputting what is required to be measured. Early examples of manual monitoring using TS include Kuhlmann and Glaser (2002) where a total station was used to take reflectorless measurements to monitor a bridge using benchmark points. The project required movement to be detected as well as to show how the shape of the bridge was changing every 6 years. Merkle and Myers (2006) used a total station to monitor five bridges during their strengthening process by using a reference baseline. The case study showed the benefits of using geodetic equipment

for measuring the structure during static loading testing where other geotechnical devices were difficult to set up in the environment.

Automatic monitoring is suitable when monitoring structures is required continuously or where it is not safe or practical for a surveyor to be in proximity to the instrument. This is very common for the railway industry. A simple overview of the concept of current state of the art automatic monitoring systems provided by Leica Geosystems is shown in Figure 3.5 .

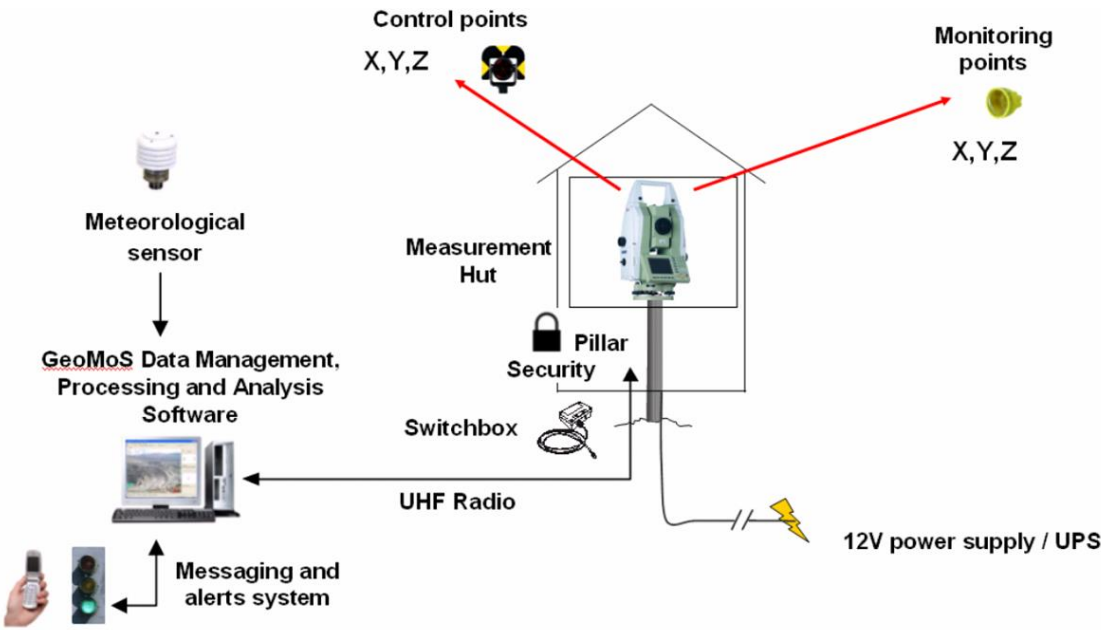


Figure 3.5: Typical automatic monitoring system configuration – image taken from Whitworth (2010)

This particular automatic monitoring system is provided by Leica which is called GeoMos². This structure shown in Figure 3.5 is not dissimilar to the monitoring tools that are provided to Network Rail by specialist monitoring contractors, for example Sol Data, Datum and itmsoil. All measurements are stored on a SQL server database. Within GeoMos are two modules: Monitor and Analyzer, where Monitor controls the operation of the total station and Analyzer is used to visualise the discrete point results graphically and/or numerically (Berberan et al., 2007). Monitoring specialists have created and developed their own equivalent to these modules. Essentially the total station requires power to acquire the data and a method to connect to a database (Figure 3.5 shows UHF radio but GPRS, Bluetooth, 3G are examples of other methods of

² URL: http://www.leica-geosystems.co.uk/en/Leica-GeoMoS_4802.htm (last accessed October 2015)

connection) where the results can be displayed according to the user requirements which have been pre-defined. For example, this can be in changes in coordinates/displacements in X,Y,Z. For monitoring track, track twist and cant (see Chapter 2) are usually required, where the SQL database is used to calculate these parameters.

An example of automatic monitoring at London Bridge station is of the railway track. Currently major construction works are taking place in the vicinity of the track, which remains operational, and therefore monitoring of it is required at all times to ensure the safety of passengers. This type of setup involves installing the instrument on a weather-proof bracket (if exposed to outdoor conditions) where there is a line of sight to the targets on the track. Figure 3.6 provides a typical example of a total station monitoring setup in a tunnel environment.

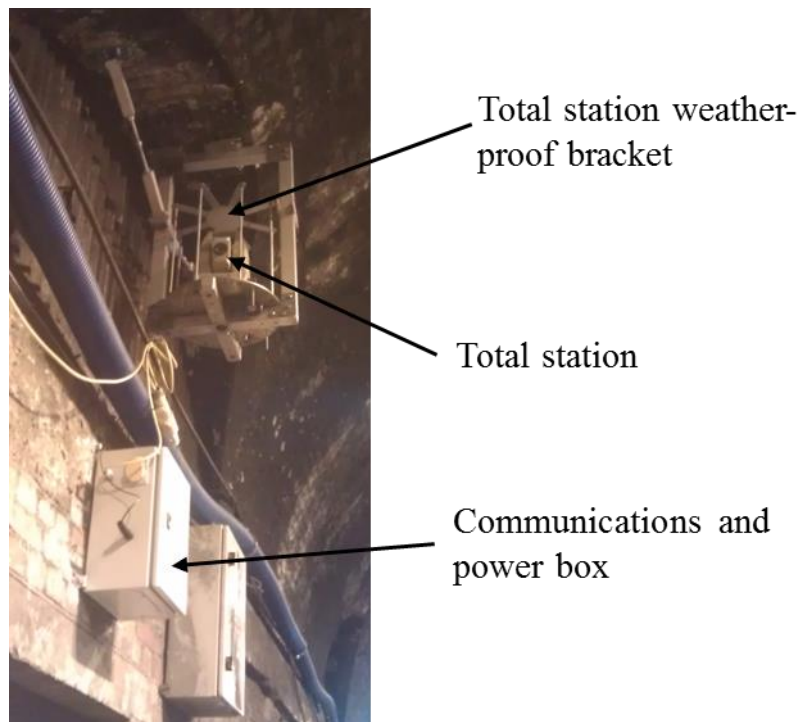


Figure 3.6: Typical automatic monitoring setup using a total station

The measurement “routine” to observe to the prisms or targets must be initialised before the system can be fully automated. This routine is usually done manually, where each prism would have to be “read” by a surveyor from the instrument before automatic readings can be deployed. However since the development of imaging functionality total stations (e.g. the Leica TS15i and Leica MS50) this can now be done remotely using an image or live image feed to the total station from a remote controller. A communications and power box (including a datalogger) is used to feed power to

the instrument as well as record and send the measurement data to a server which is then analysed and displayed in formats according to the client/engineer's requirements (e.g. a change in X,Y and/or Z, twist, cant) usually through an online web interface. The delivery and communication of monitoring information is described in more detail in section 3.4.

Based on the interviews carried out in Chapter 2 it can be seen that this is often the most expensive part of automatic monitoring. The data logger is required to be in proximity to the total station. A dial-up connection is used to connect to the server. Particularly for underground/tunnel and bridge monitoring, it is often hard to get a signal to the dial-up connection which often results in a "jam" in the network for the monitoring data. This requires a specialist to access the box and reset the system. Therefore this requires special access to this box, which is usually only accessible during engineering hours. This affects the reliability of the system particularly due to the real-time monitoring requirement. It also incurs a huge cost to gain access to send someone during engineering hours, which can be up to once a week depending on the quality of the connection. According to Leica the current state of the art monitoring instruments (e.g. TS/TM30) are designed to work continuously for approximately 8,000 hours before a system calibration is required. As is normal with technology, a system may fail unexpectedly and would require immediate replacement. Therefore this access requirement is also an issue for maintenance of the total station. This also requires a replacement total station to be installed whilst the other one is being calibrated and then access again to reinstall it once it has been calibrated. This is expensive and time consuming with a risk of monitoring measurements not being captured sufficiently. Chapter 4 presents an experiment of using total stations with varying calibration histories to test their performance and capability for detecting displacement.

One of the earliest uses of automatic monitoring using TS is described by Hill and Sippel (2002) where a total station was used to continuously monitor a landslide for relative movement. Due to the adverse weather conditions at the altitude of the area, continuous monitoring was not possible and therefore only intermittent measurements could be analysed. Cosser et al. (2003) and Psimoulis and Stiros (2007) researched the potential of automatic dynamic monitoring of bridges using the precise target pointing as well as ATR functionality of TS. Due to the rate at which measurements were made

(~1Hz), Cosser et al. (2003) found that it was possible to carry out slow dynamic deformation monitoring. However with a newer generation total station which had better ATR capabilities it was possible for Psimoulis and Stiros (2007) to carry out dynamic monitoring with frequency measurements of up to 3Hz. An example of a recent large-scale use of automatic monitoring is at Paddington Station for the Crossrail project. The Crossrail Project involves the construction of a new railway line stretching 118 kilometres, which runs through Central London and has an estimated cost of £14.8bn. A total of 52 total stations and over 1,800 prisms were installed in the Paddington area to monitor buildings and railway track during the tunnelling process. Figure 3.7 depicts the vast monitoring network (white lines) covered by the 52 total stations surrounding Paddington Station (Binder, 2014). In this case Leica GeoMos was used to collate the data. More information about the network adjustment process for this type of project is provided in section 3.3.3.



Figure 3.7: Example of large-scale automatic monitoring network on the CrossRail project including 52 total stations - image taken from Binder (2014)

It can be seen that monitoring using total stations manually and automatically have been well established, particularly in the rail industry, and there has been little change in this method with respect to monitoring in the last decade or so. This is currently one of the default methods of monitoring during railway infrastructure projects such as TLP and Crossrail. The only developments have been on the instrumentation side where more accurate and faster measurements can be taken from a total station. In

order to keep up with the amount of measurements being acquired, there has been an increase in the speed of data communication back to the stakeholder or client for inspection. Instrumentation suppliers are producing total stations that are more intuitive for a non-expert which opens up the market for users, especially for deformation monitoring where large construction sites need multiple staff for manual monitoring checks. However this can be detrimental when there may be limited knowledge of the requirement for the network adjustment/analysis stage. This could have a knock-on effect where changes in co-ordinates from previous epochs could be taken at face value, rather than taking into consideration other factors such as error propagation.

3.2.3 Terrestrial laser scanning

Terrestrial laser scanners are able to measure angles and distances to an object surface at a high speed using a laser (**L**ight **A**mplification by **S**timulated **E**mission of **R**adiation) beam in order to produce 3D co-ordinates. Based on metrology terminology, it is often referred to as an optical non-contact technique due to its ability to measure a surface without the need of physically touching or probing the object, which is based on wave optics and the electro-magnetic spectrum. Terrestrial laser scanning (TLS) has become an invaluable method of data capture within the surveying industry compared to using the more traditional total station. This has resulted in a wide variety of applications, including in the railway industry, in which TLS can be used to record 3D information accurately. For example the digitisation of cultural heritage objects, producing 3D models to provide asset information of a building e.g. through BIM (building information modelling), recording crime scenes which allows a virtual fly-through and enables this information to be used in court as evidence, aiding visual effect sequences by providing 3D geometry for films and television and so on.

Figure 3.8 provides a sample of current state-of-the-art TLS systems available from manufacturers including Faro, Leica Geosystems, Topcon, Reigl and Zoller + Fröhlich (Z+F). The TLS systems used in this study are Leica and Faro models. More information of the instrument specifications can be found in the Appendix A.



Figure 3.8: Array of current TLS systems available starting on the left going clockwise: Reigl VZ-1000; Topcon GLS-2000; Faro Focus 3D X130 and X330; Leica ScanStation P20; Z+F 5010C

The main advantage of TLS, as opposed to traditional survey techniques, is the ability to remotely capture large volumes of 3D data at a high speed with reasonably high accuracy. Set against this is that the metric qualities of the 3D data are highly dependent on the reflectance and local geometry of the surfaces under observation and sample those surfaces in a regular grid dictated by angular instrument settings rather than the features being measured. As the technology has matured, manufacturers have produced scanners that have become faster with an increasing level of accuracy. Current state of the art TLS systems, for example the Leica ScanStation P20, has a single 3D point accuracy of approximately 3mm, with an angular accuracy of 8" (see Appendix A). The range accuracy is dependent on the principle of distance measurement of the system. For TLS there are two main types of technologies for distance measurement: phase and time-of-flight measurement. Both types of these TLS systems are used in this research.

The phase measurement method can be compared to that of the total station distance measurement described in section 3.2.2 and Figure 3.3. Due to the well-defined return signal the range capability of the TLS systems using the phase measurement is around 100 metres (see Appendix A). From experience of using these types of scanners at long ranges, the optimum operating range, based on the quality of the point cloud produced, is approximately 60-80 metres. Distance measurement accuracy using the

phase measurement is very high at the 1-3mm level (Vosselman and Maas, 2010). The scan rate of phase-based TLS systems is very fast at approximately 1 million points per second.

The time-of-flight or pulsed method computes the distance by sending a laser pulse from the scanner to the object and detects the time taken between the transmitted and received signal. This type of measurement is also used in airborne laser scanning systems. Figure 3.9 provides a representation of the time-of-flight principle.

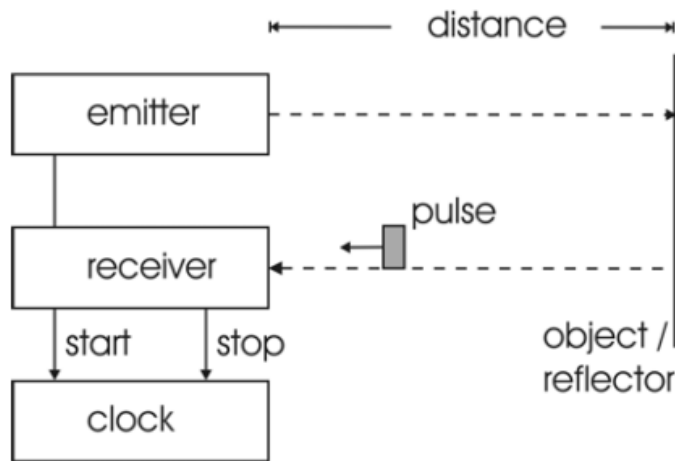


Figure 3.9: Time-of-flight distance measurement principle taken from Kahlmann et al. (2006)

The distance or range, d , can be calculated by the following equation:

$$d = c \times \frac{t}{2}$$

where c is the speed of light and t is the time taken between the emitted and received signal.

Time-of-flight scanners allow measurements of larger distances of over 100 metres up to 1 kilometre. Due to the pulsed based method, the speed of data capture is much slower with scan rates of 50-60,000 points per second (see Appendix A). However, during this study in late 2012, the Leica ScanStation P20 scanner was introduced to the TLS market with a scan rate of up to 1 million points per second, matching the phase based TLS scan rate. It is termed by the manufacturer as an ultra-high speed time-of-flight scanner enhanced by Waveform Digitising technology. Despite an improvement of the speed of the data capture, the accuracy of the range measurement for time-of-flight systems remains slightly lower at around 5-10mm (Vosselman and

Maas, 2010). When a new system is released the manufacturer produces a datasheet or specification to provide an indication of the performance of the scanner. However these do not always provide clear information on the accuracy and precision of the system. This is probably due to the vast number of scenarios in which the scanner could be used e.g. scanning different surfaces at different ranges. Therefore it can be difficult for the manufacturer to condense this information into one specification. Also, some of the parameters used in the specification are not consistent between models, making it difficult to compare the models from the same manufacturer.

Since the release of the first terrestrial laser scanner, which is claimed to be the Cyrax 2500, there has been a huge investment of typical survey equipment providers in the development of this technology. At the time of submitting this thesis Leica Geosystems have very recently introduced a new set of time-of-flight base scanners (ScanStation P30/40) which, according to the manufacturer's specification, has an improvement on the range accuracy down to $1.2\text{mm} + 10\text{ppm}$ compared to the $\pm 3\text{mm}$ or more range accuracy previously specified. Even though other TLS manufacturers are competing with the accuracy and scan rate levels of the system, other features which make the system more practical for a surveyor have been incorporated. For example Faro have produced the Focus line of TLS systems which are very small and light-weight. This makes it easier for scanning in areas with limited access but also makes it more portable across larger construction sites. The user interface of the system has been designed to allow users other than surveyors to use the system. For example, ScanLAB are a company of architects who use these systems for typical and atypical surveying jobs with no known surveying background knowledge. This opens up the user market for this type of system but it is important that the integrity of the data is maintained and that the final output is fit for purpose. Topcon have produced a model which can scan but also read to prisms to allow only one instrument to be required on site, rather than having a total station purely for measuring targets or geo-referencing (see section 3.2.3.1). More recently GPS has been integrated into TLS systems to allow geo-referencing of point clouds. This is discussed further in section 3.2.3.1. Reigl have focused on having a long range capability of the system, which has been a very useful tool for scanning mines for documentation as well as monitoring purposes

It is now typical for a TLS system to have an on-board camera; this allows a coloured point cloud to be formed as well as provide a live-feed for the surveyor to determine

areas to scan. The quality of this camera tends to be quite low and has the same resolution as a typical mobile phone. If high quality images are required, a digital SLR (single lens reflex) camera can be attached onto the scanner (e.g. Canon or Nikon), similar to the Reigl scanner setup shown in Figure 3.8. It is possible to stitch these images to the point cloud so that there is a colour value for each point scanned. It is common practice to produce HDR (high dynamic range) images to stitch to the point cloud. This allows a greater dynamic range of brightness and higher resolution compared to a standard digital image on-board the scanner. This is particularly useful when scanning dark spaces which is typical on construction sites and plants. As HDR has become a popular option for imaging when using TLS systems the quality of the image sensor on-board is improving. Z + F have produced a scanner with HDR technology on-board which is aligned to the laser scanner, producing a HDR image for the entire point cloud without the need of attaching a separate camera. Leica have followed suit by having on-board HDR capability of the images produced from the on-board camera.

Another development was the introduction of a hybrid total station, or “MultiStation”, produced by Leica Geosystems in 2013 (see Appendix A). This integrates discrete point measurement technology used in a total station along with continuous point measurement technology used in TLS systems and a live video feed. The main differences to the Topcon’s scanner and prism reading capability is it allows patches to be selected by the user for scanning, rather than full 360° scans which need to be geo-referenced. Therefore it can be useful where accurate measurements to a prism are required, but also areas of the object need to be scanned in more detail. The imaging also allows the user to remotely access the total station’s line of sight without being next to the instrument. A potential for this is in automatic monitoring where more information may be required if there is unusual activity and access to the site is limited or time consuming. It also reduces the need for having two separate instruments on site to carry out measurements. As this type of instrument is relatively new, there is very little literature giving feedback of its capabilities. The only known work at the time of submitting this thesis is from Ehrhart and Lienhart (2015) where the use of the built-in imaging system for deformation monitoring is explored. This thesis explores the use of this model of total station in Chapter 4.

It can be seen that there has been a vast development in the technologies incorporated into a TLS system. As well as improving the speed and accuracy of the system, more practical and user friendly capabilities for the expert and non-expert have been incorporated to maximise the potential of applications using TLS.

3.2.3.1 Terrestrial laser scanning targeting & point cloud processing

TLS targets come in different shapes and sizes depending on the manufacturer and type of TLS system being used. Based on the Leica and Faro TLS systems used in this research the main types of targets used in this research are planar and spherical-based targets. Examples of these are shown in Figure 3.10.

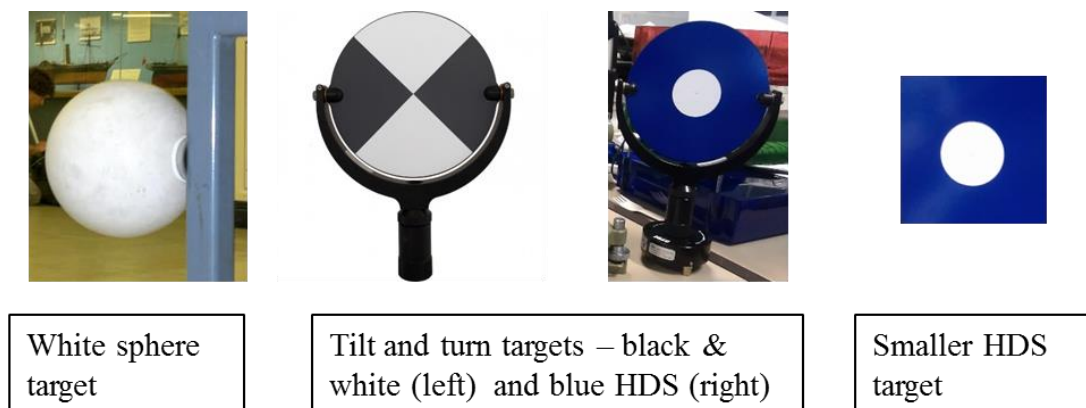


Figure 3.10: Typical TLS targets - sphere and planar based (not to scale)

The sphere and tilt and turn targets can be mounted on a tribrach and the smaller HDS targets can have an adhesive or magnetic backing to allow attachment to any surface type. The HDS (blue and white central circle) targets have a small retro-reflective centre which can only be read by Leica time-of-flight scanners. The sphere and black and white targets can be captured accurately by most TLS systems and the centres can be automatically extracted using point cloud processing software such as Leica Cyclone³ or Faro Scene⁴. Examples of target centre extraction from sphere and black and white targets using Leica Cyclone is shown in Figure 3.11.

TLS targets can be used to accurately overlap scans of a space where multiple scans are required, and to ensure the geometry of the area remained intact. With respect to

³ URL: http://hds.leica-geosystems.com/en/Leica-Cyclone_6515.htm (last accessed 17th September 2015)

⁴ URL: <http://www.faro.com/en-us/products/faro-software/scene/overview> (last accessed 17th September 2015)

deformation monitoring, an entire object or structure is usually required to be monitored, therefore numerous scans with multiple scanner setup positions is usually required, resulting in the need for accurate registration.

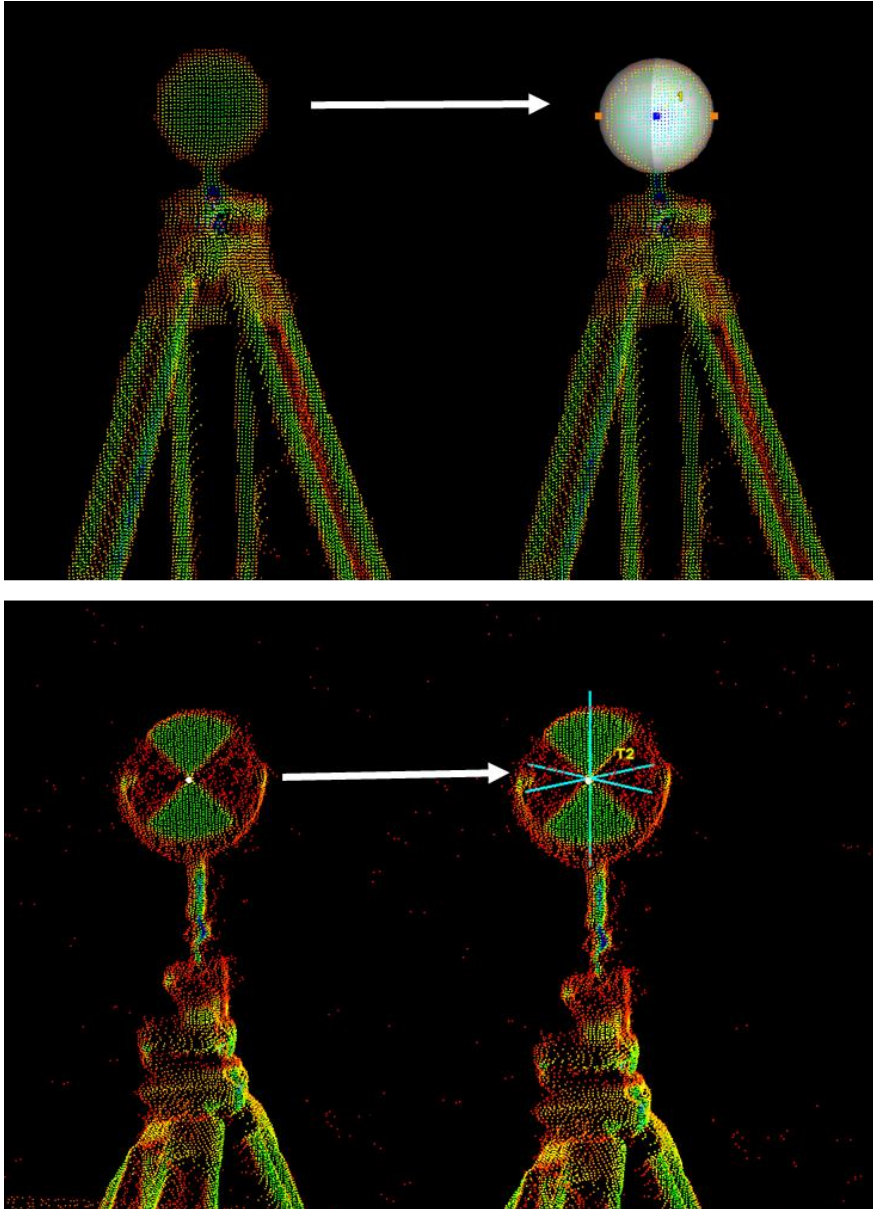


Figure 3.11: Target centre extraction of sphere (top) and black and white (bottom) target

By extracting the centres of TLS targets between multiple scans this allows common points between the overlapping point clouds to be transformed into a single co-ordinate system using a six-parameter, rigid transformation (Gordon et al., 2001; Vosselman and Maas, 2010). An example of a successful registration of four different scans is shown in Figure 3.12. Each final scan position in relation to each other is represented

by the yellow triangles (indicated with a red circle) and the point cloud from each scan is shown in a different colour (i.e. green, yellow, blue and green).

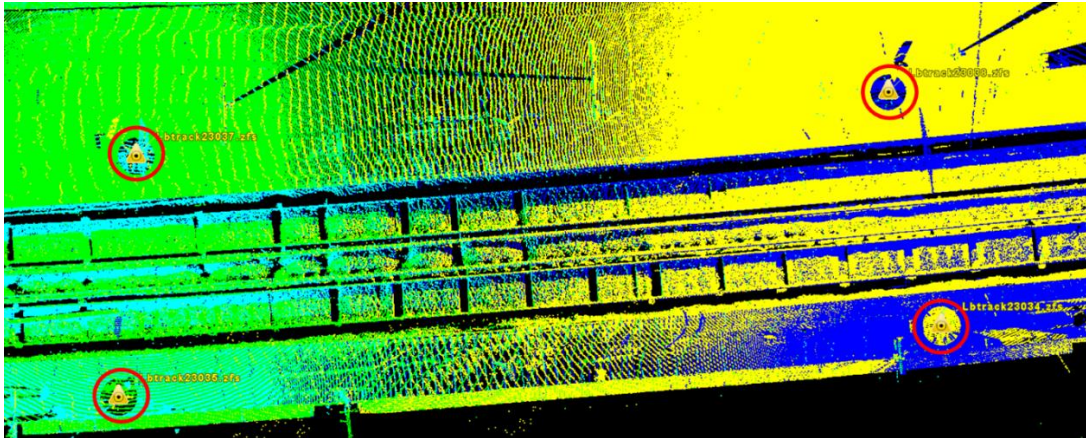


Figure 3.12: Example of point cloud registration in Leica Cyclone

In order to achieve an accurate registration the following needs to be taken into consideration: target position in relation to the scanner and other targets, target type and scanning resolution of target (Berckerik-Gerber et al., 2011). A more detailed description of TLS systems and target-based registration can be found in “*Airborne and Terrestrial Laser Scanning*” by Vosselman and Maas (2010). Along with the target centre extraction, target-based registration can be carried out within point cloud processing software, e.g. Leica Cyclone and Faro Scene. Practical application of target-based registration using Leica Cyclone is described in Chapter 5 and 6. This is the most widely used software for point cloud registration within the surveying industry.

Target-less point cloud or cloud-to-cloud registration is possible without the use of targets, for example through the well-established iterative closest point (ICP) method (Besl and McKay, 1992) or feature-based methods. ICP is based on the search of pairs of nearest points (using a nearest neighbour approach) between two point clouds and estimating the rigid transformation, which then allows them to be aligned. The rigid transformation is then applied to the “reference” point cloud and the procedure is iterated until convergence. The use of the ICP algorithm in this thesis is described in more detail in Chapter 6 where cloud-to-cloud registration is applied.

Feature-based registration uses geometric primitives such as planes, spheres and cylinders extracted from the point clouds. Once the parameters of the features have been estimated by geometric fitting, the registration parameters are estimated by

minimising the sum of the squared differences between model parameters (Vosselman and Maas, 2010).

For the majority of survey projects, particularly on construction sites, the data are required to be delivered on a fixed co-ordinate system. For TLS this process is known as geo-referencing (Schuhmacher and Böhm, 2005). This can be carried out by co-ordinating TLS targets or points of interest using a total station which gives millimetric accuracy (Allan, 2007; Lerma Garcia et al., 2008; Uren and Price, 2010), or by GPS which gives centimetre to metre levels of accuracy (Schuhmacher and Böhm, 2005; Reshetyuk, 2010). It can often be hard and time consuming to geo-reference a point cloud if targets are not used due to the difficulty in defining a corresponding point between a point cloud and a pre-determined reference point. If there is not enough overlap between scans, it is difficult for the ICP technique to be initiated (Chow et al., 2010). More recently technology has also allowed scan geo-referencing via the integration of GPS within the scanner, for example a Reigl VZ-6000 (Riegl, 2014) and Faro X330 (FARO, 2014) system.

Since the development of low cost sensors such as the Kinect sensor for the Microsoft Xbox 360 console which was released in late 2010, there was a requirement for handling real-time point clouds efficiently. This brought about the development of the Point Cloud Library (PCL). It is an open-source cross-platform library written in C++ to allow point cloud and 3D geometry processing. The PCL framework consists of a number of state-of-the art algorithms including filtering, registration, model fitting and segmentation of point clouds (Rusu and Cousins, 2011). A more comprehensive list of the modular libraries can be seen on the PCL website⁵ and a screenshot of the libraries available are shown in Figure 3.13.

PCL has allowed users to optimise the performance of point cloud processing and easily integrate it into their own project rather than relying on “black box” processing software such as Leica Geosystems Cyclone where the libraries of the algorithms used for processing, for example point cloud registration, is not easily accessible. Figure 3.14 represents the basic interface that is used in all the algorithms within PCL.

⁵ PCL Documentation - <http://pointclouds.org/documentation/> (last accessed 22nd September 2015)

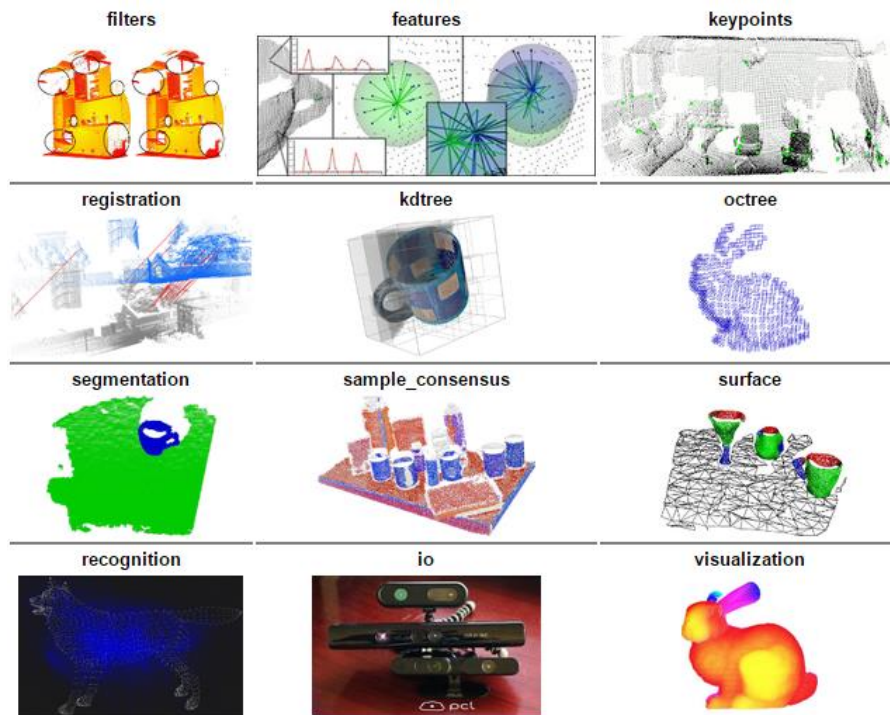


Figure 3.13: Libraries available in PCL - taken from PCL documentation website

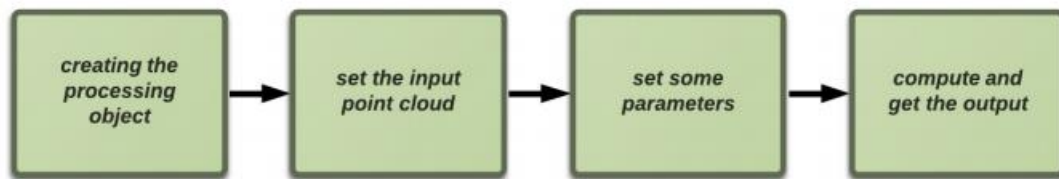


Figure 3.14: Basic interface scheme for PCL code – image taken from Boehm et al. (2013)

PCL has become a very useful tool for the robotics community (Rusu and Cousins, 2011) as well for researchers in point cloud processing. For example, the iQmulus project, which is funded by the European Commission, aims to “develop a platform that provides the needed functionalities to integrate latest research results in data processing and visualisation to tackle important real-life challenges in geospatial applications”⁶. Due to its efficiency and convenience PCL is used as a core library for point cloud processing, in particular the feature extraction and classification task (Boehm et al., 2013).

⁶ Quote taken from iQmulus website - <http://iqmulus.eu/project-overview/at-a-glance> (last accessed 22nd September 2015)

3.2.3.2 *Examples of the applications of terrestrial laser scanning within the railway industry*

Once a point cloud has been registered and geo-referenced, it can be used in many different ways to produce deliverables depending on the user/clients requirements. Some of these are common across industries, including the railway, heritage and construction industry for example. TLS data has been used on the Thameslink Programme as far back as 2002 (Gleeson, 2011).

One example is to deliver the registered point cloud directly to the client (in this case NR) through a web-enabled panoramic point cloud viewer, such as Leica TruView⁷ or Faro WebShare⁸. It provides a rendered view of a point cloud in colour/black and white to allow the user to virtually fly-through a scene without having to go and visit it. It allows basic 3D measurements to be made as well as superimposing simple 3D models into the scene. An example of the Leica TruView availability at TLP of the as-built surveys at London Bridge Station is shown in Figure 3.15. It shows how large volumes of scan data can be easily accessed by all parties working on TLP.

As well as producing TruViews of stations and parts of the TLP route, other applications of using TLS data along the TLP include producing 3D as-built models (which can then be used to produce building information models) and wireframes, comparing design models to surface models, 3D virtual reality signal sighting models to ensure signals are obstruction free and so on. More information of these examples can be found in Gleeson (2011).

Another example of using TLS data within a railway context is through kinematic scanning systems, such as those provided by the Amberg Group. Amberg systems provide rail and tunnel surveying solutions which are widely used in the railway industry across the world. For example, the Swiss Federal Railways (SBB) often use the Amberg Trolley (GRP 5000) to carry out clearance surveys of their vast amount of tunnels. This involves putting a TLS scanner onto a trolley and pushing this along track or through a tunnel. An example of this is shown in Figure 3.16.

⁷ URL: http://hds.leica-geosystems.com/en/Leica-TruView_63960.htm (last accessed 24th October 2015)

⁸ URL: <http://www.faro.com/faro-3d-app-center/stand-alone-apps/scene-webshare-server> (last accessed 24th October)

1. Thameslink Explorer Portal to access TruViews (can be accessed by all TLP staff)

2. Different locations of scans available for this particular station

3. Each yellow triangle represents a single 360° scan

4. Point cloud can be viewed in colour/intensity through panoramic view

5. Simple mark-up and measurements can be made and saved

The image is a composite of three parts. On the left is a screenshot of the 'Thameslink Explorer' website. The top navigation bar includes 'Thameslink Explorer', 'The TLP Integrated Management System', and 'GRIP How Thameslink applies GRIP'. A red circle highlights the 'TruView Surveys' link. Below this are links for 'Reserve a number', 'System Access', and 'Templates'. On the right side of the website, there are links for 'Thameslink Website', 'A Quick Guide', 'MOSS User Guide', and 'PV User Guide'. A red circle highlights the 'TruView Surveys' link. Below the website is a large 360-degree point cloud scan of a station platform, showing a dense grid of yellow triangles representing individual scans. A red circle highlights one of these triangles. On the right side of the point cloud is a 3D model of the station interior, showing a long, narrow hall with a high ceiling and a series of arches. A red arrow points from the highlighted triangle in the point cloud to the 3D model. Below the 3D model is a screenshot of the TruView software interface, showing a 3D view of the station interior with various measurement tools and a red arrow pointing to a specific measurement.

Figure 3.15: Example of handling large volumes of point cloud data at TLP using TruView



Figure 3.16: Configuration of Amberg Clearance GRP 5000 - image taken from Amberg (2015)

The scanner carries out profile measurements in 2D to provide clearance analysis between the measured object and design model. If the scanner position is tracked using GPS or a total station, track geometry information such as twist, cant and gauge can be extracted. Figure 3.17 provides some screenshots of the available output from clearance analysis as well as the track geometry parameters. Even though this method can provide important track monitoring parameters required by the engineer during a project like the London Bridge Redevelopment Project, it requires direct access to the track without any trains passing (i.e. through possessions) and doesn't provide real-time monitoring. It provides more of a condition survey solution of the track and its surroundings. Therefore this type of method is deployed on a less regular basis, for example annually, to obtain track geometry.

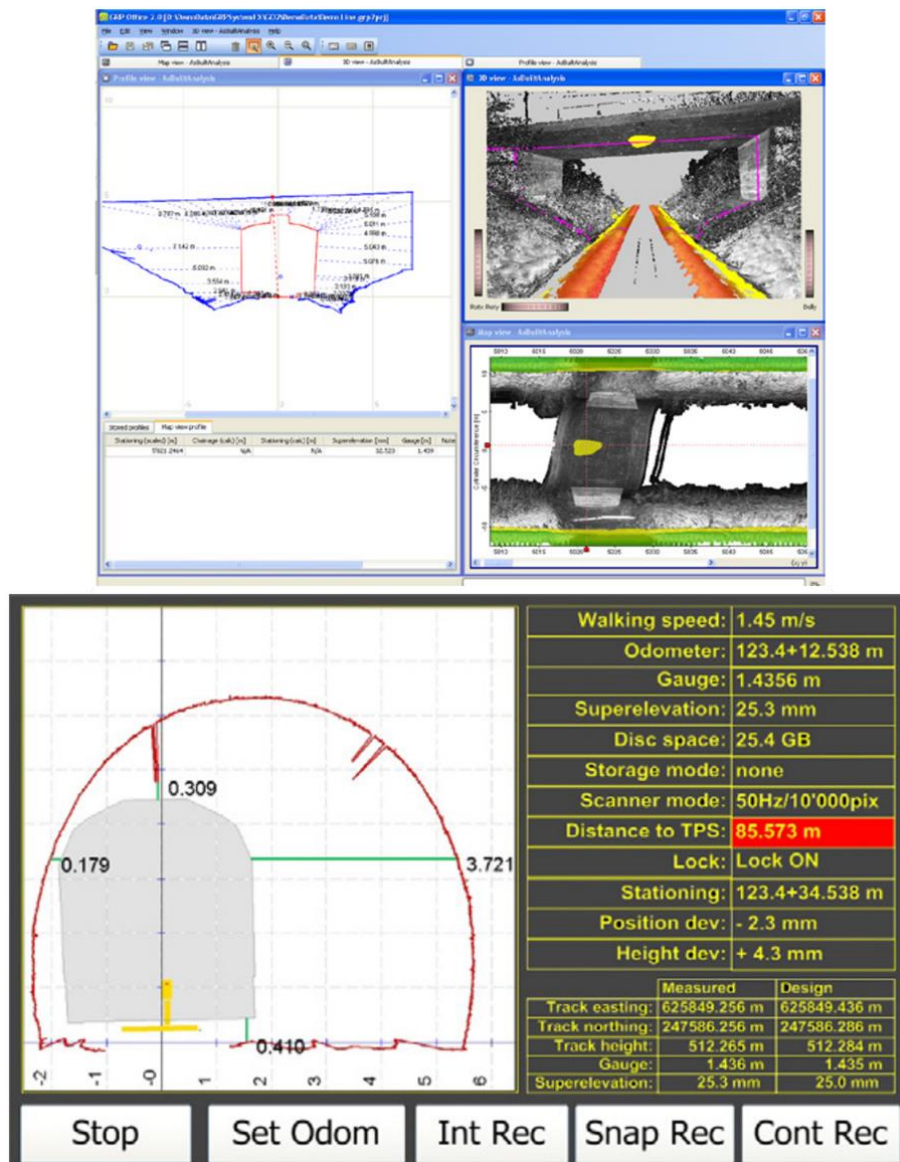


Figure 3.17: Typical clearance analysis and track parameter output from kinematic TLS of railway

Overall it can be seen that TLS is a very useful tool that allows fast data capture and accurate measurements to be made, particularly for the railway industry. It also shows how large volumes of data can be displayed in different contexts depending on the overall user requirements. Therefore by taking advantage of this tool, there is motivation to see whether TLS would be applicable for deformation monitoring of railway infrastructure, particularly during major construction projects. The next section provides a review of the current state of the art with respect to TLS and deformation monitoring.

3.2.3.3 Terrestrial laser scanning & deformation monitoring applications

The ability for TLS to acquire high resolution coverage of an object or surface compared to traditional surveying techniques, such as total stations, is an important advantage, especially for monitoring the deformation of surfaces. Therefore since the development of TLS systems in terms of speed and accuracy there has been a huge uptake in the application of deformation monitoring, particularly in the last 5-10 years.

Case studies show how the benefits of static TLS can be used as a monitoring/inspection tool for a wide variety of natural and man-made structures during the lifetime of this research study, for example: rockfall events (Abellán et al., 2009 & 2011; Alba and Scaioni, 2010); dams and locks (Lindenbergh and Pfeifer, 2005; Alba et al., 2006; Schneider, 2006); steel beams (Gordon et al., 2005; Park et al., 2007); bridges and underpasses (Werner and Morris, 2010; Riveiro et al., 2011; Puente et al., 2012; Kopáček, 2013); and tunnels (Nuttens et al., 2010, 2012, 2014) as well as more unique monitoring situations, for example Vežočník (2009) which required a high pressure underground pipeline within a geologically unstable area to be monitored.

Park et al. (2007) describe how structural deformations tend to be relatively small, in the order of a few millimetres or centimetres. Based on the instrumentation specifications, the analysis tends to take place at the same level of detail as the resolution of the scanner (Lindenbergh and Pietrzyk, 2015). This can be overcome by exploiting the high redundancy of the observed surfaces. The deformation analysis tools using TLS is discussed in more detail in section 3.3.4.

At the time of starting this study, there was no known literature into the application of monitoring railway track. This was due to the sub-centimetre level of accuracy that was being achieved, which was restricted by the accuracy requirements close to the resolution of the scanner. However, over the past few years vendors have been producing TLS systems which are faster and more accurate. This has allowed the potential of TLS to be used as a tool for monitoring railway track, particularly in the past two years where work by Liu et al. (2013) and Meng et al. (2014) have shown millimetric levels of accuracy and precision with regards to measuring railway track for monitoring purposes. This study has also looked at the use of static TLS and findings in comparison to the above work is described in more detail in Chapter 6.

The main advantages of using TLS in these applications was the non-contact measurement capability, i.e. the ability to remotely record the surface of a structure/object, over a short period of time. However, most of these examples show that TLS has been carried out on an ad-hoc basis and there is no known work of using TLS for continuous monitoring. There is uncertainty of the capability of the motors designed for TLS systems to run continuously. As their application within deformation monitoring is relatively new, it is thought that vendors are not designing the instruments to run continuously, whereas specialist monitoring total stations are designed to run 24 hours a day, 7 days a week. It can be seen that instruments are becoming faster and more accurate and the design of these instruments may need to be adapted to allow for longer-term monitoring projects.

Overall it can be seen that as TLS systems are getting more accurate and faster with data capture their use within deformation monitoring is emerging. However, the process workflow for deformation monitoring is not as established as it is for total station and CRP monitoring (see section 3.3)

3.2.4 Close-range photogrammetry

Photogrammetry “*encompasses methods of image measurement and interpretation in order to derive the shape and location of an object from one or more photographs of that object*” (Luhmann et al., 2014). It allows accurate 3D reconstruction of an object in a digital form, for example a point cloud. Photogrammetry is a very traditional method of acquiring 3D information and has been used in surveying for many applications, particularly for mapping purposes and producing digital terrain models using aerial photographs (Burnside, 1979). Close-range photogrammetry (CRP) is essentially the use of terrestrial-based images (as opposed to aerial images) at a distance of less than 300m from the object of interest to produce a 3D model (Luhmann et al., 2014). With advances in electronics, IT, computers and storage capacity, digital photogrammetry has allowed high quality and efficient production of 3D models.

CRP is a non-contact measurement technique which uses central projection imaging as its fundamental mathematical model. A representation of the principles for photogrammetry is shown in Figure 3.18. The shape and position of an object are determined by reconstructing bundles of rays for each image point P' along with the corresponding perspective centre O' , which defines the spatial direction of the ray to the corresponding object point P . In order for every image ray to be defined in 3D

object space, the image geometry within the camera and the location of the imaging system in the object space must be known.

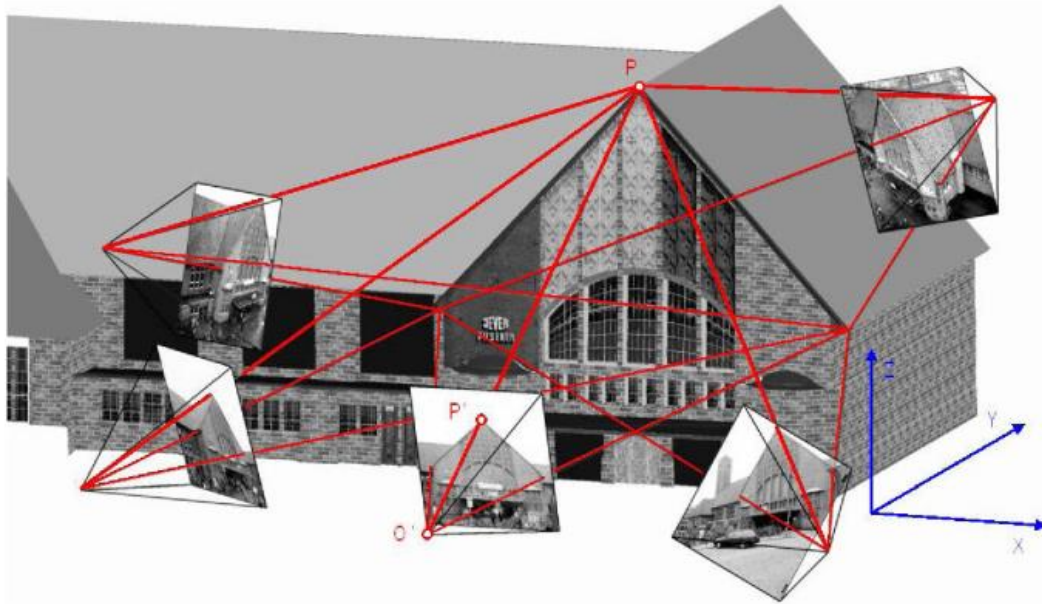


Figure 3.18: Principle of photogrammetric measurement – image taken from Luhmann et al. (2014)

Inner orientation parameters provide the internal geometric model of the camera. Based on the model of the pinhole camera, the most important reference location is the perspective centre O , in which all image rays pass. Figure 3.19 provides an image of the pinhole camera model. The interior orientation defines the position of the perspective centre relative to a reference system in the camera, i.e. the image coordinate system, as well as the departures from the ideal central project, i.e. image distortion. The most important parameter of the interior orientation is the principal distance, c . This is the distance between the image plane and the perspective centre (Luhmann et al., 2014). The determination of the inner orientation parameters is also referred to as camera calibration. The calibration parameters are estimated by the bundle adjustment, which is described below. Depending on the accuracy requirements and site conditions, the time and form of calibration varies. This could include a one-time factory calibration, annual check and a calibration either before or during object measurement/reconstruction (Luhmann et al., 2014). For this study the lab work in Chapter 4 allowed calibration to be integrated during object reconstruction, whereas the site work in Chapter 6 required calibration immediately before object measurement using a calibration object.

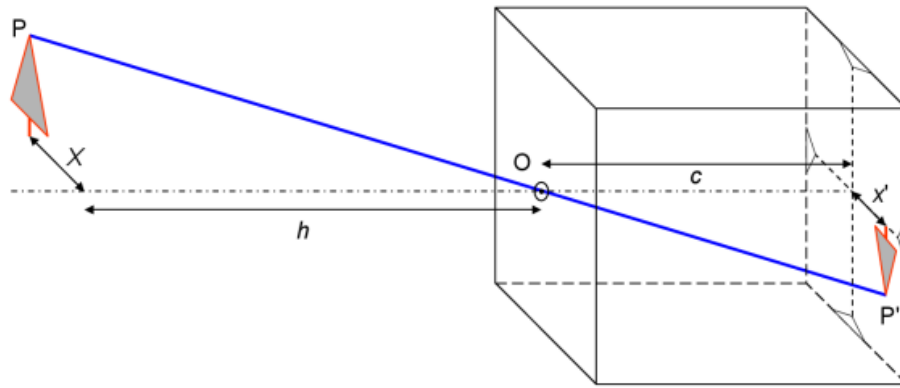


Figure 3.19: Pinhole camera model - image taken from Luhmann et al. (2014)

The exterior orientation parameters define the spatial position and orientation of the camera with respect to a global co-ordinate system. These are described as angles expressing the rotation of the image co-ordinate system with respect to the global system and are calculated indirectly, after image co-ordinates of the object points have been measured (Luhmann et al., 2014).

The measured image points correspond to a spatial direction from the projection centre to the object point. The length of the direction vector is initially unknown as every object point lying on the line of the vector generates the same image point. The object point can be located on the image ray. As a result every image generated a spatial “*bundle of rays*”, which is defined by the imaged points and the perspective centre (Luhmann et al., 2014). Once these bundle of rays from multiple images are intersected, a dense network is created a bundle adjustment can be applied. This is termed as an over-determined system of equations which allows an adjustment technique which is used to simultaneously estimate the 3D object co-ordinates, interior and exterior orientation parameters as well as statistical information about the accuracy and reliability. The most widely used adjustment technique used is least squares estimation (LSE). This type of adjustment is also used for estimating unknown parameters in a network of observations from geodetic techniques, such as total stations. The process is described in more detail in section 3.3.

3.2.4.1 CRP targeting

As with most geodetic observations, targets are required to measure locations on an object. In CRP they can be used to measure control or reference points which allows the image scale to be determined when producing object co-ordinates. It also allows automatic point identification and measurements as well as accuracy improvement,

especially when object feature points cannot be identified accurately on natural features.

There are many different target types and sizes which are dependent upon the image configuration, such as the viewing directions, image scale and resolution as well as the illumination levels available. The most typically used target type is the retro-reflective target which is circular in shape and consists of retro-reflective material, similar to the retro-reflective target centres used with TLS systems. The retro-reflective targets must be well illuminated to allow a high contrast in the images. Figure 3.20 shows the mixture of circular retro-reflective target types used in this study for calibration purposes.



Figure 3.20: Retro-reflective photogrammetry targets

Whilst the use of targets in CRP is established as an accurate, precise and reliable measurement technique (Luhmann et al. 2014), its use to generate point clouds from natural features is highly dependent on the image quality of those features and the geometry of the network of images captured during the survey. All image-based methods rely on the identification of common points or regions in two or more views with automated matching algorithms determining homologous location. Local image texture is essential for successful matching between images (Baltsavias, 1991). In structural monitoring applications, which often happen in dark cluttered environments, key challenges centre on image geometry and image quality. Image geometry requires careful selection of camera views to make sure that every feature appears on at least two convergent views. Image quality is highly dependent on being able to illuminate all of the features of interest at the time the photography is taken, for example the arches imaged in Chapter 6 were illuminated by electronic flash.

The development and widely accessible software for image matching and 3D reconstruction has provided an ideal opportunity to investigate an “ad hoc” method of

acquiring a point cloud without the use of targets and comparing it to the output of TLS to investigate its potential as a monitoring tool for this environment. One such example is Structure-from-Motion (SfM) which has been applied to a variety of applications, such as heritage imaging and archaeology (Hess, 2015), as an alternative to using the more expensive and less portable TLS system. SfM algorithms were developed to allow automatic generations of 3D models from unordered image collections. The approach requires multiple images of an object or scene from different camera positions. Simultaneously the camera parameters and orientations can be calculated through feature detection and full pairwise image matching. This then allows a sparse 3D reconstruction point cloud of the object. Dense reconstruction is then applied using multiview stereo (MVS) which efficiently filters out noisy data and increases the number resolution of the point cloud by two or three orders of magnitude (James and Robson, 2012). Despite a dense 3D reconstruction, the point cloud does not have any scale or geospatial information. Therefore control measurements of the scene are required, which can be easily obtained before or after image acquisition by using a total station, for example. Another method of applying scale would be to have a scale bar in the scene of a known length.

There are different open source solutions that carry out SfM. This study uses Visual SFM⁹ which is able to carry out feature detection and full pairwise image matching along with a bundle adjustment. Its relatively friendly user interface allows non-experts in the field to automatically produce a 3D point cloud of an object. SfM is capable of producing comparable levels of point cloud quality to TLS but requires significant post-processing in comparison to TLS, e.g. Riveiro et al. (2013) and Westoby et al. (2012). Unlike TLS, which is a polar measurement technique, CRP will fail when a feature of interest is only visible in one image due to occlusion in other images in the network. These aspects are encountered and discussed in Chapter 6.

3.2.4.2 CRP & deformation monitoring applications

Luhmann et al. (2014) discuss how CRP can be applied for deformation monitoring, particularly in environments with access and time restrictions. Traditionally the areas to be monitored are targeted within a stable network that contains multiple reference points. CRP has the advantage of rapidly capturing a surface from a low cost mobile

⁹ URL: <http://ccwu.me/vsfm/index.html> (last accessed September 28th 2015)

camera to generate single points or to generate a point cloud for monitoring to be carried out. Maas and Hempel (2006) discuss how the techniques of digital photogrammetry allow a valuable option of measuring displacements or deformations, particularly due to the highly automated data processing as well as high precision capabilities.

Literature shows examples of applying CRP successfully for structural monitoring at different scales, from monitoring hair cracks on 10 x 10cm textile reinforced probes up to the measurement of structural deflections of complex buildings (Maas and Hempel, 2006). Due to time and cost restrictions, components of bridges tend to be tested which has led to multiple tests on elements such as beams and columns. Whiteman et al. (2002) showed that vertical deflections of a concrete beam could be measured with a precision of $\pm 0.25\text{mm}$ at 1σ . The main advantage was the 3D deformation information compared to a contact sensor such as linear-variable-differential transformers LVDT, which provides 1D information. It also showed the “unrestricted” measurement range compared to the LVDT. Jiang et al. (2008) provide a comprehensive list of examples from previous work that successfully employed photogrammetry to measure cracks, deflections and deformations of bridges providing sub-millimetre levels of precision. The authors emphasise that the availability of inexpensive off-the-shelf cameras and photogrammetry software has made CRP more affordable and feasible for bridge engineering applications. However CRP does not appear to be a popular approach despite successful demonstration of it on sites and comparable levels of accuracy to conventional surveying methods.

Lee and Basset (2006) described how CRP was used to measure strain of a model tunnel in 2D using the displacement co-ordinates photogrammetric targets. The method provided reliable and precise data at the micron level when circular retro-reflective targets were used. With the development of technology and reduction in cost of digital cameras and equipment, Alba et al. (2010) were able to monitor a real tunnel cross-section for changes in its shape using CRP. The results demonstrated a sub-millimetre level of accuracy for measuring a tunnel approximately 12 m wide which compared to the total station results, providing a cheaper solution with respect to instrumentation costs. However multi-epoch analysis showed issues relating to the stability of the camera and its calibration.

This study looks at the removing the need for attaching targets to a structure that requires monitoring and explores the potential of applying SfM. Despite the uptake of SfM photogrammetry in many different applications, there is no known literature relating to SfM specifically relating to structural monitoring, particularly within a railway environment. One of the reasons could be due to the significant amount of post-processing required, particularly compared to producing a point cloud from TLS. Westoby et al. (2012) found that despite the data acquisition time using SfM being half of that compared to TLS, producing the geo-referenced dense point cloud took six times longer compared to TLS. The resolution of both datasets were comparable and consisted of sufficient resolution in order to reveal bedrock structures.

Even though SfM doesn't require targets for the image matching procedure, the initial output doesn't contain any scale information. This requires further measurement or the presence of scale bars/ ground control points to ensure the metric accuracy of the point cloud, which in turn allows accurate deformation monitoring. Golparvar-Fard et al. (2011) scaled the SfM point cloud using a measuring tape and concluded that the SfM point cloud accuracy was less than the TLS point cloud and recommended that TLS should be used for accurate survey requirements. However the authors did suggest that SfM was useful in applications such as "performance monitoring" of a construction site to understand the project status or even a post-disaster site where access is restricted and hazardous. This study looks further into analysing and comparing point cloud quality between TLS and SfM point clouds in the laboratory (Chapter 4) and site environment (Chapter 6).

3.2.5 Laser trackers

A laser tracker is typically used in high precision metrology applications where there is a need for high accuracy and precision of measurements. This tends to be on large free-form surfaces, for example aircraft wings during their alignment, in order to produce high-precision and range measurements of accuracies at the sub-millimetre or better level. Laser trackers are not typically used for engineering surveying monitoring due the smaller volume of measurement space. For example, the AT401 laser tracker, according to the manufacturer's specification, has a maximum measurement range of 80 metres. Although in practice this was found to be approximately 50 metres (see Appendix A), whereas a total station can measure ranges of the order of a kilometre. The laser tracker tends to be used in the laboratory environment where environmental

factors affecting the measurement can be controlled. This instrumentation also tends to be a lot more expensive than a total station and is comparable to a high-end laser scanner.

It is only recently that laser trackers have become more portable and even have a similar appearance to a total station, as evidenced by Figure 3.21.



Figure 3.21: State of the art total station (left) and laser tracker (right)

As well as the appearance, the measurement concept is similar to the total station, where angle encoders are used to provide horizontal and vertical angle measurements. The range or distance is typically measured using an absolute optical ranging-measuring technique or interferometry. The laser tracker used in this study, the Leica Absolute Tracker AT401, contains an absolute distance meter (ADM) which produces a much higher level of accuracy compared to the total station, with a distance measurement accuracy of 0.01mm. Laser trackers are a contact measuring technique and require the use of a target. They use a directed laser beam to measure 3D coordinates of a specialised target called a retro-reflecting corner cube (Luhmann et al., 2014). The corner cube is typically mounted in a spherical housing and referred to as an SMR (spherically mounted retro-reflector), which is shown in Figure 3.22.



Figure 3.22: Example of SMR target

The instrument can be setup on a tripod or stand to measure a set of individual points. They can also be used to carry out dynamic tracking of moving objects, for example tracking the shape of a deforming object, as long as SMR targets or tooling balls are attached.

Based on the similar measurement processes to a total station and the capability of measuring to a network of different target types using nests, the laser tracker allows the potential of a gold standard of an order of magnitude or better than a total station. This baseline measurement allows a comparison between the total station measurements to be made. There are no known methods of this application within engineering surveying. Chapter 4 provides a method of using a laser tracker to test the performance of different total stations with varying calibration histories using long established standardised methods in industrial metrology ((VDI/VDE 2634), which is explained in more detail in section 3.3.3.2. This work has led to a key contribution to this thesis.

3.2.6 Summary of engineering surveying measurement techniques

It can be seen that surveying instrumentation has developed over time, and continues to evolve towards more accurate and more automated solutions. For example, automatic levels have gone from being a rather manual process whereas more recently digital levelling has allowed measurements to be read and processed automatically and precisely do determine the change in height. Total stations were developed based on angle and range measurement tools to allow an instant 3D co-ordinate to be measured. Once total stations were produced their development has continued; the ATR functionality has introduced the automation of data capture process up through improved target measurement accuracy; only recently a hybrid scanning total station has been produced which allows an improvement of target measurement accuracy as

well as the capability of surface measurements. A laser tracker has also evolved towards a total station setup whilst providing measurement accuracy and precision to an order of magnitude higher than a total station.

Terrestrial laser scanning is able to automatically pick up a surface measurement without the use of a target. However the biggest challenge is overcoming the single point accuracy which is currently lower than a total station. However, as instrumentation provided by the manufacturer is becoming faster and more accurate, the application of TLS is starting to have an impact on the deformation monitoring industry. There are uncertainties with TLS measurements to different surfaces and there is a demand of a “surface library” to gain an understanding of the interaction between the laser and various surfaces.

The concept of photogrammetry dates back to using photography to record a scene from a camera. Aerial photogrammetry has been well established in order to carry out topographic surveys in order to produce contour maps. Since that time the technique has moved forward rapidly paralleling advancements in computer processing technology and the move from photographic systems to digital sensing. A significant part of CRP is the reducing cost of accessibility to the technique as imaging sensors have become consumer items and advances in fully automatic processing have enabled users with an internet connection to produce 3D data from images.

The development of automation and accurate non-contact surface measurement that TLS and CRP provides excellent potentials for a targetless deformation monitoring approach required by this study. The next section describes the data processing methods required to produce accurate information from the measurement acquisition process.

3.3 The role of network adjustment

3.3.1 Network design

Any type of survey, including a deformation monitoring survey, is designed, measured and computed for a particular purpose. Therefore any survey executed will vary by method and costs depending on its purpose. Consequently a selection process of the methods, number of measurements, types of instruments and procedures to be used must be carried out. This process is known as network design.

It is important that this stage is “*distinguished from the execution of the survey which is carried out as a result of the design*” (Cooper, 1987). Once the survey has been completed it is important to see whether or not the survey has met the criteria and whether it was fit for purpose. As described in Chapter 2, there is little evidence of network design being carried out on monitoring network surveys on the Thameslink Programme (TLP). The lack of this makes it harder from an assurance point of view when establishing whether the monitoring specifications have been met or not.

In general, for assessing the quality of network design the following things need to be considered: economy, precision and reliability. Economy is expressed as the cost of carrying out the observations; precision is expressed as the measure of the network’s capability in propagating random errors (expressed by the *a posteriori* covariance matrix of the co-ordinates); reliability describes the ability of redundant observations to check errors (Grafarend et al., 1985). Network quality is described in more detail in 3.3.3.2.

For deformation monitoring networks it is important that the aforementioned is considered as well as the expected levels of displacements and the accuracy requirements from the system. At TLP the expected displacement levels are communicated in the form of a zone of impact map of the site with contour levels of movement expected over the project lifetime. The accuracy requirements are then specified by the geotechnical engineers which is based on the levels of movement expected. However, in reality the expected displacement and accuracy requirements are not always known in enough advance of the monitoring deployment which makes the design and planning process difficult, especially when trying to be economic. At Network Rail apart from specific track monitoring specifications (see Chapter 2) there are limited standards with regards to monitoring different types of infrastructure during a project, for example arches, viaducts, embankments and so on. This is due to each environment or scenario being very different from project to project. Despite limited information on the expected deformation levels and accuracies, it is important that a network design is carried out to provide some sort of indication of the performance of the network and whether it is fit for purpose. Grafarend et al. (1985) describe how the analysis of deforming networks with a weak design results in difficulties in discrimination between a measurement error and a displacement of a network point.

In order to achieve the outputs desired from a deformation monitoring network, the process of network design is crucial. In order to solve for all these aspects of network design simultaneously, a well-established classification method consisting of 4 steps can be used (Grafarend et al., 1985):

- Zero-Order Design – searching for an optimal datum or co-ordinate system
- First-Order Design – optimising the location of the points and observation plan (provided the precision of the observations is known)
- Second-Order Design – the optimal distribution of weight to the observations in a fixed configuration
- Third-Order Design – optimal improvement of an existing network or existing design by adding additional points or observations

Substantial work has been carried out in order to develop tools to apply these steps for network design through a simulation process. The development of simulation methods for network design is not within the scope of this research, but more information can be found in Kuang (1996).

3.3.1.1 Pre-analysis

Network design can be facilitated by carrying out a pre-analysis. This allows a design of the network to be simulated to allow modifications in the network to achieve the requirements of the monitoring network without having to physically go and take measurements on a site/have actual observations. This is particularly useful for deformation monitoring where there are monitoring requirements in terms of accuracy that need to be achieved. There are different types of software packages that have been developed by authors as well as ones that are commercially available to carry out a pre-analysis (Setan, 1997; Bird, 2009). A widely known and commercially available software package used in the surveying industry that has pre-analysis capabilities is called STAR*NET, which has been developed by MicroSurvey¹⁰. It is typically used for applying a rigorous network adjustment using levelling, total station and GPS observations through least squares estimation. Network adjustment and analysis is described in more detail in section 3.3.3.

¹⁰ URL: <http://www.microsurvey.com/products/starnet/> (last accessed 21st September 2015)

The pre-analysis function allows the user to modify network configurations such as instrument and target locations, the number of measurements taken as well as the type of each observation being inputted into the network (e.g. distances, angles, heights). It also allows the effect of different grades of instruments, for example total stations with differing angular and distance accuracies, to be compared. This comparison tool is particularly useful for designing a monitoring network to allow an economic and precise monitoring design scheme to be established. STAR*NET, through least squares estimation, analyses the geometric strength of the network using the approximate instrument/target positions as well as the instrument accuracies that are supplied, which are sourced from the manufacturer's specification. Therefore this type of network design assumes that an instrument is within calibration and performing as expected based on the manufacturer's specification. In reality, there are errors present either in the instrument or observations which must be corrected for in order to produce accurate measurements. The different type of error sources and methods of eliminating them when applying network adjustment is discussed further in section 3.3.2.

The predicted accuracy of each of the monitoring target positions can be analysed based on the computation of the error ellipses for that particular target/station. An error ellipse provides a representation of measurement uncertainty and is derived from elements of the covariance matrix of the estimated co-ordinates (described in detail in section 3.3.3.1). An example of an error ellipse in relation to the estimated station co-ordinate (Point A) is shown in Figure 3.23.

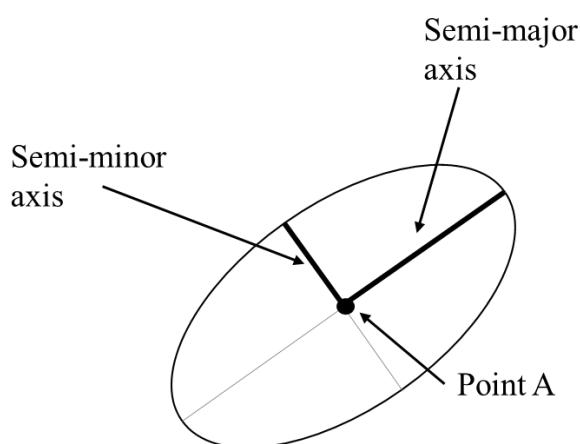


Figure adapted from MicroSurvey STAR*NET (2014)

Figure 3.23: An example of an error ellipse

The size of the ellipse is a measure of the precision of the computed point position, i.e. a smaller ellipse means that the point has greater precision than a larger ellipse. The outputs from STAR*NET provide the dimensions of the ellipse, i.e. the semi-major and semi-minor axes. The relative sizes provide an indication of which points in the network are weaker than others. The shape and orientation of the ellipse indicates how the network can be strengthened. For example, an elongated error ellipse represents a larger uncertainty in one of the co-ordinates. This could be improved by an additional set of angle or distance measurements to that station. A circular ellipse means that the point is balanced in X and Y. For general design purposes the main objective is establishing where the uncertainty is at its best and worst; ideally all uncertainties would be in the same direction. Overall key information can be gained from error ellipses via their variation in size and direction (Kyle et al, 2001). Once the station/target co-ordinate error ellipses through the design are within the tolerance of the monitoring accuracy requirements, the pre-analysis and network design is complete. The design can then be used to compare to the results from the actual network measurements. An example of applying network design of an existing monitoring network on TLP to see if it is fit for purpose is shown in Chapter 6.

3.3.2 Outlier detection and system calibration

As stated earlier, network design is based on the assumption that the instrumentation being used to take observations is performing as expected. For example, when implementing the pre-analysis tool in STAR*NET, the input instrument parameters for network design are usually derived from the manufacturer's specification. However, in reality, there are different types of errors that can occur when carrying out measurements. Due to human, instrumental and environmental factors the observation data is prone to gross, systematic and random errors. The LSE process provides residuals which can contain all these error types. In order to remove these errors, assumptions of the stochastic properties of the residuals must be made and corrected for. In this case an outlier is defined as a residual (i.e. the difference between the estimated value of the observation and its corresponding measured value) (Casparly and Rüeger, 2000) and outlier detection can be checked using different statistical techniques, of which some are described below.

3.3.2.1 *Gross errors*

Gross errors are also known as blunders and are considered as errors of a large magnitude. These are mainly caused by inexperience of the observer or misinterpretation of the results. For example, misreading a levelling staff or sighting to the wrong target will produce a blunder. Standard survey practices have been designed to allow for blunders to be detected and rejected. For example, repeating measurements several times allows any values significantly different from the mean to be detected (Kuang, 1996; Uren and Price, 2010). In photogrammetry gross errors could include incorrectly numbering images or errors in point identification. Baarda's Data Snooping test can be used as a method of removing gross errors, however it is based on the assumption that only one gross error exists at any one time (Casparly and Rüeger, 2000). Once the observation has been eliminated the LSE procedure is re-run and can be repeated until there are no gross errors present in the observations. For this study, along with ensuring redundancy in the observations, the blunder detect tool in STAR*NET was used to detect gross errors.

3.3.2.2 *Systematic errors*

Systematic errors are those which follow a pattern or mathematical law that may take the form of a constant. They tend to have the same magnitude and sign in a series of measurements. The main issue is that the systematic error is part of the measurement until a procedure is applied to remove them. A simple example of systematic error with a total station is the prism constant. If this is ignored, it is an error that will be present in all the observations. This could have a knock-on effect, particularly for deformation monitoring observations, where observations could be perceived as movement, when in fact there is an instrumentation error present.

In order to minimise systematic errors in observations, it is essential to carry out instrument calibration. Calibration allows error modelling and corrections to be made to the proceeding observations. It is recommended that full calibration is carried out by the manufacturer for a total station, however due to transportation of the instrument, mechanical shock, temperature changes and general wear and tear of the instrument, it is critical for a total station to be checked regularly. Methods of instrumentation checks, such as horizontal/vertical collimation, tilting axis error and ATR collimation, are described in Uren and Price (2010). Newer state of the art instruments can carry

out electronic self-calibration on board the total station using these well-established technique to measure and correct for systematic errors.

Since the commercial release of TLS systems, work has been carried out to model systematic errors present in TLS systems to allow a self-calibration procedure to be applied independently of a manufacturer (Lichti et al, 2000; Reshetyuk, 2006; Al-Manasir and Lichti, 2015) in a similar manner to a total station self-calibration. These include producing models for systematic errors of parameters such as range accuracy and precision, single point accuracy and precision as well as elevation angle. As well as thorough experimentation, correction models have been based on similarities to other surveying instrument construction, e.g. total stations and cameras when being used for photogrammetry. Newer TLS systems from Leica Geosystems, such as the ScanStation P20, have a self-calibration function on-board the instrument to carry out checks by placing targets around a scene in certain positions to carry out specific parameter checks, e.g. angular parameters.

3.3.2.3 *Random errors*

Random errors are errors which do not follow a pattern and are not constant. They cannot be removed from observations but statistical principles can be applied to analyse them. Generally it is assumed that the random errors in observations within surveying follow a normal distribution. One of the statistical testing procedures to check if the residuals from the LSE are due to random errors in the observations, i.e. are normally distributed, is the Chi-Square test (χ^2). It provides a method to test the “goodness of fit” of the random error in the observations to a normal distribution. The χ^2 value can be compared by:

$$\chi^2 = \sum_{i=1}^k \frac{(O_i - E_i)^2}{E_i}$$

Where O is the observed value and E is the expected value. The χ^2 value that has been calculated can then be compared to values obtained from a chi-squares distribution table. The confidence level of 95% for network adjustments is usually carried out with a two-tailed test. If the test passes, the null hypothesis is accepted which means there are no systematic or gross errors in the observations and the random errors are normally distributed. However if the test fails, the data is thought to contain non-random errors, i.e. systematic errors or blunders, and further inspection and testing of

the observation data is required. This type of test is available within the STAR*NET adjustment package where the confidence levels can be adjusted based on the project requirements. Another example of where the Chi-Square test is applied in this thesis can be found in Chapter 5, where residuals from plane fitting of a section of planar point cloud of track is plotted to see whether there are any systematic errors present in the data.

3.3.3 Deformation analysis of networks with redundant measurements

Deformation analysis can be applied on 1D, 2D and 3D monitoring networks. When using geodetic methods for deformation analysis, particularly for engineering applications, it is typical for a two-step process to be applied (Setan and Singh, 2001):

1. Independent adjustment of the network of each epoch
2. Deformation detection between the two epochs

For geodetic measurements – especially total station observations – the first step, i.e. the adjustment process, generally involves least squares estimation (LSE) of each epoch (Setan, 1995; Choudhury et al 2009). This is described in more detail in section 3.3.3.1. Once the adjustment has taken place it is important to check for any outliers in the observational data that may be affecting the quality of the output of the adjustment. A very brief overview of the different errors present in observations as well as methods to remove them was provided in section 3.3.2. The process of outlier removal is an iterative one and can be removed through each iteration of LSE. Once outliers have been removed, it is important to understand the quality of the network before any deformation detection takes place between two epochs. An overview of investigating network quality is described in 3.3.3.2. The second step is typically carried out by calculating the changes in co-ordinates between the epochs (Caspary and Rüeger, 2000; Setan, 1995).

Networks that have a higher number of observations than the unknown parameters are termed as networks with redundant measurements, where the number of degrees of freedom is the number of observations minus the number of unknown parameters. Examples of these redundant measurements can be derived from geodetic observations and photogrammetry, for example a combination of angle and distance measurements using a total station (as discussed in 3.2.2) and the dense network of “bundle of rays” in photogrammetry (discussed in section 3.2.4). As there are redundant measurements in both of these cases there is no unique solution for the unknown parameters and these

can be estimated based on functional and stochastic models using least squares estimation (LSE) to determine 3D co-ordinates.

3.3.3.1 Least squares estimation

LSE is a well-established adjustment method in surveying. The redundant set of measurements are useful for 3 reasons: checking for gross errors/outliers; providing the precision of the co-ordinates; gaining an insight into the quality of the network together with statistical information about accuracy and reliability. These are well established measures within the surveying industry and are described throughout this section.

The functional model relating the measurements and parameters to be estimated can be expressed as:

$$\mathbf{l} = f(\mathbf{x})$$

where l is the vector of the observations and x is the vector of the parameters to be estimated. The functions of the equation are non-linear. Using Taylor's theorem (Caspary and Rüeger, 2000), a linearised form of the observation equation can be written in matrix form as:

$$\mathbf{l} + \mathbf{v} = \mathbf{A}\hat{\mathbf{x}}$$

where \mathbf{A} is the design matrix, which consists of the derivatives which describe the functional relation between the unknown parameters (which are calculated from the approximate values). $\hat{\mathbf{x}}$ is the vector of unknown parameters, \mathbf{l} is the vector of the observations and \mathbf{v} is the vector of the residuals (Caspary and Rüeger, 2000).

The stochastic model is defined by the covariance matrix, C , because it is the only component that contains information about the accuracy of the observations during the adjustment process. It is determined based on the standard deviation of the observation (σ_i) and the correlation coefficients between the observations (ρ_{ij}). Further details on deriving the covariance matrix can be found in Caspary and Rüeger (2000), Setan (1995), for example. It is useful when determining the quality of the observations once LSE has been applied – see section 3.3.3.2.

The weights of the observations, based on the standard deviation, produce the weight matrix, \mathbf{P} . For observations considered to be equal in accuracy, the weights are simplified to $p_i = 1$ (Luhmann et al, 2014). For observations with varying accuracy,

the corresponding weights are estimated from the a priori standard deviations of the original observations (s_i) and the observation of unit weight (s_0) where $p_i = \frac{s_0^2}{s_i^2}$ for observation i .

The least squares estimation method, also known as the Gauss-Markov linear model, is based on the idea that the unknown parameters are estimated with maximum probability. It makes an assumption that there are no gross or systematic errors in the observations in order to calculate the residuals:

$$\mathbf{v}^T \cdot \mathbf{P} \cdot \mathbf{v} \Rightarrow \min$$

Therefore for each observation, i , there is one equation which is adjusted using the LSE procedure:

$$v_i = \hat{x} - l_i$$

LSE is an iterative process that is performed until corrections to the parameters become insignificant, i.e. minimising the sum of the squared residuals (Mikhail, 1976).

A very brief overview of the LSE method for network adjustment has been provided here, however a more detailed description of the process can be found in many geodetic network observation/analysis books such as Mikhail (1976), Cooper (1987), Setan (1995) and Capsary (2000).

3.3.3.2 *Network quality*

Once the network has been adjusted and screened for observational errors, the quality of the network and assessment of the achieved accuracy is important, particularly when carrying out deformation analysis. As stated in section 3.3.1, the quality of a network is described by precision, reliability and economy. This research focuses on the precision and reliability of the observations to ensure that any errors in the data are not misconstrued as deformation, whilst achieving the objective with a minimum instrument and human effort/cost.

Network precision measures

Network precision describes how the precision of the observations affects the results through the network geometry. It provides a measure of the network's characteristics in propagating random errors, with the assumption that gross errors and/or systematic errors have been removed (Kuang, 1996). A precision measure can either be local or

global, where local precision measures focus on a specific set of points in the network and global measures refer to the whole network. This thesis uses local precision measures when assessing the quality of the network. Generally the variance and covariance matrices, derived from the LSE process, provide these precision measures. There are many aspects of network precision and the main ones widely used in the surveying community are discussed here.

In a 2D network an immediate local measure of accuracy is the standard deviations of the co-ordinates (σ_x and σ_y) which can be readily computed using the variance (σ_0^2)

$$\sigma_x = \sigma_0 \sqrt{q_{xx}} \text{ and } \sigma_y = \sigma_0 \sqrt{q_{yy}}$$

Where cofactors q are the diagonal elements of the covariance matrix. Standard deviation of the station co-ordinates provide the uncertainty in the computed co-ordinates, typically at 1σ .

Alternatively to the standard deviation a root mean square value (RMS) can also be reported. It is the square root of the arithmetic mean of the squares of a set of numbers/sample. In this case the set of numbers are the differences between the measured and nominal values (residuals). This is frequently used as a precision measure output when fitting a geometric primitive to a point cloud using LSE, e.g. plane, sphere, and cylinder. This study uses the RMS as a precision quality measure when applying plane fitting to point clouds obtained from TLS and CRP point cloud data when measuring to the track and brick surface in the laboratory (Chapter 4). When applying plane fitting in this study, an open-source point cloud analysis tool, CloudCompare¹¹, is used to calculate the RMS as well as extract the residuals. Further details of this process is provided in Chapter 4.

A well-established method of visually displaying the precision of a network is by plotting error ellipses, which was briefly described and shown in section 3.3.1.1. Error ellipses represent the area of uncertainty around a given points; they can be absolute (referring to the uncertainty of one point) or relative (referring to the uncertainty between two points). They are generalisations of the standard deviations derived from the LSE process. The semi-major and semi-minor axes are functions of the eigenvalues

¹¹ URL: <http://www.danielgm.net/cc/> (last accessed October 2015)

and eigenvectors, which is a fundamental approach to the analysis of the covariance matrix. The interpretation of the size and shape of error ellipses is also provided in section 3.3.1.1. Detailed material of all the matrix and precision measure computations that have been very briefly described here can be found in Kuang (19996) and Caspary and Rüeiger (2000).

Packages such as STAR*NET provide precision quality measures such as standard deviations of the computed cop-ordinates as well as plots and geometric information of relative and absolute error ellipses in the output listing once the adjustment has taken place, where confidence levels can be adjusted by the user according to the application.

Network reliability measures

Network reliability describes how a network reacts to small biases in the observation data. It denotes the robustness of the network and its ability to resist undetectable gross errors in the observations. The concept of network reliability originates from Baarda (1968). There are two types of checks for reliability in a network: internal and external. Internal reliability is associated with the ability of a network to detect gross errors by tests of hypothesis made with a specific confidence level, whilst external reliability is related to the effect of undetected gross errors on the LSE (Kuang, 1996). As stated earlier, in order for LSE to work effectively the data needs to be free of any gross or systematic errors and therefore many techniques for “data screening” pre and post-adjustment have been developed. For example the “blunder detect” function in STAR*NET attempts to isolate observation with blunders by successively deweighting the observations that do not fit into the network. Further reading of network reliability can be found in Caspary and Rüeiger (2000) and Kuang (1996). Once the outliers have been detected, they can be removed and the adjustment can be re-run to improve the output residuals.

Accuracy measures

Accuracy “*describes the closeness of agreement between a result and a measurement standard or accepted reference*” (Luhmann et al, 2014). Therefore accuracy measures can only be used if a comparison or reference data of higher accuracy is performed. In order to establish whether a measuring system is achieving its accuracy, there are long established standardised methods in industrial metrology (VDI/VDE 2634). These are

usually applicable to co-ordinate measuring machines (CMMs) and instruments with optical sensing heads. One of these tests is called length error. The length error, E , is the difference between a measured (displayed) length L_m and the calibrated reference length L_r :

$$E = L_m - L_r$$

The length error can be used to analyse the accuracy of a length measurement (Luhmann et al, 2014). In Chapter 4 the length error is used to test the accuracy of total station instrumentation in the laboratory where the calibrated reference length is sourced from a laser tracker, which has a much higher instrumentation accuracy, usually by an order of magnitude.

3.3.3.3 *Detection of deformation*

Another rigorous method has been established for estimating the point group displacements in a monitoring network, termed congruency testing (Setan and Singh, 2001). The objective of the test is to detect whether or not the point group being considered for deformation has remained stable. The point group can consist of all points common between epochs, points establishing the reference points or those belonging to a specific part of the network (Caspary and Rieger, 2000). The procedure of congruency testing is not within the scope of this thesis but further reading can be found in Setan (1997). Once congruency testing has passed, modelling of deformation can be applied.

As described at the beginning of this section a two-step analysis is usually applied to deformation analysis. Once adjustment has been carried out on each epoch independently, the detection of displacement between the two epochs can be applied. There are different deformation models which can be used based on geodetic observations including from total stations and photogrammetry. These include measuring the differences in 1, 2 and 3D co-ordinates, spatial distances, azimuths and zeniths. Depending on the requirement of the monitoring scheme, the most appropriate deformation model can be applied to the observations (Caspary and Rieger, 2000). Setan and Ibrahim (2003) developed a tool for integrating the output from STAR*NET and an in-house deformation detection software for 2D and 3D, in which error ellipses are shown in 2D. The workflow is shown in Figure 3.24, where the output from STAR*NET is fed into the main menu of DEFORM99 (the deformation detection tool).

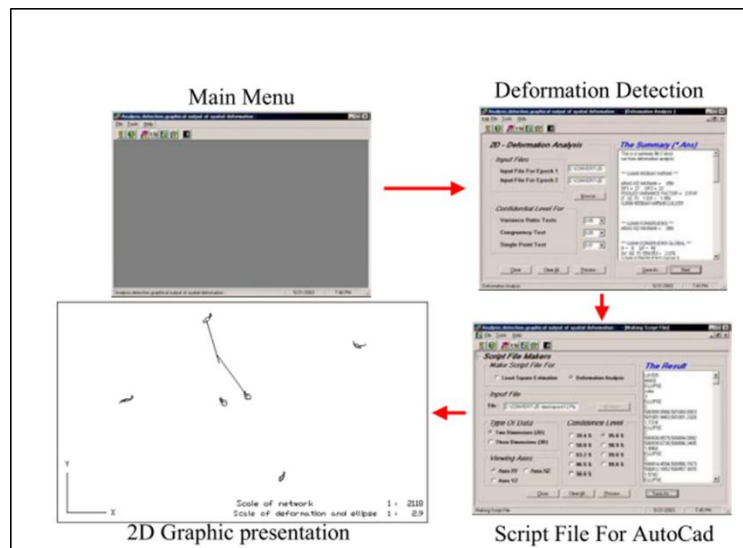


Figure 3.24: Bespoke deformation detection tool developed by Setan and Ibrahim (2003) – image taken from this paper

Currently at London Bridge Station the method of deformation detection in the masonry arches at London Bridge is to calculate the X,Y and Z co-ordinates and compare these individually to the measurements of the same target from epoch 0, i.e. the baseline measurement. For track monitoring, the cant and twist is extracted based on a combination of the Z height difference and distance between the tracks (see Chapter 2). Despite this process of “deformation detection” there is little evidence of data analysis to gain an insight into the data quality, e.g. a network adjustment with relative error ellipses (see section 3.3) for each of the monitoring points measured¹². However when comparing this to other monitoring schemes applied in the railway industry, there is evidence of network adjustment being applied to automatic monitoring measurements using total stations.

Berberan et al (2007) were able to provide an automatic, robust and accurate computation of deformation of a tunnel in Lisbon that had been damaged during its construction, using four motorised total stations. Due to the limitations of a thorough network analysis within GeoMos, EpochSuite (an adjustment software) was integrated into GeoMos, via the SQL database, in order to minimise error propagation as well as outlier detection (see section 3.3). Tse and Luk (2011) also carried out network design using a least squares adjustment tool for automatic monitoring of a tunnel in Hong

¹² Based on my attendance at monitoring meetings to implement a monitoring scheme as well as analyse monitoring data from the monitoring specialist

Kong during the extension. A recent example of a very large-scale monitoring network in the UK was at London Paddington Station, which was required during the construction of the new Crossrail station (see section 3.2.2.2). Different network designs were proposed and error ellipses of the monitoring points were produced to ensure accuracy requirements were met so that false triggers were not set off (Binder, 2014) . Despite worldwide evidence of network design for automatic total station monitoring in a railway environment, there is little evidence of this on TLP. One of the reasons for this is that the monitoring contractors don't always have background knowledge of engineering surveying, but instead have specialist skills in computer processing and handling large volumes of data. Therefore, this gap in knowledge has resulted in a monitoring system with unknown levels of quality with regards to the measurements taking place.

An informative workflow of a “best practice” network design and adjustment process with respect to deformation monitoring over a series of epochs is provided by Caspary and Rüeeger (2000) which is shown in Figure 3.25.

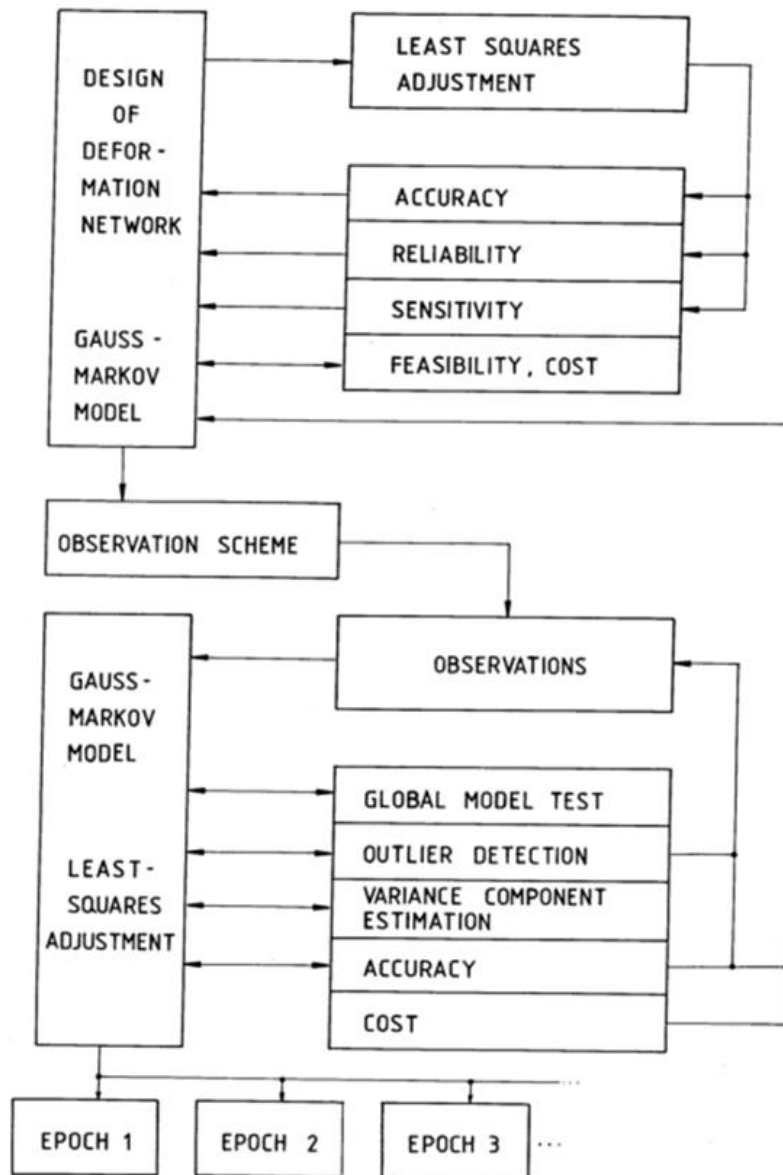


Figure 3.25: Flow diagram of network design and adjustments for deformation monitoring – taken from Caspary and Rieger (2000)

3.3.4 Deformation analysis of networks with single measurements

Compared to networks of observations with redundant measurements to points, the procedures for deformation monitoring (i.e. applying adjustment and producing quality measures etc) using single measurements to points is not possible. Therefore there is no built-in check if a blunder is made or if there are any systematic errors when measuring the angle or distance to a point. An example of this in surveying is radial traversing where a single distance and angle is measured from a known point to tie in another point. Although this method provides the ability to co-ordinate control points more quickly, it is only possible to check the results obtained between the points surveyed (Uren and Price, 2010). Therefore the quality of the measurements are purely

relying on the calibration of the instrument as there are no other ways of checking for errors of the measurements.

Another example of single point measurement is with TLS data where individual points are never exactly measured twice. However the technique does provide redundant information of the surface. The following section describes how this surface measurement can be exploited and tested for deformation.

3.3.4.1 TLS deformation analysis

It is typical for multiple scans to be used to measure the surface of an object or feature for deformation analysis. Therefore it is important that care is taken when applying point cloud registration to ensure the integrity of the data for the analysis process. As discussed in section 3.2.3.1, registration should be carried out accurately through either targeting, which allows a global reference system to be established, or through surface-based methods such as ICP (Besl and McKay). In this thesis, target-based registration to allow accurate geo-referencing to the site co-ordinate system is applied in Chapter 5 and registration between multi-epoch scans using the ICP algorithm is applied in Chapter 6.

Point cloud extraction

In order to utilise TLS point cloud data for applications such as monitoring, extraction and segmentation of the relevant features from the point cloud is an integral part of the data processing step (Lari and Habib, 2014). Vosselman et al (2004) state that typical man-made objects such as planes, cylinders and spheres are shapes that can be easily extracted from the point cloud based on their geometric parameters. Research into efficient and accurate point cloud extraction procedures has become a wide area of interest and is well reported (Schnabel et al., 2007; Awwad et al., 2010; Lari and Habib, 2014). An object such as a rail or assembly of objects such as a railway track could be segmented and extracted based on its planar elements by applying accurate local surface fitting. Popular plane fitting methods include least squares estimation (LSE), Principal Component Analysis and the RANSAC algorithm (Nurunnabi et al., 2012). Each method has its own advantages with respect to robustness, reliability and sensitivity to outliers. The approach used for the work described in Chapter 5 utilises the LSE method which, as described earlier in section 3.3.3.1, is based on the long established principle of minimising the sum of the squared residuals.

When exploring methods of deformation analysis there are generally two types of analysis: point-wise and object wise deformation analysis. Vosselman and Maas (2010) also describe change detection as a method of monitoring, however this type of monitoring is to purely detect whether a particular scene has changed over epochs, for example whether a car has been added or removed from a scene. On the other hand deformation analysis is aimed at quantifying the changes by modelling the parameters present in the scene and comparing them over time.

Point-wise deformation analysis

Point-wise deformation analysis can be divided into three different classes of comparison: measurement to measurement; measurement to surface; and surface to surface (Vosselman and Maas, 2010). A similar approach to these classes of comparisons is applied in Experiment 4 in Chapter 4 where the displacement of a brick surface is measured and analysed using different point-wise and object-wise (see below) techniques.

The measurement to measurement comparison requires the instrument, i.e. TLS system, to remain fixed and comparisons can be made using a “virtual target” to measure to a fixed horizontal and vertical angle with respect to a spherical co-ordinate system. This type of monitoring has been used for calculating volumes of mining excavations (Vosselman and Maas, 2010).

Measurement to surface comparisons are carried out by creating a surface of a baseline epoch (e.g. a triangular mesh) and comparing proceeding epoch scans, i.e. the points are compared back to the surface. This method allows fast computation of the differences between epochs excavations (Vosselman and Maas, 2010). An example of this method was explored by Alba et al (2006) where the shortest distance between a point from the scan and the surface of a baseline scan of a dam was compared (through a triangular mesh and polynomial surface). Even though displacement surface maps provided a dense and accurate representation of the deformation of the order of a few millimetres, the deformation rates were close to the geo-referencing and registration errors which affected propagated into the deformation analysis. It was recommended that TLS could be used for periodical monitoring whilst other sensors (levelling, TS and collimators) were being used for continuous monitoring. There are many tools

available that can be used to create surface meshes, e.g. Polyworks¹³, MeshLab¹⁴ and CloudCompare. In this study Geomagic Studio¹⁵ was used based on its capability of handling large volumes of data with large co-ordinates (i.e. geo-referenced to a site grid).

Surface to surface comparisons allow meshes of the surface to be compared over multiple epochs which enables noise and data reduction. The disadvantage of this is that further processing is required compared to the other comparison techniques. An example of this type of comparison was carried out by Lemy et al (2006) where the displacement of a tunnel was measured. By producing a surface mesh which allowed reduction in noise levels the scanner was able to detect movement with an accuracy of $\pm 5\text{mm}$ compared to the $\leq 1\text{cm}$ accuracy of a single point from the TLS system. However issues with generating differential elevation maps onto a stable reference system was encountered. A similar approach for comparing multi-epoch TLS surface scans is explored in Chapter 6.

Object-orientated deformation analysis

Object-orientated deformation analysis methods allow highly redundant measurements of a surface to be exploited to “counter-balance” the low precision of the single point measurement, compared to that of a total station. This is carried out by identifying primitive objects in a time series and parameterising their motion over time. Primitives include fitting planes, spheres, and cylinders to the point cloud surface which can be estimated using LSE. The main advantage of this type of method is the high quality of the deformation parameters of interest with respect to the quality of the original TLS data (Monserrat and Crosetto, 2008). However the main challenge for this type of analysis is identifying a suitable object to represent the point cloud. However, due to structures often conforming to geometric primitives, this has become a popular approach for structural deformation monitoring.

Gordon and Lichti (2007) fitted a simple polynomial to a beam, using principles of beam deflection, to detect vertical deformation. It was found that by modelling the surface of the beam, displacements with an accuracy of $\pm 0.29\text{mm}$ (at a range of 3 metres) could be observed. This proved that it was capable of high precision detection

¹³ URL: <http://www.innovmetric.com/en/products/polyworks-modeler> (last accessed October 2015)

¹⁴ URL: <http://meshlab.sourceforge.net/> (last accessed October 2015)

¹⁵ URL: <http://www.geomagic.com/en/> (last accessed October 2015)

to the same level as photogrammetry, as well as providing the extra advantages that TLS present. Gordon and Lichti (2007) emphasised the importance of the physical setup of the TLS and that it should be positioned to "maximise capture of the surface that would best represent the deformation". In a laboratory environment Laefer et al (2014) were able to detect cracks of a masonry wall that were 5 mm wide with a precision of 1mm by using plane fitting techniques. On a larger-scale Kopáček et al (2013) and Erdélyi et al (2014) were able to detect deformation of a bridge and roof respectively using planar surfaces by applying single value decomposition with an accuracy and precision in the order of a few millimetres. Puente et al (2012) used mobile TLS to evaluate geometrical deformations of a concrete arch shaped underpass by analysing the arch profiles to achieve deformation measurements between 1-5 mm. The application of TLS for measuring tunnel deformations and carrying out inspections during and after their construction has been applied using primitive fitting. Nuttens et al (2010, 2012 and 2014) have used state of the art TLS technologies (phase and time-of-flight based systems) to scan newly built concrete tunnels and monitor them over a period of time to determine their "ovalization" through calculating the best-fit of a cylinder on tunnel sections. The authors show that by comparing the point cloud to the CAD design model of the tunnel, millimetric levels of precision could be achieved and that sub-millimetre deformations could be detected and measured by combining TLS and strain gauge measurements. Another example of using TLS in a tunnel environment is presented by Koon et al (2009) where plane fitting was applied to detect defects in the concrete liner of a tunnel. By assuming small segments of the tunnel lining as planar, histograms of the residuals of the plane fit (applied through LSE) was used to detect physical defects. A similar process to this is used in Chapter 5 where plane fitting is applied to remove artefacts from the planar web of the railway track.

Recent examples of railway track monitoring analysis using TLS

When starting this study there was no known literature related to using TLS as a tool for monitoring railway track. However with the advancement of data acquisition and processing, investigation into the capabilities of TLS to accurately detect and extract rail track geometry for deformation monitoring has widened in the past two years and runs in parallel with the key contributions provided in this thesis.

Meng et al. (2013) present a laboratory method for extracting track from static TLS data to obtain 3D track reference geometry with the potential to calculate deformations from subsequent scans. Results showed a mean difference of 2mm in the horizontal and 3mm in the vertical between the ground truth and the mesh. However it is uncertain as to whether the model conforms to the physical form of the track. Liu et al. (2013) used static TLS to extract track geometry for deformation monitoring of high speed rail to achieve an accuracy of better than 3mm. Further analysis of these findings in relation to extracting track geometry using static TLS track in this thesis are described in more detail in Chapter 6. Overall it can be seen there is a consensus of achieving accuracies of better than 3mm, however there is a need to improve this level to fulfil the engineer's requirements for track monitoring.

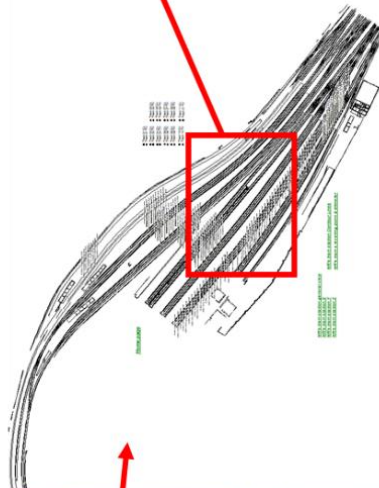
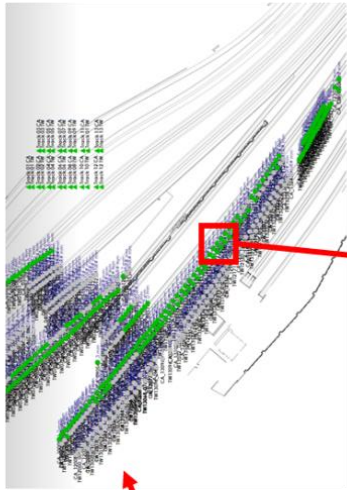
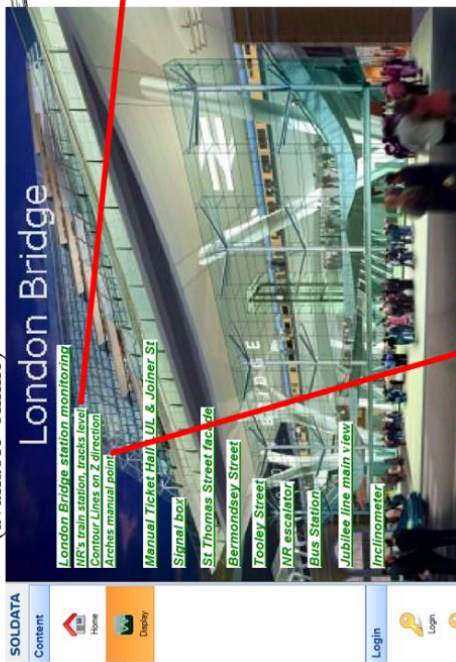
It can be seen that many different methodologies have been developed in order to use scan data from TLS for deformation analysis. Even though they can be categorised into point-wise and object-orientated deformation analysis tools, they are not as well-established as the network adjustment tools available for target-based monitoring. One of the reasons for this is that each structure required to be monitored is unique and that different tools could be used based on the shape and size of the object. However it is thought that through testing of different types of object, a library of surfaces and objects required to be monitored could be developed to allow users to determine which methods are most suitable. This study explores the measurement of brick and track surfaces, typically encountered in a railway environment, in order to detect deformation. The laboratory testing of these surfaces is investigated in Chapter 4, followed by large-scale testing of these surfaces on live monitoring sites in Chapter 5 and 6.

3.4 Data information and communication

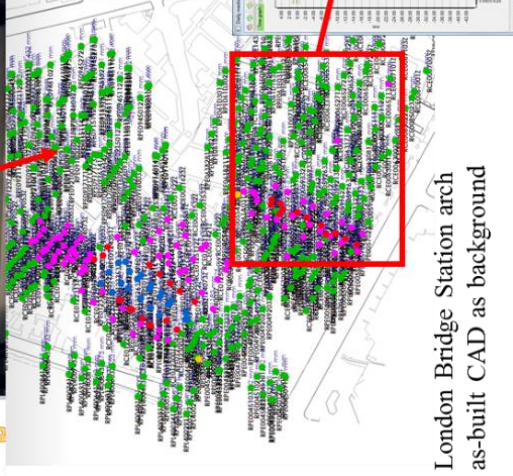
Once deformation measurements have been analysed they should be presented to the relevant parties (for example an engineer) in a suitable manner to allow them to inspect a structure or understand any patterns of movement. The deformation detection results can be presented through co-ordinate changes or displacements in 1, 2 or 3D using tables/spreadsheets or graph plots. For example, the monitoring contractor at London Bridge presents deformation data (from total station measurements) of the masonry brick arches as displacements in X, Y and Z or longitudinal displacements. The results are usually displayed with respect to an as-built CAD drawing of the area to provide

context to the engineer. In terms of track parameter monitoring, the change in twist and cant has been pre-calculated, based on the calculations provided in Chapter 2, which allows the engineer to easily understand any deflections or movements occurring at track level. Based on the red, amber, green trigger alarms predetermined by the engineers in the EPP, the values are shown in their associated threshold category. Figure 3.26 provides an overview of these types of visualisation tools available to the available to the engineer using Geoscope software, the real-time data management system for monitoring.

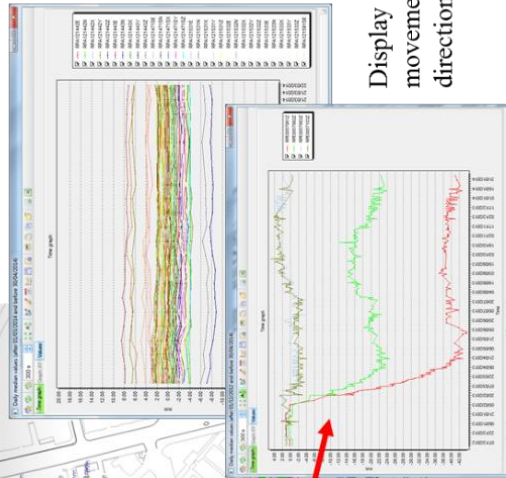
London Bridge monitoring homepage
(available online)



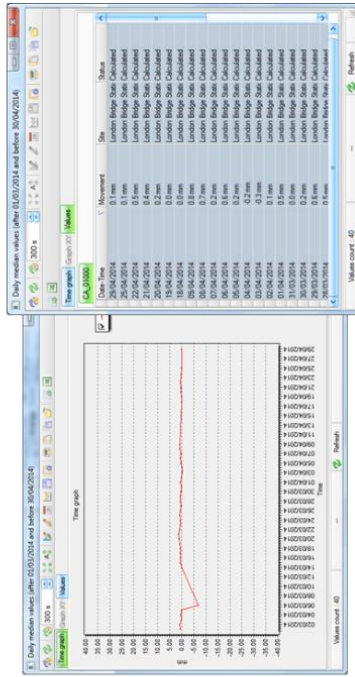
London Bridge Station track
as-built CAD as background



London Bridge Station arch
as-built CAD as background



Display of relative
movements of arches in Z
direction through graphs



Display of track parameters
(e.g. cant and twist) through
graphs/tables

Figure 3.26: Typical method of communicating monitoring data on TLP

Another example of the monitoring results from a deforming set of arches at London Bridge Station, where the expected levels of movement were exceeded and set off alarms, is shown in Chapter 6.

This type of data presentation through tables and graphs is not dissimilar to the typical output provided by automatic monitoring packages from monitoring contractors as well as vendors. For example, Leica produce the same type of analysis outputs as ones shown above in their monitoring package GeoMos, with tables and/or graphs. Smoothing filters can be applied to the raw datasets to reduce the “noise” from continuous monitoring data from a total station. This allows the engineer to see the “trend” from the raw measurements. The basis of the smoothing algorithm is unknown, however it appears to be based on a trend line. An example of applying a smoothing filter using GeoMos is shown in Figure 3.27, where the smoothing filters are shown in blue and green.

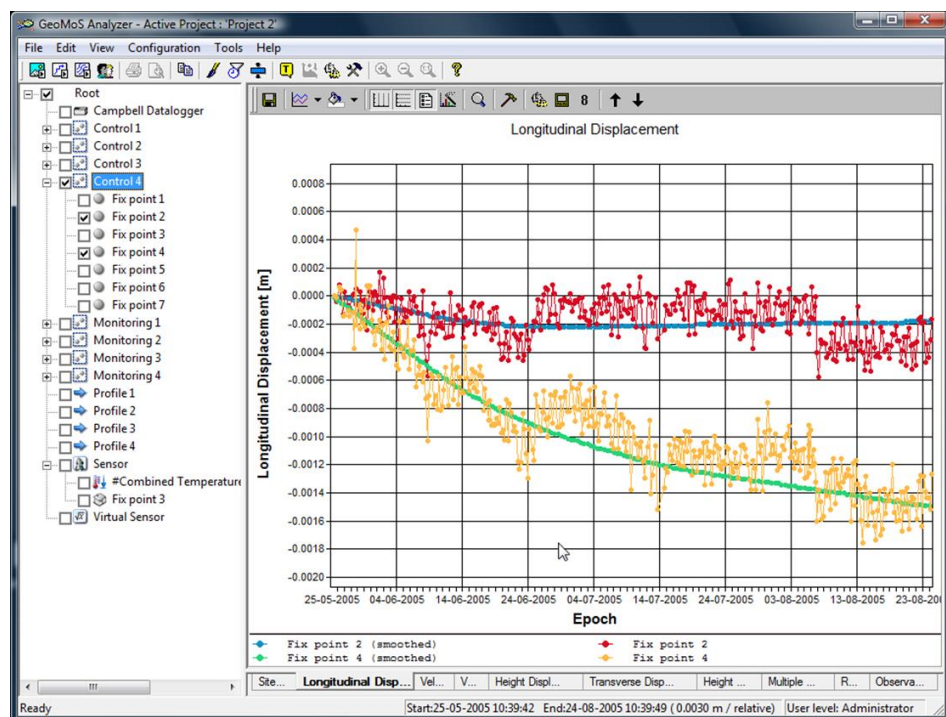


Figure 3.27: Application of smoothing filters to monitoring observations

The benefit of these types of packages is the flexibility in choosing how the data are displayed. This allows the same data to be presented to each stakeholder based on their individual needs. For example, an asset owner of a building being monitored in the vicinity of the construction work would require a different understanding of movements compared to a ground engineering team. Geoscope allows the engineer more rights to manage the data more easily. For example, if the engineer wants to see

if there are any patterns in displacement of surrounding arches, they are able to create a group of the prisms being measured so that the same points don't need to be repeatedly selected for inspection.

As described in Chapter 2 one of the issues with current monitoring systems is that these types of data analysis and presentation lack a provision of data quality information, i.e. the deformation measurements being presented do not come with any type of confidence levels or uncertainty. However based on the well-established monitoring analysis techniques described in section 3.3.3, deformations are presented through displacement plots using vectors and error ellipses. An example taken from Caspary and Rieger (2000) is shown below in Figure 3.28. The monitoring network of a dam is presented with the estimated deformations (vectors) along with their 95% confidence ellipses. The datum is derived from the stable reference points which are shaded.

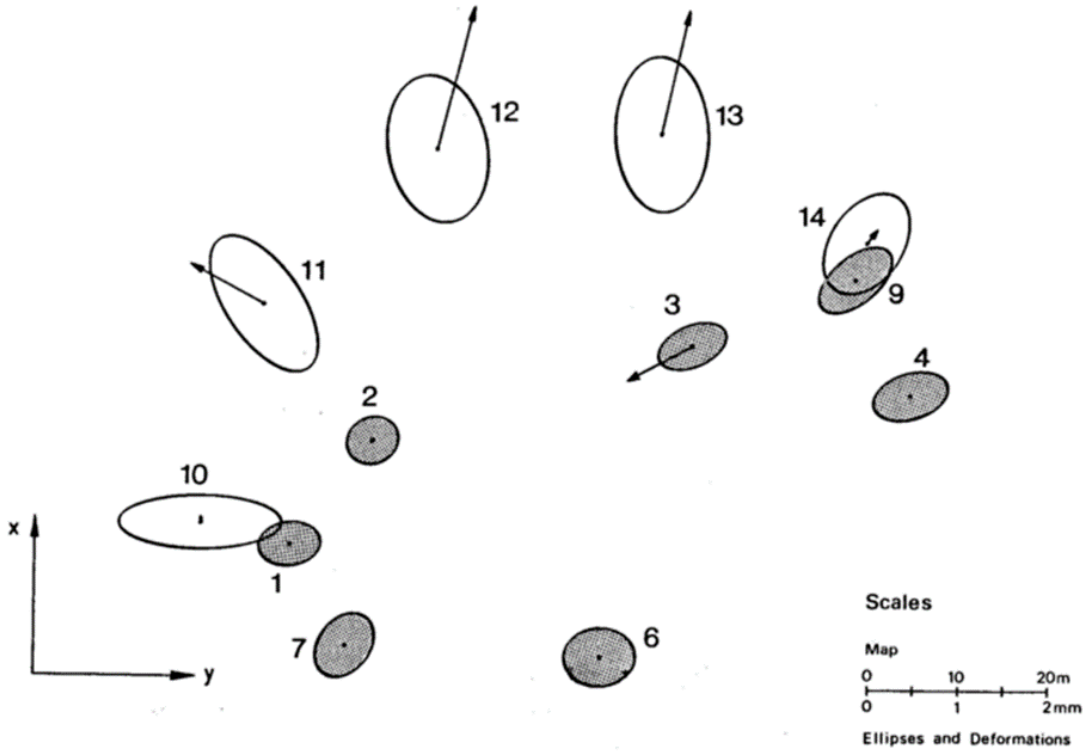


Figure 3.28: Example of presenting deformations with 95% confidence ellipses – image taken from Caspary and Rieger (2000)

This already provides better understanding of the data quality of the measurements with respect to the estimated deformation vectors in comparison to the current data presentation methods. Even though this is lacking geospatial context of the monitoring environment, this can be easily rectified. There is no evidence of this type of

deformation analysis display on current automatic monitoring packages provided by the vendors or monitoring specialists. Setan and Ibrahim (2003) created a workflow by taking output data from a STAR*NET adjustment file and feeding it into an in-house piece of 2D and 3D deformation detection software to produce deformation analysis and graphical presentation whilst reporting the data quality through error ellipses. Within photogrammetry displacement vector fields are a common method of displaying deformation results. An example of this is presented by Maas and Hampel (2006), which is shown in Figure 3.29, where road pavement deformation measurement was carried out by attaching signalized targets resulting in 2D displacement vectors between sequential measurements.

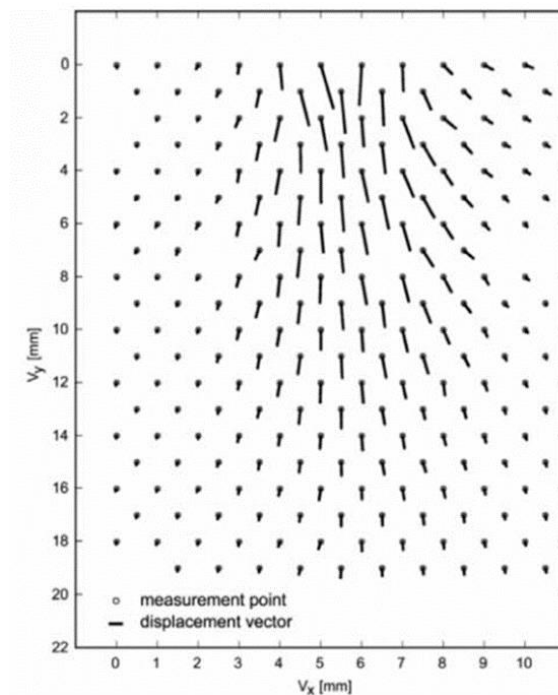


Figure 3.29: Road pavement deformation measurement through 2D deformation vector field - image taken from Maas and Hampel (2006)

This type of data presentation has the potential to be used in the context of manual and automatic monitoring at NR as it allows the engineer to analyse measurement points relative to each other as a “whole” easily, rather than having to manually create groups of the targets of interest. Therefore any systematic behaviours or patterns of movement of a structure could be detected straight away.

With the more recent use of TLS for deformation monitoring, there have been some examples of the visualisation of deformation monitoring of surfaces. Alba et al (2006) present colour-coded deformation maps by comparing different surfaces derived from

two scans of a portion of a dam (approx. 136m in height x 381 metres in length), shown in Figure 3.30. Even though this provides a method of displaying deformation to a millimetric level of precision, the methods used for producing these displacement maps is not provided.

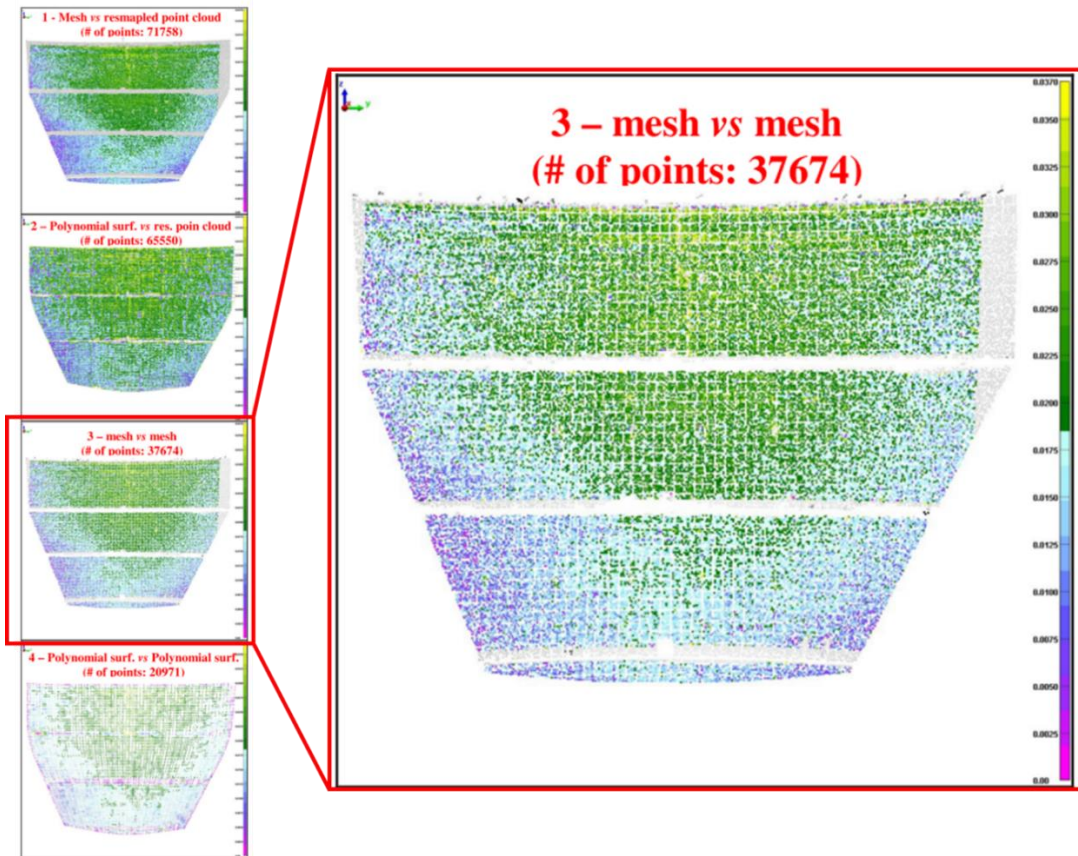


Figure 3.30: Deformation maps of different surface approximations using TLS – image taken from Alba et al (2006)

On a smaller scale Lemy et al (2006), generated similar methods of “displaying the evolution of surface topography” when monitoring tunnel wall displacements throughout and after its excavation. The patches are approximately 12 x 16cm. An overview of these are provided in Figure 3.31, where the top image shows a point cloud comparison between a baseline and test epoch and the bottom image shows a differential elevation map from comparing the same two epochs. Similarly to Alba et al (2006) there is minimal information on the production of these models. Despite the very extreme level of scales of these objects, there is little information on handling these types of datasets, particularly when comparing two point clouds or surfaces.

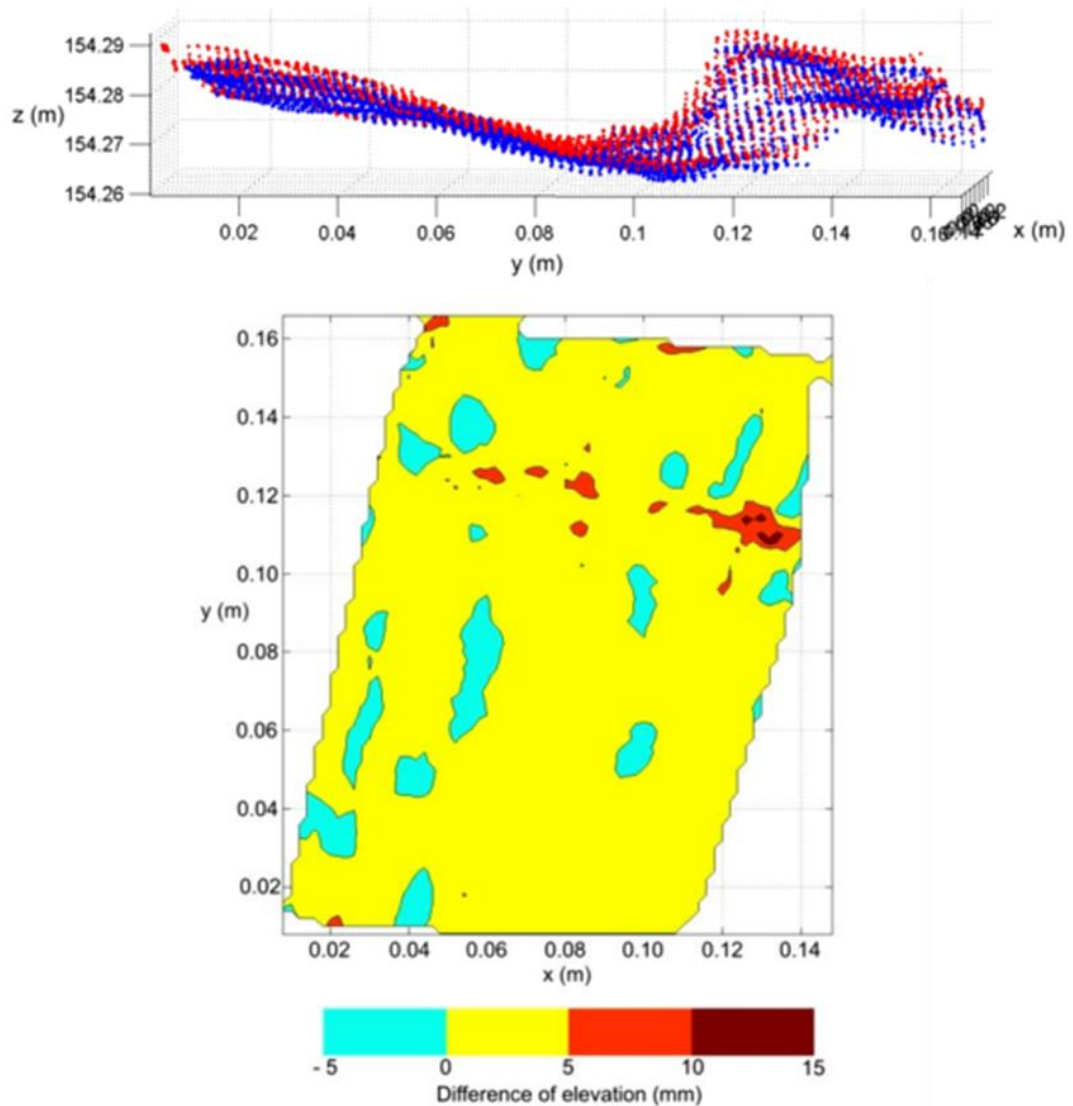


Figure 3.31: Different methods of displaying change in surface topography of a tunnel wall - image taken from Lemy et al (2006)

In general it can be seen that despite millimetric accuracy and precision being achieved in the literature where TLS is applied for deformation monitoring, there is limited discussion on how this monitoring information can be communicated back to engineers, or other interested parties such as stakeholders, to see the outputs from the TLS measurements, for example: Riveiro et al (2011, 2013); Kang (2012); Erdélyi et al (2014); and Nuttens et al (2014).

This thesis looks to explore the methods of communicating deformation monitoring data obtained from TLS back to an engineer. This is an important final step of deformation analysis. Different tools for measuring and displaying deformation within a laboratory environment are explored and presented in Chapter 4. Based on the

laboratory findings Chapter 6 provides a case study where TLS monitoring data were presented to the engineers in different ways to establish a fit for purpose solution.

3.5 Chapter Summary

This chapter has provided an overview of the variety of engineering surveying measurement techniques used in this study. It highlights the opportunities that these techniques provide in the context of deformation monitoring through target and surface-based measurements.

Within the railway industry it can be seen that the default method applied for monitoring is through total station and prism-based methods by measuring to a network of points manually or through an automatic system. Section 3.3 has shown that the processing of these types of observations is well-established from an academic standpoint, where the use of network design and analysis provides a rigorous way of analysing the observations as well as providing quality measures of the data, which then allows deformation detection to be carried out. However, currently on the London Bridge Redevelopment Project and generally on TLP, it can be seen that there is a gap in this measurement analysis process where there is little evidence of network design, adjustment and measurements appear to be analysed at face value. This is a very significant issue with respect to providing assurance of the safety of passengers and surrounding structures. There is also little evidence of regular instrumentation checks for errors, e.g. systematic errors, which could affect the monitoring results and be perceived as movement if the measurements are taken at face value. One of the reasons for this is where the skillsets of the monitoring specialists lie; it appears there is more of a focus on handling large volumes of discrete information through IT and computer processing skills, particularly in the UK, where there is limited knowledge of network adjustments and data quality.

This thesis focuses on ensuring data quality of measurements to a network of targets as well as surfaces to allow an accurate and precise targetless monitoring approach to be developed, based on Network Rail's requirements of this study. It can be seen that there is little work on measuring surfaces as a method of replacing targets to overcome the cost and maintenance issues associated with prisms. Even though there is limited literature with respect to targetless monitoring within a railway environment, it can be seen that TLS and CRP techniques are working towards millimetric levels of precision with regards to surface measurement of structures. This study takes this potential

forward by applying these tests within both a laboratory and site scale whilst maintaining a high level of data quality.

Previous work has shown short-term ad-hoc projects of monitoring using TLS or CRP, where a few examples present methods of presenting this deformation. However their (TLS and CRP) use within an engineering context and whether they are fit for purpose, is unknown. This EngD has provided an opportunity to apply testing to a set of live monitoring sites over the 3 to 4 years of the project. This study explores different methods of communicating this deformation information back to the Network Rail/contractor engineer where there was a requirement to monitor a set of deforming arches and railway track to determine if these methods provide a fit for purpose solution whilst removing the need for prisms.

The next chapter presents the laboratory testing carried out to understand the instrument capabilities of point and surface-based monitoring using total stations, TLS and CRP, where surface-based tests focus on railway track and masonry brick surfaces.

Chapter 4 - Instrumentation performance tests through point and surface-based measurements within a laboratory environment

Chapter 3 provided a review of the current engineering surveying techniques used in deformation monitoring. It presented the fundamental need for the performance of monitoring instrumentation to be regularly tested. It is an essential step in the monitoring process to truly understand its capabilities as there's a risk that an instrument's error may be perceived as movement, which in turn could lead to false alarm triggers being set off. Consequently this could stop the operation of the railway. Based on time spent with observing monitoring systems at Network Rail TLP and the interviews carried out in Chapter 2, there is very little evidence of this type of testing carried out in reality in the UK. This issue is addressed by carrying out four experiments to test instrument capabilities of point and surface-based monitoring within a laboratory environment.

The first half of the chapter describes two experiments investigating instrument performance of conventional instrumentation, i.e. total stations, used for monitoring railway infrastructure such as track and structures. Terrestrial laser scanning (TLS) is also introduced to see the capabilities of target-based measurements compared to the conventional instruments. A state of the art laser tracker is also implemented into these experiments to highlight the need for an accurate baseline measurement to allow comparisons between instruments to be made.

As this study looks into the potential of non-contact and targetless solutions for monitoring, the performance of TLS and close-range photogrammetry (CRP) measuring directly to the railway infrastructure surfaces is investigated. A similar set of experiments highlights the potential of surface-based measurements when compared to the results from the target-based performance tests. The surfaces investigated in this thesis are railway track (Experiment 3) and masonry brick (Experiment 4).

4.1 Target-based instrumentation testing

This section discusses target-based tests carried out on state of the art instrumentation typically used in the surveying and monitoring industry. A state of the art laser tracker,

typically used in metrology, was used in both tests to allow a baseline measure for the survey instrumentation measurements.

4.1.1 Experiment 1: Network performance

The importance of network design for deformation monitoring and the difficulty in discriminating between a measurement error and displacement (Grafarend et al., 1985) was highlighted in Chapter 3 section 3.3.1. The aim of this experiment was to test the performance of state of the art instrumentation measuring to a network of fixed points. This was to highlight the importance of implementing network analysis, particularly for deformation monitoring and to determine whether errors were instrument or network based.

4.1.1.1 Methodology

Ten 1.5” drift magnetic nests (Figure 4.2a) were securely installed across the space of the indoor laboratory (approximately 11 x 5 metres) at a variety of heights and distances to create a network of points. The nests allowed reliable measurements to be made to the target centre using both a laser tracker and the total stations. Three instrument stations (S1-S3) were established based on their lines of sight to all the targets. To ensure the stations were in a stable position, heavy instrument stands were used. A traverse of the stations was carried out to provide co-ordinates of the instrument stations on an arbitrary grid. A 2D plan of the Stations (S1-3) and Nest positions (N1-10) is shown in Figure 4.1.

The AT401 laser tracker and TS15i, TS30, TM30 total stations were used in this experiment. For the laser tracker to measure to the nests a 1.5” spherically mounted retro-reflector (SMR) was used (Figure 4.2b). The laser tracker uses ATR to measure automatically to the SMR target. As the total station was unable to read the SMR target a 1.5” target adapter (Figure 4.2c), which has the same centre point as the SMR, was used. The readings from the total station to the target were read using the reflectorless mode.

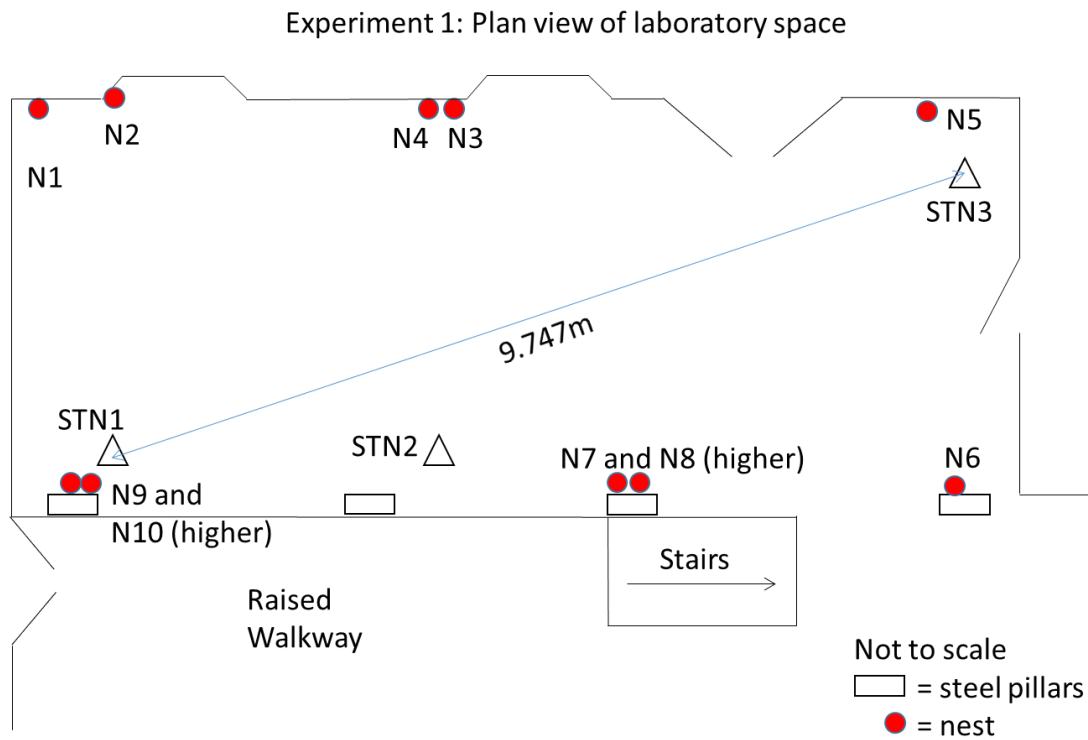


Figure 4.1: Plan view of lab space and position of stations (S1-3) and Nests (N1-10)



Figure 4.2 a) 1.5" magnetic nest (left); b) 1.5" SMR target (centre); c) 1.5" target adapter (right)

Readings to the targets were taken from each station by observing all targets in sequence in one face of the instrument followed by the same in the second face. This process was repeated so that there were two rounds of measurements for each point measured. The readings from each of the instruments were imported into STAR*NET (see Chapter 3 section 3.3). When applying a network adjustment in the software, a minimally constrained network was used so that any measurement blunders could be easily isolated and detected. In this case station S1, an arbitrary point ARB1 and a bearing between S1 and nest N1 was used to constrain the network. All observations were put through the blunder detect tool to remove any gross errors in the input data.

The output of the network adjustment in STAR*NET allows relative error ellipses to be produced (see Chapter 3 section 3.3.1.1 and 3.3.3.2). Relative error ellipses describe the relative precision between two points. Figure 4.3 represents a relative error ellipse between two points.

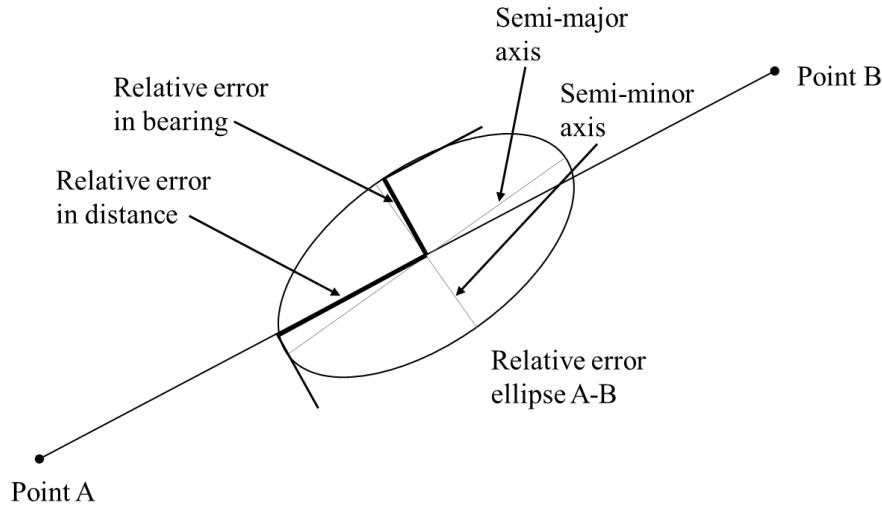


Figure adapted from MicroSurvey STAR*NET (2014)

Figure 4.3: Schematic of relative error ellipse between two points

The size of the error ellipse is a measure of the uncertainty of the computed point position. The relative error ellipses between the nests were computed to allow comparisons between all of the instruments' precision. The error ellipses also provide a way of analysing the strength of the survey network. A typical network adjustment plot from STAR*NET can be seen in Figure 4.4 where the error ellipses are displayed in red. These have been exaggerated for visualisation purposes. The error ellipses show a very low uncertainty in the relative distance error between the nest positions, however it does show a high level of uncertainty in the relative error in the bearing between the nest positions.

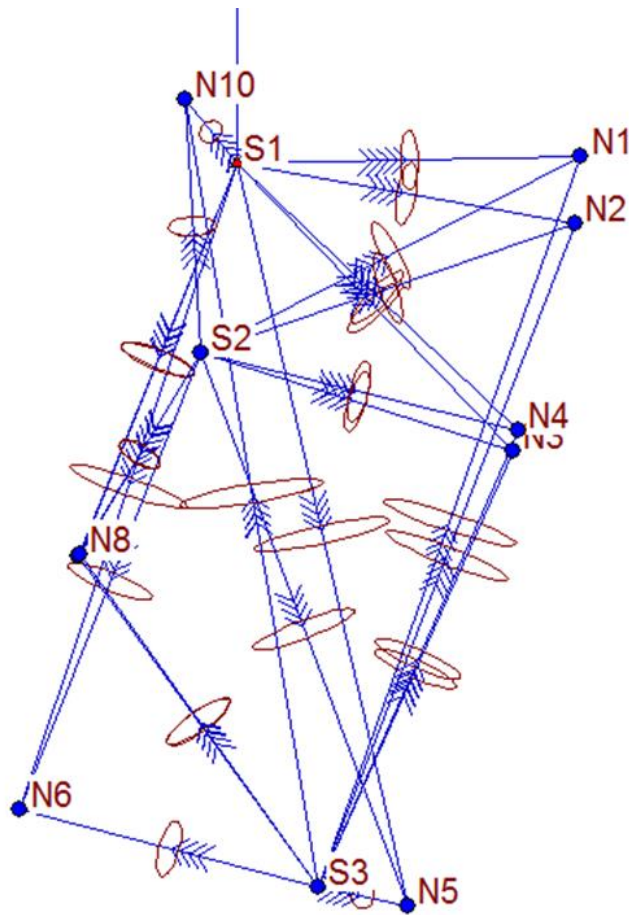


Figure 4.4: An example of a network adjustment plot using STAR*NET

A pre-analysis (see Chapter 3 section 3.3.1.1) was carried out for the network of targets from each of the stations for each instrument used. This allows a list of approximate co-ordinates to be established as well as computing the expected error ellipses based on the instrumentation parameters inputted into STAR*NET (based on the manufacturer's specification), without having to provide any real observations. This allows the expected error ellipses to be compared to the observed error ellipses. For an accurate comparison it must be ensured that the rounds of angles/redundancy of the observations is taken into consideration and that it matches the measured observations when using the pre-analysis function.

The length error was also calculated from the output of the adjustment. The length error is a standardised method (VDI/VDE 2634) used for testing acceptance and re-verification of optical measuring non-contact 3D measuring systems in industrial metrology (see Chapter 3 section 3.3.3.2). The length error E is defined as “the difference between a measured (displayed) length L_m and the calibrated reference length L_r ”:

$$E = L_m - L_r$$

Based on the specifications with respect to the accuracy and precision of the laser tracker, the AT401 was used as the calibrated reference length, L_r . Therefore the length error of the total stations were used to analyse the accuracy of the length measurement based on the laser tracker.

Based on the guidelines for testing optical 3D systems, the length error can be displayed and analysed by plotting the measured length against the length error (Luhmann et al. 2014). In order for the acceptance of a system, the maximum permissible error (MPE) is a length-dependent value that must not be exceeded. The MPE is expressed as

$$MPE(E) = A + K.L \leq B$$

where E = length error; A, K = machine-specific constants; L = measured length, B = maximum permitted deviation of length measurement. For the laser tracker, the MPE is provided. The total station machine-specific constants can be calculated based on the accuracy measurements in the manufacturer's specification.

4.1.1.2 Results and analysis

All the predicted and observed relative error ellipses were computed (1σ). The output listing from the network adjustment in STAR*NET provides the size of the semi-major and semi-minor axes.

It should be noted that the AT401 predicted and observed measurements are based on SMR target readings, providing the highest accuracy possible for this network. However the total station observed measurements in this section are based on reflectorless readings to the reflective targets due to incompatibility of an accurate prism-based target fitting into the nests. For further information on reflectorless readings, please refer to section 3.2.2.1. Figure 4.5 shows the predicted precision of the points in the network if a prism target, i.e. the highest accuracy measurement for the total station, was available.

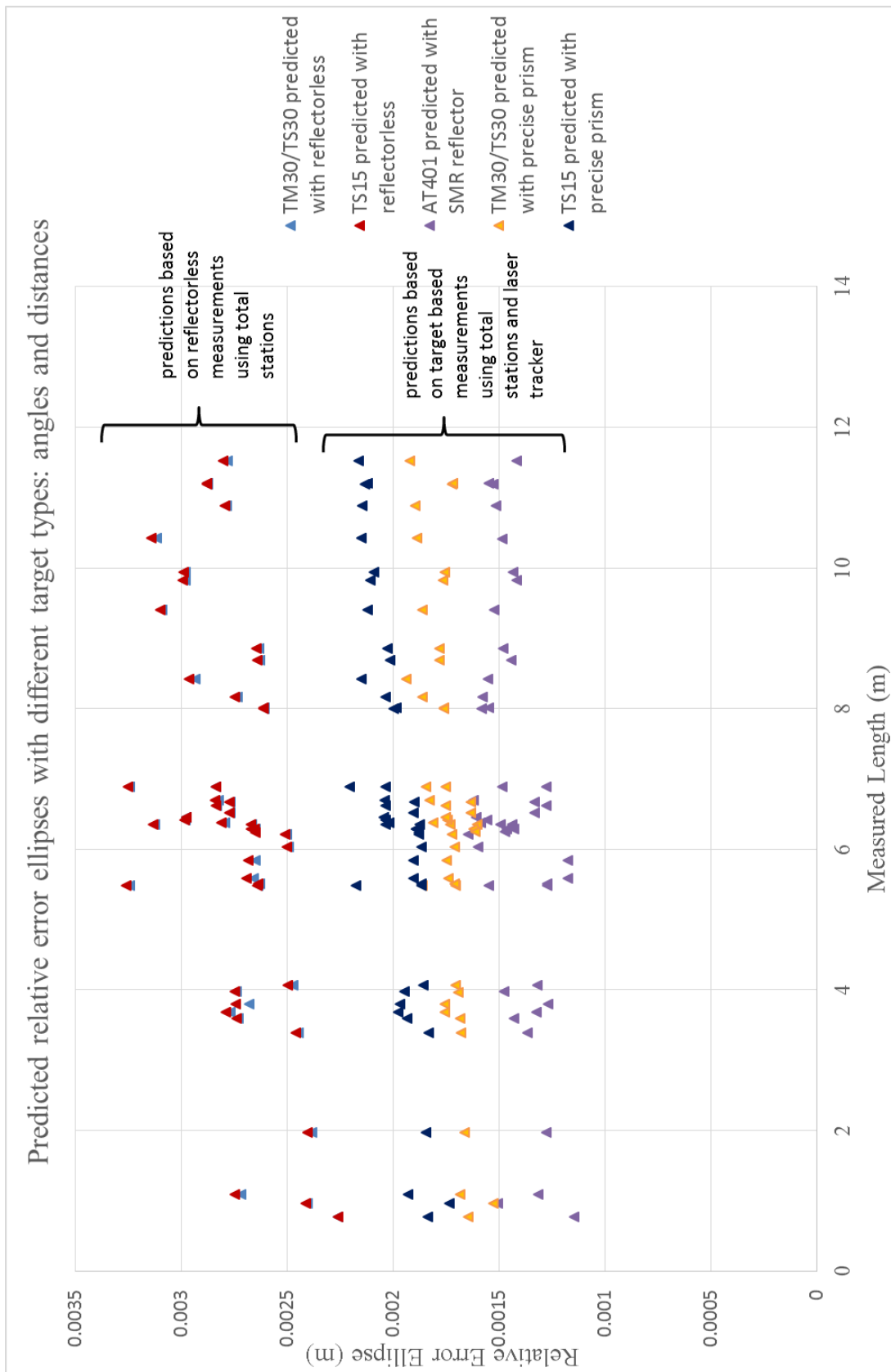


Figure 4.5: Predicted relative error ellipses (semi-major axis) of prism and reflectorless target measurements based on instrument specification

As expected, the graph shows that the SMR/prism target-based measurements would produce the most precise results, with the AT401 providing the most precise coordinates at the millimetre level for this particular network. The total stations' coordinate precision approximately doubles when using reflectorless measurements. Based on the manufacturer's specification the TS30/TM30 is predicted to have a precision of the point co-ordinates between 1.5 and 2mm using prisms. This is followed by the TS15's predictions around the 2mm level. This type of result provides a "best case scenario" of expected precision from the instruments for this network if measuring to a prism or in reflectorless mode.

The top section of the graph shows the predictions of using reflectorless measurements from the total stations (as the laser tracker is unable to take reflectorless measurements). It shows that they have a similar performance in their reflectorless mode compared to the prism based mode, showing that the laser used in the two instruments is very similar. These results show a "worst case scenario" of the instruments' performance in the network. With respect to monitoring in the railway environment, this is a useful comparison to have in case prisms cannot be measured, for example the line of sight to track is blocked with machinery or trains and a reflectorless surface measurement in proximity to the prism is required as a backup.

With respect to monitoring, this provides a way of reporting the expected performance of the instrument within a network. This is particularly useful for automatic continuous monitoring when the instrument is fixed. In this context the precision of the total stations is up to 3mm which is based on the network's geometry. Therefore when measurements to these points are repeated, the co-ordinates will be within 3mm and the point will not necessarily have moved 3mm.

The observed and predicted relative error ellipses between each of the nests from each of the instruments were plotted against the measured length to determine the precision of the points as the range from the instrument increased. This provides an internal prediction and performance of the instruments and is shown in Figure 4.6.

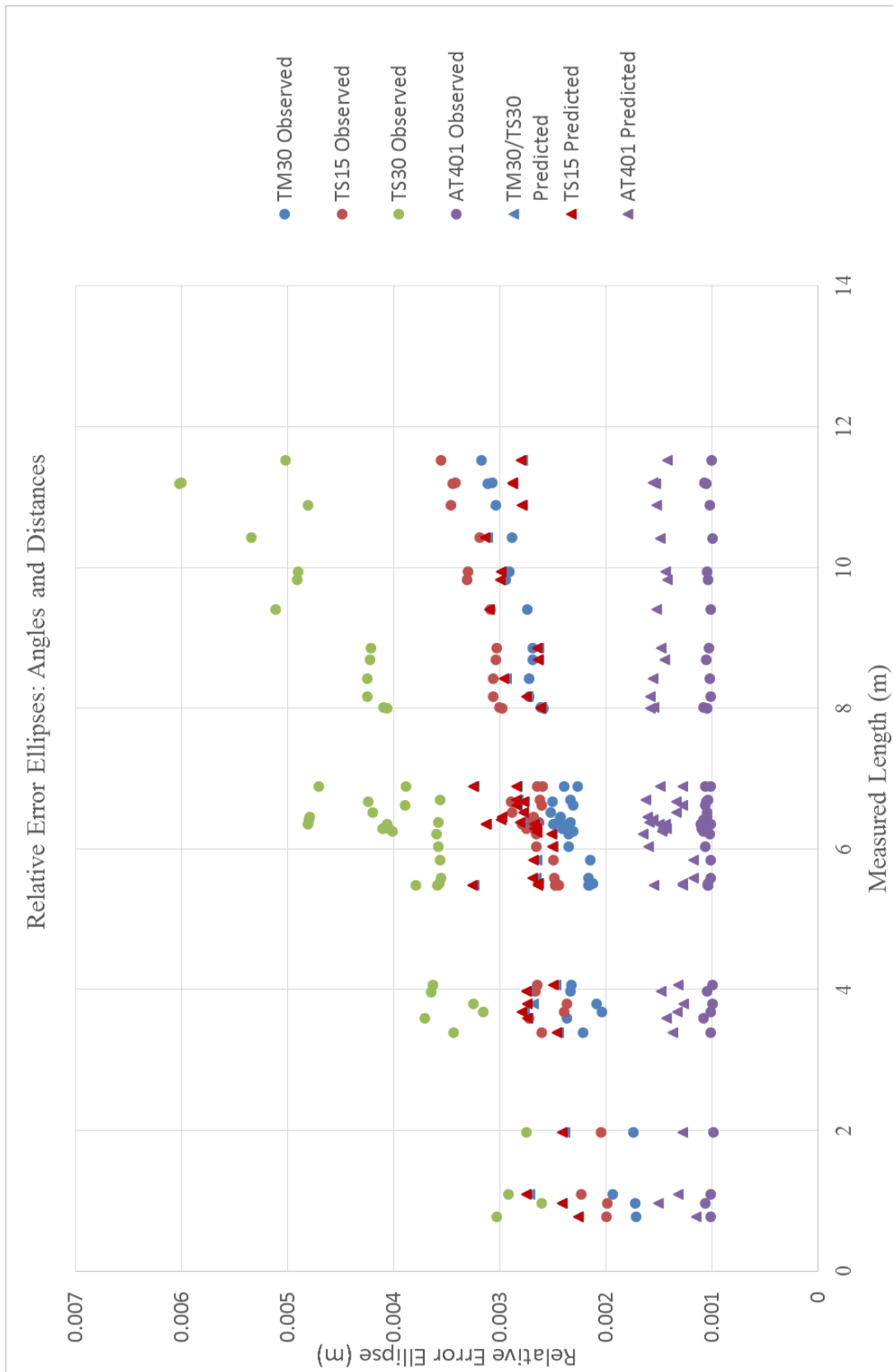


Figure 4.6: Relative error ellipses (semi-major axis) - observed (circle) against predicted (triangle)

For this network all the total stations show an increase in uncertainty as the range from the instrument increases. However the AT401 does not conform to this trend and

therefore has a more accurate and precise level of measurements in angles and distances, which is expected from the laser tracker based on its specification. Therefore it shows that the laser tracker provides a good baseline when comparing the capabilities between the total stations.

The observed error ellipses from the AT401 are producing an uncertainty between the points at the 1mm level whereas the predicted level of uncertainty is slightly higher between 1.2 and 1.6mm. This shows that for this network the AT401 is performing slightly better than expected at all ranges for this network.

As the TS15 and TS30/TM30 have very similar specifications in angular and distance accuracy (see Appendix A) the predicted performance of the total stations is very similar for this network. The graph shows that the TS15 and TM30 are producing the level of uncertainty predicted for this network. For ranges less than 7 metres the instruments are both performing better than expected.

The observed relative error ellipses from the TS30 show a high discrepancy from the predicted relative ellipses, with the highest uncertainty of 6mm at a range of just under 12 metres (which was the maximum range considered in this experiment). As the points were fixed when measurements were taken, it can be seen that against the TS30's predicted performance there is an instrument issue. This unexpected level of uncertainty implies that there is an error in either the angles or distance measurements using this particular total station and further investigation is required. This plot has allowed this unexpected uncertainty to be shown. However if network analysis had not been carried out, this uncertainty between the two points could vary by up to 6mm if measurements were repeated. This could then be translated into movement rather than an instrument error and therefore set off triggers unnecessarily.

The length errors were plotted against the measured length along with the *MPE*, using the AT401 as the reference measured lengths. This is shown in Figure 4.7.

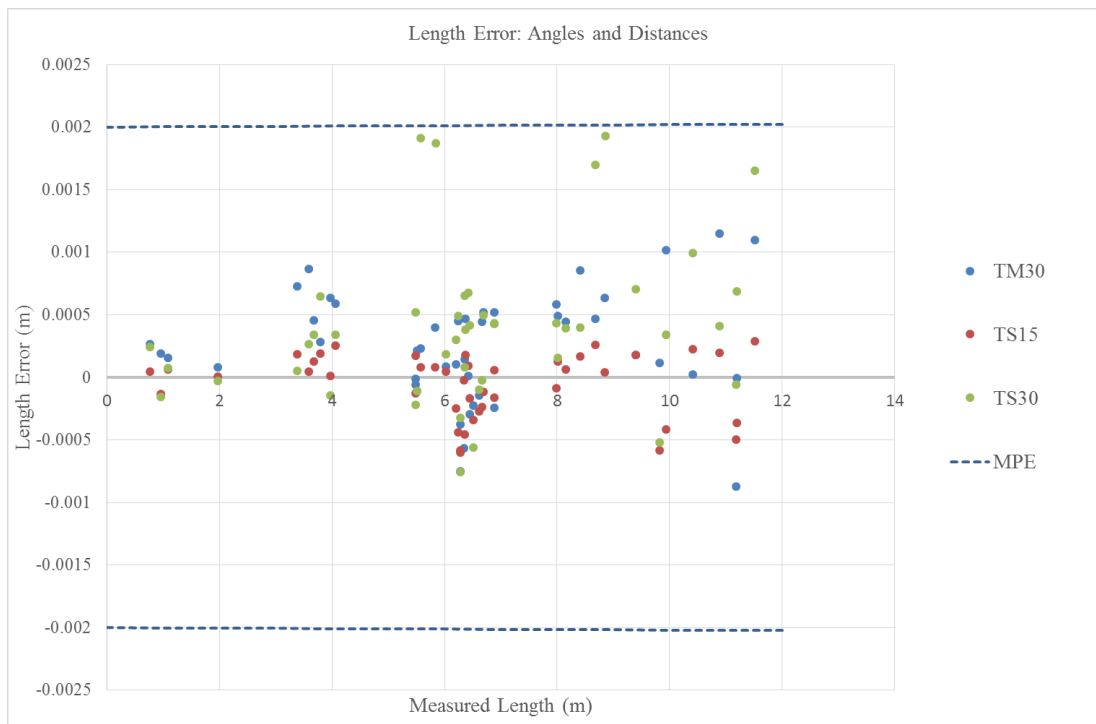


Figure 4.7: Length measurement errors and MPE boundary

The length errors show a skew towards the positive length error values, showing that the measured lengths from the total stations are longer than the reference length. It would be expected that the points would be spread more evenly across the space within the *MPE* boundary lines. All the instruments' length errors are within the *MPE*. However it can be seen that the TS30 length errors are on the border of the *MPE* at ranges of 5-11 metres. This complements the findings from the relative error ellipses and shows that there is an instrument error present in the TS30.

As the relative error ellipses and length errors are based on angle and distance measurements from all stations to all points in the network, a way of investigating the source of the TS30 error is to determine if this is a recurring instrument error from all stations in the network or specific ones. Therefore the relative error ellipses (1σ) and length error measurements can be plotted according to the stations the measurements were acquired from. This is shown in Figure 4.8 and Figure 4.9.

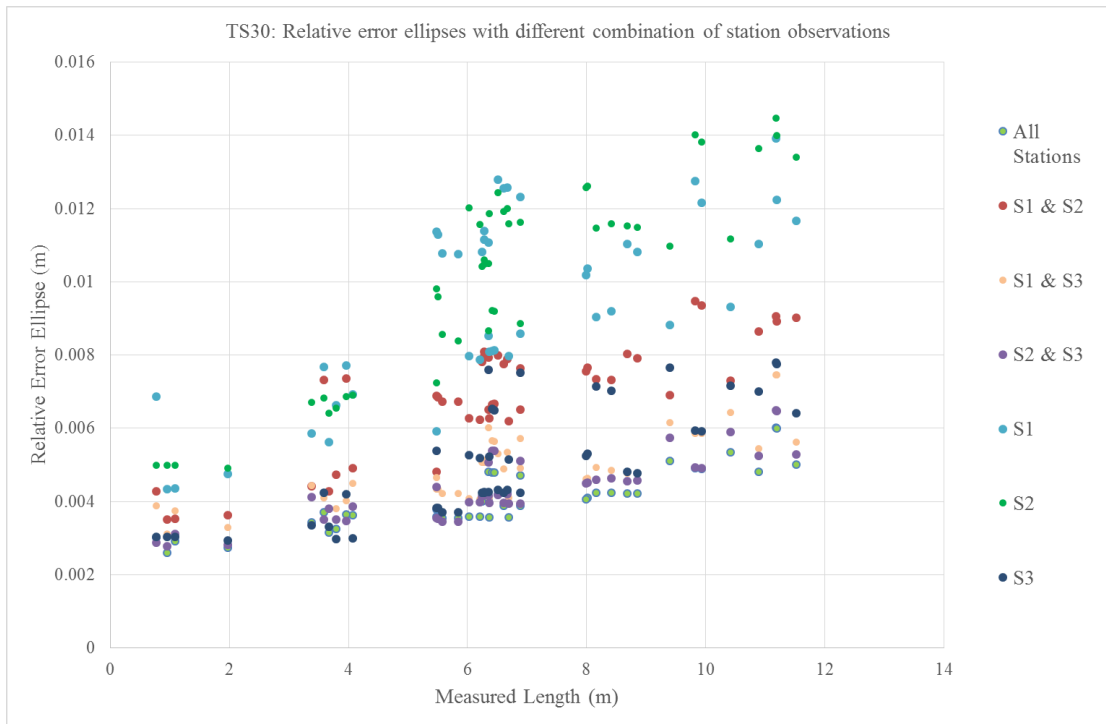


Figure 4.8: TS30 relative error ellipse of network from different stations

Figure 4.8 shows that the uncertainty of the position between points in the network increases to approximately 15mm when observations from only S1 or S2 are used in the network adjustment, which is an incredibly high level of uncertainty for this working range. When only S3 measurements are put through the network adjustment, the uncertainty remains similar to that of all the stations combined. The graph also shows that the uncertainty remains low when all stations are being used, i.e. when there is redundant data, for the network adjustment. Therefore this shows that the source of the instrument errors is in the measurements taken from S1 and S2. From a monitoring point of view, if either only S1 or only S2 were monitoring stations reading to the nests as monitoring points, which is typical for a monitoring network for railway track, there would be an uncertainty of 5mm and 15mm at a range of 2m and 11m respectively. This is extremely high for such a short range. The station/nest co-ordinate error ellipse in the output listing in STAR*NET provides the uncertainty of the nest position lying within that particular station's ellipse region. Therefore when comparing the measurements from S1 only using the TS30 (inadequate) and TM30 (performing as expected), the uncertainty of the nest position is up to 9mm for the TS30 and 3mm for the TM30 for a network of points at the 12m range. Therefore the level of uncertainty of the TS30 is three times higher than expected. Therefore if network analysis hadn't

been carried out, this 9mm level of uncertainty could have been observed as movement rather than an error in the instrument.



Figure 4.9: Length error of network from different stations with the TS30

Figure 4.9 shows that based on the length error values the TS30 when measuring from S1& S2 and S1&S3, the length error goes beyond its MPE. This shows that the measurements from these stations do not conform to their tolerances and confirms the need to investigate further into the angle and distance measurements from S1 and S2.

The results from the error ellipses and length errors show an error based on the angles and/or distance measurements from S1 and/or S2 when run through the network adjustment. Therefore in order to deduce the instrument errors in the TS30, the angles and distance measurements need to be extracted and run independently through a network adjustment. As there are only three stations in this network, it is not possible for STAR*NET to run a “distances only” 3D adjustment through trilateration. A fourth station would be required to calculate this. An alternative and more appropriate method for analysing the quality of the distance measurements would be to use an optical rail and interferometer, for example used by Gassner et al. (2011) when investigating the distance measurement performance of the AT401 laser tracker.

This network setup does allow an adjustment to be run by using only the angle measurements, with a single distance required to scale the network. The results from

calculating the relative error ellipses (1σ) and length errors from the angles only network adjustment is shown in Figure 4.10 and Figure 4.11.

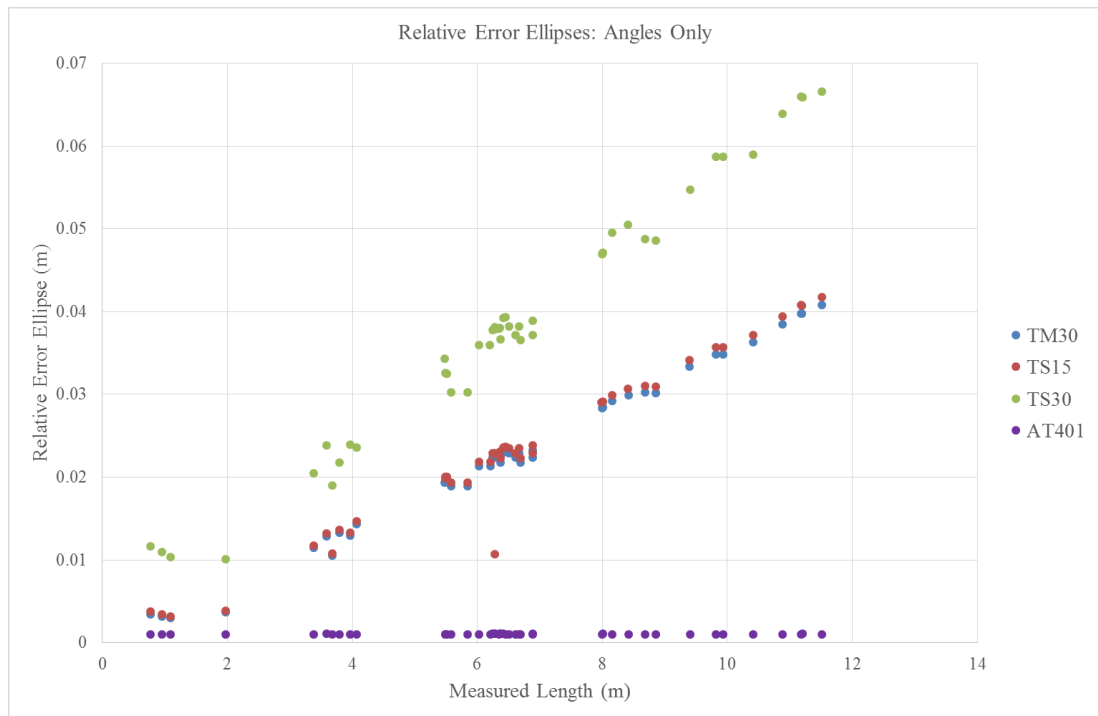


Figure 4.10: Relative error ellipses (semi-major axis) for angles only measurements from instruments



Figure 4.11: Length errors for angles only measurements from total stations

The AT401 angle measurement precision is very high, with a consistent 1mm level of uncertainty at all the ranges up to 11 metres. This is similar to the uncertainty with the combined angle and distance measurements. Despite working with the tracker at a similar range, Gassner et al. (2011) found that angle accuracy was comparable to total stations. Figure 4.10 shows that the AT401 is performing much better than the total station for this particular network.

By eliminating the distance measurements, it can be seen that the TS30 angle measurements are affecting the uncertainty of the co-ordinates when compared to the TS15/TM30 (with a similar specification as the TS30). The length errors of the TS30 are wide-ranging between +3mm and -5mm. Based on the results from the error ellipses with the combined angle and distance measurements, it is likely that the angle measurements from S1 and S2 are the source of the error which requires further investigation.

STAR*NET outputs the residuals from the adjustment of the distance, zenith and direction observations. From the standard errors, which is a weighted value based on the parameters inputted into STAR*NET, standardised residuals are computed. This is the residual of an observation divided by its standard error (MicroSurvey, 2014). Therefore this is the ratio between the observation's fit in the adjustment and the estimated strength. This becomes a unit-less quantity to allow comparisons of the adjustments of the different types of observations (i.e. distances, zenith and direction observations). As the TM30 did not produce any unexpected errors and has the same performance specification as the TS30, the standardised residuals between the TM30 and TS30 for all of the observations from S1 and S2 were compared. The distance, zenith and direction standardised residuals are shown in Figure 4.12, Figure 4.13 and Figure 4.14 respectively.

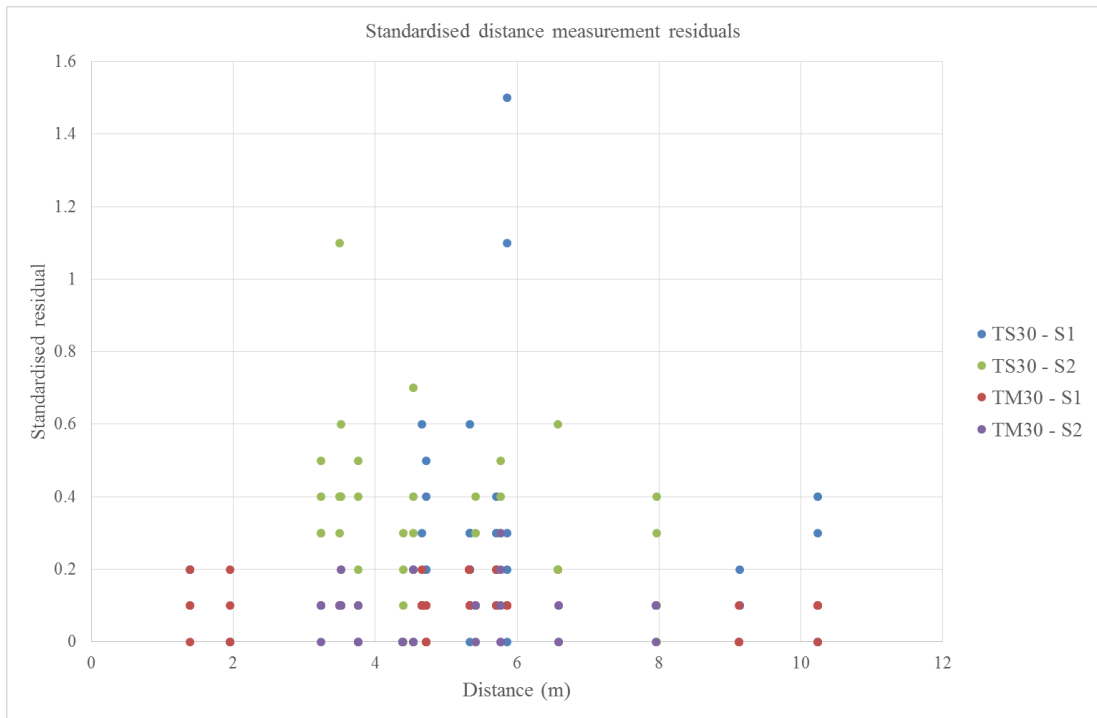


Figure 4.12: Standardised distance residuals of TS30 and TM30 from S1 and S2

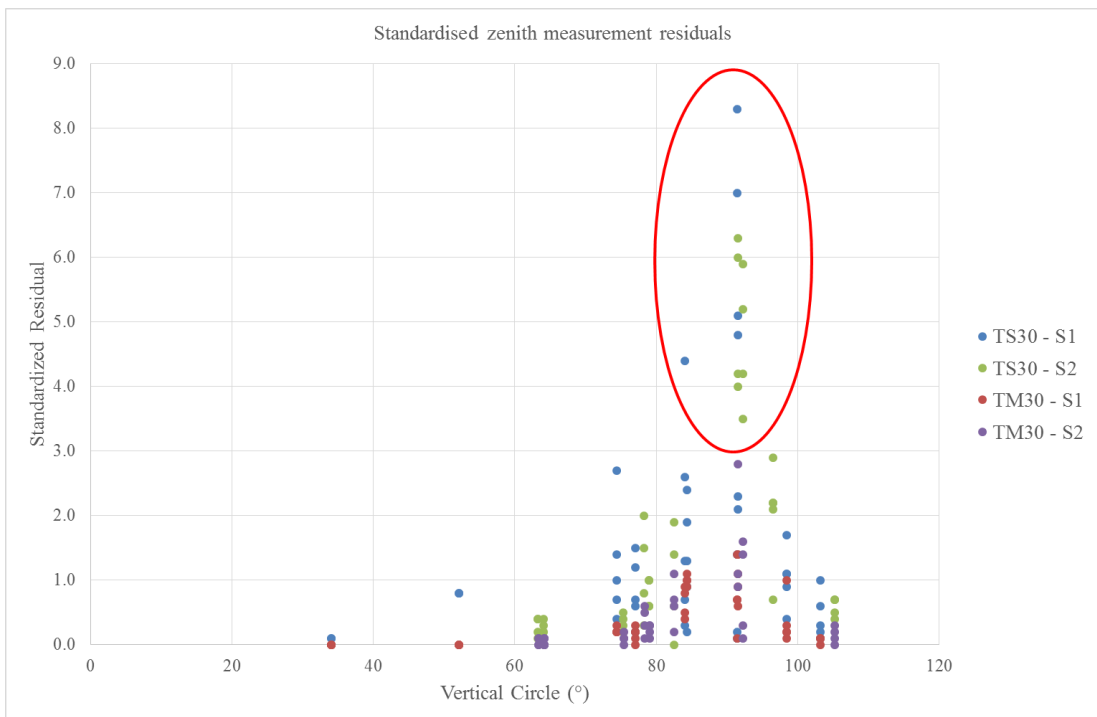


Figure 4.13: Standardised zenith residuals of TS30 and TMS30 from S1 and S2

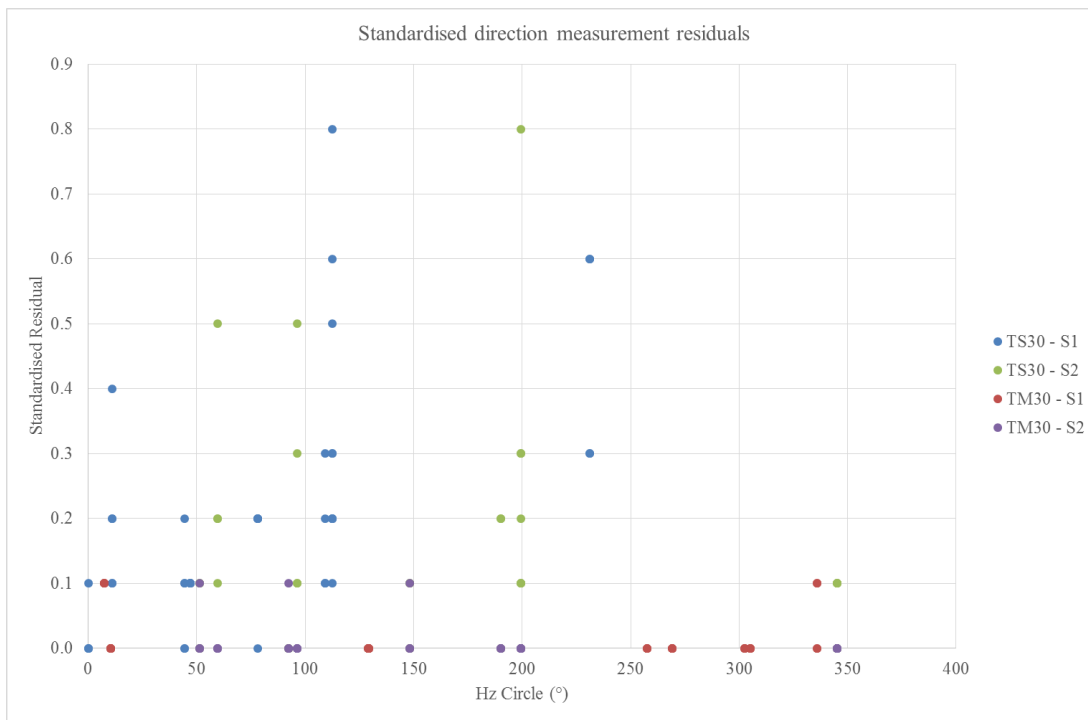


Figure 4.14: Standardised direction residuals of TS30 and TM30 from S1 and S2

For the distance and direction observations, the ratio between the observations fit and estimated strength is around 1.0. This shows that the fit is better than expected for these observations for both the TS30 and TM30 instrument. When analysing the zenith observations for the instruments it can be seen that TM30 is also producing residuals of a ratio of 1.0. However the zenith angles from the TS30 produce standardised residuals of greater than 8.0. It can be seen that the highest residuals are occurring at the horizontal circle reading of around 90° , which is highlighted in red in Figure 4.13. This error is present for readings from S1 and S2 whereas readings on other parts of the circle produce a smaller magnitude of standardised residuals. This implies that there is an instrument error when on that particular area of the circle. On further investigation, these errors occur for both faces of the total station readings implying this is not a vertical index error. These measurements are not blunders as they are not randomly distributed across the vertical circle readings and are highly systematic. Therefore this shows that the instrument has an internal error in the vertical circle reading. To rectify this, the instrument should be sent back to the manufacturer for calibration.

A comparison was made between the semi-major relative error ellipses of the TM30 measurements from S1 with two rounds of angles against one round of angles. This was to see the effect of a reduced redundancy of measurements in the case of limited

time availability for instrumentation testing. The results showed that the average of the error ellipses, i.e. uncertainty, for the TM30 observations for this network were 4.0 mm and 3.0 mm for one and two rounds of measurements respectively. This was compared to the predicted error ellipses of 4.2mm and 2.9mm respectively. These results confirm that the instrument performed as expected but also show the significance of having redundant measurements. The predicted values were also calculated for three and four rounds of angles which showed error ellipses with an average of 2.4mm and 2.1mm respectively. This could not be done with the observed data as only two rounds of angles were taken for this experiment. The latter set of results indicate the uncertainty beginning to tail off despite the increase in redundancy of the measurements. The predicted results do show that between one and four rounds of angles, the size of the error ellipse is halved. However the biggest difference in size of the error ellipse is between having one and two rounds of angles, where the precision is increased by a millimetre. When testing instruments this is an important improvement in the precision of the instrument. Therefore if testing were to be applied to future instruments, it would be suggested that at least two rounds of measurements need to be taken to points if there wasn't sufficient time to accommodate multiple station setups.

4.1.1.3 Conclusions

The purpose of this experiment was to highlight the importance of network analysis to establish the presence of measurement errors from total stations to a network of points. In this experiment relative error ellipses were used to analyse the precision of the instrument's performance in the network. The length error was used as a check for the length accuracy as well as an acceptance test for its performance.

A prediction of the expected performance of the total stations in the network was determined to allow a comparison to the observed measurements to be quickly made in order to reveal any instrumentation errors that may be present.

It showed that the laser tracker was a suitable baseline measure for comparing the capabilities of the total stations. The TS15 and TM30 total stations were also performing as expected with an approximate precision of 2-3mm for this network setup. However there was a large discrepancy of the TS30 observed measurements to the predicted ones with a relative uncertainty between points of up to 15mm. By using

the relative error ellipses and length error calculations, the source of this error could be determined. The angle measurements were run through the network adjustment independently and the standardised residuals for the distance, zenith and direction observations were plotted. This showed an instrument error on the vertical circle reading and required the instrument to be sent back to the manufacturer for calibration.

In a monitoring environment, if the instrument was fixed and continuously measuring with the error on the vertical circle, the measurement error could have been disguised and translated into movements of the target of up to 9mm based on the station coordinate error ellipses. Depending on the structure being monitored, this could falsely raise the alarm for movement. Therefore this highlights the importance of a simple instrument check before and during its deployment.

Redundancy of the measurements in the laboratory, as well as on site, has an impact on the precision of the overall output. Based on the results in this experiment at least two rounds of angles should be taken to increase the precision of the overall output and therefore improve the integrity of the results. If there is limited time when carrying out the laboratory testing and multiple station setup is not possible, increasing the redundancy of the measurements can increase the precision of the results.

The predicted results were able to show the capabilities of the total stations when applying prism and reflectorless-based measurements. This provides an indication of the performance that can be expected from a “worst case” scenarios if measurement to prism was not possible at the time, for example an obstructed line of sight due to obstructing vehicles or passing trains.

4.1.2 Experiment 2: Target-based measurement capability

Based on the knowledge gained from the performance of a laser tracker and total stations in a network environment, the next investigation is to test the range accuracy of these instruments when a target is moved. From the monitoring specifications, millimetre levels of movement is typically predicted on structures such as arches or buildings and is therefore required to be monitored using total stations. Therefore an experiment was set up in a laboratory environment to see how different survey instrumentation performs when there is a known level of movement of a target. This experiment also allowed a TLS system’s point based capabilities to be tested and

directly compared to the laser tracker and total station's capabilities and therefore investigate its potential for monitoring.

4.1.2.1 Methodology

The laser tracker AT401, total stations TS30 and TS15 and ScanStation2 TLS system were used in this experiment to allow three different survey grade instruments to be compared. Currently there isn't a common target that allows accurate measurements from these three different instrumentations. Therefore a target array consisting of the three bespoke target types was developed and created for this experiment, which is shown in Figure 4.15. The target array consists of an aluminium plate with five 0.5 inch diameter holes which allowed the tooling balls, which are associated with the laser tracker, to be firmly glued in using a glue gun. For this experiment they were called T1-T5 from left to right. Four blue reflective HDS targets, associated with the TLS system, were stuck to the plate using their strong adhesive backing. These were called L1-L4 from left to right. The precise prism (Leica GPH1P), associated with making precise measurements using a total station, was fixed to the centre of the plate using screws. This target was called MP for the experiment.

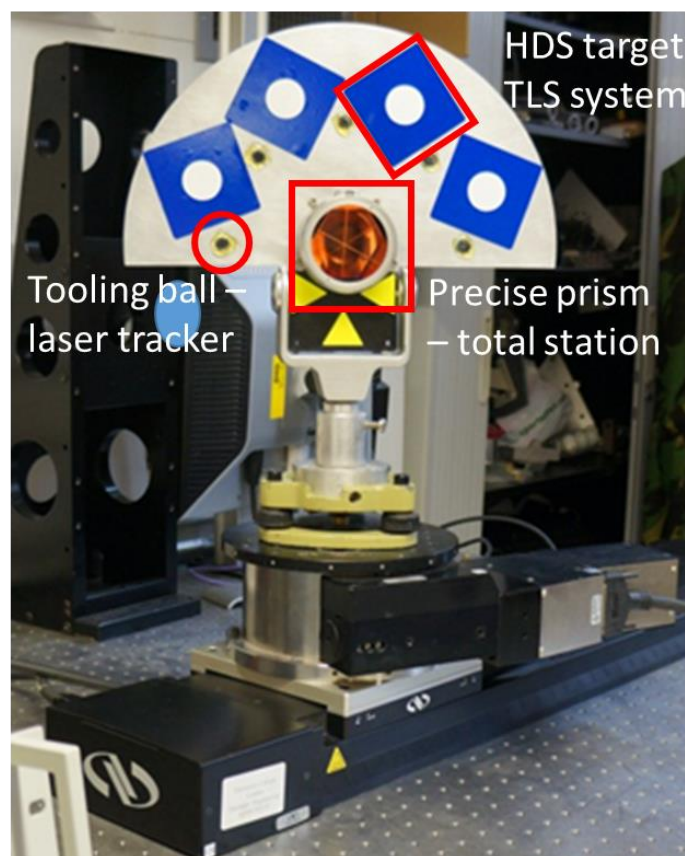


Figure 4.15: Target array for range displacement measurements; HDS targets L1-L4 from left to right; tooling balls T1-T5 from left to right; precise prism MP (centre)

The target array was fixed to a highly precise motorised linear translation stage (Newport Motion Controller MM4006) using a tribrach, which was securely attached to a control unit which allowed small translations to be applied. According to the manufacturer's specification the translation stage had an accuracy of 25 microns which was suitable for the level of movement being detected in this experiment.

The instruments were set up at the longest range possible from the translation stage in the laboratory, which was approximately 6 metres away. Heavy duty tripods were used to ensure the instruments were stable throughout the measurement process. The instruments were aligned by eye so that they were approximately perpendicular to the target array and that the telescope was approximately setup at the same height as the targets. This was to allow only the range measurements to be taken into consideration when the movements were applied. Figure 4.16 provides an image of the test setup.



Figure 4.16: Target array testing setup

The following linear range translations were applied to the target array: 25mm, 10mm, 5mm, 2mm, 1mm and 0.5mm. These values cover a wide range of structural movement that is typically predicted by an engineer on a monitoring project, for example the arches at London Bridge Station. To have redundancy of the observations, three sets of distance measurements to each target from each of the instruments were taken after each translation was applied.

When test readings took place, it was established that the total stations were able to read to the tooling ball targets, and the laser tracker was able to read to the monitoring prism using their respective ATR modes. Therefore all viable measurements took place in the ATR mode. The laser scanner was unable to accurately measure to the tooling balls and precise prism. The laser tracker was unable to read the reflective centre of the HDS TLS target, however the total stations were used in reflectorless mode to read the TLS target centre by eye.

4.1.2.2 Results and analysis

The results are shown in order of target type measured: tooling ball, monitoring prism and laser scanner target.

Table 4.1 shows each of the differential distances calculated from the observations of the different instruments against the movement applied to the translation stage for measurements to the tooling balls. It also shows the precision of each of the instrument measurements to the targets at the maximum allowable range in the laboratory of 6m.

Linear movement of motorised linear translation stage (in mm) $\pm 0.025\text{mm}$		Differential distance measurements from instruments in millimetres								
	Tooling Ball	AT401			TS30			TS15		
25.0000	T1	24.9913	24.9913	24.9973	24	25	25	24.9	24.8	24.9
	T2	25.0017	25.0047	25.0047	25	25	25	25.0	25.1	25.0
	T3	24.9957	24.9967	24.9997	24	24	24	24.6	24.7	24.8
	T4	24.9743	24.9763	24.9793	25	25	25	25.0	24.9	25.0
	T5	24.9605	24.9625	24.9665	25	25	25	23.8	23.5	23.9
10.0000	T1	n/a*	9.9780	9.9770	10	10	9	10.0	9.8	10.0
	T2	9.9860	9.9840	9.9820	10	10	10	10.1	10.1	10.1
	T3	9.9837	9.9867	9.9847	10	10	10	9.8	9.8	10.1
	T4	9.9813	9.9833	9.9833	10	10	10	10.1	10.1	9.8
	T5	9.9757	9.9757	9.9737	10	10	10	9.9	9.8	9.7
5.0000	T1	4.9895	4.9875	4.9855	4	5	5	4.8	4.6	4.8
	T2	4.9890	4.9880	4.9890	5	5	5	4.7	4.7	4.6
	T3	4.9907	4.9897	4.9897	5	5	5	5.1	5.1	4.8
	T4	4.9887	4.9857	4.9867	5	5	5	5.0	5.0	5.2
	T5	4.9867	4.9857	4.9827	5	5	5	5.0	5.0	5.0
2.0000	T1	1.9900	1.9920	1.9890	2	1	1	1.7	1.9	2.0
	T2	1.9913	1.9923	1.9903	2	2	2	2.1	1.7	1.9
	T3	1.9917	1.9927	1.9907	2	2	2	1.9	2.1	1.8
	T4	1.9927	1.9907	1.9897	2	2	2	1.9	2.2	2.1
	T5	1.9927	1.9897	1.9897	2	2	2	2.2	1.9	2.1
1.0000	T1	0.9967	0.9887	0.9877	1	1	2	0.9	1.0	0.7
	T2	0.9960	0.9890	0.9870	1	1	1	1.0	1.1	1.1
	T3	0.9930	0.9900	0.9880	1	1	1	0.9	0.9	1.0
	T4	0.9907	0.9907	0.9887	1	1	1	0.8	0.9	0.9
	T5	0.9890	0.9880	0.9860	1	1	1	0.9	0.8	0.9
0.5000	T1	0.4927	0.4907	0.4887	0	0	0	0.5	0.6	0.6
	T2	0.4933	0.4923	0.4923	0	0	0	0.4	0.3	0.5
	T3	0.4937	0.4927	0.4917	1	1	1	0.7	0.7	0.8
	T4	0.4937	0.4917	0.4917	1	1	1	0.4	0.5	0.5
	T5	0.4953	0.4933	0.4903	1	1	0	0.9	0.5	0.5
Precision of range measurement to target (approx. 6m)		0.0018mm			0.1mm			0.1mm		

* = no measurement taken

Table 4.1: Measured translations from instruments to tooling balls

It can be seen that the TS30 results for distance measurement don't have the same number of significant figures as the TS15. After the tests had taken place, it was discovered that the display settings for the range measurement has been altered and was not at its full precision with respect to significant figures (i.e. sub-millimetre). As this instrument had been borrowed from Network Rail, it had been deployed elsewhere and the tests could not be repeated. However the distance measurements between the total stations are comparable and precision of the range measurements are equal with a very high precision for a total station of 0.1mm. The results show that the AT401 has a micron level of precision for the distance measurements and the overall precision of the range measurement is 1.8 microns which is nearly two orders of magnitude higher than the total station. This confirms the validity of using the laser tracker as a baseline measure for comparing the performance of total stations. In order to assess the

accuracy of the instruments, the residuals of the measurements to each of the tooling balls was calculated. As the TS30 did not provide sufficient information in the distance measurements, the residuals for the AT401 and TS15 linear translations were calculated. The results are shown in Table 4.2.

Tooling Ball	Instrument observed – expected residuals (absolute) for linear translations in mm		
		AT401	TS15
T1	average	0.01	0.1
	st. deviation	0.005	0.2
T2	average	0.01	0.1
	st. deviation	0.006	0.2
T3	average	0.01	0.1
	st. deviation	0.004	0.2
T4	average	0.01	0.0
	st. deviation	0.006	0.1
T5	average	0.02	0.2
	st. deviation	0.011	0.5

Table 4.2: Residuals of measurements to tooling balls from laser tracker and total station

The tracker results show a very good accuracy and precision from the instruments. Based on the manufacturer’s specification the range accuracy is ± 0.01 mm. The results show a comparable level of performance apart from the results from measurements to the T5 tooling ball. The total station results show a sub-millimetre level of accuracy and precision. From the specification the expected accuracy performance is 1mm. This level of accuracy is expected due to the range employed for this test. Even though the TS15 residuals are well within specification for this test, the tooling ball T5 also appears to have the largest residuals and therefore lowest accuracy and precision. Even though the sample size of this dataset is small, this was investigated by plotting all of the distance measurements residuals of the tooling balls from the laser tracker and total station against the residuals without the T5 measurements. These are shown as histograms in Figure 4.17 .

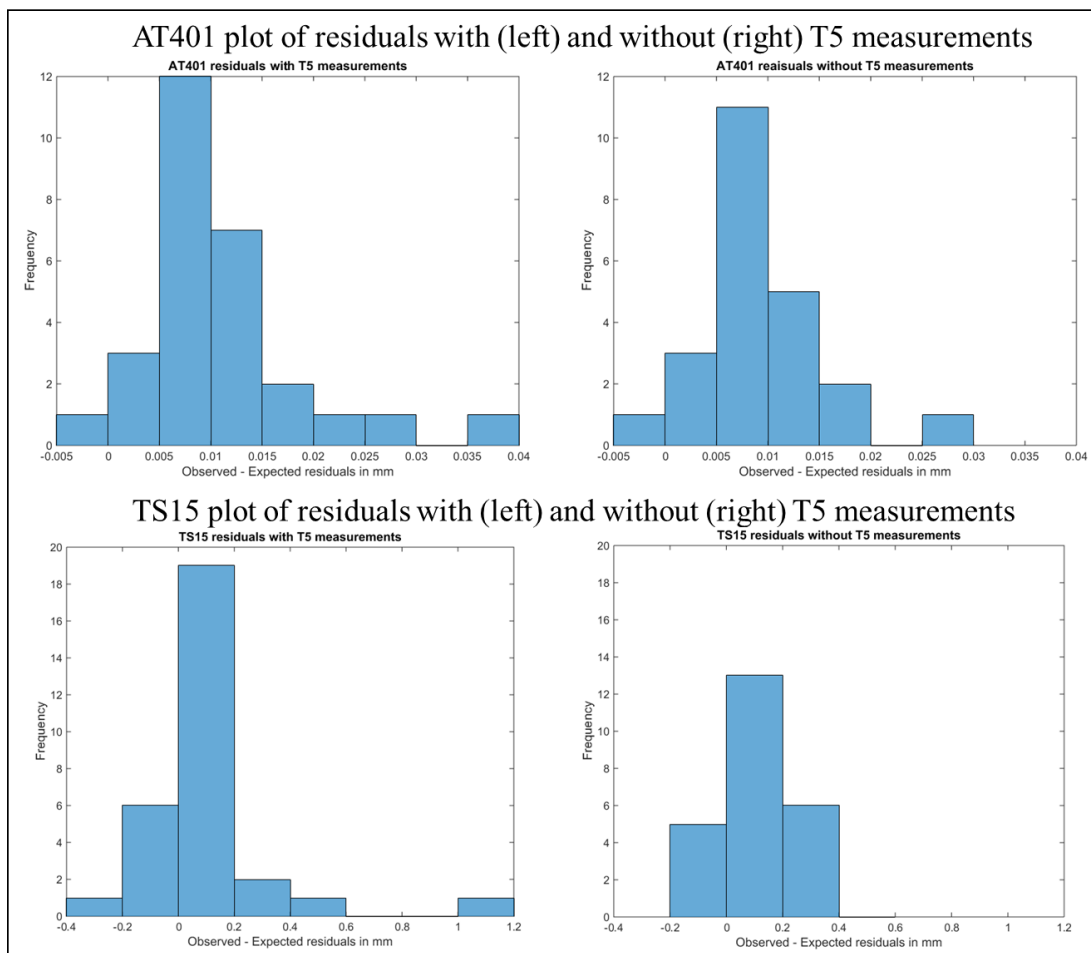


Figure 4.17: Histogram of residuals of tooling balls with and without T5

Despite a very small sample of data the right hand side histograms, i.e. without T5 measurement, both show a tendency towards a normal distribution. This was confirmed by applying the chi-squared test in MATLAB to both instruments. This shows that there is sufficient evidence to show that the residuals are normally distributed. The chi-squared test was also applied to the residuals inclusive of the T5 measurements from both of the instruments. These failed the chi-squared test which shows there is not enough evidence to say these residuals are normally distributed. This result implies a systematic bias in the T5 residuals. When looking closely at the measurements to T5 in Table 4.1, the precision is low compared to the other tooling balls. This implies that the tooling ball may have not been centred correctly when measurements were made to the ball or may have become loose after gluing it to the metal plate. The consistency in the T5 tooling ball residuals between the laser tracker and total station confirm that there is a systematic error occurring. Therefore it must be ensured the tooling balls are firmly glued to the monitoring array.

Table 4.3 shows the linear translation measurements when the laser tracker and total stations were observing to the precise prism. It also includes the precision of the measurements to the target at the range of approximately 6 metres.

Linear movement of monitoring prism using motorised linear translation stage (in mm) $\pm 0.025\text{mm}$	Differential distance measurements from instruments to precise prism in millimetres								
	AT401			TS30			TS15		
25.0000	n/a	n/a	n/a	25	25	25	24.9	24.7	24.6
10.000	9.9763	9.9763	9.9753	10	10	10	9.9	9.8	9.8
5.0000	4.9913	4.9933	4.9923	5	5	5	5.1	4.9	5.1
2.0000	1.9860	1.9860	1.9850	2	2	2	1.8	1.9	1.9
1.0000	0.9993	0.9993	0.9983	1	1	1	1.1	1.2	1.2
0.5000	0.4833	0.4833	0.4823	1	0	0	0.3	0.1	0.4
Precision of range measurement to target (approx. 6m)	0.001mm			0.1mm			0.1mm		

Table 4.3: Measured translations from instruments to precise prism

Despite a much smaller sample size compared to the tooling balls, the precision of the AT401 measurements compares to its precision results for the tooling balls, with a precision of 1 micron. Both the total stations show a 0.1mm level of precision which also matches its precision when measuring to the tooling balls. This table shows that the tooling balls and precise prism can be read accurately from the laser tracker as well as total stations. This could be useful for providing a good baseline of prism measurements from a laser tracker in a set of arches where total station monitoring is required. It also shows that a total station could read tooling balls instead of prisms if there is limited space for the larger prism target. However, based on the results it must be ensured that the tooling ball is correctly aligned to the instrumentation.

As the experiment was carried out at the same time as the tooling balls, the full precision issue with the TS30 is still present. However, the residuals from the AT401 and TS15 could be calculated and the results are shown in Table 4.4.

Instrument observed – expected residuals (absolute) for linear translations of monitoring prism in mm			
Movement on translation stage		AT401	TS15
25	average st. deviation	n/a	0.2 0.2
10	average st. deviation	0.02 0.001	0.2 0.1
5	average st. deviation	0.01 0.001	0.0 0.1
2	average st. deviation	0.01 0.001	0.1 0.1
1	average st. deviation	0.00 0.001	0.2 0.1
0.5	average st. deviation	0.02 0.001	0.2 0.2

Table 4.4: Residuals of measurements to precise prism from laser tracker and total station

These results confirm the high accuracy and precision performance of both types of instrumentation and the comparability of the readings of the same instrumentation to the tooling balls. Even though there is a very small sample of observations, the residuals were plotted and passed the chi-squared test for both instruments. This shows that there is no evidence of systematic errors when both instruments are reading the precise prism.

In order for the TLS targets to be measured by the total station, reflectorless mode was switched on and the measurements were repeatedly taken by eye to each of the targets. For point-based measurements from the TLS system, the target centre was acquired using Cyclone. The tool allows the user to select a point in the vicinity of the target centre and a vertex is created in the centre using a built-in algorithm in Cyclone. Figure 4.18 shows a point cloud of the target array based on the intensity of the return signal using the ScanStation2. It shows all four TLS targets (dark blue) with a green circle and a blue dot which is the reflective centre of the target. Cyclone then creates a vertex (light blue) denoting the target centre. According to the manufacturer's specification the vertex position is within a $\pm 2\text{mm}$ standard deviation of the target's centre. For the MRes (1st year) report of this research project, results showed that the target centres could be repeatedly measured with a precision of $\pm 2\text{mm}$ over a period of time, based on a total station survey to the target centres (Soni, 2011).

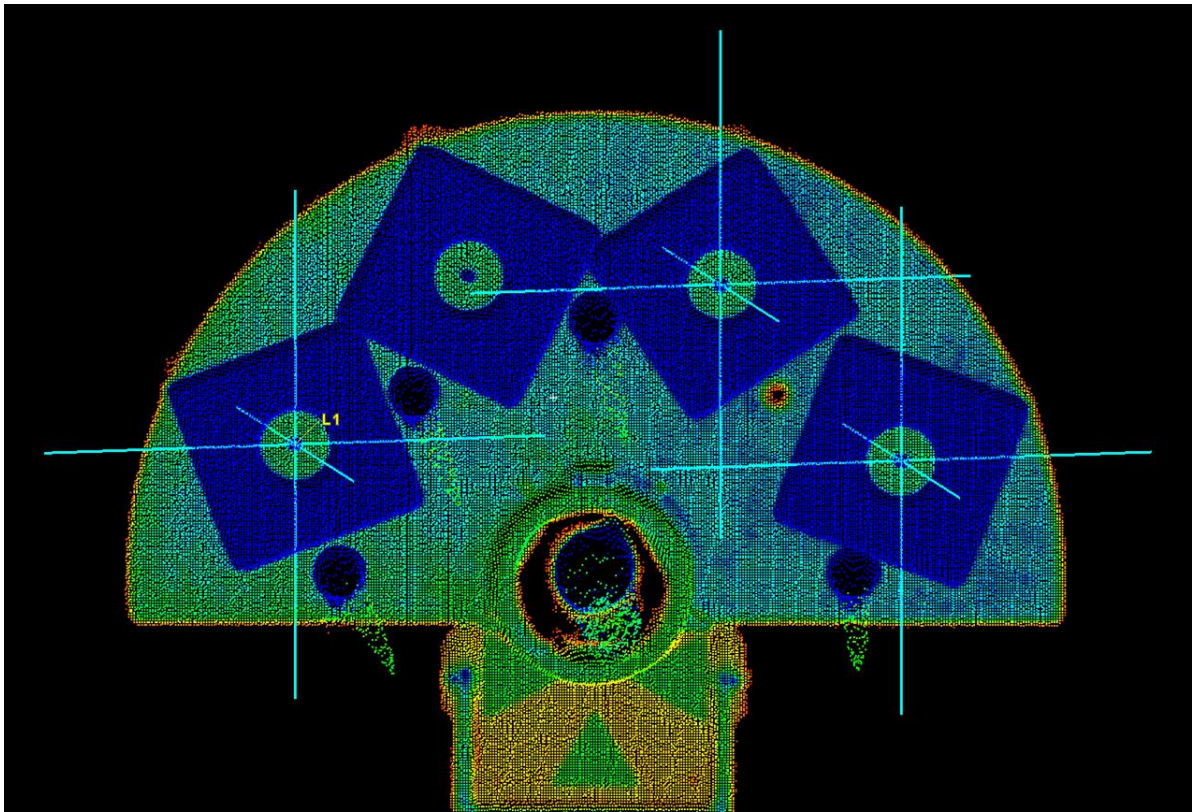


Figure 4.18: Point cloud of target array with target acquisition

The point cloud also shows the noise effect of scanning the highly reflective tooling ball and precise prism. The return noise shows a “green trail”, based on intensity return, of noise acquired by the scanner. This confirms the inability to laser scan the glass-based targets tailored for a laser tracker and total station.

Table 4.5 shows the range measurements from the TS30, TS15 and ScanStation2 to each of the TLS targets. It also shows the precision of the range measurement of the instrument approximately 6 metres away from the targets.

Linear movement using motorised linear translation stage (in mm) $\pm 0.025\text{mm}$		Differential distance measurements from instruments in millimetres								
	TLS HDS target	TS30 (reflectorless mode)			TS15 (reflectorless mode)			ScanStation2		
25.0000	L1	24	24	24	26.9	26.9	26.5	25.6	25.5	25.3
	L2	24	25	25	20.9	21.1	21.2	25.3	25.0	25.0
	L3	25	25	25	20.6	20.3	20.7	25.0	24.8	25.0
	L4	25	25	25	26.9	26.8	26.8	25.2	25.3	25.1
10.0000	L1	9	9	9	7.9	8.0	7.8	10.3	10.2	9.8
	L2	9	9	9	12.3	12.2	12.6	10.1	10.2	9.6
	L3	10	10	10	13.2	13.2	13.3	9.7	9.9	9.4
	L4	10	10	10	8.4	8.6	8.5	9.9	9.8	9.7
5.0000	L1	4	4	4	4.9	4.9	5.0	4.8	4.9	4.7
	L2	5	5	5	4.7	4.7	4.8	5.3	5.3	5.1
	L3	5	5	5	5.6	5.4	5.7	5.1	5.1	5.2
	L4	5	5	5	5.4	5.4	5.5	5.3	5.3	5.2
2.0000	L1	2	2	2	1.8	1.7	1.6	1.5	1.8	2.0
	L2	2	2	2	2.6	2.4	2.7	1.9	2.3	2.2
	L3	2	2	2	2.7	2.7	2.7	2.1	2.1	2.3
	L4	2	2	2	1.3	0.9	0.7	1.9	1.7	1.9
1.0000	L1	1	1	1	0.8	0.7	0.8	0.9	1.5	1.2
	L2	1	1	1	1.1	1.1	1.2	1.2	1.2	1.0
	L3	1	1	1	0.9	1	1	1.5	1.2	1.0
	L4	1	0	1	0.7	0.8	0.8	1.7	1.4	1.2
0.5000	L1	1	1	1	0.7	0.6	0.8	0.7	0.7	1.0
	L2	1	1	1	0.6	0.5	0.5	0.8	0.8	0.5
	L3	1	1	1	0.8	0.7	0.7	0.4	0.5	0.3
	L4	0	0	0	0.7	0.8	0.8	0.1	0.1	0.3
Precision of range measurement to target (approx. 6m)		0.04mm			0.1mm			0.3mm		

Table 4.5: Measured translations from instruments to TLS targets

From the table it can be seen that the TS15 is measuring differential distances of between 20mm and 27mm which is a high discrepancy compared to the 25mm movement from the translation stage. With respect to a monitoring environment with a red trigger level of 25mm, if using the TS15 in reflectorless mode, this level of movement is likely to set off the alarm compared to the TS30 which is producing more precise results with a higher accuracy. Therefore this shows a very poor performance, particularly for monitoring, of the TS15 when measuring in reflectorless mode.

The range precision of the TS30 measurements to the TLS targets is better than the precision to the prism and tooling balls. It is thought that this precision is high due to the limited number of significant figures displayed on the total station. Further work would repeat the measurements with a higher number of significant figures. The TS15 shows the same range precision compared to the precision of the tooling balls and prism measurements despite a poor accuracy. This demonstrates that the instrument is able to produce the same precision of 0.1mm with the ATR and reflectorless mode at

this range. The TLS system shows a slightly lower level of precision than the total stations but this still remains at the sub-millimetre level.

Table 4.6 shows the average residuals for each of the laser scanner targets from the TS15 and ScanStation2.

TLS reflectorless target	Instrument observed – expected residuals (absolute) for linear displacements in mm		
		TS15	ScanStation 2
L1	average	0.11	0.12
	st. deviation	1.17	0.32
L2	average	0.18	0.11
	st. deviation	1.94	0.21
L3	average	0.3	0.01
	st. deviation	2.34	0.25
L4	average	0.03	0.05
	st. deviation	1.13	0.34

Table 4.6: Residuals of measurements to TLS targets from total station and TLS system

Even though both the instruments are performing to their respective precision specifications, the TLS system is producing a higher accuracy and precision when measuring to its own target type. This is because of the difference between the measurement processes of the two instruments. The total station is likely to incur a lower precision when manually reading to the target repeatedly. For example, there will be human errors when navigating the cross-hair onto the centre compared to the instrument using the ATR mode to find and measure the prism. There is also potentially a weakness in the return signal when the total station is measuring to the target surface compared to a glass prism, therefore affecting the distance measurement accuracies and precision. The TLS, on the other hand, uses an automated method for calculating the target centre and is designed to be accurate and precise. When comparing these results to the prism reading residuals, it can be seen that the ScanStation2 is performing to a similar level as the TS15 to the prism target. This shows that the instruments are reading to their bespoke targets with their highest accuracy and precision.

To see the differences in the accuracy of the instruments, the residuals of the measurements were plotted in a histogram. These can be seen in Figure 4.19.

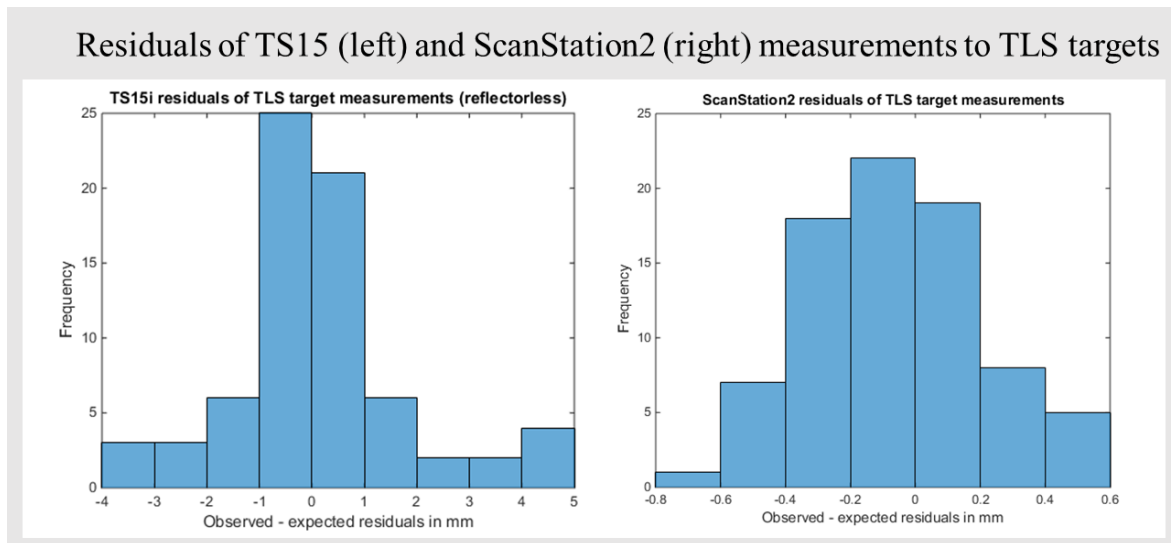


Figure 4.19: Histogram of residuals of total station and TLS system measurements to TLS targets

A chi-squared test was carried out on both data sets and the results showed that there was not enough evidence to show that the TS15 residuals were normally distributed whereas the ScanStation2 residuals were normally distributed. The plot from the total station shows residuals of up to ± 5 mm, but the residuals of the TLS target centre measurements are within ± 1 mm. This confirms that there is a bias in the measurements from the TS15 in comparison to the ScanStation2's automated measurement to the target centre. This is a particularly high error for the TS15 at this working range. There was evidence of a similar level of error present on a separate fieldwork project to this laboratory testing when using the reflectorless mode. The instrument was subsequently sent for calibration. Further work could apply the test procedure once the instrument had returned from calibration to confirm the instrument error.

4.1.2.3 Conclusions

This experiment has shown a comparison between the accuracy and precision of a laser tracker, total station and TLS when measuring static linear movements of a target array using a translation stage. As there is no single target that allows readings to be accurately measured from each of these instruments, a target array with multiple target types was created and developed for this experiment.

The ability to “read” both the tooling balls and prism using the laser tracker and total stations demonstrates the potential of using the laser tracker as a highly accurate and

precise baseline measurement for total station and prism-based monitoring for structures such as railway track or arches. It could also be used as an interim measure along with total station monitoring confirming the performance of the total station measurements.

The results show that the laser tracker can measure to a tooling ball and precise prism with the same level of accuracy and precision of approximately 10 microns and 1 micron respectively when using the ATR function. This shows that the instrument is performing to specification at this range.

The total station is also able to measure to a tooling ball and precise prism with a similar level of accuracy and precision at a sub-millimetre level of approximately 0.1 and 0.2mm respectively when using the ATR function. However when the ATR function is turned off to read the laser scanner targets, the accuracy remains similar but precision becomes worse. This is thought to be due to the bias when making the observations by eye to the reflective surface as opposed to the built-in ATR function.

The TLS results show that the accuracy and precision of measuring target-based movement is 0.1mm and 0.3mm respectively. This sub-millimetre level is a similar level to that of the total station results. Therefore TLS can be seen as a comparable method to total stations for target-based monitoring when applying linear movements.

4.2 Surface-based instrumentation testing

The aim of these tests was to determine what could be accurately captured from the surfaces typical in the railway environment, e.g. the railway track and brick, without the use of targets and determine if these accuracies are comparable to point-based measurement capabilities and whether these values were sufficient for monitoring requirements at Network Rail. The non-contact technologies investigated in this study are terrestrial laser scanning (TLS) and close-range photogrammetry (CRP).

4.2.1 Experiment 3: Surface-based measurement of laboratory rail

In order for TLS or CRP to be used for track monitoring, sufficient coverage of the rail surface must be acquired. If sufficient coverage could be obtained by TLS or CRP, this information would then need to be converted into accurate track geometry such as the track cant and twist (see Chapter 2 section 2.6.1). It would be also useful to measure the track gauge. Currently the prism-based monitoring method is not possible as the prisms are attached to the sleepers. This section details the laboratory tests to determine

the quality of the coverage from these two methods. It also provides a novel procedure for approximating the physical location of a piece of rail.

A section of rail approximately 1.5 metres long was provided by Network Rail TLP in order to carry out the laboratory tests of surface-based measurements through TLS and CRP. An image of the section of rail used for the laboratory tests is shown in Figure 4.20. The model of this type of rail is known as CEN56E1. This is a standard rail type which is used for the terminating tracks at London Bridge Station.

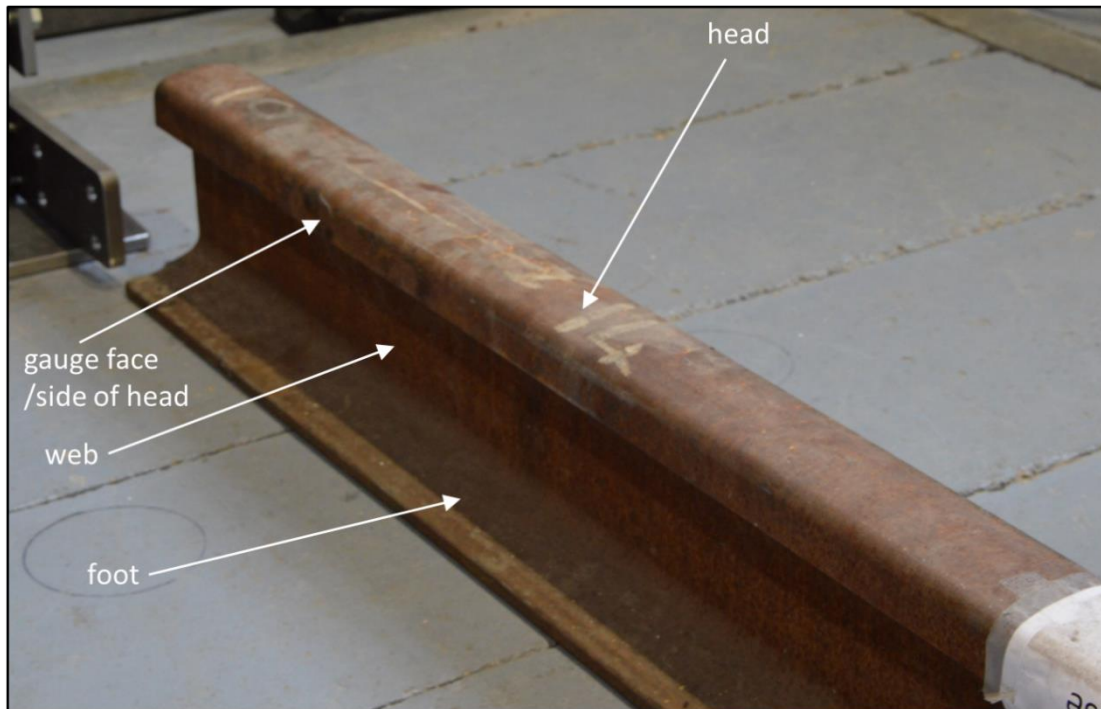


Figure 4.20: CEN56E1 rail used for the laboratory tests

The methods for capturing the rail surface using TLS and CRP are described in sections 4.2.1.1 and 4.2.1.2 respectively.

4.2.1.1 Terrestrial laser scanning (TLS) measurements acquisition

In order to provide an accurate account of the coverage of railway track available from a TLS system on a live site at platform level, the lab track was placed approximately at the same distance and height between the platform and track level. These approximations were based on an initial test scan carried out at London Bridge Station at the allowed safe distance from the platform. Figure 4.21 provides a mock-up of the allowed distance and height between the TLS from the edge of the platform and the set of railway tracks to be observed. It was only possible to scan one side of the rail using the TLS systems at this required distance and height from the rail in the laboratory.

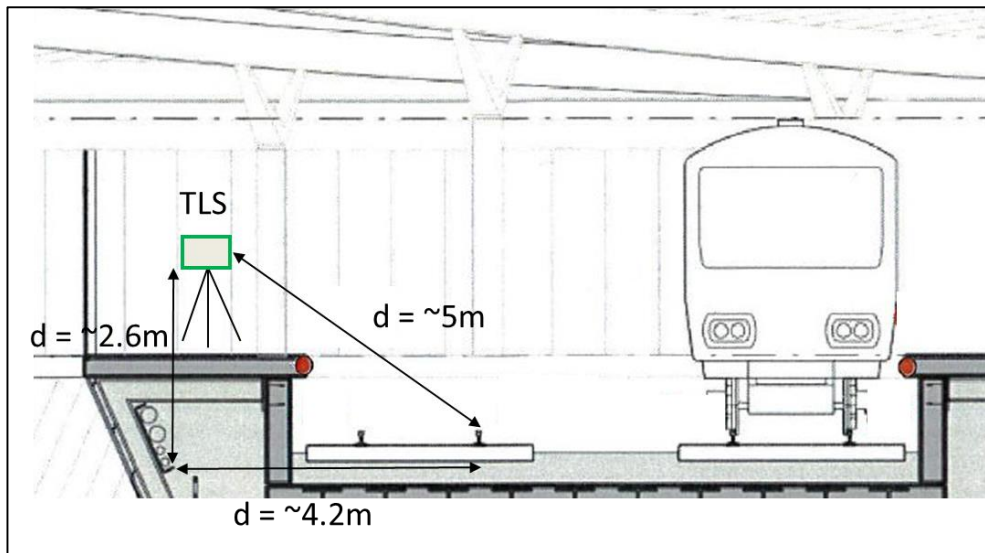


Figure 4.21: Expected height and distance of scanner to track (not to scale), (image taken and adapted from London Bridge Monitoring Specification, Network Rail (2013))

At the time of the laboratory tests, the following state of the art survey grade TLS systems with differing range measurement properties were used to scan the rail track: Leica ScanStation C10 (time-of-flight), HDS7000 (phase-based), ScanStation P20 (hybrid time-of-flight) and the Faro Focus 120 (phase-based). The hybrid scanning total station, the Leica MS50 (time-of-flight), had recently been released and the scan function of this was used to see the quality of the scans in comparison to the TLS systems. All scanners acquired the rail surface with a resolution set to 1mm, which is the highest resolution available for most of the scanners. For this experiment the Leica ScanStation P20 and Faro Focus 120 were available on a different date to the other TLS systems. Due to restricted access in moving the rail in the laboratory space on that date, it was only possible to scan from approximately half of the range (~2.5 metres) compared to the other TLS systems used. The scans were imported and cleaned in Cyclone to produce a 500mm cross-section from each TLS system. The processing of this data is described in Section 4.2.1.3. The time taken using the TLS was between 5 minutes and 30 minutes (the MS50 scans with a slower rate of 1,000 points per second). The processing time to import the scans in Cyclone to acquire a 500mm cross-section was approximately 10 minutes. Therefore the total time to produce the cross-section using TLS was between approximately 20 and 40 minutes.

4.2.1.2 Close-range photogrammetry (CRP) measurement acquisition

To compare the TLS outputs of measuring the rail without the use of targets, CRP using Structure from Motion was applied to the same section of the track. A Nikon

D3200 camera was used with a wide angle 16mm fish-eye lens to capture a network of images of the railway track as well as determine the calibration of the camera (determination of the interior orientation). Camera calibration was carried out using VMS, which outputs a camera calibration file. More information on the camera calibration process can be found in Luhmann et al. (2014). In order to obtain significant coverage of the rail, images needed to be acquired within close proximity of the rail and therefore the simulated platform to track height and distances could not be applied.

Based on the calibration process, the network of images were then corrected for distortion using UCL's Lens Distortion Correction (LDC) software and a fish-eye correction model. The corrected images were run through Visual SFM version 0.5.22 - an open source Structure from Motion bundle adjustment based tool - to carry out feature detection and full pairwise image matching. The dense 3D reconstruction function was then run to produce a point cloud of the rail. The CRP point cloud was then scaled in Geomagic Studio using points in the laboratory that had been surveyed using a total station. This provided a scaled 3D point cloud of the rail. As CRP is a passive system, the capture to point cloud cross-section production time took significantly longer than an active TLS system. The data acquisition time was similar to TLS taking approximately 10 minutes, plus a further 20 minutes for images for calibration to ensure a sufficient number of overlap and targets were captured between images. The calibration process took approximately 1 hour, where selecting the common targets took the most time. The Structure from Motion tool took approximately 1 hour to run to produce a dense reconstruction of the space including the brick surface (see Experiment 4/section 4.2.2). The dense reconstruction of this space used a total of 58 images. This process had been streamlined after optimising the parameters to be inputted to produce a dense point cloud. The scaling process then took a further 10 minutes to allow an accurate point cloud to be produced. In total the time taken from data capture to producing the point cloud took approximately 3 hours.

4.2.1.3 Initial TLS and CRP output of rail surface

After the point cloud of the lab rail had been acquired using TLS and CRP techniques, the raw point cloud cross-sections were examined to give an indication of the coverage quality of the different type of instruments. Figure 4.22 shows the cross-sections, in orthographic view, of the lab rail using the time-of-flight and phase-based scanners as well as the CRP point cloud against its rail design model.

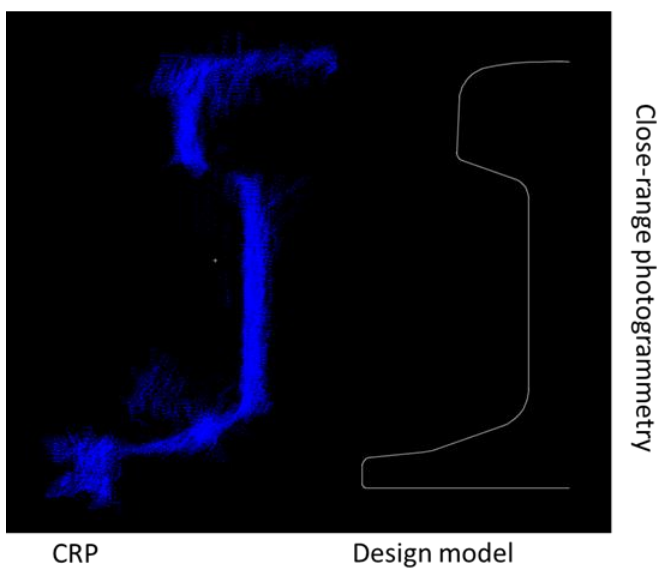
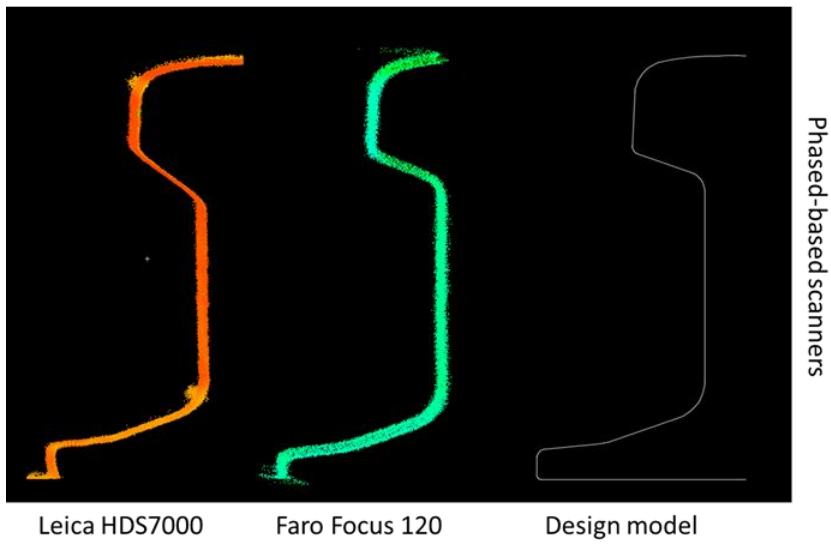


Figure 4.22: Cross-sections of lab rail through TLS and CRP in orthographic view

The point cloud colours are based on the intensity of the scan which is automatically allocated into Cyclone. Due to the angle between the TLS systems and rail (to imitate the angle between the platform and the track), the area between the gauge face and the top of the web of the track (highlighted in the red circle of the design rail model in Figure 4.22) is occluded and the point cloud doesn't accurately represent this part of the track and therefore must be cleaned. Therefore this step will be required when applying TLS on a live track site. However there is a substantial amount of coverage of the laboratory rail surface including the head, web and foot of the rail when compared to the design rail model.

The time-of-flight scanners show a variation in noise level of the rail surface with the C10 appearing to be the "noisiest" with a thick layer representing the cross-section, whereas the P20 and scanning total station MS50 appear to accurately show the head, web and foot of the track. The phase based scanners also show an accurate representation of the geometry of the rail with the Focus appearing to be the most similar to the rail model. This is most likely due to the closer range that it was scanned at compared to the other TLS systems.

The point cloud cross-section from the CRP surface measurement appears quite noisy, particularly around the curved parts of the surface compared to the planar area of the rail. This is analysed in the next section.

4.2.1.4 Plane fitting of TLS and CRP rail surface measurement

The noise quality of the point clouds can be analysed statistically by applying local plane fits using LSE to the areas known to be planar (Clark and Robson, 2004). Based on this type of rail design model the web of the track is planar. For simplicity Figure 4.23 will be used when referring to planar areas of the rail. Local plane fits were applied to the PL2 section of each of point clouds by manually extracting it from the cross-section.

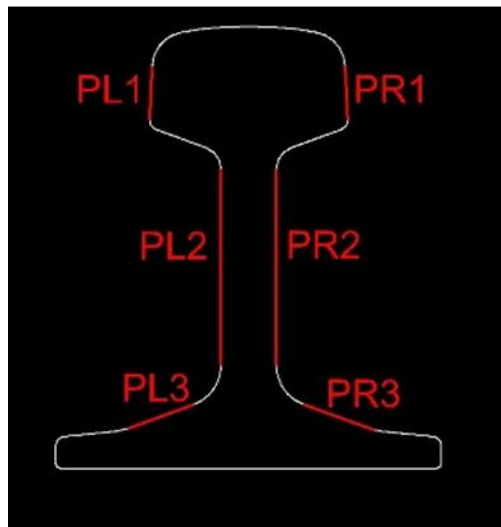


Figure 4.23: Planar based naming reference for rail

Local plane fitting was carried out using CloudCompare as it provides the root mean square error (RMS) of the plane fitting procedure as well as the residuals. The RMS of the residuals of the local plane fits of PL2, the range scanned and number of points of the section is shown in Table 4.7.

	Time-of-flight scanners			Phase-based scanners		Close-range photogrammetry
Instrument used	C10	P20	MS50	HDS7000	Faro Focus 120	Nikon D3200
Maximum range from scanner	5.6m	2.5m	5.4m	5.3m	2.6m	~1.5m
RMS of plane fit to PL2	2.5mm	0.5mm	0.9mm	0.6mm	0.9mm	1.5mm
No. of points in PL2	42,658	13,463	33,207	53,584	10,716	30,010

Table 4.7: RMS of local plane fit to PL2 using TLS and CRP

The number of points of the web of the rail are roughly the same for each of the scanners apart from the P20 and Focus120. This is because these scanners were setup closer to the track and therefore had more of an occlusion to the web of the rail. Therefore there is less coverage of the web of the rail from these scanners. However the RMS plane fits from these scans compared to the others show that there was sufficient coverage of the web despite the occlusions.

The results show that the plane fits with the largest RMS is the C10 with 2.5mm. Based on the point cloud cross-sections shown in Figure 4.22, these results confirm the high level of noise present. The specification of the C10¹⁶ indicates that the modelled surface noise of the scanner is 2mm. Therefore this particular scanner is noisier than expected, especially at a short range of approximately 5 metres compared to the 300 metre range the scanner can measure to. The CRP plane fit is slightly better than the C10 with an RMS of 1.5mm. Despite the high noise levels around the curved parts of the rail, these results confirm a millimetre level of fitting to the web of the rail. The remainder of the time of flight and phased based scanners demonstrate the capability of these scanners to produce a sub-millimetric level of fitting with the P20 and HDS7000 producing the best results for their scanner type. The specifications of the Faro Focus 120, MS50, P20 and HDS7000 do not provide information of the expected modelled surface noise but the sub-millimetre level of fitting is higher than expected based on the millimetre level of range noise to a dark surface expected from all of the scanners, based on the full manufacturer specifications (see Appendix A).

To compare the quality of the plane fits for each of the instruments, the residuals of the plane fits were plotted in a histogram. Figure 4.24 and Figure 4.25 show the histograms for the time of flight and phased based scanners respectively. Figure 4.26 shows the residuals for the CRP plane fit.

¹⁶ C10 full specification: http://hds.leica-geosystems.com/downloads123/hds/hds/ScanStation%20C10/brochures-datasheet/Leica_ScanStation_C10_DS_en.pdf

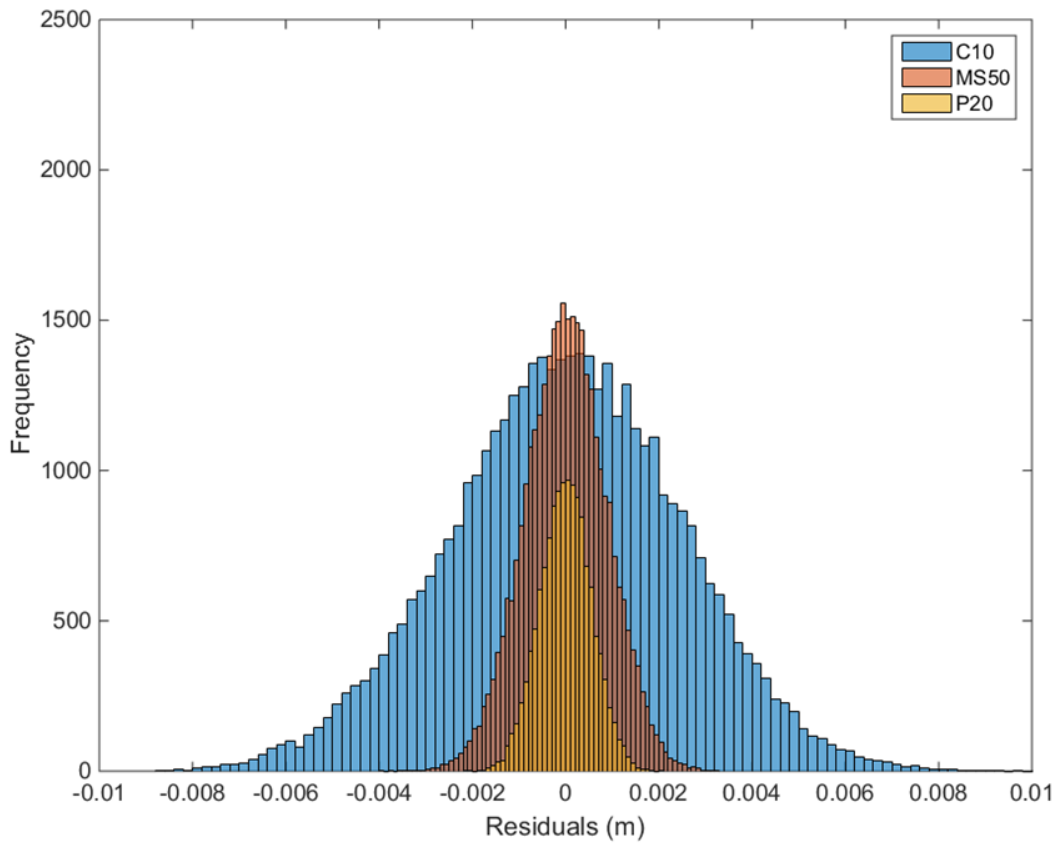


Figure 4.24: Histogram of time of flight scanners plane fitting residuals to web of rail

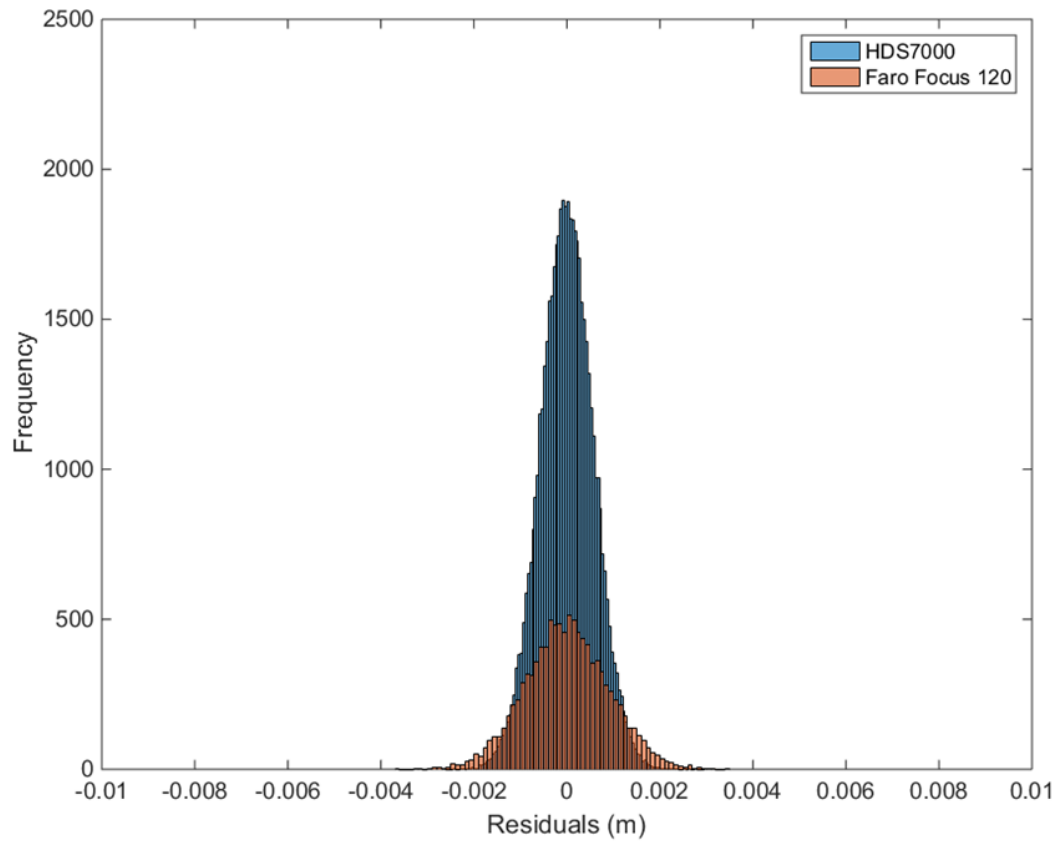


Figure 4.25: Histogram of phase based scanners plane fitting residuals to web of rail

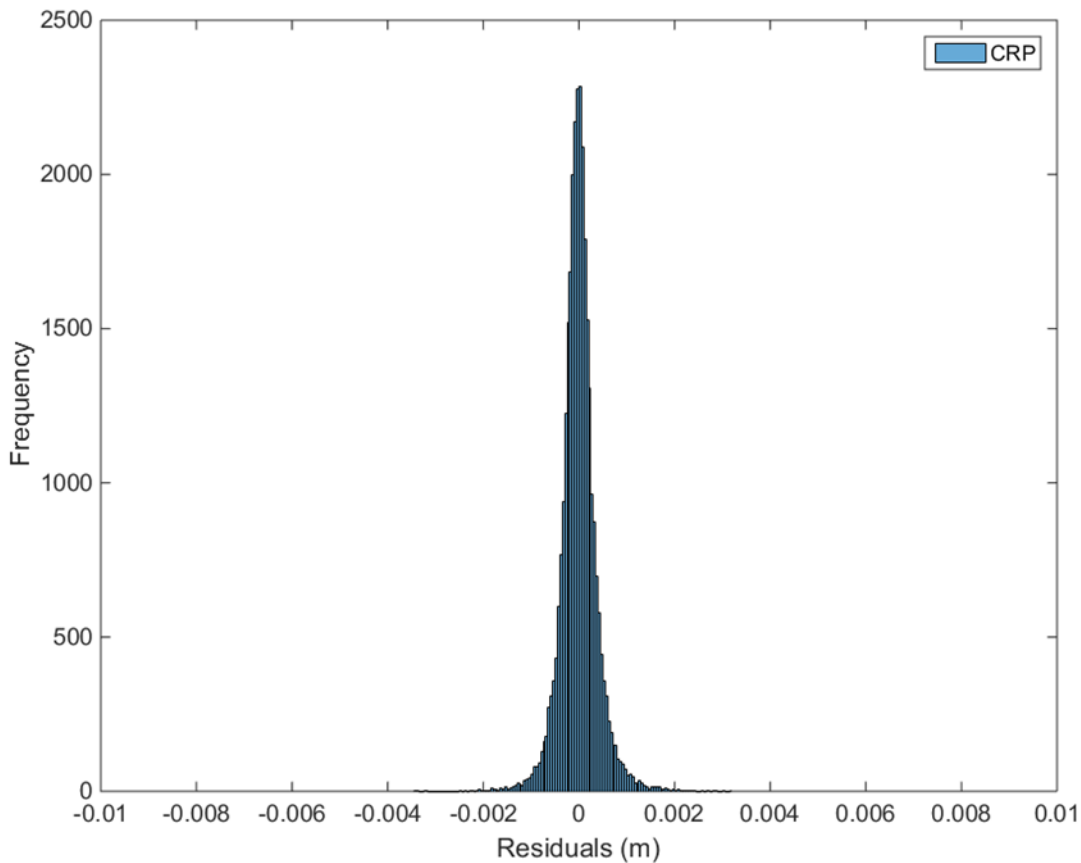


Figure 4.26: Histogram of CRP plane fitting residuals to web of rail

Figure 4.24 shows the C10 has a poor precision for the planar fit with residuals of up to 10mm compared to the MS50 and P20 which are showing a good accuracy and precision of the plane fit to the web of the rail. As the MS50 and P20 have different sample sizes, an F-test was carried out to see if the variances of the residuals were statistically different. To determine if the variances are significantly different, the F value calculated from the equation below is compared to the F distribution table which is dependent upon the degrees of freedom (ν) for each sample. The F value can be determined by the following:

$$F_{[\nu_A, \nu_B]} = \frac{S_A^2}{S_B^2}$$

where A, B = datasets to be compared, s = the variance of the dataset and ν = the degrees of freedom.

In this case the calculated F-value for the MS50 and P20 data (0.389) was less than the critical value (0.976) which showed that the variances are not significantly different.

Therefore the two datasets are comparable with respect to their plane fitting residuals, implying similar levels of noise between the TLS systems.

From Figure 4.25 it can be seen that both the HDS7000 and Focus 120 have a very good accuracy but the precision for the Focus 120 is poor compared to the very precise HDS7000. Comparing these values to the histogram in Figure 4.26 it can be seen that the plane fitting using CRP is very accurate, however the precision is not as good as the HDS7000 or P20.

Overall it can be seen that the most accurate and precise TLS systems for the plane fitting procedure of rail is the HDS7000 and P20. The CRP point cloud shows a similar level of accuracy to these two TLS systems but the precision is slightly worse.

In order to determine the track geometry required by the engineers, an accurate fitting process of the whole point cloud to a reference model must be established. The results of the plane fitting in section has given an indication of the potential quality of rail fitting process locally for the web of the track. Based on these results, a rail fitting process was created and developed based on the live railway track monitoring site. This is discussed in detail in section 5.7.

4.2.2 Experiment 4: Surface-based measurement and range translation performance of brick

Another surface that was measured and tested in the laboratory, using TLS and CRP as a non-contact and targetless solution, was brick. According to the London Bridge Station monitoring specification arches are required to be monitored monthly, weekly or daily with at least $\pm 3\text{mm}$ accuracy. Therefore the objective of this test was to establish how well the surface could be measured using TLS and CRP and whether either of these could be used to detect movement of the brick to this level of accuracy. At the time of the initial surface based testing in the laboratory, the only available TLS system was the phase-based Faro Focus 120. However, this was the same system that the survey contractors at London Bridge Station had that would be accessible for their site testing. Therefore the lab performance testing of this TLS system would provide an indication of the expected performance of the contractor's scanner when used in the arches. The MS50 scanning total station was released after the Focus 120 had been used in the laboratory and arches test. Therefore this instrument was used to see its capability as well as allow a time-of-flight type of scan to be compared. The same

camera used for the CRP railway track surface measurement was used in this experiment (Nikon D3200 + 16mm fish-eye lens).

4.2.2.1 Surface-based measurement of brick

A small sample of a brick wall, approximately 20cm x 20cm, was created. This is shown in Figure 4.27 .

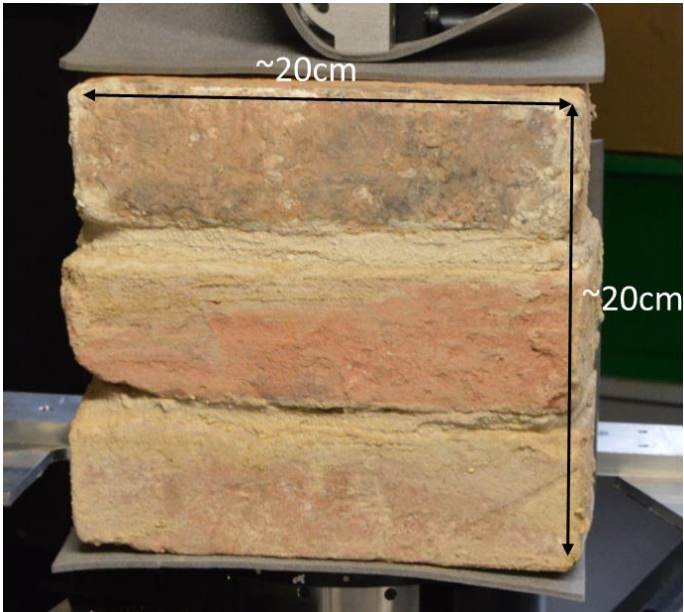


Figure 4.27: Sample of brick wall used for laboratory tests

The surface was then scanned using the Focus 120 as well as the scanning total station MS50 at approximately 6 metres from the scanners at a 1mm resolution. CRP was applied to the same surface using a similar methodology described for the track surface measurement acquisition in Section 4.2.1.2. The point cloud of the surface from each of the instruments is shown in Figure 4.28.

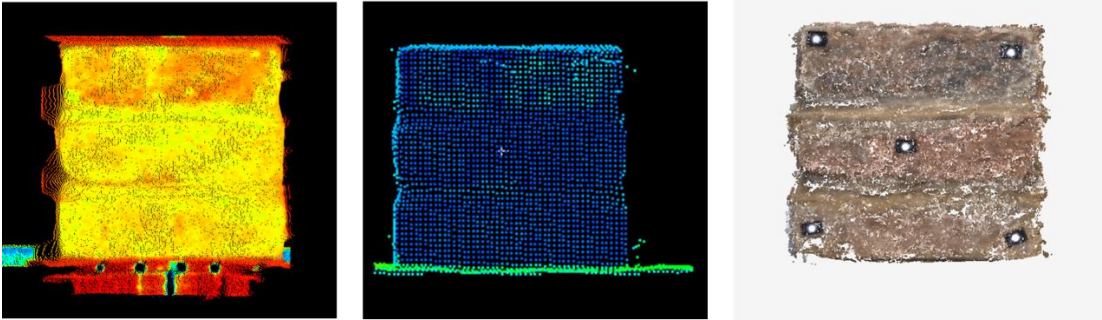


Figure 4.28: Point cloud from MS50, Focus 120 and CRP respectively from left to right

Based on the work from Monserrat and Crossetto (2008) and similarly to section 4.2.1.4, in order to gain an understanding of the quality of the point clouds when scanning this surface, geometric primitive modelling was used. Despite the sample

brick not being perfectly planar, it allowed an approximation for the surface comparison between the instruments to be made. Therefore it would be expected that the RMS is not as close to zero as with the plane fitting of the rail web. Table 4.8 provides the results of the plane fitting process from the different instruments.

	Time-of-flight scanner	Phase-based scanner	Close-range photogrammetry
Instrument	MS50	Faro Focus 120	CRP
RMS of plane fit of masonry brick wall	1.9mm	2.1mm	1.8mm
No. of points	42,028	33,833	61,959

Table 4.8: RMS of plane fitting to brick wall

The results show a comparable level of performance between these three different instruments when applying plane fitting. This RMS level of fit around the 2mm level also matches the findings from Laefer et al. (2014), where plane fitting was applied to a test brick surface using TLS to determine crack detection limits. As expected the RMS of the residuals are high in comparison to the web of the rail plane fit as it is known that this surface is not perfectly planar. However the results demonstrate the sensitivity of the methods to detect change of better than 2mm to a surface of unknown surface planarity.

In order to have a better understanding of the noise levels of the instrument's surface measurements, the same planar patch from a single brick was selected from each of the point clouds and plane fitting was applied. The results are shown in Table 4.9.

	Time-of-flight scanner	Phase-based scanner	Close-range photogrammetry
Instrument	MS50	Faro Focus 120	CRP
RMS of plane fitting of planar patch of brick	0.7mm	0.8mm	0.7mm

Table 4.9: RMS of plane fits to planar patch of a single brick

These results show a sub-millimetre capability of fitting to the planar surface for each of the instruments used. These results agree with the RMS values from plane fitting of the web of the railway track in section 4.2.1.4, where the surface of the track was

known to be planar. Based on the results from the track plane fitting, these results confirm that the instruments are performing as expected.

4.2.2.2 Methodology

In order to test the accuracy of these instruments to detect movement of the brick wall without the use of targets, the object was set up on the translation stage in a similar way to the range translation performance experiment presented in section 4.1.2. The TLS systems' setup for this experiment is fairly straight forward as the measurements are taken based on knowing that the TLS system is stationary on a fixed point. In order to obtain suitable coverage of the surface CRP requires images to be taken around the object and therefore the camera cannot be stationary, particularly when there aren't any targets attached. Therefore CRP was not used in this particular experiment.

The TLS systems were set up in a similar way to the target-based experiment, approximately 6 metres away from the translation stage on a heavy-duty tripod. An example of the laboratory setup is shown in Figure 4.29 with the MS50 and brick wall on the translation stage highlighted in white.



Figure 4.29: Brick wall translation test (white box) with the MS50

The same movements as the target based experiment were applied to the translation stage: 25mm, 10mm, 5mm, 2mm, 1mm and 0.5mm. After each movement, scans of

the brick were acquired. The point clouds were exported from Leica Cyclone into CloudCompare to allow a distance comparison to be made. In order to analyse the deformations, the three different methods of point-wise comparisons discussed by Vosselman and Maas (2010) were applied: point to point, point to plane, and surface to surface. There are functions in CloudCompare that allows the first two of these comparisons to be made. Firstly, the “Cloud to Cloud distance” tool calculates the 3D distances between a reference and model point cloud which outputs a mean distance and standard deviation. The second tool is the “Cloud to mesh distance” function which uses the reference model/mesh as a baseline to compute the distance between the point cloud (which has moved) and the mesh (baseline). This also provides an average distance along with the standard deviation. For both comparison tools a colour coded surface displacement map of the surface and histogram of the residuals from the reference cloud or mesh is outputted. An example of this is shown in Figure 4.30.

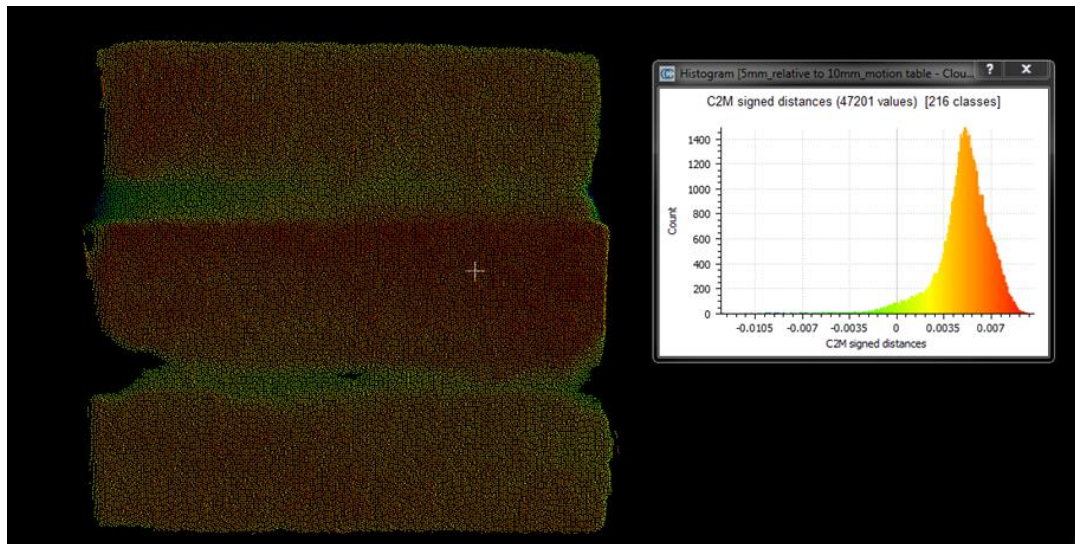


Figure 4.30: Colour surface displacement and histogram output from distance comparison in CloudCompare

For the third deformation analysis method, Geomagic Qualify 2013 was used to allow a mesh to mesh surface comparison of the “reference” and “test” model. A mesh is created by converting the point cloud into a polygonal surface mesh. The “3D Compare” function allows a reference and test object to be identified. The 3D deviations between the reference and test model are then calculated and reported. Figure 4.31 provides a figure of the 3D deviation process. The test object can be either a point cloud or surface mesh. For this comparison the test object was a surface mesh.

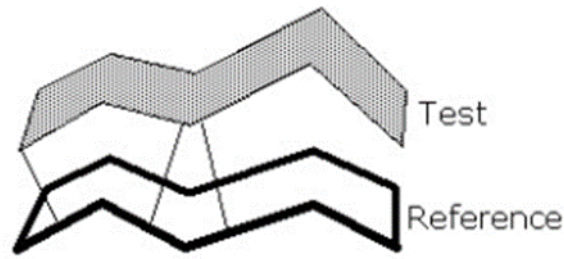


Figure 4.31: Geomagic Qualify 2013 3D Deviation Comparison concept

The output of the 3D deviation tool is also a colour coded surface displacement map alongside the average distance and standard deviation between the two meshes. However the residuals of the deviations are not available from this software. Figure 4.32 provides an example of the output when comparing the 3D deviation between the baseline and test meshes, with the scale shown in metres.

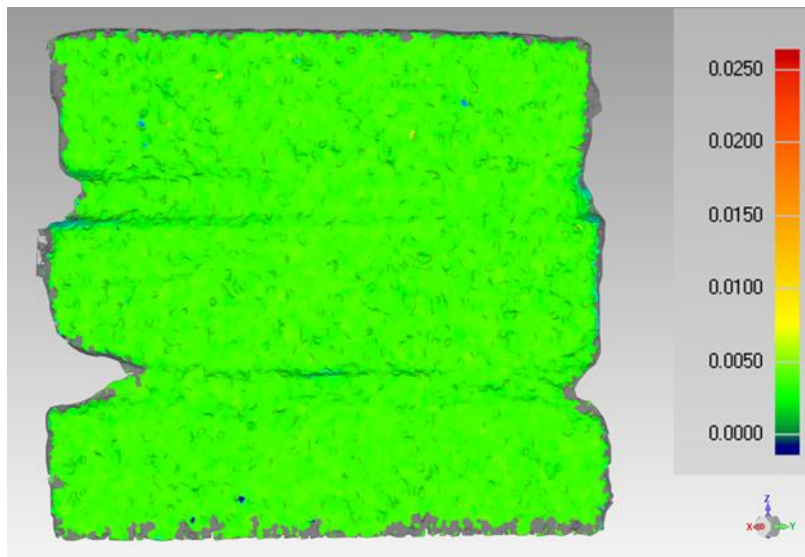


Figure 4.32: Geomagic Qualify 2013 3D deviation output (in metres)

4.2.2.3 Results and analysis

Similarly to the results shown in Section 4.1.2.2 of the target based range translation test, the cloud to cloud, cloud to planar mesh and surface mesh to surface mesh differential distances from the Focus 120 and MS50 undergoing different translations is shown in Table 4.10. The residuals (average) and precision (standard deviation) of the three different distance comparison methods of the TLS systems are shown in Table 4.11.

Distance comparison method (software used)		Cloud to Cloud Distance Comparison (CloudCompare)		Cloud to Planar Mesh Distance Comparison (CloudCompare)		Surface Mesh to Surface Mesh Distance Comparison (Geomagic Qualify)	
Movement on translation stage (mm)		Faro Focus 120	MS50	Faro Focus 120	MS50	Faro Focus 120	MS50
25.0	average displacement	23.4	23.2	24.5	24.9	24.4	25.0
10.0		9.0	8.7	9.6	10.1	9.1	9.5
5.0		5.2	4.1	5.2	5.0	5.2	4.6
2.0		2.6	1.6	2.3	2.1	2.1	1.8
1.0		1.4	0.9	0.5	0.9	0.9	0.8
0.5		1.1	0.7	0.3	0.5	0.3	0.5

Table 4.10: Measured translations from TLS instrument to brick surface on translation stage

		Instrument observed – expected residuals (absolute) for linear translations in mm					
		Cloud to Cloud Distance Comparison		Cloud to Planar Mesh Distance Comparison		Surface Mesh to Surface Mesh Distance Comparison (Geomagic Qualify)	
Movement on translation stage (mm)		Faro Focus 120	Leica MS50	Faro Focus 120	Leica MS50	Faro Focus 120	Leica MS50
25.0	average	1.6	1.8	0.5	0.1	0.6	0.0
	st. deviation	1.3	1.2	2.0	1.9	0.5	0.7
10.0	average	1.0	1.3	0.4	0.1	0.6	0.5
	st. deviation	1.1	0.8	2.5	1.9	0.9	0.9
5.0	average	0.2	0.9	0.2	0.0	0.9	0.4
	st. deviation	0.7	0.7	2.5	2.0	0.2	0.8
2.0	average	0.6	0.4	0.3	0.1	0.7	0.2
	st. deviation	0.6	0.5	2.3	1.8	0.1	0.4
1.0	average	0.4	0.1	0.5	0.1	0.8	0.2
	st. deviation	0.7	0.5	2.4	1.8	0.1	0.5
0.5	average	0.6	0.2	0.2	0.0	0.6	0.0
	st. deviation	0.6	0.3	1.9	2.0	0.2	0.4

Table 4.11: Residuals of measurements from instrument to brick surface

Table 4.11 shows that the accuracy of the distance measurement overall are better than $\pm 2\text{mm}$ for each of the distance comparison tools. This is an acceptable value based on the manufacturer’s specifications as well as the monitoring specification’s accuracy requirement of $\pm 3\text{mm}$.

The cloud to cloud distance comparison has the lowest accuracy of better than $\pm 1.8\text{mm}$ and precision of approximately $\pm 1\text{mm}$. The scanner never hits the surface on the same point twice and therefore when comparing two different point clouds, the distance

between two points will never exactly be the corresponding points between the two different scans.

The cloud to planar mesh distance comparison shows a very high accuracy of better than $\pm 0.5\text{mm}$. However the precision of this tool is very low with precision values of $\pm 2.5\text{mm}$. This shows that the planar fit of around 2mm is limiting the precision of the results.

The results from the surface mesh to surface mesh show a very high accuracy and precision when detecting movements of the translation stage at the sub-millimetre level with the Faro 120 producing an average accuracy and precision of 0.3mm and 0.7mm respectively. The MS50 is performing slightly better with an average accuracy and precision of 0.2mm and 0.6mm respectively. The high accuracy and high precision is based on exploiting the redundant surface information and producing a mesh as opposed to fitting a plane. It can be seen that the results from the tool in Geomagic are the best overall. These results are very promising and comparable to those from the total station for target based measurements, where sub-millimetre levels of accuracy and precision of 0.1mm and 0.2mm respectively is achieved. Therefore it can be said that the TLS systems show a similar capability of sub-millimetre levels of performance as the total station at this range for these level of movements.

4.2.2.4 Conclusions

This experiment was carried out to investigate the TLS and CRP capabilities of measuring to a brick surface. Similarly to the track surface measurement, planar fitting was applied to gain an understanding of the point cloud noise levels of the scan. As the brick wall was not perfectly planar, the plane fit RMS was approximately 2mm from the TLS systems and through CRP, which matches the findings from Laefer et al (2014).

Three different types of displacement comparisons were carried out between the reference and test brick wall position: cloud to cloud, cloud to planar mesh and surface mesh to surface mesh.

The most accurate and precise results were produced when calculating the distances between two surface meshes. The sub-millimetre level of accuracy and precision from the surface to surface comparison is comparable to results from the total station measuring to targets on the translation stage. The ability to detect small changes in

displacement shows the potential of TLS for measuring to brick surfaces at larger scale, such as the London Bridge arches.

The cloud to cloud and cloud to planar displacement techniques produced an accuracy of better than $\pm 2\text{mm}$ which is very promising based on the $\pm 3\text{mm}$ accuracy specifications of monitoring masonry arches at London Bridge Station. The lowest precision for the measurements was when the cloud to planar mesh comparison tool was used. This was low due to the brick wall being approximated as a plane, where the brick isn't perfectly planar.

The MS50 produced a slightly higher accuracy and precision compared to the Focus 120. The data acquisition time for this small sample of brick wall was approximately 5 minutes and 1 minute respectively. The MS50 took slightly longer due to the scan rate of 1,000 points per second compared to the 1 million points per second from the Focus 120. Similarly to the railway track experiment, the results show the flexibility of the MS50 for discrete and surface-based measurements, particularly for localised scanning of features that might need to be monitored regularly over time. Due to access to the Focus 120 on the site and results achieved in the laboratory, this was the TLS system that was chosen for the site test of the masonry brick arches.

4.3 Chapter Summary

Network design and analysis: Experiment 1 presented a method of testing instrumentation performance through the well-established network design and analysis processes to show whether or not a total station is performing to specification. This type of network analysis through least squares estimation is well established in literature and is essential for deformation monitoring to ensure errors in measurement are not perceived as actual movement. By using metrology instrumentation observations it shows the flexibility of using network analysis as well as providing a gold standard to show the strength of a network and its performance.

Target measurement capability: Experiment 2 provided a method of testing a laser tracker, laser scanner and total station's level of accuracy and precision when applying static linear movements of targets ranging from 0.5mm up to 25mm. The results showed that the laser scanner was able to measure to the same sub-millimetre level of accuracy and precision (0.1mm and 0.3mm respectively) as the total station (0.1mm and 0.2mm respectively) when reading to its respective target type. This test provided

a method of checking capabilities of monitoring instrumentation for detecting displacements of targets. The test also provided a method of testing three different instrumentation types, i.e. laser tracker, terrestrial laser scanner and total station, simultaneously by creating a target array of the different target types.

Measuring an engineered surface: Experiment 3 provided a way of analysing the quality of point cloud outputs from terrestrial laser scanning (TLS) and close-range photogrammetry (CRP) when measuring the surface of a typical rail track used in the UK rail industry (CEN56E1). By applying plane fitting to the flattest surface of the rail (i.e. the web of the rail) it allows the user to quickly understand the noise levels of the instrument to this particular surface. The results show that a sub-millimetre level of plane fitting (0.5mm) is possible using TLS, indicating the potential quality achievable for rail fitting in order to measure track parameters essential for track monitoring. This process is taken forward through the practical application of track monitoring in Chapter 5.

Measuring an arbitrary surface: Experiment 4 showed a method for analysing the quality of the point cloud outputs from TLS and CRP when measuring to a surface with an unknown level of flatness, in this case a brick surface. Similarly to Experiment 2, linear movements were applied to the brick surface to allow the accuracy and precision of the targetless displacements to be measured. 3 different types of point cloud data processing techniques were applied for measuring surface displacement: cloud to cloud; cloud to planar mesh; and surface mesh to surface mesh. The results showed a sub-millimetre level of accuracy and precision (0.2mm and 0.6mm respectively) when measuring the linear displacements between surface meshes from the TLS data. This compares to the accuracy and precision levels of target based measurements. This data processing technique is taken forward when measuring displacements of a set of deforming brick arches in Chapter 6.

4.4 Opportunities and challenges for Network Rail

4.4.1 Opportunities

- Testing monitoring instrumentation before, during and after deployment to check the performance of an instrument in a controlled environment. The test procedure would provide validation of an instrument that might not be performing to its specification and would state whether the instrument required to be sent to the manufacturer for calibration. The tests could also be applied to newer technology being introduced to see its capabilities with respect to the current technology.
- Similarly to field testing in surveying (e.g. 2-peg test used for levelling), the network testing procedure could be setup in a laboratory space but also on site where a network of targets or points could be setup.
- All the experiments carried out in this chapter could be automated to reduce the processing time and allow the user to see in near real-time how well the instrument in question is performing. An instrument could be set up on a fixed position to allow data capture to be speeded up. For example reading to targets/prisms could be automated by creating an observation “schedule” which allows the observations to be made automatically once set up on a fixed position. For the capture of surfaces using TLS, a pre-defined window could be created to pick up that particular feature from a fixed position. Analysis of the observations in STAR*NET/Geomagic/CloudCompare could be automated by creating a macro or plug-in to the software. This would then allow the user to see the analysed results instantaneously. The instrument could also be left to run continuously if required to carry out dynamic testing in a controlled environment.
- Metrology instrumentation, despite being a more expensive solution, can be used to provide a more precise and accurate method of monitoring using the same principles of measurement as a total station. For example, network design, adjustment and analysis of redundant observations to targets can be applied. This would be particularly useful for a baseline measurement
- This chapter highlights simple instrumentation testing which could be incorporated into the monitoring specification for a project to provide assurance to the engineers of the instrument’s performance as well as to check that the specifications are being adhered to.

4.4.2 Challenges

- Network Rail currently doesn't have a dedicated lab testing facility to undertake laboratory tests in-house as all survey and monitoring work is sub-contracted out.
- There is a lack of in-house expertise at Network Rail for carrying out assurance of all aspects of the monitoring procedure on projects, i.e. from network design through to quality checking the output data.
- Network Rail rely on the contractors to perform assurance checks i.e. the work is sub-contracted. During research of the workflow for monitoring at NR TLP (described in Chapter 2) there was little evidence from the monitoring industry that there is good practice of network design and adjustment. However, based on the findings from this chapter, the need for instrument testing could be emphasised and incorporated into the monitoring contract to enforce this as best practice.
- The methods identified in Experiment 1 allow checks on instrumentation performance. Further research would be required to ascertain and compensate for instrument drift, which is very important when assessing continuous monitoring.

Chapter 5 – London Bridge Station site test: monitoring of railway track

The aim of this chapter is to validate the terrestrial laser scanning (TLS) findings from the rail surface measurement experiment in the laboratory (see Chapter 4 experiment 3). This enables a novel rail fitting method to be developed to extract track geometry parameters, which are required by the engineers. Based on the quality of fitting, a comparison can then be made between the track geometry values derived from TLS and from the conventional prism-based monitoring data from a total station.

5.1 Site Challenges

Ultimately the biggest challenge for this site is to have enough surface coverage of the track in order to calculate track geometry parameters and validate these based on the current track monitoring prism setup. Despite carrying out the laboratory tests in a way that simulated the platform and track environment, there are a number of challenges and logistical issues when scanning a live track environment that cannot be created in the laboratory. The main challenges met during this live monitoring site testing are described here.

Firstly in order to access the platform, a notice period of at least one week is required. It must be ensured that no other major works are taking place in the area and trains must not be berthed on the platforms as this would occlude surface measurement to the track. Logistically, this can take a few weeks to have all these requirements in place before data capture can be carried out. In this case the data capture needed to be acquired during engineering hours to avoid passing trains. When working on platform level, safety rules must be adhered to, for example equipment must be setup at least 2.5 metres away from the edge of the platform if a track possession has not been acquired. One of the challenges from the TLS data capture point of view is the reality of coverage of all the tracks from one TLS setup. If this is not achievable a method of incorporating two scans accurately to achieve the same level of plane fitting as in the laboratory must be explored. During data capture there are environmental factors that could affect the TLS data such as weather (as this is an outdoor environment) and dust from construction work in the vicinity may affect the data and sensor. The data capture was carried out during engineering hours, this could result in occlusions of capturing

surface information by passing workers. As this type of data capture is dealing with a larger area than in the laboratory, there are challenges with dealing with a much larger dataset in order to extract sections automatically along the track line.

5.2 Data Capture

As described in Chapter 2, London Bridge Station is a major transport hub in Central London. As part of the Thameslink Programme, the station is required to undergo a full refurbishment to accommodate the upgrade of the major railway line running through it to allow an increase in the number of passenger carriages as well as the frequency of trains. The station is required to remain operational during the entire project which started in 2012 and is due to finish in 2018. During the refurbishment, the tracks and platforms are required to be monitored throughout the project as they fall within the zone of impact during demolition and construction work. Currently the track monitoring system consists of robotic total stations measuring to prisms mounted on the sleeper adjacent to each running rail and on the platform wall along the length of platform and track. A mixture of tamper proof and L-bar prisms were installed over the test period. An image of the tamper proof and L-bar prisms attached to the sleeper along with their visibility in a point cloud are shown in Figure 5.1.

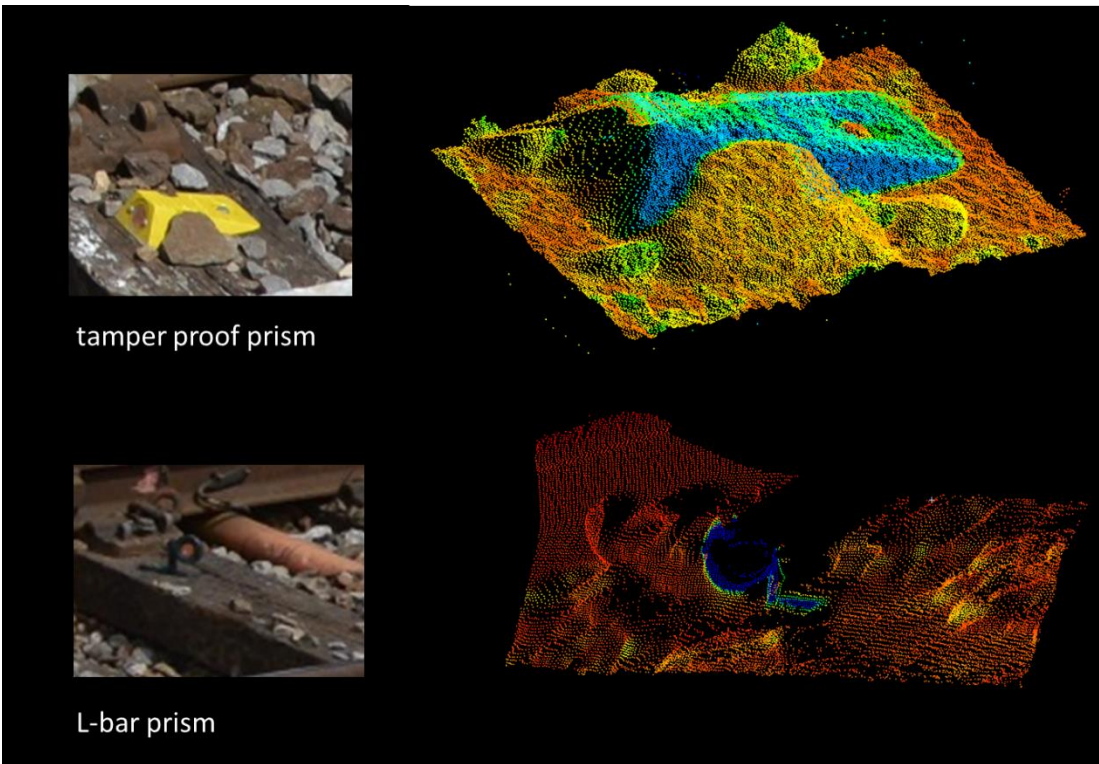


Figure 5.1 Image and point cloud of tamper proof and L-bar prisms typically used for total station monitoring, not to scale

The track test area was chosen based on its requirement to be monitored throughout the study (through prism based monitoring) and would also remain untouched by the demolition team until the data capture phase of the study was due to be complete. The test area of track is approximately 25m long. This section of rail contains two running lines with a raised electric third rail running in between these. Based on the plane fitting experiment using the model track in laboratory described in Chapter 2 (experiment 3), the Leica HDS7000 was used for the railway track site tests at London Bridge.

Typically for deformation monitoring, at least three epochs of data capture is required before detection can be assessed (Caspary and Rieger, 2000). Therefore the track test area was scanned over four epochs whilst being monitored through prism-based monitoring. Four epochs were chosen across the 18 month period of the data capture stage. Table 5.1 shows the times of data capture on this site:

Reference	TLS Capture date	TLS used
Epoch 1	August 2012	HDS7000
Epoch 2	February 2013	HDS7000
Epoch 3	May 2013	ScanStation P20
Epoch 4	March 2014	HDS7000

Table 5.1: Epochs of TLS Data Acquisition at London Bridge Tracks

It should be noted that for Epoch 3 the newly released ScanStation P20 was used as an alternative. Even though this resulted in discontinuity, laboratory tests carried out in Chapter 4 showed that this system was able to perform at a comparable level to the HDS7000. Therefore this provided an opportunity to compare the quality of data of the same surfaces from a state of the art phased-based and time-of-flight TLS under site conditions.

In order to comply with Network Rail’s health and safety regulations of working in proximity to live track, the scanner was setup 2.5 metres away from the edge of the elevated platform. Two 360° scans on the eastern side of the test area (referred to as Scan A and B) were carried out, one on each side of the platform to ensure both sides of the rail was captured. The scanner was also setup in alignment with the prisms on

track so that comparisons could be made between the track geometry from the TS and TLS systems. Figure 5.2 shows the approximate scanner positions (green) with respect to the track and prism placement (red).

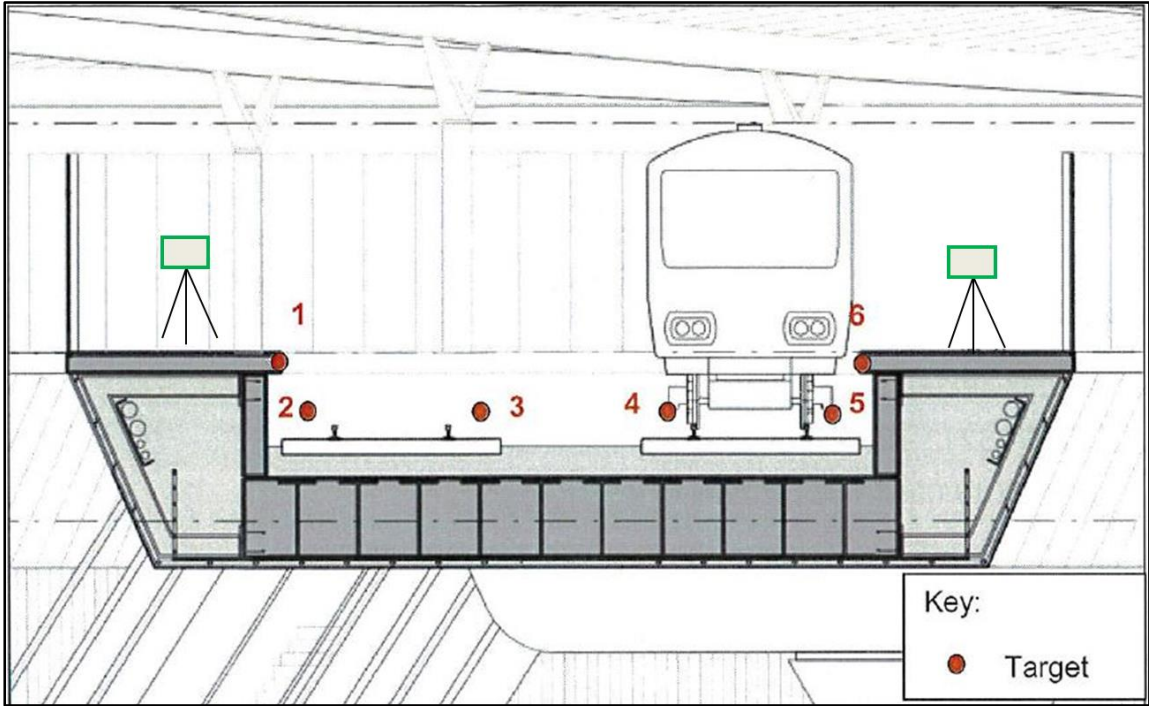


Figure 5.2: Scan positions at platform level (image taken and adapted from London Bridge Monitoring Specification, Network Rail (2013))

In order to compare the accuracy of the scans from a longer range, this process was repeated and a second set of scans was setup approximately 25m west of the test area (referred to as Scan C and D). Each scan was approximately 20 minutes each; according to the manufacturer’s specification this type of scan provides a point resolution of 2-3mm at a 10m range from the scanner. Figure 5.3 illustrates the TLS setup from the top view looking down, where scan positions are represented by yellow triangles. For each epoch the TLS was setup roughly in the same position as Epoch 1 and no permanent marker was used. This was to reduce the time required on-site.

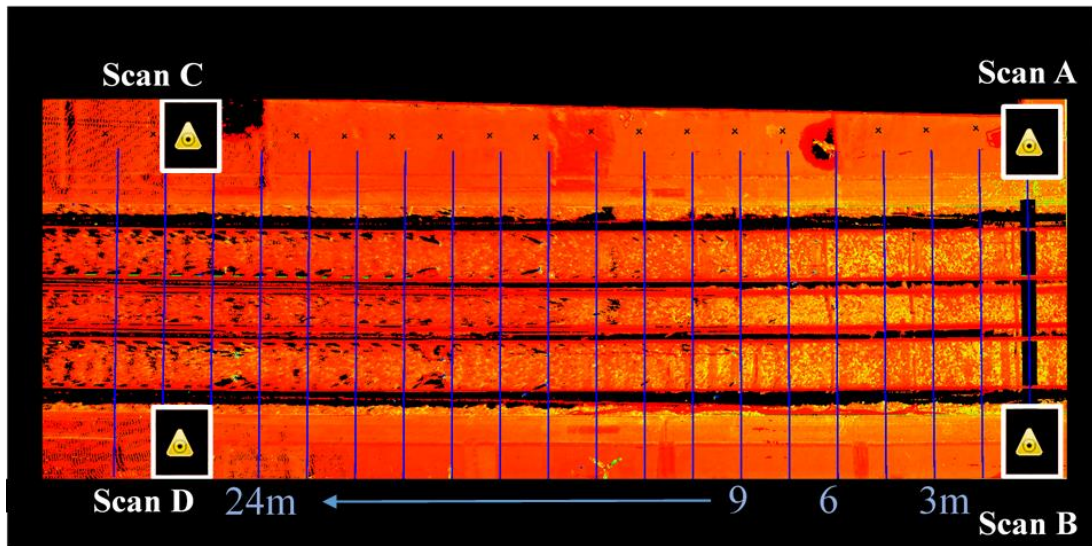


Figure 5.3: Scanner positions (top view) including cross-section locations and track labelling

A combination of spheres and black and white tilt and turn checkerboard targets were distributed at various heights across the platforms within the area of interest (see Chapter 3 section 3.2.3.1). Based on previous knowledge and studies on point cloud registration (Becerik-Gerber et al., 2011), targets were used to be able to achieve the highest possible registration between the scans in Cyclone. The targets were observed using the Leica TS15i total station and the scans were geo-referenced by observing to prisms that were already being used as a reference for the prism-based track monitoring system deployed by monitoring contractors. The total station observations were processed in a similar way to experiment 1 in Chapter 2, where STAR*NET was used to provide the target co-ordinates through a least squares network adjustment using a minimally constrained network. Figure 5.4 provides a network plot of the reference prisms and target positions. The red circles show the station co-ordinate error ellipse which is the uncertainty of that station's position. The diagram shows an exaggeration in the error ellipses. The target positions are labelled TARG01-06.

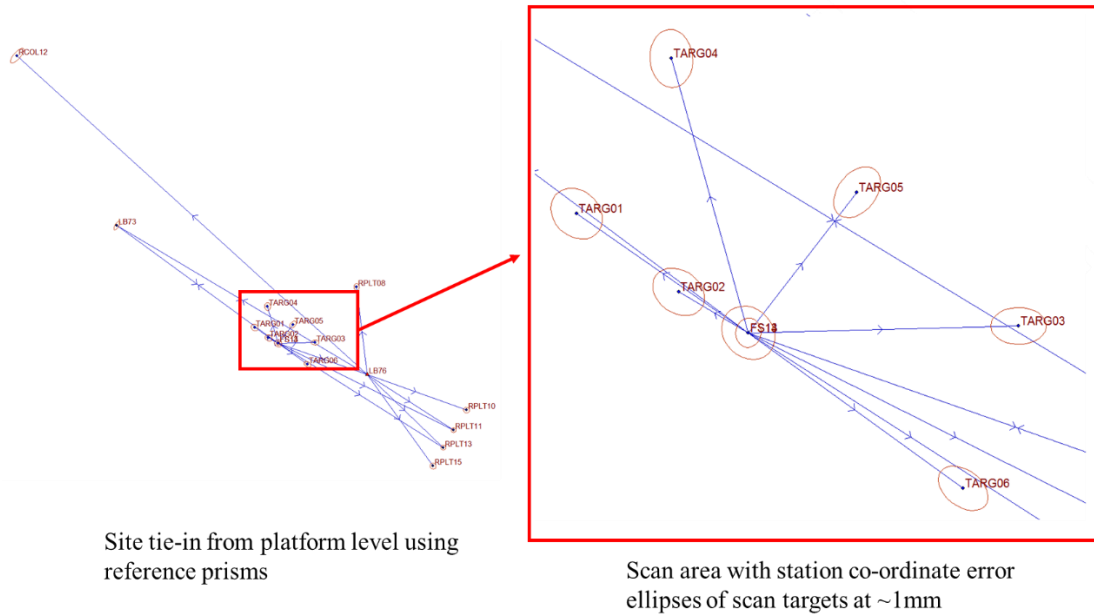


Figure 5.4: Network plot from STAR*NET for scanner target positions

The error listings show that the station co-ordinate standard deviations are on average 1.0mm. Therefore there is uncertainty of 1mm of the position of the target positions, highlighting the high quality of the survey network. The adjusted co-ordinates were used for the registration process which is outlined in Section 5.4

5.3 Importing Raw Scans

When importing HDS7000 and P20 raw scans into Cyclone it must be ensured that the most recent version of Cyclone is being used. This is to ensure that any bugs present in previous versions, usually related to importing scans, have been resolved. When the epoch 4 scans took place in March 2014 the HDS7000 scanner had become discontinued by Leica and a new version of Cyclone had been released (8.0.1) in parallel with the release of the (then) new ScanStation P20 in March 2013. Therefore when importing the P20 files from epoch 3, the version of Cyclone had to be upgraded in order to handle the point cloud. However file import support for the HDS7000's .ZFS file format became troublesome in the newer version. A single 360° scan from one position would come in “segmented” and in different orientations. Figure 5.5 shows an example of this issue where one full scan has become segmented into three separate scans which have been coloured differently for visualisation purposes: default intensity coloured (1), blue (2) and green (3).

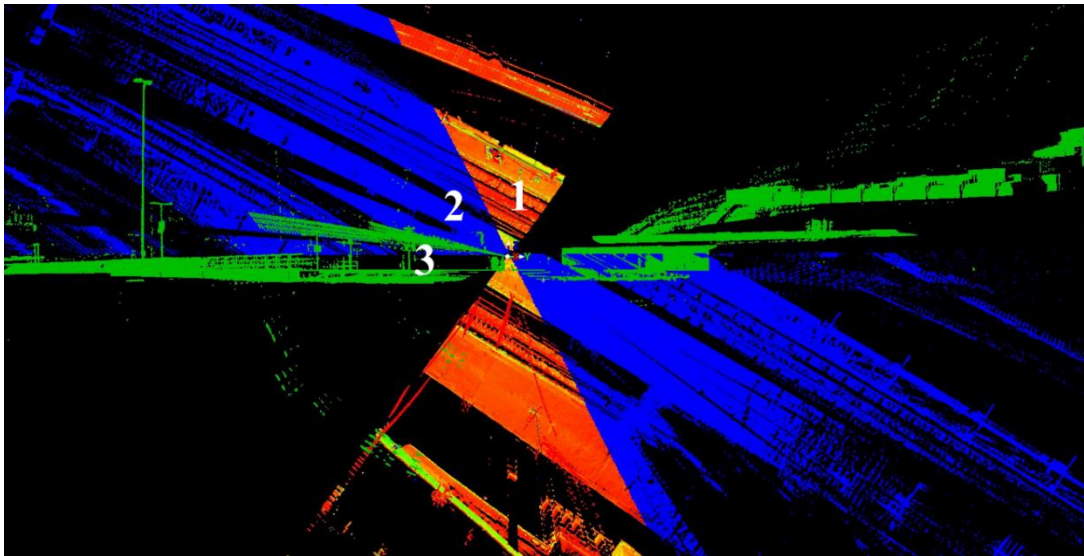


Figure 5.5: Segmented scan when importing .ZFS file into Cyclone 8.0

Clouds 1 and 2 appear to fit together as normal when importing the scans and show the top view of the tracks and platform. However cloud 3 has become rotated with respect to the other 2 clouds and shows a profile view of the platform as if it was a separate scan in a different co-ordinate system. This technical issue was reported to Leica Geosystems but an immediate solution was not available until the release of the next Cyclone update. Due to the urgency to ensure this was a software issue and not a hardware issue (and the scans could be registered together), an older version of Cyclone, 7.3, was used to import the data. However it is not possible to step back a version of Cyclone on the same machine and the old version must be installed on a separate machine. When the files were imported into the older version of Cyclone, each scan came in as one full scan and there was no need to re-scan the area. On the release of the newer version of Cyclone 8.1.3, this issue had been resolved. This shows that there can be a risk and effect of a TLS workflow and continuity when using different scanners and upgrading software versions.

5.4 Point Cloud Registration

Once the scans had been imported into Cyclone, the registration could be carried out in Cyclone itself. According to the literature for the software, the ICP algorithm is used for the registration process.

Each of the target centres were acquired in a similar way to experiment two in Chapter 4 (see Figure 4.18), using the algorithm within Cyclone. The laboratory tests showed that this algorithm was able to acquire the target centre to a sub-millimetre precision

compared to the $\pm 2\text{mm}$ precision stated in the specification. Figure 5.6 provides an example of the algorithm applied to the black and white tilt and turn targets. It must be ensured that these targets are scanned at a high resolution so that the software is able to acquire the centre accurately (at least 3mm point spacing).

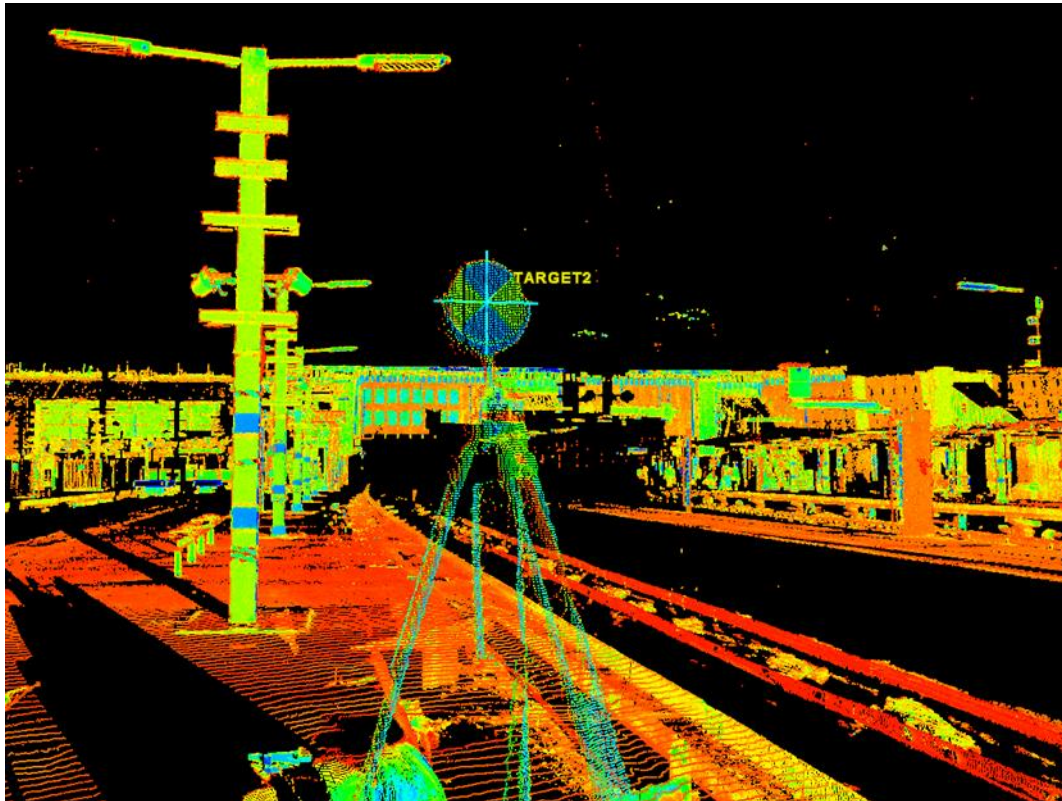


Figure 5.6: Tilt and turn target centre acquisition in Cyclone

Once the targets had been acquired, these were geo-referenced by using the target coordinates obtained during data capture, discussed in section 5.2. For each of the epochs the registration reported a mean absolute error of 1mm in Cyclone. It is important that the registration errors at this stage are minimal as this affects the quality of the track geometry measurements later on.

5.5 Track Extraction from Point Cloud

Once a registered point cloud has been obtained, the aim of the overall process is to be able to measure the twist and cant of the track from the point cloud at regular intervals over the test area. As the scans have been geo-referenced against an established track survey datum, track detection within the point cloud is not necessary for this study. In literature describing the quality of rail extraction, authors have not provided evidence of the tools that have been used to create sections and whether this process has been carried out automatically (e.g. Liu et al., 2013). Instead of carrying out track detection,

a methodology for track extraction is required. Given that prism monitoring is required every three metres across the track in the test area, the track extraction method requires cross-sections coinciding with the prism locations. This section explores 2D and 3D extraction of the point cloud.

5.5.1 2D cross-section extraction

Geomagic Qualify 2013, which was used in Chapter 4 Experiment 4, can also be used to create cross-sections through point cloud data, which can then be exported into standardised point cloud formats. The “*Section Through Object*” function allows the user to cut sections of defined thickness based on a reference plane or line. For a 2D fitting process to be carried out 1mm thick sections of track were extracted, where the user defines the location of the required “cut” manually. Figure 5.7 provides an example of a 1mm thick cross-section through the track on site relative to the lab track.

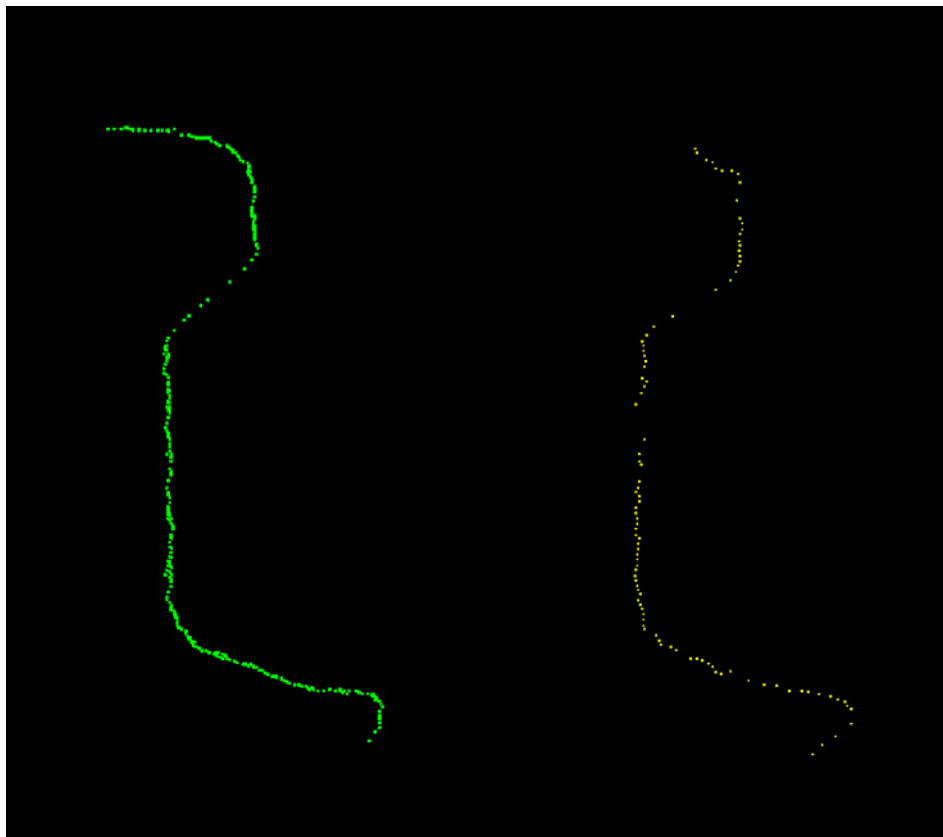


Figure 5.7: 1mm cross-section of track from laboratory rail (left) and site rail (right)

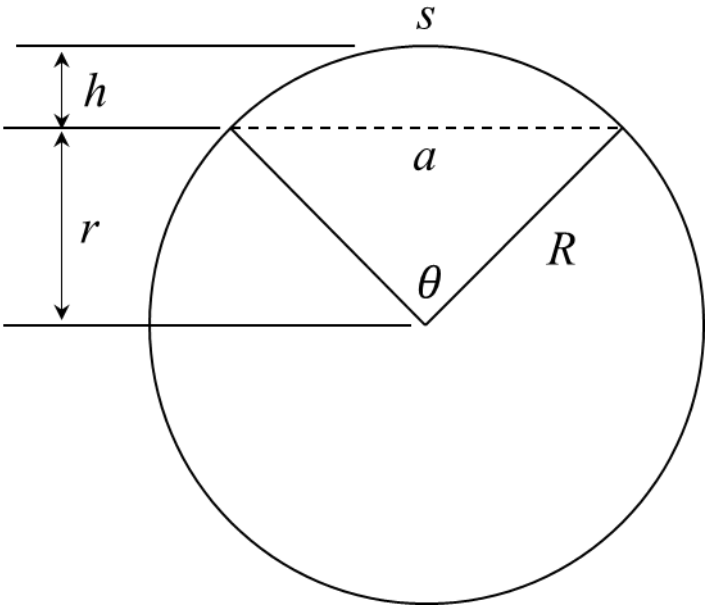
It can be seen that the 1mm cross-section of track obtained from site is very sparse compared to the lab track, with only 100 points in total. This is due to the larger range between the scanner and track compared to the laboratory tests. In order to carry out a

rail fit to a design model, there is not enough feature information from a 2D section of the track. This was confirmed by an unsuccessful registration process of the 2D section to the design rail model in Geomagic and CloudCompare. Therefore a “thicker” cross-section is required in order to carry out the rail fitting process, i.e. a 3D cross-section.

5.5.2 3D cross-section extraction

5.5.2.1 Determining cross-section length

In order to determine the thickness of the cross-section to be extracted for this type of rail fitting, any curvature of the track must be eliminated. Therefore the largest cross-section of track that can be assumed to be straight needs to be calculated. In order to calculate the rate of change in rail curvature, the minimum railway curve radius is required. Based on the TLP track and its maximum speed of 30mph the minimum railway curvature radius is 90 metres (provided by Network Rail track engineers). Using the circular segment formula below (which is based on trigonometry), the chord length, a , is required to determine the largest straight length of the track:



Where R is the radius of the circle, a as the chord length, s the arc length, h the height of the arced portion, and r the height of the triangular portion.

The length of the chord can be determined:

$$a = 2 R \sin\left(\frac{1}{2}\theta\right)$$

$$\begin{aligned}
a &= 2 r \tan\left(\frac{1}{2} \theta\right) \\
&= 2\sqrt{R^2 - r^2} \\
&= 2\sqrt{h(2R - h)}
\end{aligned}$$

In this case h is 1mm. This assumption was based on the plane fitting tests on the rail in the laboratory which is similar to that used at London Bridge. Plane fits were applied to the web of the rail to demonstrate baseline measurement capabilities of the scanners (section 4.2.1.4). R , in this context is the minimum railway curvature radius, is 90m. This results in a chord length of 0.85m. Therefore based on the curvature of the rail with a 1mm tolerance the maximum length of cross-section of track that can be assumed as straight is 850mm. For simplicity for the remainder of the study, 500mm was taken as the required cross-section length. This length of cross-section was used in the laboratory testing to allow comparisons of the quality of the rail fitting between site and lab testing to be easily made.

5.5.2.2 *Extraction tools*

The aim of the extraction process was to find an accurate and relatively automatic method of extracting point cloud at regular intervals. Three different point cloud handling tools that are commonly used by the laser scanning community were explored for extracting 3D cross-sections of track: Geomagic Qualify (see Chapter 4 Experiment 4), Microstation V8i¹⁷ (a 3D CAD modelling software used at Network Rail) and Cyclone (see section 3.2.3). The advantages and disadvantages of these tools are summarised below.

As shown in Section 5.5.1, Geomagic Qualify is able to extract cross-sections of any length defined by the user. The advantage of the tool is that it can handle large volumes of point cloud data. However in order to create the sections, the physical location of the cut has to be manually selected by the user by eye. For this study a 500mm cross-section is required to be extracted every 3 metres. Geomagic doesn't have a CAD level of measurement tools to allow the user to easily measure and note where the next

¹⁷ URL: <https://www.bentley.com/en/products/product-line/modeling-and-visualization-software/microstation> (last accessed February 2016)

section needs to be extracted. Figure 5.8 provides an example of the extraction tool and current drawbacks.

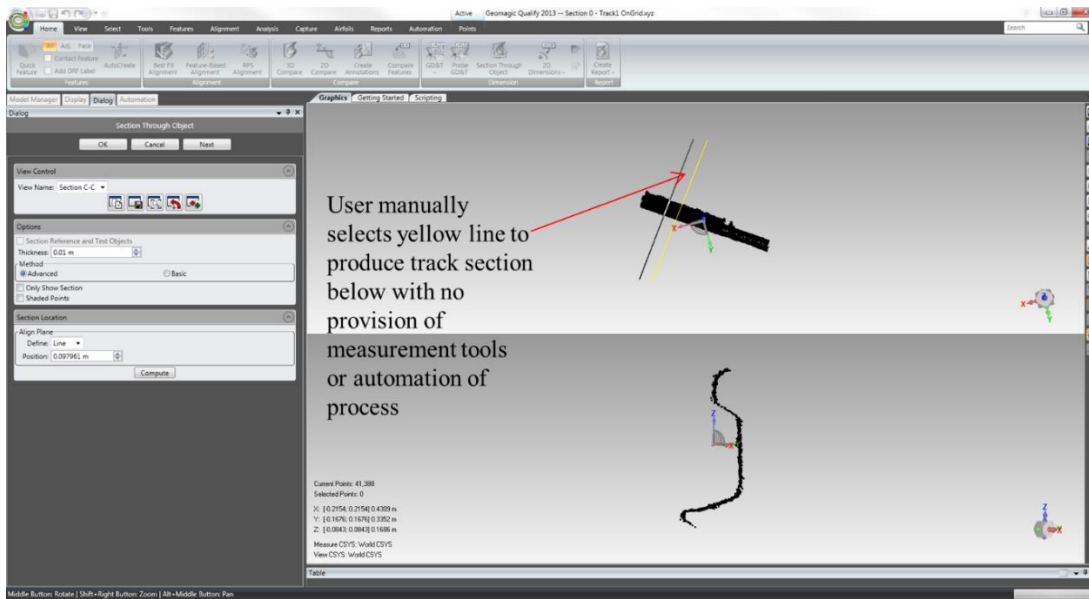


Figure 5.8: Example of extracting cross-sections in Geomagic Qualify 2013

Therefore this is a very manual tool with inaccuracies in the placement of cross-section extraction, which is vital for a direct comparison to the prism-based monitoring readings. In order to increase the accuracy and level of automation of extracting process, a CAD package with point cloud handling tools is required.

Microstation V8i is the CAD package used at Network Rail. The requirement of automatic extraction of CAD data at regular intervals is achievable through a command line function. Therefore there is a potential to achieve this with the point cloud data once it has been imported. With the advancement of laser scanning and the availability of point cloud data handling tools in CAD packages, Microstation has developed a “point cloud toolbox” which allows the user to import scan files in various standard formats (e.g. E57, XYZ), including scanner manufacturer’s proprietary file formats (e.g. Leica, Faro and Rieg). Typically the data are then used to create 3D models. In order to import the data, the software converts the scan files into its proprietary format from Pointools .POD files. Before file conversion, the conversion settings must be checked by the user as the default settings heavily sample down the data to 50mm. Figure 5.9 shows the different spatial filter settings provided by the point tool conversion in Microstation depending on the type of scan data.

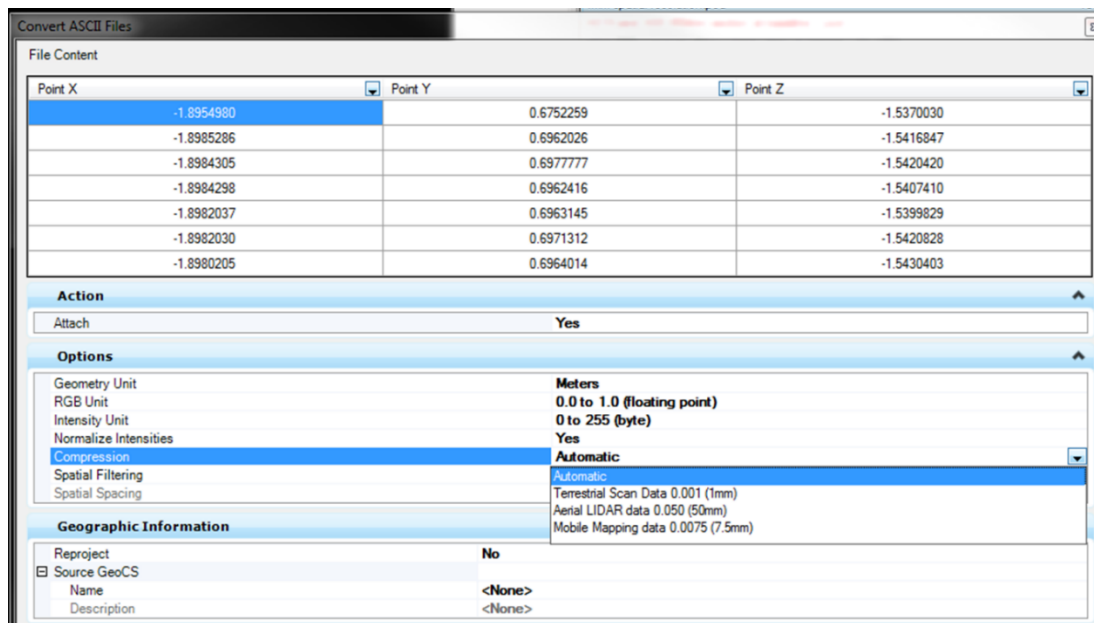


Figure 5.9: Spatial filtering settings in Microstation V8i

There is limited documentation on this spatial filtering process. For monitoring and this particular study it is important to retain the integrity of the point cloud data. Therefore any filtering could affect the quality of the fitting process later on, even at the 1mm filtering level. Despite the filtering process, it is possible to produce the cross-sections at the required intervals automatically which resolves the issues earlier with Geomagic Qualify. However the next step of the process will require a fitting or registration process. As there are no point cloud registration tools within Microstation, it would require the point cloud cross-sections to be exported out of Microstation. As well as this becoming a laborious process of the importing and exporting point cloud data with the risk of losing the point cloud integrity, the limitation here is that this toolbox only allows its Pointtools .POD file format to be exported. This format is problematic when importing into point cloud registration tools such as Cyclone, CloudCompare or Geomagic Studio.

Therefore a tool that allows automatic extraction that retains the data's integrity with a minimal data importing and exporting process is key. After investigation into each of the point cloud data handling software, the Section Manager tool was identified within Cyclone as the most useful. This tool is not as well-known as other features in Cyclone, e.g. the registration tool, and has not been found in literature for extracting sections to date. The tool was originally developed for extracting road surface information to detect changes in level of the road over various intervals. In order to create the cross-sections a reference line, also known as an "alignment" in Cyclone, is

required. In this case the point cloud data are geo-referenced and therefore the Network Rail as-built track survey lines from the CAD model can be used as a reference line to ensure the cross-sections are cut at the corresponding chainage/meterage of the monitoring prisms. If the data are not geo-referenced a reference line can be created relative to the track, for example the platform. The user can then create sections by defining a start and end point (in this case the area of interest), the height and width of the section and the spacing between each section. Figure 5.10 provides an example of before and after the automatic extraction process within the test area. Cross-sections can then be automatically extracted for each of the epochs based on the same track reference line.

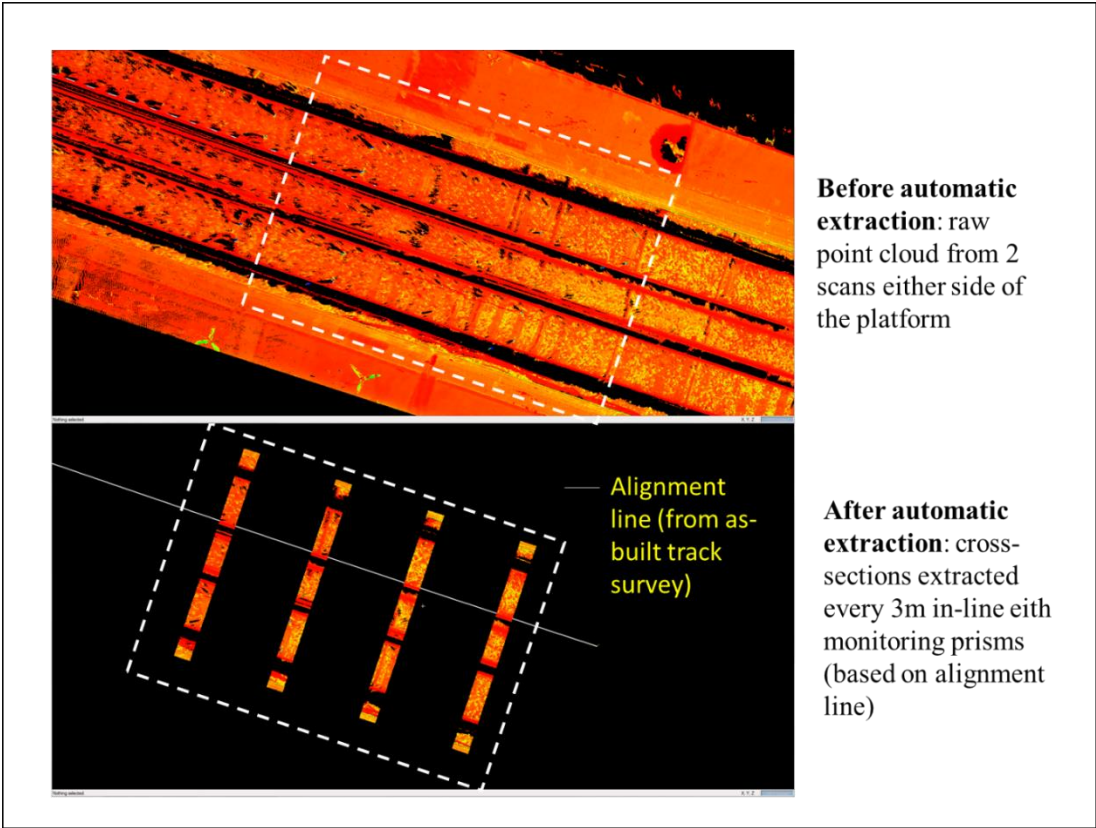


Figure 5.10: Automatic cross-section extraction using Cyclone (top view)

5.6 Data Cleaning

In the laboratory tests, the rail section was “clean” and unused and therefore didn’t have any shiny surfaces or artefacts attached to it and therefore no data cleaning was required. However on site, a very shiny surface is created when the wheel of the train and rail interact. This produces a high level of noise when scanning the surface, particularly as it encompasses edges. Therefore the extracted point cloud cross-

sections must be cleaned to remove spurious top rail surface data (shown in Figure 5.14) before an accurate fit can be established.

5.6.1 Edge Effects

A typical extracted cross-section from two scans either side of the platform is shown in Figure 5.11. Visual inspection of the cross-sections highlighted many occlusions from the line of sight between the scanner positions and track. In this case Track 1 and Track 4 are occluded by the platform edge whereas Track 2 and 3 are occluded by the raised third rail.



Figure 5.11: Coverage of track from Scan A and B - NOT TO SCALE

On further inspection, random noise appears to be present in the registered scans, highlighted in Figure 5.12.

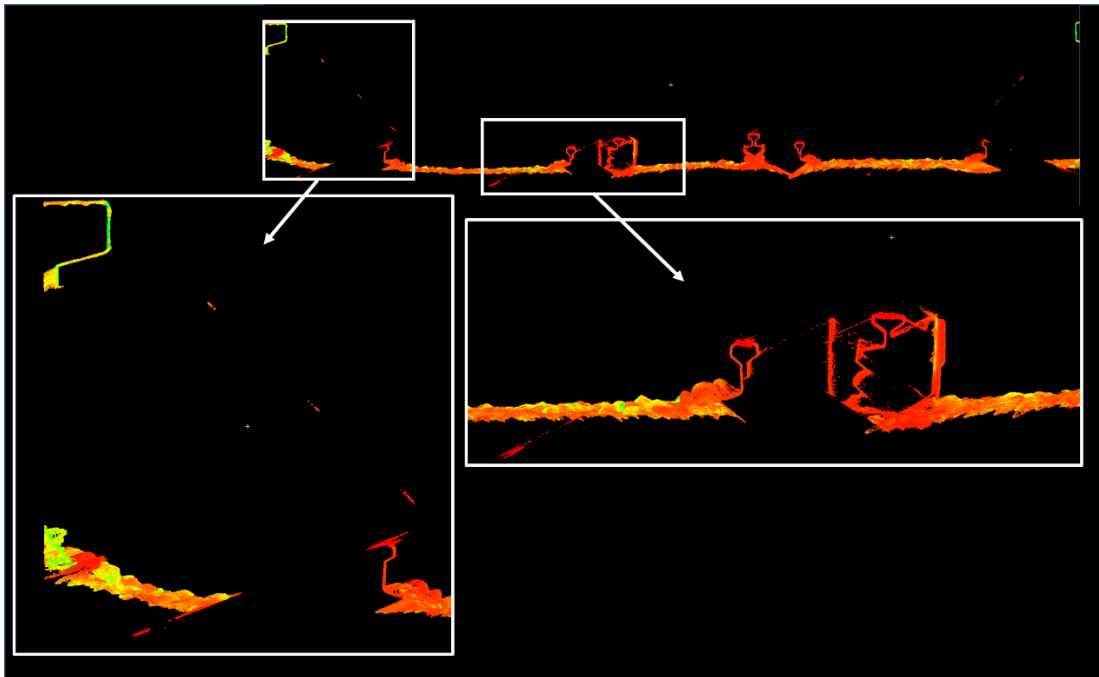


Figure 5.12: Random noise in extracted cross-section

It can be seen that this is not random noise and these “point traces” can be directed back towards the scanner locations, shown in green in Figure 5.13.

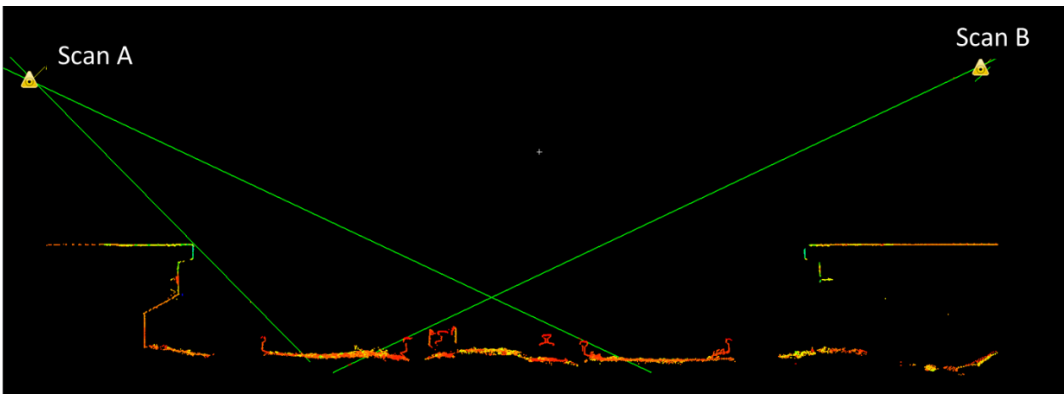


Figure 5.13: Point traces directed back to scanner locations

Even though the “noise” is sparse, the edge effects in proximity to the track needs to be cleaned. Figure 5.14 shows a cross-section of a design model of rail in comparison to the scanned rail from the HDS7000 and P20 scanner respectively.



Figure 5.14: Cross-section of rail from the design model, HDS7000 (green) and P20 (blue) laser scanner

Despite more coverage of the surface of the rail compared to the laboratory tests, visual comparison of the registered scanner point clouds from the site to the design model highlight many occlusions from the line of sight between the scanner position and track, as well as pixel “edge effects” characterised most notably for the P20, by systematic point traces directed back towards the scanner locations (despite the same filtering options applied when importing the data into Cyclone). These areas can be manually cleaned up for the analysis. Data from the head of the rail is also much noisier from both scanners compared to the laboratory testing due to interaction between the scanner laser and the complex reflective surface formed on the steel as trains pass over it, whereas the track in the laboratory was unused and therefore had no shiny surfaces. However portions of the rail section do remain consistent between the site scans, for

example the sides of the rail head, the web and the foot. These consistencies support measurement for web thickness and position.

5.6.2 Artefact Removal

Based on visual inspection of the extracted cross-sections, a key requirement is to remove obvious artefacts in proximity or attached to the rail that will affect the quality of the fitting process. Artefacts include ballast, base plates, rivets and track welds. Figure 5.15 shows an example of an extracted cross-section with an artefact. The blue circles highlight a feature apparent in the data. On close inspection it can be seen that this feature is a track weld and needs to be cleaned so that it does not adversely affect plane fitting. In this case the track weld is approximately 80mm long out of the 500mm cross-section.

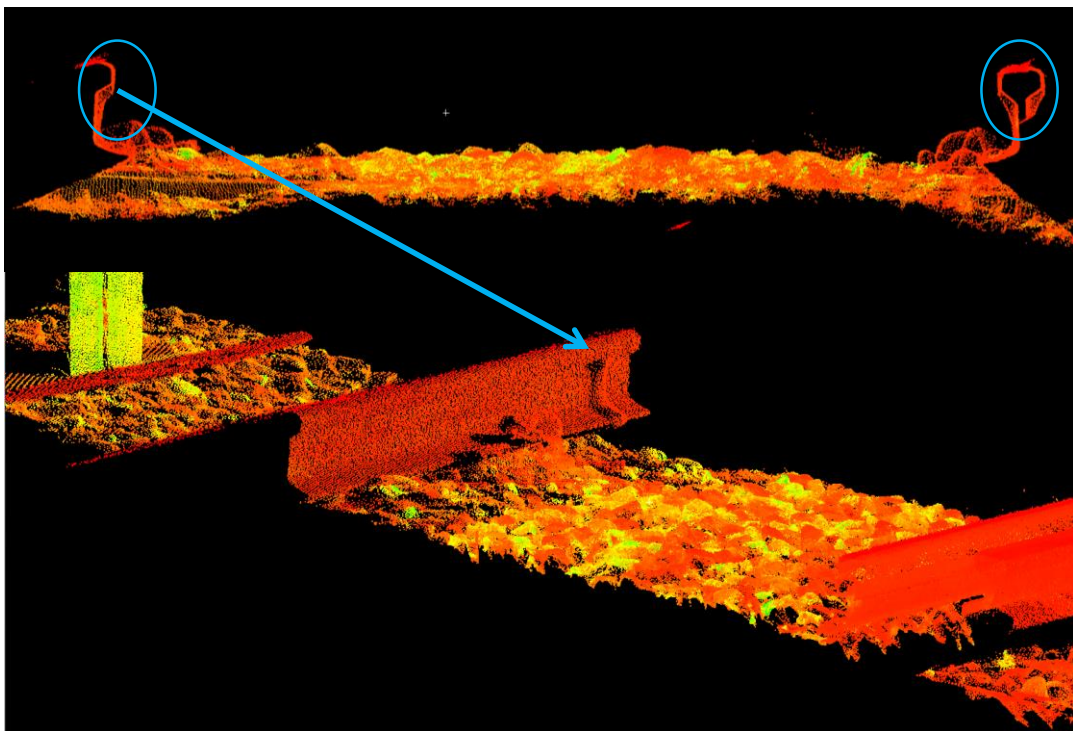


Figure 5.15: Example of typical artefact associated with the track

Outlier detection is not suitable for artefact removal in this situation. This is because the artefact to be removed is not comprised of random data but is highly systematic due to the surface that it represents. Figure 5.16 provides a top-view of the weld to demonstrate this.

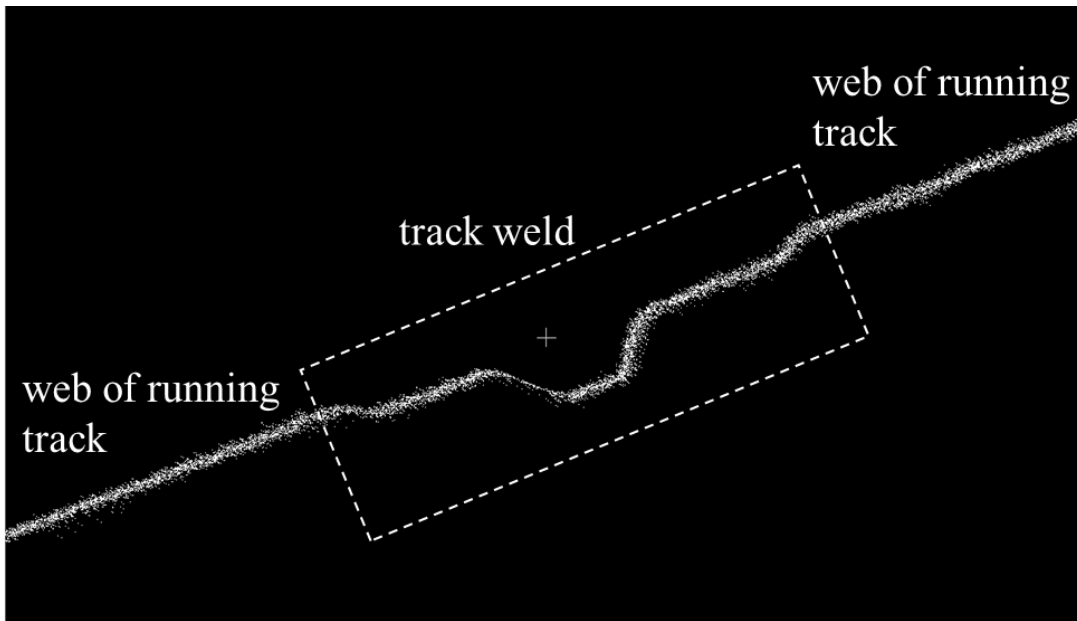


Figure 5.16: Track weld artefact (top view)

This artefact can be automatically removed by applying local plane fitting, using least squares estimation, to the web of the track and analysing the spread of the distribution of the plane fit residuals. In this example the RMS of the fit with the artefact is 2.6mm. Figure 5.17 shows a colour coded histogram, using CloudCompare, of the residuals of the plane fit. The blue, green and yellow areas represent the track weld and show large residuals in relation to the plane fit, whereas orange (web of the track) has very small residuals.

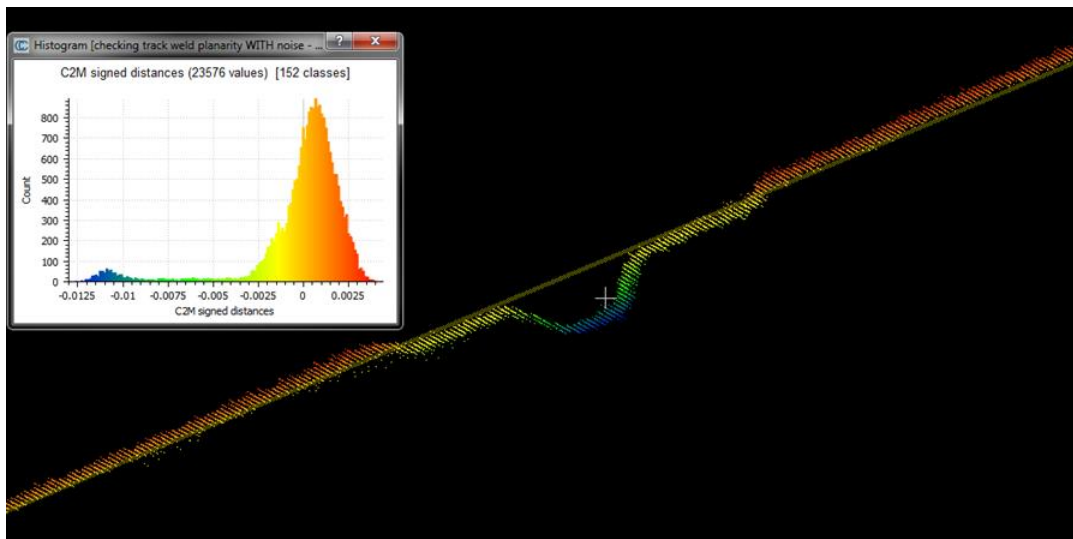


Figure 5.17: Colour coded histogram of plane fit of track weld artefact

The residuals can be exported from CloudCompare and analysed in more detail. Figure 5.18a shows the same histogram of the residuals from the plane fit with the artefact using MATLAB. The graph shows a bimodal distribution with the left peak

corresponding to the weld. Isolating this artefact arrives at a better plane fit with an RMS of 0.6mm and the histogram of these residuals in Figure 5.18b shows a tendency towards a normal distribution.

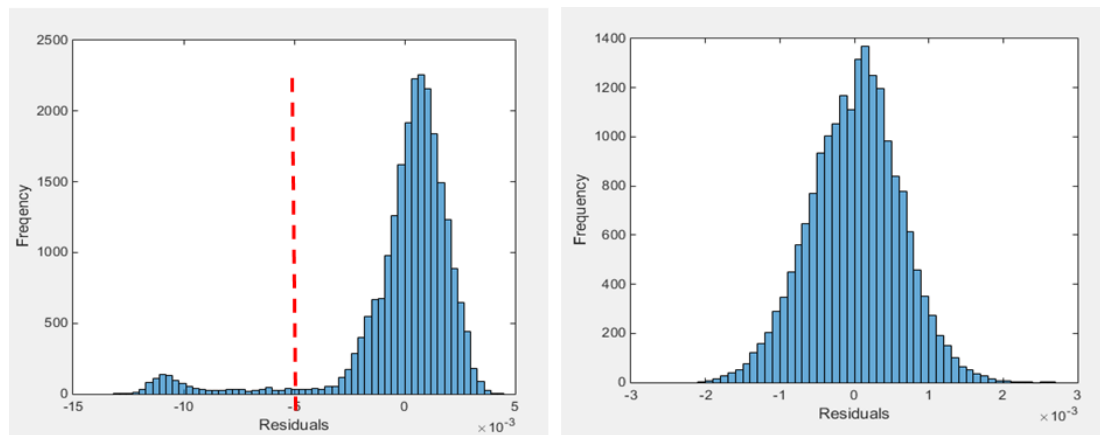


Figure 5.18a) Histogram of residuals *without* data cleaning of weld artefact (left) and b) *with* data cleaning (right) in metres

The distribution in Figure 5.18b compares to the residuals of the plane fit to the web element of reference track scanned in the laboratory (section 4.2.1.4), shown again here in Figure 5.19. The RMS of the plane fit of the web of the track here also corresponds to that of the laboratory track when using the HDS7000, i.e. 0.6mm. This shows that the scanner is performing to the same quality level in the laboratory and on site when capturing the web of the track.

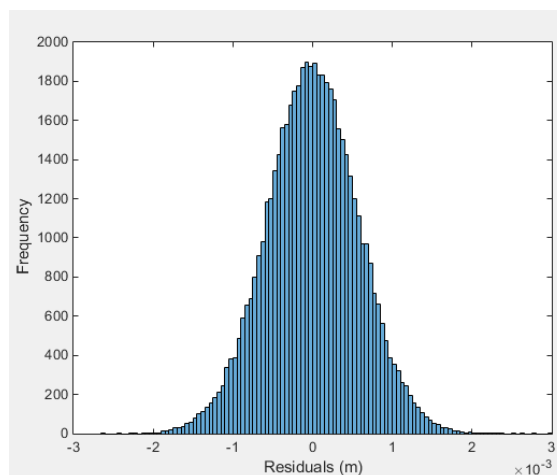


Figure 5.19: Histogram of residuals of reference lab track from the HDS7000

Another example of an artefact that can occur are cable connections. These can be for train signalling block detection (forming a circuit which is connected by the train wheel axles to show wheels are present and hence a train is occupying that section of the track, i.e. signal block) of the track. Similarly to the track weld example, visual

inspection of the cross-section shows a subtle feature extruding from the rail web. In total the cable connections take up approximately 110mm of the cross-section. Figure 5.20 provides a typical example of a point cloud cross-section containing a rivet as well as its appearance in reality.

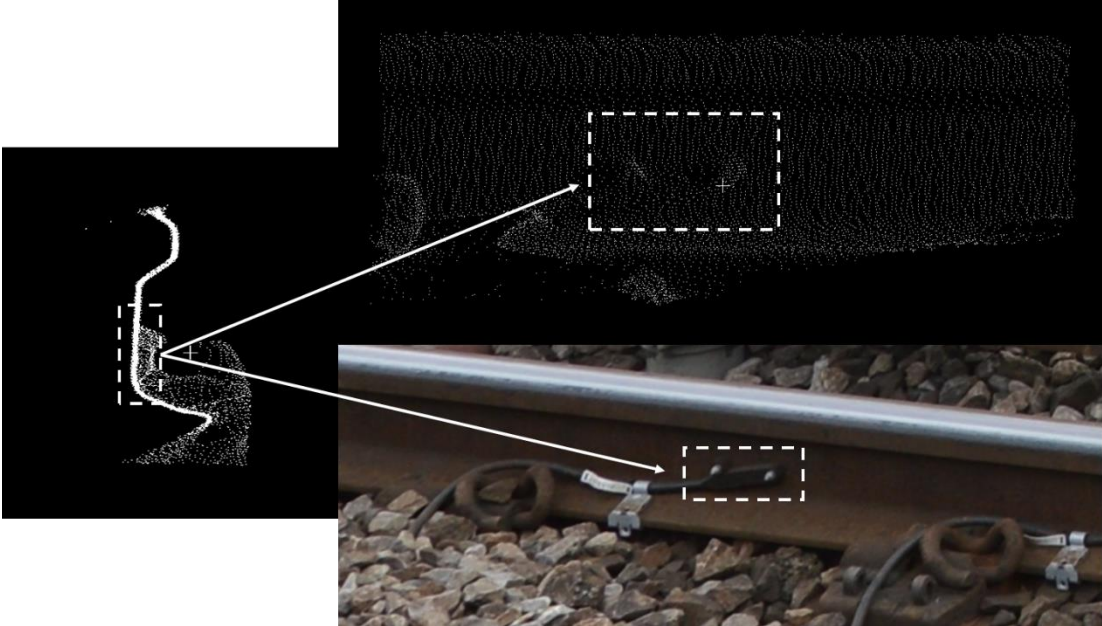


Figure 5.20: Track cable connection artefact profile (left), corresponding face-on view (top right) and image of feature (bottom right)

The plane fitting method for removing the track weld artefact can be validated to remove the rivet artefact on the web of the rail. Figure 5.21a and b provides the results from the plane fitting removal process of the cable connection with residuals with and without the artefact removed plotted as a histogram.

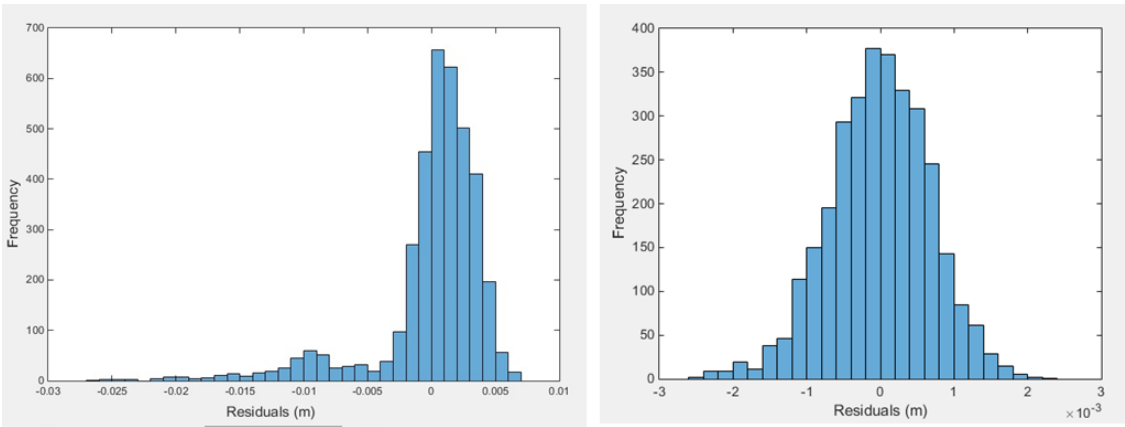


Figure 5.21a) histogram of residuals **without** data cleaning of rivet artefact (left) and b) **with** data cleaning (right)

Despite the shape of the histogram in Figure 5.19, the residuals from the reference point cloud are not normally distributed which is evidenced by failure of the chi-square

test. This is also true for the “cleaned” rail data shown in Figure 5.18b and Figure 5.21b. Therefore the assumption to iteratively remove the secondary peak based on a chi-squared limit test cannot be readily adopted. However it can be seen that there is consistency in the offset between the histograms and upon further inspection a consistent offset of 0.3mm from 0.0mm in both histograms could be seen. It is clear from the plot of reference (i.e. lab test) residuals that planes can be used for artefact removal. Therefore ongoing work is required to form a robust statistical process. The appearance of a systematic error in the histogram follows findings from Al-Manasir and Lichti (2015) and further work would be required understand the interaction between the TLS system and different surfaces.

5.7 Rail Track Fitting

In order to determine the track geometry required by the engineers, an accurate fitting process of the track point cloud to a reference model must be established. The results of the plane fitting provide an indication of the potential quality of rail fitting process locally for the web of the track (i.e. sub-millimetric). Therefore two different methods of rail fitting processes are explored: curvature and plane-based fitting.

5.7.1 Rail fitting inclusive of curvature

Based on the point cloud cross-sections and design model it can be seen that the curved parts L1, L2 and L3, shown in Figure 5.22, provide enough coverage for a fitting process to the design rail model to establish its position.

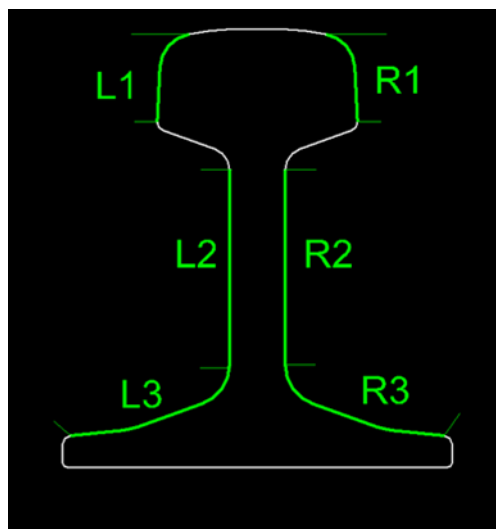


Figure 5.22: Rail curvature based naming reference

CloudCompare allows a point cloud to be registered to a design model whilst providing statistical information on the registration process. Therefore the rail cross-section point cloud can be registered to the design rail model. An initial alignment was applied to the different entities to bring them into the same co-ordinate system. This is carried out by selecting common points between the two “models”. Based on the coverage of the point clouds the side of the head and foot can be used for alignment. A fine registration can then be applied, using the ICP algorithm (see section 3.2.3.1), to accurately register the point cloud to the reference model. An example of the output of fine registration in CloudCompare is shown in Figure 5.23, where the reference model of the track is black and the point cloud registered to the model is green.

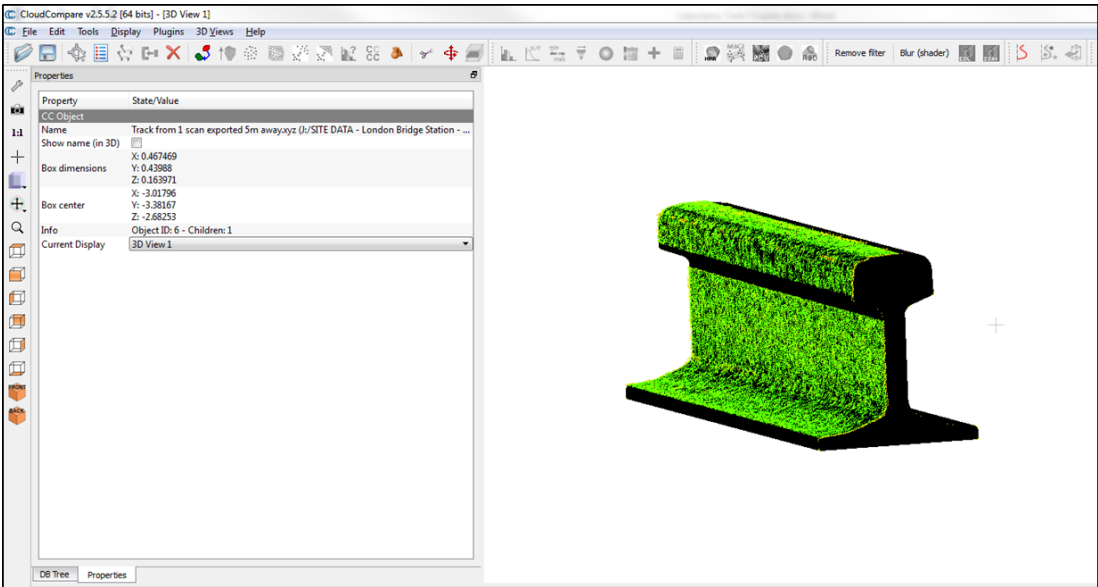


Figure 5.23: CloudCompare example of fine registration of rail point cloud to design model

The aim of this procedure is to investigate the quality of the fitting process when including all viable point clouds of the rail cross-section, i.e. with the most coverage. In order to obtain the best possible registration for the fitting procedure, a well-populated cross-section should be chosen. In this case the cross-section closest to the position of Scan A and Scan B (see Figure 5.3) at the 0 metre chainage is used. For this cross-section the scanners are positioned approximately 4m from the left of the web and 7m from the right of the web of the rail.

A series of fine registrations, using the ICP algorithm, were carried out to see which features from the point cloud align best to the reference model. A registration of the whole section with and without the “noisy head” can also be carried out to see the effect on the quality of the registration.

Table 5.2 summarises the RMS values from registering different sections of the point cloud (represented in orange) of the track to the 3D reference model (represented in blue) from the HDS700 scanner at Epoch 1 and P20 scanner from Epoch 3. The table also shows the RMS of the plane fits to the left and right web of the rail.

The RMS of the registration of the entire section of rail, including the head of the rail, shows a fit of 5.3mm and 7.5mm from the HDS7000 and P20 respectively. This low level quality of rail fitting from the site scans are due to the noise from the top of the head of the rail affecting the fit to the model.

Data fitting to individual portions of the rail show a fairly consistent fit with all sections registering to better than 3mm. All the RMS values from the HDS7000 show slightly better rail fitting than the P20, implying that data from the P20 are slightly noisier.

From these results it can be established that the closer, left side of the section of rail, consistently gives the best fit to the model for both scanner types (shown in bold in Table 5.2). These areas can be considered as the most “trusted” when aligning to the track reference model. A further registration for this part of track can be computed to compare capability between left hand (near) and right hand (far) sides of the rail, which is also shown in Table 5.2.

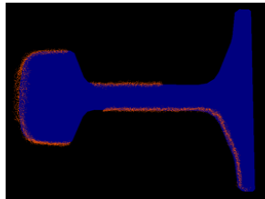
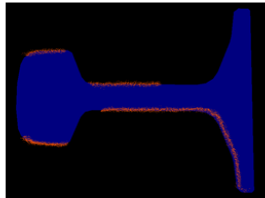
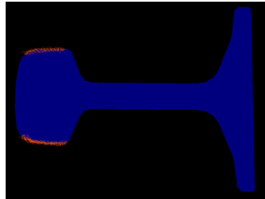
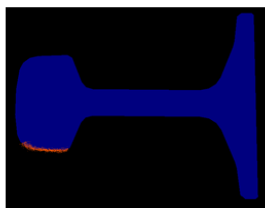
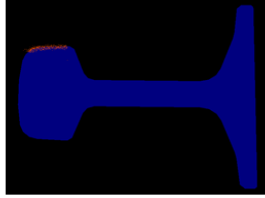
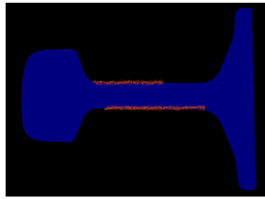
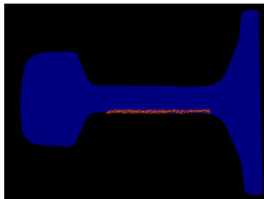
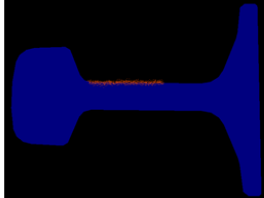
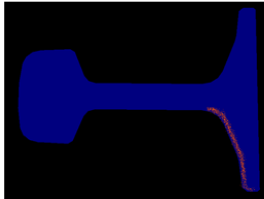
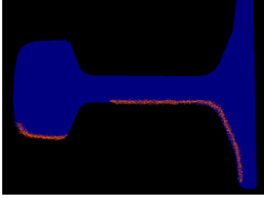
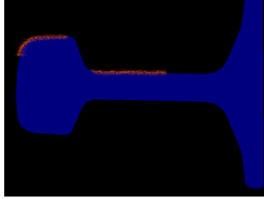
Section compared	Full profile (with top of rail)	Full profile (without top of rail)	Head	Head – near rail	Head – far rail	Web
Extracted point cloud of rail (orange) compared to reference model (blue)						
HDS7000 RMS (mm)	5.3	2.5	2.5	2.4	2.6	2.4
P20 RMS (mm)	7.5	2.8	2.9	2.6	2.6	2.7
Section compared	Web – left	Web – right	Foot		Left section	Right section
Extracted point cloud of rail (orange) compared to reference model (blue)						
HDS7000 RMS (mm)	2.4 Plane fit RMS = 0.8	2.5 Plane fit RMS = 1.3	2.4		2.4	2.6
P20 RMS (mm)	2.5 Plane fit RMS = 1.1	2.6 Plane fit RMS = 1.3	2.6		2.6	2.7

Table 5.2: Summary of RMS values of fitting point cloud to modelled rail

The results show that “globally” the left section of the track is able to fit to 2.4mm and 2.6mm from the HDS7000 and P20 respectively. This is compared to the points from the right hand side of the track producing an RMS of 2.6 and 2.7mm respectively for the HDS7000 and P20. This shows that the fit to the 3D model is slightly better with the points from a single scan position compared to a combined scan (two scanning positions). The reasons for this could be due to a smaller range from the scanner and therefore smaller spot size of the laser hitting the surface, or an increased range noise due to decreased laser return strength with range. This test shows that the left side of the track: i.e. the head, web and rail of the track provides the best alignment to the 3D reference model with an RMS of 2.4mm and 2.6mm from Scanners A and B respectively. When both sides of the track profile are registered to the model the registration RMS increases to 2.5mm and 2.8mm respectively. However as this incorporates two different scans, the effect of the 1mm RMS target based registrations might have an effect on the overall fit. Overall, without the noise from the head of the rail data, all sections are able to fit to the model with an RMS of better than 3mm.

The quality of the point cloud fits to the design model can be investigated in more detail by plotting the residuals of the RMS as a histogram, also known as a 3D comparison. Based on the earlier registration results the full profile with and without the rail head as well as the side of the rail nearest to the scanner (in this case the left side) can be compared. Results are shown in Figure 5.24.

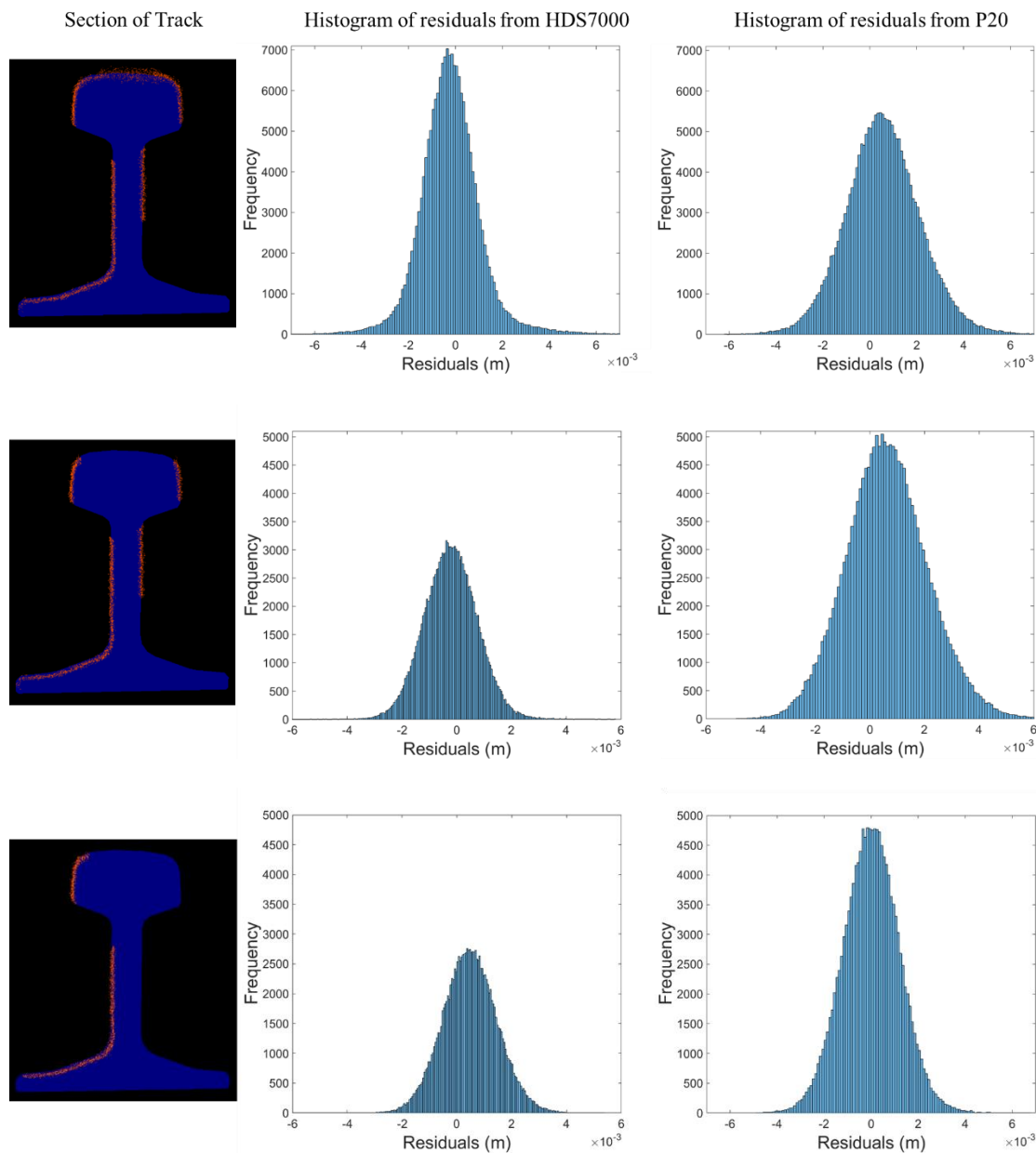


Figure 5.24: 3D Comparison results from the HDS7000 and P20

Inspection of the histograms from each scanner shows that overall the P20 has a consistent bias with the spread of residuals, of up to 7mm, skewed to the right. This implies a systematic error in the data from the scanner. This systematic bias in the data could be due to the accuracy of the scanning system as a whole. A way of verifying this would be to decrease the point cloud extraction area to see if the skewness was still present for a small sample of the point cloud profile, i.e. a 2D comparison method. The HDS7000, on the other hand, shows a small spread of residuals for the most trusted area followed by wider spread of residuals as more “areas” of the point cloud profile are added to the comparison. This shows that as the coverage of the track profile increases, other factors are affecting the quality of the fit, for example, the registration

and quality of the right hand side of the scan from a longer range as well as the noise from the top of the head of the scan. Results from the chi-square test show that the residuals from the 3D comparison technique do not show a normal distribution, highlighting the presence of a systematic error in the TLS systems. Further work would investigate the presence of systematic errors in these TLS systems, in particular when measuring to different surfaces.

To validate these site test results of the rail fitting process, the same curvature fitting procedure was applied to the point clouds from the laboratory testing, using different scanners. The results from the fitting process is shown in Table 5.3.

	Time-of-flight scanners			Phase-based scanners		Close-range photogrammetry
Point to model registration RMS	C10	P20	MS50	HDS7000	Faro Focus 120	CRP
	3.1mm	2.5mm	2.5mm	2.4mm	2.5mm	3.1mm

Table 5.3 : RMS of rail fitting procedure inclusive of rail curvature (L1,L2, L3) in laboratory

The laboratory test results show that the rail fitting process inclusive of the track curvature from HDS7000 and P20 showed a registration RMS of 2.4 and 2.5mm respectively. The results from Table 5.2 show that the rail fitting of the same part of track on site produce results of 2.4mm and 2.6mm respectively. This validates the results in the laboratory from the fitting process as well as confirming the comparable levels of performance of the scanner in the laboratory and site environment.

When looking back at the literature, Meng et al. (2014) were able to show a 2 to 3mm level of agreement between the mesh of a mini railway track (approximately 120m in length with a gauge of approximately 184mm) and the ground truth. The results from Table 5.2 and Table 5.3 show equal levels of agreement but also highlight particular rail sections that show the best fit from a point cloud whilst reducing the number of processing steps required to achieve this. Oude Elberink et al. (2014) also considered the point data but made a line extraction based on the rail head to achieve an RMS better than 20mm when compared to the final model. Results from the left section (side of the rail nearest to the scanner) track fitting described here demonstrate fit from ICP

of better than 3mm can be achieved which fits in with Oude Elberink et al.'s (2014) suggestion of using the foot of the track to extract accurate rail geometry.

This work has shown that an RMS of better than 3mm can be achieved when registering different sections of the track – including the head, web and foot as well as curved parts of the track profile – to the design model through a novel technique. The rail fitting and localised plane fitting results validate those achieved in the laboratory which shows the scanners ability to achieve the same level of fitting when there are external challenges such as a noisier surface, larger range from the scanner and many occlusions.

The findings from this section have been published in the International Archives of the Photogrammetry, Remote Sensing and Spatial Information Sciences (ISPRS) (Soni et al., 2014) and presented at the ISPRS Technical Commission V Symposium in 2014.

Based on the engineer's requirements of producing a millimetre level of accuracy for measuring track geometry, it can be seen that this level of fitting needs to be optimised to fulfil these requirements. The sub-millimetre results from the localised plane fitting of the planar sections of track highlight the capability of the scanners to produce a comparable level during the fitting process. Therefore an alternative method of carrying rail fitting using only the planar sections can be investigated.

5.7.2 Rail fitting of planar sections

The objective for this is to build upon the previous section to optimise the quality of fitting the track point cloud to the design reference model for accurate track geometry extraction. Once the rail fitting quality has been improved, the next objective is to compare the capabilities of the rail fitting at different ranges and the effects of angles of incidence from the scanner to the 4 different tracks to determine the optimum spacing between scanner positions.

The point cloud of the track can be segmented based on the planar features of the rail design model shown in Figure 5.25. The planarity of these areas of the model can be validated by applying local plane fits where the RMS should be zero.

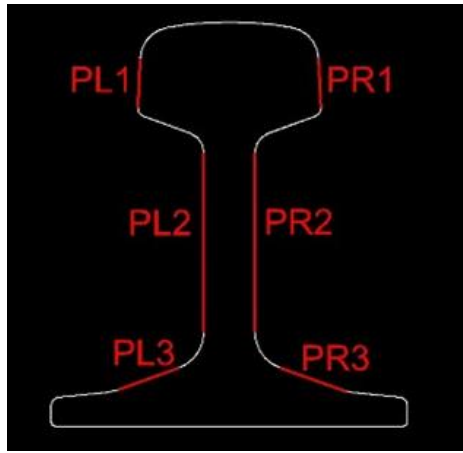


Figure 5.25: design rail geometry highlighting planar segments (in red)

Once the point cloud has been segmented into the planar sections, local plane fits can be applied to each section using CloudCompare. Results of the RMS of the residuals normal to the plane from Scan A&B and Scan C&D at the 9m chainage is shown in Table 5.4.

Local plane fits: RMS of the residuals normal to the plane (mm) from Scan A&B (~9m away)							Local plane fits: RMS of the residuals normal to the plane (mm) from Scan C&D (~15m away)						
	PL1	PL2	PL3	PR1	PR2	PR3		PL1	PL2	PL3	PR1	PR2	PR3
Track 1				0.7	0.7	0.6	Track 1				0.7	0.8	0.8
Track 2	0.5	0.4	0.6	0.7	0.6		Track 2	0.8	1.0	1.0	n/a	n/a	
Track 3	0.9	0.9		0.4	0.4	0.5	Track 3	n/a	n/a		0.4	0.5	0.8
Track 4	0.6	0.5	0.5				Track 4	1.0	0.8	0.8			

Table 5.4: Local plane fits from Scan A&B (left) and Scan C&D (right) at 9m chainage

These results demonstrate the capabilities of the scanner to produce sub-millimetric level of fitting. Despite some occlusions to Tracks 2 and 3, the level of fits are comparable between the setups and different ranges and angles to the same section of track. Overall these data provide a baseline of the expected level of fitting of the track point cloud to the rail model. This expectation can be used as a measure of the quality of the input data.

A fine registration was then carried out between the planar areas of the point cloud and the planar segments of the design rail model (i.e. PL1, 2 and 3) using CloudCompare. All 6 planar sections are not visible on each of the 4 running rails on site, due to the raised third rail or platform occlusions. However the scans are able to capture at least 3 of the planes on one side of the rail which is a minimum requirement when fitting the point cloud to the design rail model. For example, based on the cross-section in Figure 5.11, after cleaning the point cloud, Track 1 contains PR1, PR2 and PR3. Table

5.5 shows the visibility of planar features of each section of track at the 9 meter chainage.

Track Number	= visible	Planar Segment Visibility					
		PL1	PL2	PL3	PR1	PR2	PR3
Track 1							
Track 2					*	*	
Track 3		*	*				
Track 4							

* = plane not visible at 9m interval due to raised third rail occlusions from Scan C&D

Table 5.5: Track visibility of planar features

The design rail model (Figure 5.25) can be considered as a set of discrete planes rather than a single entity. This enables all registrations to be made using the ICP between the raw scan data and the plane definitions. Table 5.6 shows the results from Scan A&B of the cross-section at the 9m chainage and from Scan C&D at the same cross-section.

Registration RMS between point cloud to rail model (mm) from Scan A&B						
	Local plane fit registration			Combined plane fit registration (1 scan)	Combined plane fit registration (2 scans)	
	PL1	PL2	PL3		PR1,PR2,PR3, PL1,PL2 (i.e. planes on entire right side and visible left side)	PL1,PL2,PL3,PR1,PR2 (i.e. planes on entire left side of track and visible right side)
Track 1				1.2	n/a	n/a
Track 2	0.6	0.9	0.7	1.2	n/a	1.6
Track 3				1.5	1.6	n/a
Track 4	1.1	1.3	1.1	1.5	n/a	n/a

Registration RMS between point cloud to rail model (mm) from Scan C&D						
	Local plane fit registration			Combined plane fit registration (1 scan)	Combined plane fit registration (2 scans)	
	PL1	PL2	PL3		PR1,PR2,PR3, PL1,PL2 (i.e. planes on entire right side and visible left side)	PL1,PL2,PL3,PR1,PR2 (i.e. planes on entire left side of track and visible right side)
Track 1				1.3	n/a	n/a
Track 2	0.8	1.0	1.0	1.2	n/a	n/a
Track 3				1.3	n/a	n/a
Track 4	1.1	1.5	1.2	1.5	n/a	n/a

Table 5.6a) Registration RMS from Scan A&B (top) and b) Scan C&D (bottom)

Firstly when comparing the RMS values between both sets of scans for the local and combined plane fits, the results shows the scanner is able to achieve the same quality of fit from 9m and 15m away from the track, despite the number of points on the plane being approximately half at the 15m compared to the 9m scanning range with a

commensurate change in spot size. The comparability of these show that scanner instrument placement separations could be increased in order to speed up data capture and efficiency. Limiting on-site time and complexity is particularly important given constraints of site access and passing trains.

The RMS of the registration of the local plane fits shown in Table 5.4 provides a baseline measure against which a target quality for fitting data to the rail model for the TLS system used can be established. The left hand sides of Table 5.6a and b highlight that the RMS values of the individual registered fits to the planar segments of the rail model are slightly higher than the target value. This may be due to reduced point cloud coverage on the rail that is registered to the design model. For example, the upper web of the rail (PL2 and PR2) is always occluded by the side of the head of the rail (PL1 and PR1) when scanning from platform level. This is shown in Figure 5.14.

When looking at the registration of the combined plane fits from a single scan location (centre column in tables) that include data from at least 3 planes from one side of the rail, results show a fit of better than 1.5mm to the design rail model. These three planes provide the minimum geometric information necessary for fitting to the rail model. A focus on of the UK rail type and plane fitting has allowed this work to show an improvement by a factor of two compared to previous work (Meng et al.,2014) where the quality of fit was better than 3mm.

Similarly to the validation of the curvature based fitting, this planar based fitting result was validated by applying the same fit to the scans of the rail in the laboratory. Table 5.7 shows the RMS of the registration of the planar sections of rail to the design model.

	Time-of-flight scanners			Phase-based scanners		Close-range photogrammetry
PL1, PL2 and PR3 RMS registration to model	C10	P20	MS50	HDS7000	Faro Focus 120	CRP
	2.9mm	1.6mm	1.7mm	1.4mm	2.0mm	2.5mm

Table 5.7 : RMS of rail fitting of planar sections using laboratory track

These results show that the HDS7000 is able to achieve a planar based rail fit of 1.4mm in the laboratory which compares to the results of better than 1.5mm from the site testing.

The results from Section 5.7.1 indicated that when registering the track profile from a single scan, the spread of residuals in the registration was less compared to that of a combined scan. For planar based fitting, the registration of all visible planes for a particular track collected from scanners located either side of the track and registered together, i.e. Track 2 and 3 with 5 planes, is particularly encouraging. The RMS of the residuals are only 0.1mm higher than the single scan case implying the same quality of fit. However when plotting the histogram of residuals of a single scan versus a combined scan, the combined scan has a slight skew to the right. This is shown in Figure 5.26.

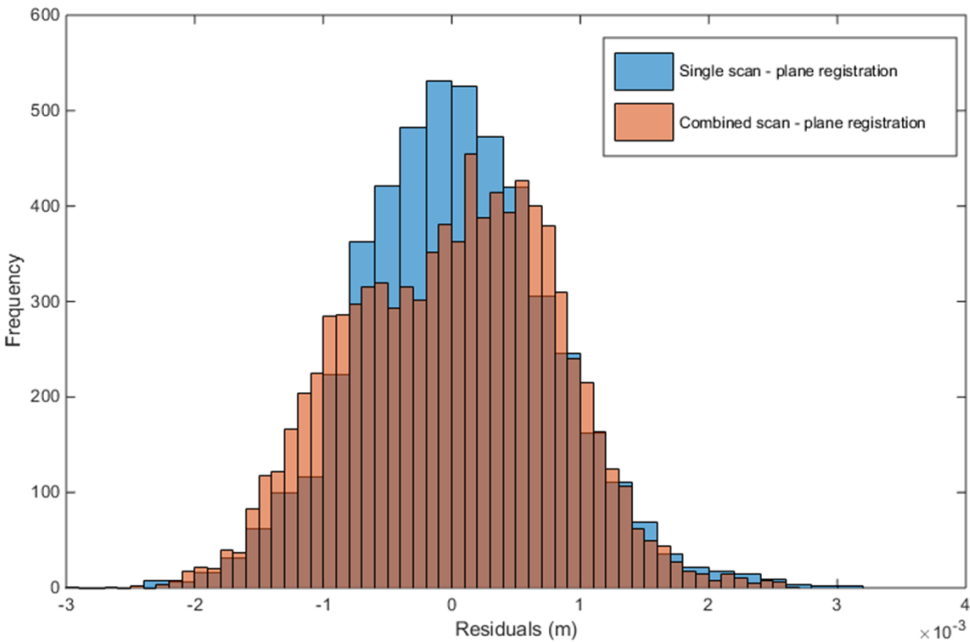


Figure 5.26: RMS registration residuals of single and combined scan

Comparing these results to the plots in Figure 5.24 confirms a systematic error in the data, the source of which is most likely to be from errors in the registration between the two scans made on either side of the platform. This highlights the need for accurate registration between the scans, even though in this case an overall RMS of 1mm was reported in the registration in Cyclone.

The methodology workflow for the data capture, extraction, cleaning and fitting procedure developed in this chapter is shown in Figure 5.27 . It must be ensured that the integrity of the point cloud data remains intact throughout the workflow in order, e.g. applying minimal or no data sampling, to achieve the best outcome.

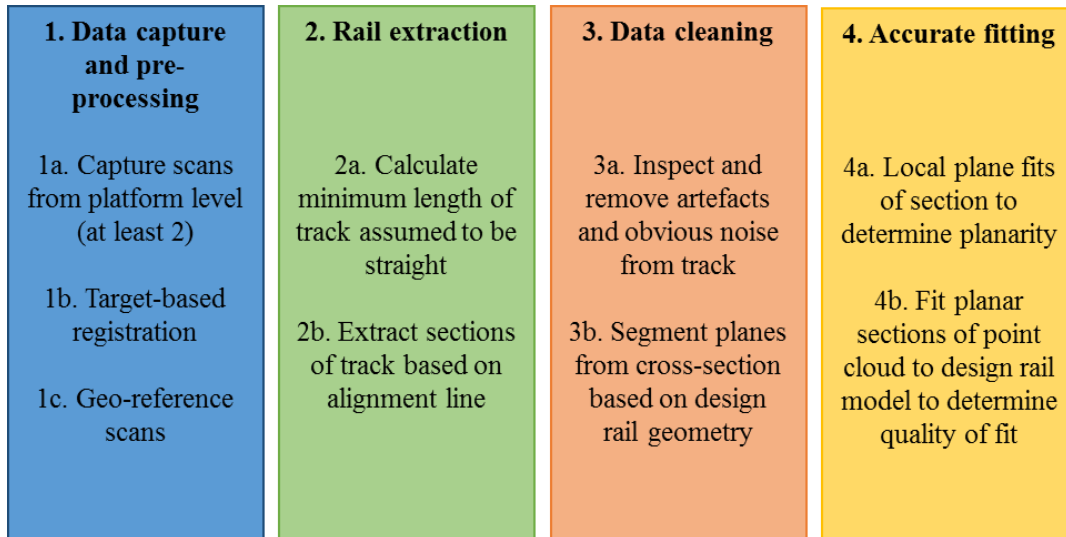


Figure 5.27: 4-step methodology workflow for accurate rail fitting

Once the point cloud has been accurately fitted to the reference model, track monitoring measurements, such as cant and twist, can be extracted directly from the model through CAD.

The findings from this section have been presented and published in the conference proceedings of the FIG Working Week 2015, Commission 6: Engineering Surveys (Soni et al., 2015).

5.8 Measuring and validating track geometry against prism-based method

Once an accurate fit of the track point cloud to the design rail model has been established, the rail model can be used to extract track monitoring parameters significant to the engineer. A CAD package allows the difference in elevation between the running tracks, i.e. cant, to be measured accurately. The twist can then be calculated by taking the difference of these cant levels between 2 cross-sections.

For this site test the scanner has been set up in-line with a set of monitoring prisms (i.e. at a chainage of 0 metres) either side of the platform. This allows this set of prisms and the subsequent ones every 3 metres being monitored for the redevelopment project to

be compared directly with the novel TLS fitting method. Scanning over four epochs would allow a way of validating the TLS method. When extracting the prism monitoring data from the monitoring contractor for the first epoch, it could be seen that the prism co-ordinates roughly aligned with the scan data, shown in Figure 5.28. This confirmed that the prism and TLS data were on corresponding co-ordinate systems.

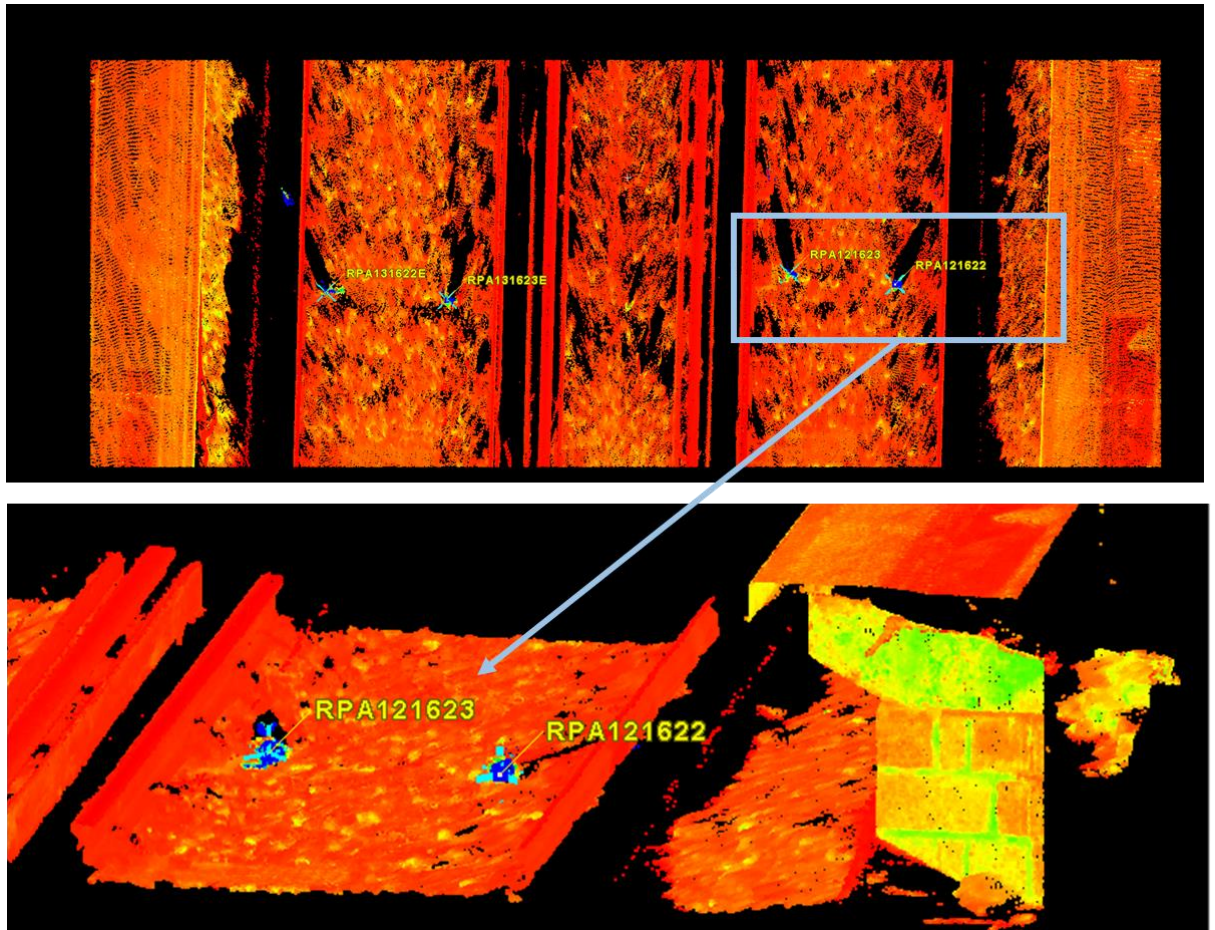


Figure 5.28: Aerial view (top) and perspective view (bottom) of monitoring prism co-ordinates (blue vertices)

Following the request for the prism monitoring data from the monitoring contractor and a significant amount of delay, it turned out that the data were not actually being recorded for the prism monitoring system on that particular section of track. This had been going on for nearly 12 months, and there was little evidence the client (Network Rail) had been informed of this. The reason for the system not recording was that the works taking place in the vicinity had blocked the prism reference system. Also, the reason why this was not resolved during the period of the study (i.e. where prisms were not being measured) is not clear. Therefore no twist and cant measurements from the prism-based method are available for the test area for epochs 1-3.

However when Epoch 3 and before Epoch 4 had taken place, the prism monitoring system had been reinstated. This allowed the prism and TLS monitoring data to be compared as intended and provided an indication of the quality of the TLS methodology.

Subsequent inspection of the prism co-ordinates and TLS cross-sections revealed a set of two cross-sections across Tracks 12 and 13 that correlated (an example of one cross-section is shown in Figure 5.28. This allowed for four track cant measurements and two twist measurements over two sets of track to be compared. It also allowed the gauge to be calculated based on the TLS results. Table 5.8 shows the cant, twist and gauge results from the prism based and TLS based monitoring setup based on the contractor’s prism reference from tracks 12 and 13.

Prism	Prism co-ordinates (surveyed by monitoring contractor) on survey grid in metres			Track geometry – all dimensions in mm				
				TS cant	TLS cant	TS twist (over 12 metres)	TLS twist	TLS gauge
RPA131622E	83385.4794	34699.929	111.0541	1.0	2.0	0.8	1.0	1436.1
RPA131623E	83385.9461	34700.5202	111.0593					
RPA131712E	83391.9884	34695.3301	111.0409	1.7	3.0			1434.4
RPA131713E	83392.5141	34696.0077	111.0385					

Prism	Prism co-ordinates (surveyed by monitoring contractor) on survey grid in metres			Track geometry – all dimensions in mm				
				TS cant	TLS cant	TS twist (over 12 metres)	TLS twist	TLS gauge
RPA121622	83388.7223	34703.6912	111.0852	-0.1	-0.8	4.9	5.9	1432.9
RPA121623	83387.8741	34702.498	111.0968					
RPA121712	83395.4634	34698.1409	111.0809	5.0	5.1			1434.0
RPA121713	83394.9282	34697.3875	111.0745					

Table 5.8: Cant, twist, and gauge comparisons between total station and TLS results

When using the cant and twist values obtained by the prism-based method (provided by the monitoring contractor) as a baseline measurement, it can be seen that the TLS method provides similar values. This particular set of results shows that TLS correlates to the prism based data approximately within 1mm. These results agree with and show a slightly higher level of accuracy to Liu et al. (2014), who were able to achieve an accuracy of 2mm for the cant measurements based on TLS compared to the track inspection car.

The prism-based method implemented on this site is unable to provide gauge information as the prisms are attached to the sleepers and the distance to the gauge face is unknown. Therefore a regular gauge survey is required by the engineers. However, due to the surface measurement nature using TLS, the gauge information can be provided easily based on the measurements made in CAD. The standard gauge of rail in the UK is 1435mm. Based on the standard rail gauge, the results from the rail fitting using TLS (yellow column in Table 5.8) show that the biggest deviation from the standard gauge is 2.1mm. These results also agree with Liu et al. (2014) who were able to achieve an accuracy of 2mm.

For this set of data TLS shows comparable results for twist and cant to total station monitoring and also highlights that the track geometry parameters can be communicated back to the engineers in their typical format required. This information could be represented visually using the point cloud information. Alongside this, the results have shown that TLS can provide a method of validating the prism based method as well as providing information when the prism based method fails to produce readings for a particular area. It also provides a visual check of the track without the engineer needing to gain access directly to the track. This allowed a detailed inspection remotely without any time restrictions, in case a trigger may have set off.

5.9 Chapter Summary

A TLS survey was carried out using a rigorous total station survey which allowed accurate registration, geo-referencing and extraction of track from the point cloud.

Experiment 3 in Chapter 4 showed that a sub-millimetre level of plane fitting, i.e. 0.6mm, to the web of the rail was achieved using the Leica HDS7000. This result was validated when using the same TLS model to apply plane fitting to the web of track on a live railway monitoring site at London Bridge Station, which also achieved a fit of 0.6mm. Not only does this validate the laboratory tests, it shows that the same level of fit can be achieved without the use of targets attached to the rail at a longer range of approximately 15 metres from the scanner without the need for track possessions. This level of plane fitting to the web along with plotting histograms of the residuals was used as a reference when detecting whether track artefacts were attached to the web of the track.

A novel rail fitting technique was developed based on fitting the point cloud of track to its CEN56E1 rail design model by using the curvature-based and planar-based features of the surface. The results showed that when curvature based fitting is applied the quality of the fit to the design model is better than 3mm. However when multiple planar-based features of the point cloud are fitted to the design model, the quality of the fit is better than 1.5mm. This can be applied to a pair of rails in order to allow track geometry to be calculated, for example cant and twist.

Validation of the track cant and twist highlighted the capability to continuously capture TLS data where the prism monitoring data were sparse or missing. The prism data allowed four common points over one epoch to be compared to the TLS data. The TLS data also allowed track gauge to be calculated which is not possible for prism monitoring because of the attachment method to the rail. In order for the twist and cant to be calculated from TLS data, there must be sufficient surface coverage of at least one side of the track. For this particular set of tracks at London Bridge Station there were two pairs of tracks and a raised third rail running between the two. Therefore due to the occluding third rail, the cant and twist values could only be extracted when a scan had been obtained either side of the platform edge.

Due to the point cloud track extraction method, regular sections of track can be extracted at any interval required by the engineer without having to install more prisms or revisiting the site, which would require a possession. For example, if prisms have been installed at 9 metre intervals and the engineer requires a detailed inspection of the track at 3 metre intervals, this can be extracted automatically from the original point cloud without any extra effort in TLS data capture or processing.

Due to accurate geo-referencing of the TLS data it allows the point cloud to be compared to the design model (on site grid) immediately on a construction site. Therefore the engineer could determine an area of interest in which the archived TLS data could be used to evaluate.

The methodology presented for extracting and measuring track from TLS data at platform level shows that track can be monitored and data tied into the site co-ordinate system with rapid mobilisation and minimal planning compared to prism based monitoring. For example, if there was a prism on track suspected of providing a “bad” reading, a possession would be required to access that target to carry out an inspection

to ensure the safety of the passengers. This would require significant planning time and costs just to gain the possession before the source of the error could be investigated. However TLS could be deployed immediately to check whether there was movement of the track.

The findings from the rail fitting procedure shows that the same level of fitting can be achieved when the scanner is approximately 15 metres away from the railway track (compared with rail fitting results 9 metres away). This shows that rail fitting can potentially be achieved from historic as-built TLS data in the vicinity of the track, providing the scan has sufficient density.

5.10 Opportunities and challenges for Network Rail

5.10.1 Opportunities

- This methodology has produced a fit for purpose solution for monitoring track using TLS; calculating cant and twist parameters required by the engineers using a non-contact solution without the need of targets directly attached to the track/sleepers is possible.
- This type of interval scanning provides an independent check of the prism system if there's a failure of the prism monitoring system, without the need for possessions (which is currently required for prism-based monitoring installation). This provides a significant reduction in cost and safety risk from an installation and maintenance perspective.
- The track monitoring method using TLS allows a "rapid response" for seeing if something has happened on or around the track with very quick mobilisation to the lineside.
- The track monitoring solution is flexible and allows any track profile separation to be extracted based on the engineer's requirements.
- The monitoring solution is also useful for short-term low interval monitoring requirements where lineside access may be difficult.
- A scanning total station, such as the MultiStation MS50 would allow a section of track to be continuously monitored if required. If a prism reading fails due to being knocked, a scan could be carried out instead. The instrument would be required to be positioned close to the track if scanning was required. If the train timetable was known then the scans could be done in between passing trains.

- Some of the point cloud processing stages could be streamlined through the automation of data processing. The Point Cloud Library (PCL), as described in Chapter 3 could be used to create a tool for automatic point cloud registration based on the planar features of the track. This would remove the need for targets on site, reducing the data capture time. Another example would be the automation of point cloud processing when removing artefacts from the web of the track, based on plotting the residuals of the plane fit described in the chapter. These types of solutions would improve the time taken between track capture and delivering the track geometry parameters to the engineers.
- If required, data processing for track monitoring could be applied to any pre-existing TLS dataset of the track if there was sufficient point cloud density.
- As scanner manufacturers are now producing TLS systems that are very accurate to the sub-millimetre level, there is potential to improve the quality of the rail fitting. The TLS capabilities of the current systems used for this study are being pushed which can be seen by the rail fitting results. Therefore a more accurate scanner will improve the overall accuracy of the track monitoring solution.
- As well as improved accuracy, TLS systems are becoming faster. If a quicker scanner could be used, this would reduce the data capture time providing an opportunity of applying the track monitoring methodology during operational hours where trains are passing.
- TLS is becoming a very accessible technology in terms of specialist skills required to adopt this method of geospatial data capture. However monitoring using TLS requires specific skills to understand and “de-code” information from sequential epochs.
- The laboratory tests have shown a way of validating what can be expected from a TLS system when scanning track through the plane fitting. Before deploying any system there needs to be a way of validating the manufacturer’s specification performance against the actual performance. Therefore the laboratory tests provide a good indication of this before being deployed onto site.

5.10.2 Challenges

- With respect to TLS replacing the current continuous automatic monitoring system (measuring to targets 24 hours a day, 7 days a week) there is uncertainty of the scanner’s performance when being run continuously as they are not currently

designed for this compared to the total station instrumentation currently used for continuous monitoring.

- If automatic monitoring was required, TLS data could be captured as trains were passing by. However there would be occlusions in the data from the passing trains, which would require some development in the data filtering process to allow the rail fitting process to be applied.
- The track monitoring method requires a line of sight to the rail at least 15 metres from the scanner when at platform level. This will be challenging on different sites depending on where the tracks are in relation to the platform, where the angle view of the scanner could be a limitation on the coverage of the surface of the track, particularly if a third rail is present.
- The need for two scans either side of the platform, for this particular set of tracks, in order to obtain track cant and twist geometry limits the flexibility of the TLS instrumentation setup.
- If there was a potential of using TLS for continuous monitoring and replacing the current total station monitoring systems, there would be a huge cost increase based on the prices of TLS systems compared to total stations. Currently there are 65 total stations running continuously at London Bridge Station. The price of an accurate survey grade TLS system is at least double that of a high grade total station. Therefore there would be a challenge to find an economic solution for monitoring using TLS in the long term. However there is potential with the Leica scanning total station MS50 which is currently approximately the same cost as a highly precise total station. Whilst these are capital costs, operational costs also need to be considered for a cost/benefit analysis. A further study would be required to assess this.

Chapter 6 - London Bridge Station site test: monitoring of masonry arches

This chapter describes the application of terrestrial laser scanning (TLS) and close-range photogrammetry (CRP), along with conventional survey techniques, to the monitoring of a set of masonry arches at London Bridge Station. Firstly, it investigates the capabilities of using TLS compared to traditional survey methods and encompasses a case where significant movements occur over an extended period of time. Inter-epoch comparison demonstrates a capability to detect change but highlights a requirement to understand the structure and data quality in making valid interpretations. Secondly, similarly to Chapter 4, this chapter compares TLS and CRP techniques as monitoring tools for creating point cloud data on the same set of masonry arches. These investigations generate significant volumes of data conferring the additional challenge of how to visualise observed changes and communicate those changes and their significance to the engineers who must make informed decisions from the data in a timely fashion.

Chapter 4 (experiment 4) showed that a similar level of accuracy and precision can be achieved when applying linear translations to a masonry surface using TLS compared to a total station being used to observe targets attached to the surface. The tests also showed that CRP is able to produce similar point cloud quality to the TLS systems within the laboratory. Therefore this showed the potential for applying TLS and CRP for monitoring masonry structures. The aim of this chapter is to validate these laboratory results by applying TLS and CRP to a live monitoring site. However site conditions are very different to a controlled laboratory environment which affects the data capture and has an effect on subsequent processing. Some of these are challenges and are described in the next section.

As described in section 2.6, London Bridge Station is currently undergoing major redevelopment as part of the Thameslink Programme. The station was constructed on a series of masonry arches, built between 1836 and the end of the 19th century. The masonry arches are located at street level directly below the platform level of the station, shown in Figure 6.1.



Figure 6.1 Image of London Bridge arches at street level with train shed visibly located overhead (image taken from NR TLP published TruView)

The arches are required to be monitored prior to and during various stages of demolition and construction works. The initial arch monitoring specification was designed to monitor movements during the deconstruction of the old train shed roof overhead. Manual monitoring, which includes prism measurement in arch arrays, has been implemented here on a daily and weekly basis depending on proximity to works and their nature. Automated monitoring has not been applied at arch level due to restricted sight lines and continuing changes to the project's monitoring requirements.

6.1 Site Challenges

When the arches test site was being designed for this study, an arch that was going to have little disruption to it during the study was chosen. This would allow easy access to the arch as well as the use of a monitoring bracket initially setup for total station monitoring. This would allow the scanner to be set up in the same position each time and a 360° scan to be carried out. The initial plan was to carry out scans at regular intervals including hourly and weekly scans to allow the scans to be compared as well as investigate the capability of TLS as a monitoring tool. The arch was also well lit which would aid with the CRP data capture. Access to height was also easily available. An image from the initial site inspection is shown in Figure 6.2.



Figure 6.2: Images from original arch test site inspection

However just before data acquisition was due to take place, the arches next door (E55 & E57) had shown evidence (through prism-based monitoring) of unexpected settlement during piling works. At this point the engineers required an additional survey method to be used to validate this movement and provide a more detailed inspection to determine how the arch structures were moving, whilst the works continued. Therefore this provided an opportunity to carry out TLS and CRP monitoring testing on a deforming set of arches. This was thought to be a unique situation to the study as there was actual displacement taking place that required to be measured.

Therefore the “new” site presented many challenges compared to the original test site. Firstly, the scale of the data capture area was significantly larger than in the laboratory as well as the original arch, where one setup was required to scan the arch. The shape of the surface scanned in the laboratory was a small masonry sample, whereas this was a set of masonry arches. Therefore multiple setups for the arches were required. One of the main challenges in data capture here included obtaining suitable access to allow sufficient coverage of the arches from TLS and CRP. The lines of sight were limited during construction work, particularly during piling works, which was when this set

of data was captured. An example of the site conditions during data capture is shown in Figure 6.3. It can be seen that there are many large obstructions such as plant vehicles, clutter and restricted access to certain areas of the site.



Figure 6.3 : Typical site conditions of arches during data capture

As the data capture was taking place during piling works, there was a lot of vibration in the test areas. Therefore scans had to be acquired in between these to ensure data quality was not affected. In the laboratory the lighting could be controlled to allow suitable CRP data capture. However Figure 6.3 shows the minimal lighting available on this site. Whilst simple, a bright camera flash can be used to provide better image contrast appropriate for image-to-image matching, as well as target and feature recognition.

6.2 Data capture

6.2.1 Total Station (TS) monitoring setup

The masonry arches were located at street level directly below the platform level of the station. The arches were required to be monitored prior to and during various stages of demolition and construction works. The initial arch monitoring specification was designed to monitor movements during the deconstruction of the old train shed roof overhead. Manual monitoring, which included prism measurement in arch arrays, was implemented on a daily and weekly basis depending on proximity to works and their

nature. Automated monitoring had not been applied at arch level due to restricted sight lines and continuing changes to work progress and monitoring requirements.

The manual monitoring prisms were installed by the construction contractor at 5m arrays through the arch at the crown and springing points (see Figure 6.4), whilst reference prisms were located outside the predicted impact zone. Reference prisms were therefore used to define a stable co-ordinate system for each monitoring epoch. Therefore a monitoring network within each arch was set up.

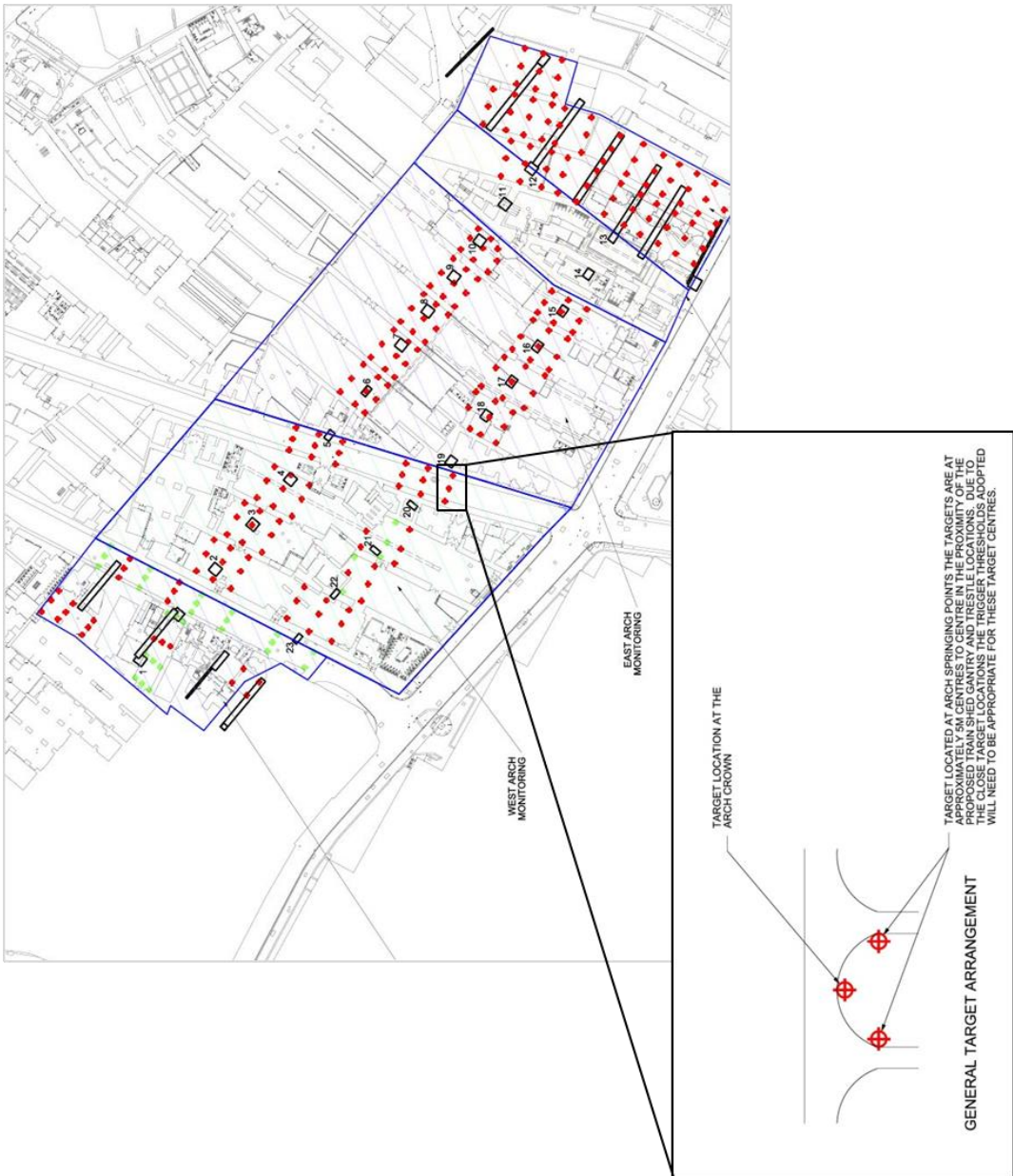


Figure 6.4: General target arrangements of arch monitoring

According to the monitoring specification for this project, all targets located on the arches were required to be monitored with an accuracy of at least +/- 3mm. A Leica

TS15 total station was used for the manual monitoring and geo-referencing. The capabilities of the instrument, based on the manufacturer's specification, are 1" for horizontal and vertical readings and 1mm + 1.5ppm (parts per million) for distance measurements to a prism (see Appendix A).

The quality of the network design for this site is affected by the limited lines of sight to the reference prisms through the long and narrow arches, which is similar to that of a tunnelling case. Ideally, reference targeting would be placed evenly across the network outside the impact zone, but this would be too invasive and uneconomical in this case. The trade-off was a weaker survey network geometry and lower accuracy when calculating the relative movement of the monitoring prisms. Similarly to the network analysis performance carried out in Chapter 2 experiment one, analysis was carried out to assess the geometric strength of the network using STAR*NET. A pre-analysis of a test area of the arches, shown in Figure 6.5, was carried out. The test area for this site was approximately 5 metres x 12 metres. There was no evidence of network analysis from the monitoring contractor. Therefore a "retrospective design" of the network was created to understand what could be achieved from the prism-based monitoring.

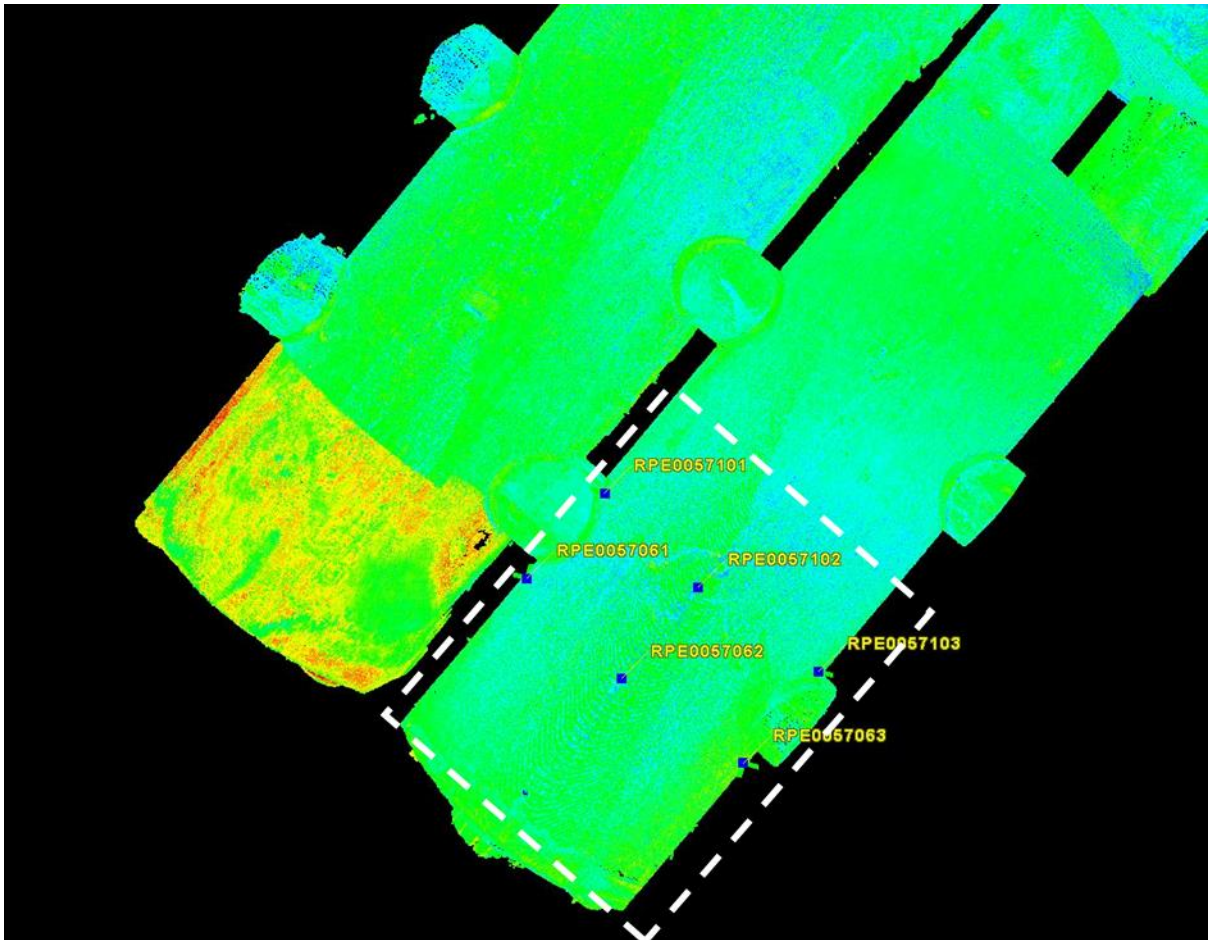


Figure 6.5: Test area (white) with monitoring prism arrays (blue)

Figure 6.6 shows a network plot of the reference (triangles) and monitoring points (squares) in the local monitoring network, including predicted error ellipses (1σ) for key target prism locations.

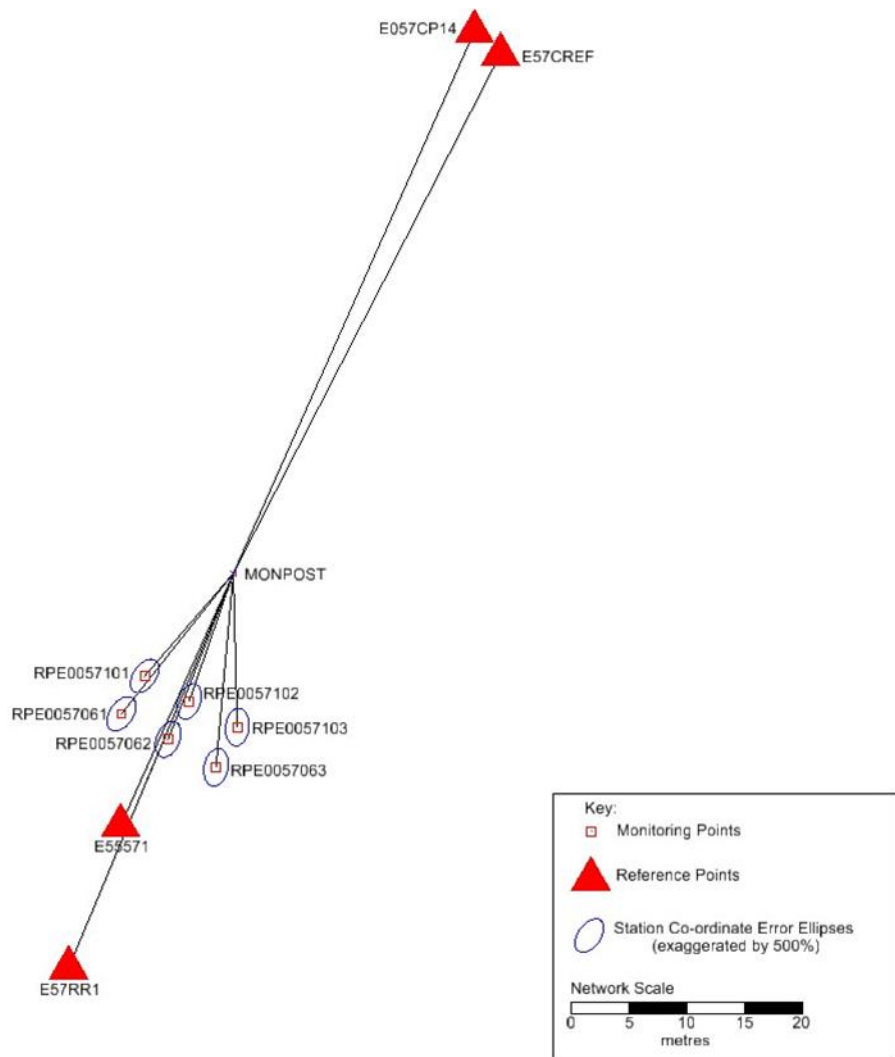


Figure 6.6: Network plot of TS15 monitoring survey of test area with error ellipses (1σ)

The standard deviations in Table 6.1 represent the precision of the monitoring target prism co-ordinates at 1σ .

Monitoring Point	Point co-ordinate standard deviation (mm)		
	E	N	EI
RPE0057061	1.0	1.2	1.0
RPE0057062	0.9	1.3	1.0
RPE0057063	0.9	1.3	1.0
RPE0057101	1.0	1.2	1.0
RPE0057102	0.9	1.3	1.0
RPE0057103	0.8	1.3	1.0

Table 6.1 : Monitoring point co-ordinate standard deviations (1σ)

It can be seen that the standard deviations of the monitoring points remain at the 1mm level. The network plot shows the error ellipses for the monitoring points have semi-major axis and semi-minor axis which are up to 3mm and 2mm respectively. Therefore, based on the +/- 3mm accuracy requirements of the arches monitoring, it can be seen that the survey is meeting the engineer's requirements.

Subsequent to the train shed deconstruction, 1D levelling (see section 3.2.1) was included in the manual monitoring to supplement the 3D observations during the piling works within the arches. The levelling network was linked to an external GPS reference network outside of the impact zone. This linkage includes a set of total station observations to define the targets within the site co-ordinate system. The levelling was partly instigated due to the logistical restrictions (access time and sight-lines during piling works) and partly as an alternative system to validate the movement in order to meet a requirement in the works specification. The co-ordinates of the monitoring points were used to geo-reference the targets used for TLS to enable inter-comparison with the levelling data.

Despite a predicted heave of up to 30mm during the removal of the train shed roof, no differential movement was detected. However during subsequent piling works, the manual prism based monitoring showed that some unexpected settlement in the arches was occurring. At this point the engineers required an additional survey method to validate this movement as well as a more detailed inspection to determine how the arch structures were moving whilst the works continued. Additional precise levelling bolts were added to the monitoring regime, and as the area was also being tested for TLS, localised scanning of the arches undergoing deformation was added to the techniques used for validation.

For this study an area defined by 2 prism arrays, comprising of 6 prisms, in the arches was chosen to compare the results from the manual monitoring to the TLS monitoring, with their co-ordinates from manual monitoring used to define a common co-ordinate system against the reference points shown in Figure 6.5 and Figure 6.6.

6.2.2 TLS monitoring setup

A Faro Focus 120 scanner, which was used in the laboratory tests of masonry brick sample (see Chapter 4 experiment 4) was available on site. Originally purchased by the Design and Build Contractor to illustrate topographic survey updates, this instrument was selected to monitor the set of arches subject to movement. The Focus

120 is a phase based scanner and according to the manufacturer's specification, the maximum operating range is 120m with a ranging error of $\pm 2\text{mm}$ (FARO, 2013). Chow et al. (2012) carried out a point-based self-calibration of this system and was able to show the ranging precision was better than 2mm to TLS signalised targets before and after the calibration procedure, agreeing with the manufacturer's specification.

Scanning was carried out on four separate epochs over an 8 week period following the detection of initial movement until the settlement appeared to have stopped. The number of scans for each epoch varied due to the limited access to the site whilst works continued. Scanned surfaces were typically at ranges of 5 metres from the scanner with a point spacing of 4mm. The ranges deployed were similar to those of the laboratory testing (see section 4.2.2) but due to time restrictions on site, the resolution of the scan was reduced from 1mm to 6mm. To increase the accuracy of the registration of scans for a particular epoch, sphere targets were used (see section 3.2.3.1). Scan-to-scan registration was carried out in Faro Scene version 5.1. Results from the TS monitoring were utilised in order to select stable areas so that each epoch could be registered to the "Epoch 0" baseline dataset (which had been scanned for as-built purposes a few months beforehand) with the ICP algorithm (Besl, 1992) available within Leica Cyclone version 8.1 software. Stable areas comprised of the base of the arches up to a height of up to approximately 1 metre distributed across the entire point cloud. Registrations indicated by the software shows an average RMS registration of 7mm. This is discussed further in section 6.3.4.

6.2.3 CRP setup

To compare the outputs of TLS without the use of targets and to show the potential of other applications for deformation monitoring in a railway environment, CRP was applied to the arch at one of the epochs. A similar method to that used in the experiment in section 4.2.1.2 was applied. A Nikon D3200 camera was used with a calibrated wide angle 16mm fish-eye lens to capture a network of images of a test section of the arch. The images were then corrected for distortion using UCL's Lens Distortion Correction (LDC) software and a fish-eye correction model using the parameters obtained from a laboratory calibration. The corrected images were run through Visual SFM version 0.5.22 to carry out feature detection and full pairwise image matching. The dense 3D reconstruction function was then run to produce a point cloud of the area. The CRP

point cloud was then scaled and compared to the TLS point cloud. 3D distances between common features within the CRP and TLS point cloud were used to compute a scale factor for the CRP point cloud. Once scaled, the same reference points could be used to approximately align the CRP data. Fine registration was then achieved using CloudCompare version 2.4 software based on the same stable regions as originally used to inter-compare the TLS data. This process resulted in a global error of 3mm. section 6.3.5 details some of the tests carried out to validate the CRP results.

6.3 Results and analysis

6.3.1 Comments on workflow

The workflow for each of the methods, including design of the sensing network through to communicating measurement data to engineers, is shown in Table 6.2. The TS workflow established the geo-reference for the system and was able to co-ordinate some half a dozen targets which were essential to both CRP and TLS geo-referencing. Without the use of TS both CRP and TLS would only have been capable of determining relative movement between epochs as opposed to absolute movement. Similarly if TS was used on its own, only a few dozen points could have been recorded rather than the complete surface geometry obtainable from either TLS or CRP.

Methodology							
Instrumentation /Method	Pre-analysis	Data Capture	Data Processing			Outputs	Communication and Reporting
TS (medium equipment cost) Several setup positions			Orientation	Network adjustment		Discrete points	Web-based reporting of movement in tabular and graphical format
TLS (high equipment cost) Several scan positions	Simulation and design of sensing network against requirements	Instrument and target placement Repetitive data capture	Registration	Network adjustment (optionally with geo-referencing)		Point cloud	Deformation displacement maps/extracted profiles
CRP (low equipment cost) Many images			Image correction and image matching	Network adjustment (optionally with scale and geo-referencing)	Dense reconstruction	Point cloud	Deformation displacement maps/extracted profiles

Table 6.2: Methodology workflow of TS, TLS and CRP for monitoring purposes

Despite having similar data acquisition times on site, CRP required significantly more “back office” time to get to the point cloud output due to the number of steps required in the workflow. It was also found that in order to process the 201 images encompassing the network for one arch required extensive computer processing power (a high end PC with 8 processor cores and 64GB RAM). The CRP point cloud output is dependent on the local surface texture and the overlapping network of convergent images that can be captured across the surface. The major limitation, with current CRP technology is that it is a passive sensor with limited capability to texture-less surfaces and results cannot be realised and checked in the field since significant post processing is required to produce the point cloud model. In contrast TLS is an active sensor providing close to real-time output of point cloud and if areas have been missed, they can be seen immediately and re-scanned during the same on-site session.

The skill set required for these survey methods differs. CRP techniques require a specialised skill set to capture the image network necessary to produce the optimum output through the workflow. Once an accurate point cloud has been acquired and registered the data processing workflow for each system is relatively similar and commonly used by those working in the engineering surveying industry. The attraction of CRP is the relatively low cost and widely available digital camera as a sensor, but this is offset by the skills needed to reliably capture the data on site. As mobile computing improves, automation of CRP capture may well reduce the required operator skills. As TLS can measure from a single station, the data capture process is somewhat easier being one of obtaining full coverage rather than the complete multi-view coverage required by CRP. Despite this, it is a relatively high cost sensor and less readily available if bespoke validation tools are required. In contrast, CRP uses low cost cameras which are more readily available.

6.3.2 Manual monitoring results

Figure 6.7 shows a graph of one of the monitoring prism readings, relative to the baseline readings in the Z direction, within the test area of the arches. This monitoring information is provided to the engineer via a web-based reporting system that highlights change through the use of pre-set trigger threshold alarms. In this study the trigger thresholds (see Chapter 2) are defined in terms of settlement where green = $\leq 10\text{mm}$ settlement, amber = $>10\text{mm}$ and $\leq 15\text{mm}$, red = $> 15\text{mm}$. The time series of the graph shows the monitoring data acquired before, during and after the piling works

began. The green arrows indicate epochs at which TLS was carried out. In this case the decision made by the engineering team was to increase the monitoring frequency and to verify the survey network link to external geo-referenced points whilst continuing the plan of work.



Figure 6.7: Graphical monitoring results from prism target RPE0057101- data taken from Sol Data Geoscope's monitoring database

Table 6.3 shows monitoring data from the two arrays of prisms in the test area (refer to Figure 6.5). The data shown in red are the recorded changes shown in Figure 6.7.

Between the 2 corresponding arrays of prisms, the results show a consistent set of movement. Significant change in movement is detected between epochs 1 and 3 (with changes of up to 25mm with respect to the first epoch), which then levels off by epoch 4. The left side of the arch is settling up to -43mm (Z direction), whilst the right side of the arch remains relatively stable. The crown of the arch shows a gradual settlement reaching 23mm which then stops by epoch 4. The results show discrepancies indicating settlement of up to 20mm between the crown and left of the arch. This settlement is considered highly significant, being an order of magnitude larger than the 3mm maximum deflection observed to the right of the arch and when compared to the 1.3mm maximum co-ordinate standard deviations (1σ) estimated from the survey network (see Table 6.1).

Array 1 (left to right) (mm) Movement in Z axis (-ve value is a settlement)						
Epoch/Target ID	RPE0057061	Δ movement RPE0057061	RPE0057062	Δ movement RPE0057062	RPE0057063	Δ movement RPE0057063
0	1		1		1	
1	-22	-23	-14	-15	-2	-3
2	-31	-9	-19	-5	-2	0
3	-41	-10	-23	-4	-1	1
4	-42	-1	-22	1	-2	-1
5	-42	0	-22	0	-1	1
6	-43	-1	-22	0	-2	-1

Array 2 (left to right) (mm) Movement in Z axis (-ve value is a settlement)						
Epoch/Target ID	RPE0057101	Δ movement RPE0057101	RPE0057102	Δ movement RPE0057102	RPE0057103	Δ movement RPE0057103
0	1		0		1	
1	-24	-25	-14	-14	-2	-3
2	-33	-9	-19	-5	-2	0
3	-42	-9	-23	-4	-2	0
4	-43	-1	-22	1	-2	0
5	-43	0	-22	0	-2	0
6	-44	-1	-22	0	-2	0

Table 6.3: Numerical manual monitoring results of arches including change in movement between epochs (mm)

6.3.3 TLS results

Direct measurement to prisms with TLS is unreliable with the Focus 120 system used in this study. However the dense and relatively complete surface information that TLS provides allows an area-wide displacement map to be computed. Data from the dense deformation displacement map can be used for inter-comparison. Profiles were also produced to provide the engineers with a more conventional understanding of the observed movement.

Based on the results from Chapter 4 experiment 4, the deformation displacement maps in Figure 6.8 were produced by comparing the meshed surfaces for each epoch to the baseline measurement in Geomagic Studio & Qualify 2013. CloudCompare was also attempted, however this software (version 2.4) as not able to handle the large volume of data incurred by the coverage of the test area. The 3D deviation tool available within Geomagic Qualify is able to calculate the deviations as the shortest distance from the test object to the reference object. The deformation displacement maps shown are in plan-view for each of the epochs compared to Epoch 0. The scale of displacement analysed is +0.05m to -0.05m. The colours are representative of the movements classed in the original trigger threshold values set for the monitoring of the arches

during the deconstruction of the train shed roof (see Section 6.3.2). The grey areas highlight where there was insufficient data overlapping between the scans. Each of the maps shows a black spot towards the north of the test area, implying a settlement of greater than 50mm. After further investigations, this was found to be an anomaly where there was a gap in the baseline data due to occlusions caused by lighting fixtures on the crown of the arch.

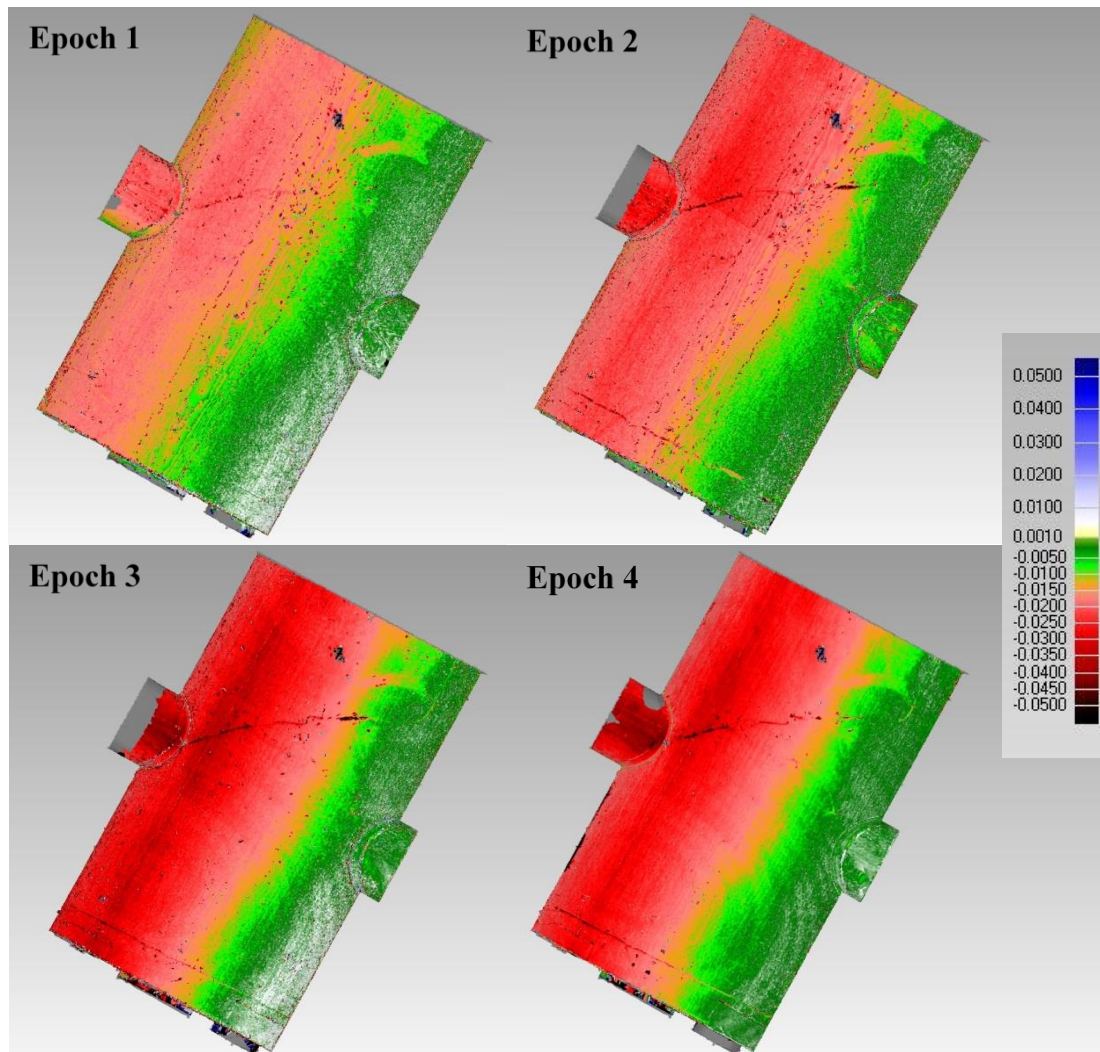


Figure 6.8: Deformation displacement map of a 5 x 12 metres area of local detail between epochs 1 and 4 (plan view, deflection in metres)

6.3.4 TS and TLS analysis

The colour scaled surface deformation displacement map highlights the settlement of the arches. Results agree with the observations from the manual monitoring data. In this case the scan data are independent of the TS monitoring survey and provide more detail of the surface of the arches. The accuracy of the displacement map is dependent on the ICP registration between the epochs calculated in Cyclone version 8.1. In Figure

6.8, where data between epochs has been compared in Geomagic Studio 2013, it is readily apparent that significant areas of the right hand portion of the arch show typical discrepancies of the order of 1mm demonstrating the validity of the registration. The surface displacement map is significant for the engineers as it firstly validates the manual monitoring results, but also provides more information about the structure for the engineer to carry out further analysis. The colours have been selected to highlight the various trigger alerts that would be set off if this was developed into a reporting system. However, one of the software limitations is that the only way of providing numerical information of the deformation is through the coloured scale.

In order to directly compare results from TLS to the prism monitoring, an attempt to extract the discrete information from the surface model in the vicinity of each prism was made. The discrepancies between the movement from the manual readings and expected readings from the scan data show variations of between 1mm and 20mm highlighting the weakness of this method, despite 5mm point spacing of the surface in proximity to the prism. An alternative method would be to apply local fitting to the TLS data to compare them to the TS dataset. However prism locations have been selected by the engineer according to the arch geometry and do not easily support local fitting (see Figure 6.9) such as the plane fits used in Section 6.3.5, necessary to ensure accurate results. In order to make direct comparisons to the prisms, physical adapters to prisms or spheres would need to be attached in the place of each prism. Alternatively a common target incorporating a prism and checkerboard could be assigned.

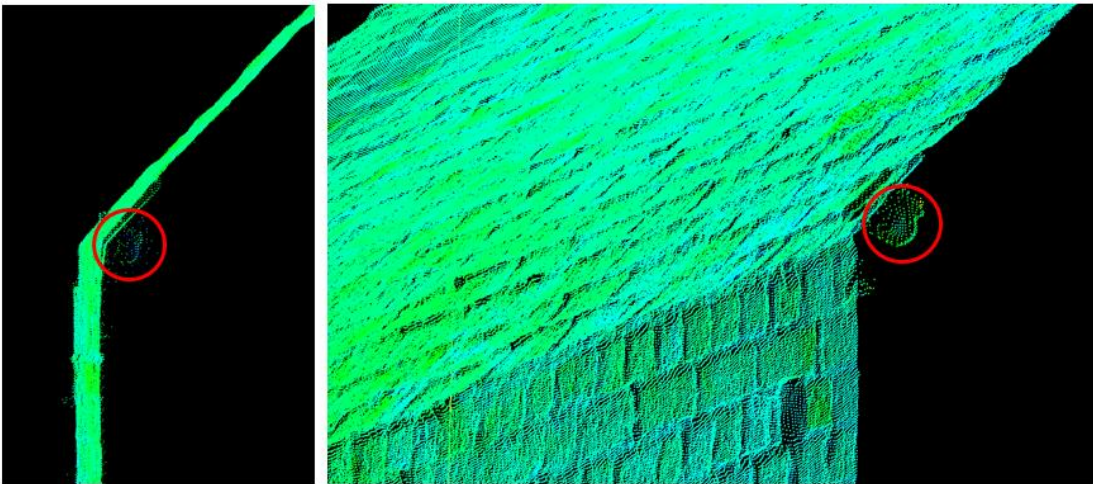


Figure 6.9: Side (left) and perspective (right) view from point cloud of prism (circled in red) aligned to springing point of arch

Profiles through the arch at each epoch were manually extracted using Microstation V8i. The profiles were constructed at approximately the same position as the prism arrays. An example is shown in Figure 6.10. Even though the exact location of the prisms cannot be identified in the scans, the difference in distance measurements provides a way of visualising discrete measurements across the array. In this example, the profile shows a set of six discrete deformation measurements that have been extracted from the scans compared to the three prism based measurements available. Even though the uncertainty between the registered datasets was approximately 7mm, it can be seen that the displacements correspond to the prism-based readings shown in Table 6.3 in the order of a few millimetres. Given the observed change in this test area, the engineer found that being able to choose both profile locations and the number of data points to be extracted per profile provided an ideal solution. Some parts of the profile have required more “extraction” than others, particularly when analysing the effect of unpredicted movement. This allowed the engineers to have flexibility with distinguishing where more localised monitoring was required to take place. This is not a practical solution for prism based monitoring as, in the simplest case, it could result in installing a very large number of prisms which would result in further costs for installation, maintenance and the time required on site. Meanwhile this need for an “extra” set of measurements would not be required if TLS was applied, as the data would contain all this information and could be used on an “as and when needed” basis. This then becomes a balance between being able to extract information to the level of accuracy required and what exact information the engineer requires to see in the reporting.

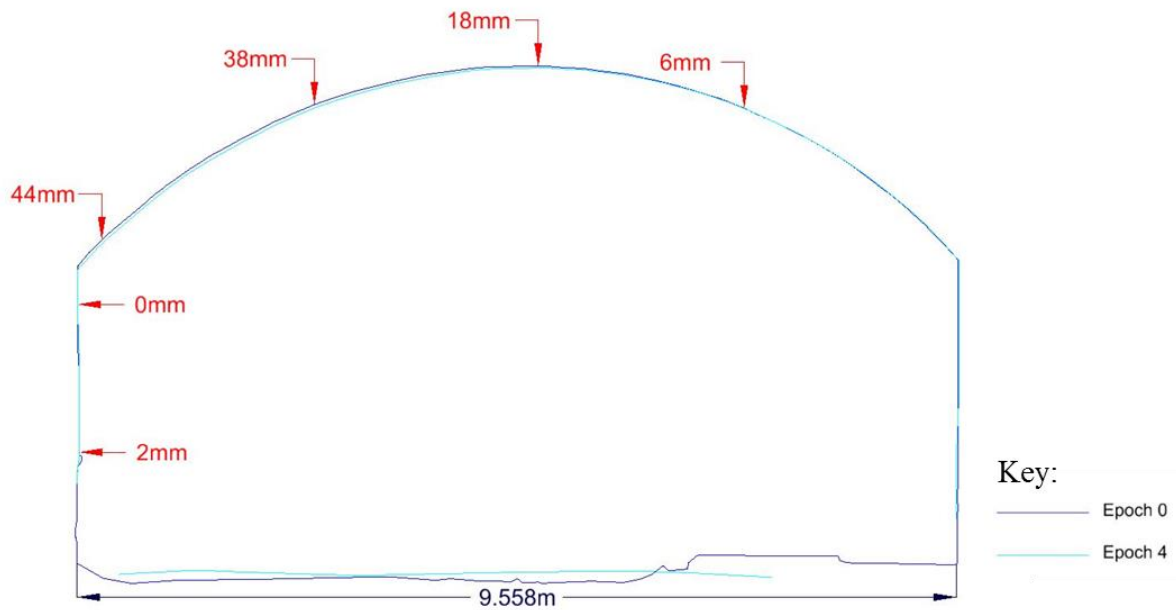


Figure 6.10: Profile of arch from TLS data with movement vector dimensions (deflections shown in red)

Geo-referencing in this particular application is challenging due to narrow sight lines. However if it could be improved, the effectiveness and independence from local deformation of the TLS would benefit, since ICP and assumptions of stable surfaces would no longer be needed.

To overcome the requirement of needing a TS and TLS system whilst maintaining a high accuracy of survey, manufacturers are producing laser scanning total stations which have the capabilities of reading prism targets accurately and scanning localised surfaces similar to a TLS system, e.g. the Leica MS50 which was used in the laboratory testing (see section 4.2.2). Whilst the scanning time is significantly longer with the first generation of these devices, these types of instruments are likely to reduce the time required when using the TS and TLS system as well as to produce discrete point measurements to a target in the arches as well as scan a surface that might require further investigation.

In practical terms local referencing on ICP is likely to remain a requirement since strengthening the TS network geometry for accurate geo-referencing in these arches would be challenging due to the long and narrow shape and therefore limited lines of sight for a network solution (see Figure 6.6). To overcome this, more TS setups would be required which, in turn, would introduce more sources of error which would be propagated through the survey network. Simulation of possible networks could be used

to optimise the solution, but initial estimates suggest that magnitude of these errors would be of the same order as the predicted movement levels.

6.3.5 CRP vs TLS

A test area within the arches was chosen to compare the processes and outputs from CRP and TLS. The workflow, shown in Table 6.2, was used to produce a scaled and registered point cloud of the same arch. An example from the CRP output can be seen in Figure 6.11

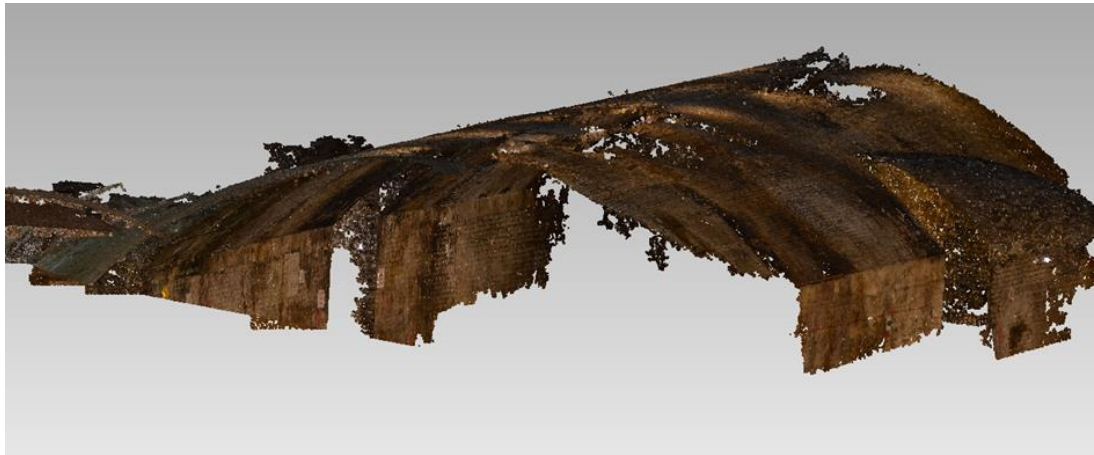


Figure 6.11: CRP point cloud of test area of masonry arches

Local comparisons between the TLS and CRP point clouds were carried out by looking at the individual patches and profiles of each of the datasets.

Patches of relatively flat areas in the corresponding point clouds were extracted and compared. By using least squares estimation, planes were fitted to these patches using CloudCompare. As the arches are not perfectly planar, the RMS of the residuals following plane fitting are limited to a relative comparison between the two surveying methods. These are shown in Table 6.4.

	RMS of the residuals, normal to the plane (mm)	
	TLS	CRP
Plane 1	7.3	11.3
Plane 2	2.2	3.0
Plane 3	1.7	1.7
Plane 4	3.5	3.3

Table 6.4: Results from plane fitting using least squares estimation

The RMS of the residuals from the plane fit show the level of noise of those particular patches from the two sensors and therefore demonstrates the sensitivity of TLS and CRP to detect change. The values for these areas are comparable between the methods as well as the laboratory testing (section 4.2.2.3) and show a millimetric level of noise. They also agree with the findings from Laefer et al. (2014) where plane fitting to a brick surface produced an RMS around the 2mm level. In this case the size of the test patch is slightly larger. The exception is Plane 1, where on closer observation a strip of wood (Figure 6.12) could be seen attached to the extracted region, this small 3D feature with its sharp edges and sharp shadowed edges has been recorded differently by the active TLS and the passive CRP system.



Figure 6.12: Image of area used for Plane 1 highlighting wooden object

Figure 6.13 shows the point cloud used for the “Plane 1” fit using the TLS and CRP data. It shows the visibility of the wooden object in both datasets. In this case the difference in the magnitude of the residuals highlights the spatial sensitivity of the methods to record fine detail, suggesting that the photogrammetric surface is more sensitive to this influence. The profile views from both data sets confirms this (lower image pair in Figure 6.13).

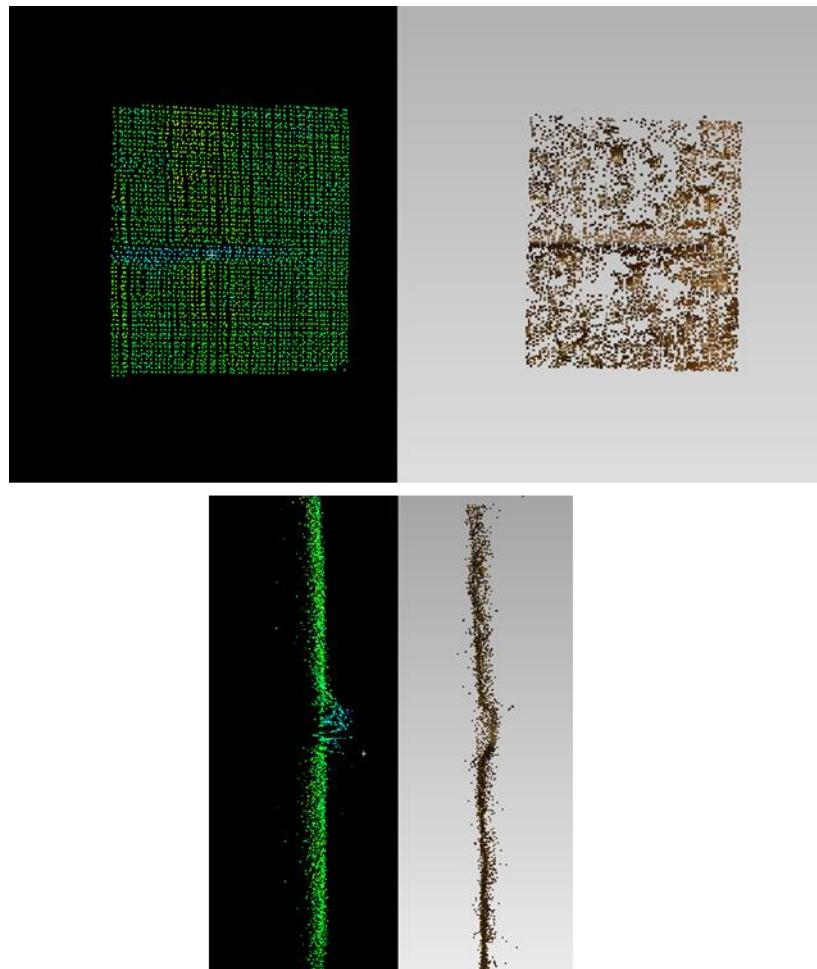


Figure 6.13: Front and side profile view of TLS (left) and CRP (right) point cloud for Plane 1

Corresponding profiles of the arch from the CRP and TLS datasets were extracted and compared. An example profile is shown in Figure 6.14 where the TLS points (which are set as the baseline dataset) are represented in dark blue and CRP in light blue. Discrepancies between two systems along the arch are shown. A close-up image of the point clouds of the area highlighted in the grey box is shown in the lower image.

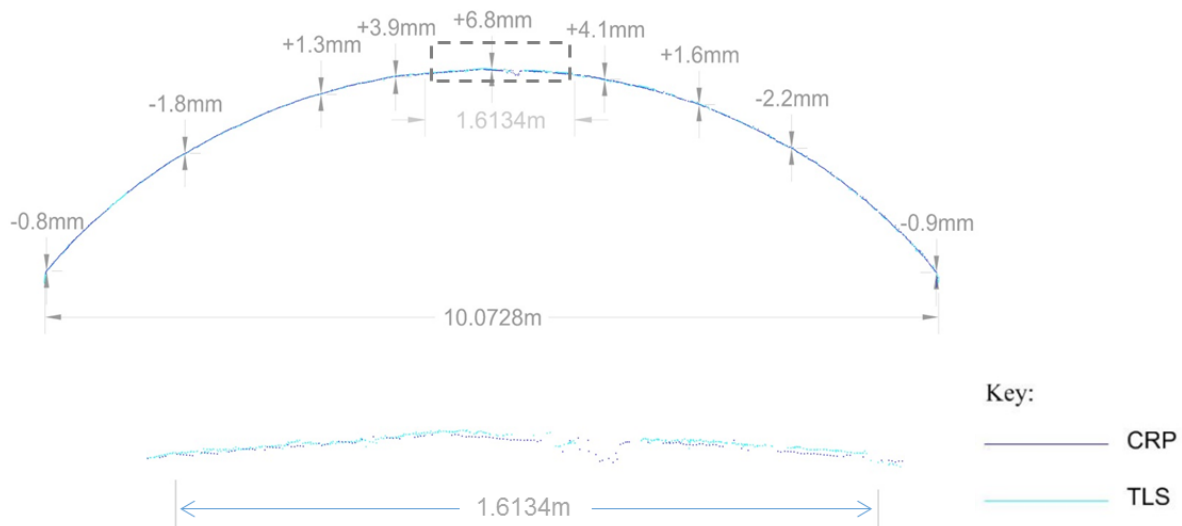


Figure 6.14: Comparison of arch profile between TLS and CRP data

As the global registration error for the TLS and CRP data was 3mm (section 6.2.3), the profile shows a relatively good fit between the two datasets. This highlights the capability of achieving, after post-processing, an accuracy of $\pm 3\text{mm}$ required by the engineers. The springing point of the arch shows a very small discrepancy between the datasets, i.e. less than 1mm, and corresponding to the boundaries of the ICP registration data selection. The level of discrepancy is higher towards the crown of the arch reaching up to 6.8mm. A possible reason for this discrepancy is the weakness in the photogrammetric image network geometry. Due to the site logistics, it was not possible to take images in proximity to the crown compared to the springing points of the arch. These discrepancy results suggest that this affected the image geometry and subsequently degraded the point cloud output. Therefore further work would be required to improve the image network so that sufficient coverage of the crown of the arch can be acquired.

The findings from this chapter have been published in the peer reviewed journal *Applied Geomatics* (Soni et al., 2015).

6.4 Chapter Summary

A TLS monitoring survey was applied to a deforming set of brick arches on a live construction site without the need of attaching targets to the structure. This provided relative movements of the arches independent of the total station (TS) monitoring that had been implemented on the site. The outcomes from TLS validated the movements of approximately 40mm from the TS monitoring over a series of epochs, with an

uncertainty of approximately 7mm based on the ICP registration between the epoch scans.

The movement measured from the TLS data was communicated to the engineers through surface displacement maps and 2D CAD profiles of the arches. From the engineering point of view the TLS data provided more “complete” information about the surface and change in shape compared to the discrete set of points provided by the TS, without the need of revisiting the site for further measurements or inspections.

The baseline point cloud which was used to compare the TLS epoch scan data was from a pre-existing topographic survey scan. This highlights the potential of using these tools and resources for where movement isn't anticipated.

Overall this highlights the “rapid response” capabilities for TLS to a deforming arch, especially when targets haven't been attached. It is a repeatable method of data capture which can be easily mobilised.

Close-range photogrammetry (CRP) was applied to one of the TLS epochs to compare the point cloud quality between the datasets. Results showed a comparable level of quality, where RMS from plane fitting to corresponding patches of the arch surface matched to better than 1mm. A comparison of the profiles of the arch from each of the datasets showed that the springing points of the arch corresponded to the 3mm registration threshold, whereas the crown of the arch had a discrepancy of nearly 7mm with the CRP data. This was due to lack of images in proximity to the crown due to limited access on site.

Whilst TLS can provide a check of the data capture whilst still on site, CRP requires significant post-processing and is dependent on the surfaces being passively imaged and the geometry of the images captured. TLS systems provide some sort of instrument capability/manufacturer's specification for the user to see if it's fit for purpose, whereas there is no instrument capability information with CRP.

With regards to TS monitoring, this chapter has shown the importance of pre-analysis for network design when investigating the capabilities of an instrument when measuring and/or monitoring an arch or tunnel environment, where there are long and narrow lines of sight. It allows the user to distinguish between weakness in geometry of the network and actual movement.

6.5 Opportunities and challenges for Network Rail

6.5.1 Opportunities

- A pre-analysis of the network design can be carried out to see if the monitoring design is fit for purpose based on the engineer's monitoring accuracy requirements.
- TLS can be easily adopted without needing target installation when there is unpredicted movement and validation of movement is required. If using prism-based monitoring, more prisms would be required to be installed, costing time and money. This type of implementation provides an alternative if there is limited access to prisms during construction work.
- Where it is physically difficult to place prisms for monitoring purposes, TLS could be applied.
- The automation of surface displacement maps and extracting cross-sections is currently available in packages such as Geomagic Qualify. This would allow sections and displacement deformation maps to be easily created depending on areas in which the engineers require further investigation.
- Another use for this automated point cloud processing tool could be to inter-compare TLS data between different contractors as a method of assurance.
- In common with monitoring track, access and skills needed to deploy TLS are readily available. A laser scanner is a common survey instrument that is often used and easily available on major construction sites, particularly with producing topographic surveys and the development of BIM. Therefore, similarly to this study, monitoring using TLS could be easily adopted with the easy access to the system on site. With respect to training requirements, data capture would be similar but further training would be required to carry out accurate comparisons between multiple scans.
- In common with the conclusions from monitoring track in Chapter 5, there is potential for a hybrid scanning total station (e.g. Leica MS50) in the monitoring industry which allows a combination of techniques to be exploited. For example:
 - This type of instrument would allow accurate geo-referencing and measurements to prism using the TS whilst having the ability to carry

out surface based measurements of patches using TLS on an as and when needed basis.

- The instrument could be used for assurance purposes, particularly validating and independently checking co-ordinate grid systems. Multiple types of measurements could be made of multiple types of targets depending on site access and time of day, e.g. prisms can be easily sighted during the day, however when there is difficulty in sighting them at night time, a scan could be carried out.
- With the development of point cloud processing tools such as Point Cloud Library, there is potential to automate the TLS solution, particularly for accurate point cloud registration.

6.5.2 Challenges

- One of the biggest challenges is the ability to co-ordinate the scans onto a site grid for a set of arches in order to provide absolute movement values. Compared to the track monitoring survey which was in an open space, the short and limited line of sights to the edge of the zone of influence made this a challenging survey. If the network analysis produces poor results, this will result in a low accuracy of point cloud geo-referencing.
- A current limitation is the accuracy of registering multi-epoch scans together. This work has shown a cloud-to-cloud registration approach. In order to increase the accuracy of this, a similar method to the track monitoring survey applied in Chapter 5 would need to be implemented by having permanent reference targets that could be read by both TS and TLs systems. This would improve the accuracy of the registration between the scans and therefore the integrity of the surface displacement maps and cross-sections. Having reference targets that are easily accessible on a construction site is challenging.
- The quality of the point cloud is dependent on the optical properties of the materials being scanned. This particular work shows the effect of scanning a brick surface, however the return signal from the scanner will be different for surfaces such as concrete or dark materials.
- Despite CRP producing a similar quality of point cloud as the TLS of the masonry surface, the process to produce this point cloud was very time consuming and required multiple processing steps for the output due to it being a passive sensor. The quality of the output is also very dependent on the image

network geometry. Compared to TLS, the application of CRP would require a highly specialised person.

Chapter 7 - Conclusions and further work

This chapter brings together all the individual chapter summaries into a single set of conclusions. Analysis of these outcomes highlight the contributions to knowledge and novelty of this work as well as giving suggestions for further work.

This research was motivated by Network Rail Thameslink Programme (TLP) where there were concerns in the effectiveness of the monitoring systems being implemented. In particular, there was an uncertainty of the benefit of using glass prisms due to multiple problems associated with their implementation and maintenance during the lifetime of the project (see Chapter 2). Fundamentally targets are designed to provide highly accurate and clearly identifiable features that permit measurement of the structure they are attached to. However compared to direct surface measurement, they are an indirect physical fixture which can give spurious readings if moved or knocked. This study investigated the potential of non-contact monitoring solutions such as terrestrial laser scanning (TLS) and close-range photogrammetry (CRP) technologies which support both target and surface measurement capabilities. The thesis investigates the performance of engineering surveying instrumentation for measuring to targets in comparison to the performance of TLS and CRP when measuring to surfaces, with the aim of detecting deformation both within laboratory and live site environments.

7.1 Contributions to knowledge

With regards to engineering surveying equipment such as total stations and terrestrial laser scanners, manufacturer's specifications are broadly achievable. This can be seen in Chapter 4 where experiments demonstrated that instrument capabilities evaluated in a laboratory can then be applied on site. It is also as evidenced by Chapter 5 & Chapter 6, for measuring points and surfaces in order to detect change at millimetric levels.

When measuring to a network of points, repeated measurements to targets in a network can be analysed using well-established network design, adjustment and analysis procedures. From an academic standpoint, this is accepted practice, however there is very little evidence of any of these procedures in practice at Network Rail on the Thameslink Programme. An overview of these procedures is provided in Chapter 3 in the context of a multi-instrument setup. It is important for these steps to be applied to observations, particularly for deformation monitoring networks, where the use of

redundant measurements provides an additional level of security in making decisions concerning the significance of any observed changes.

Chapter 4 provided an example of using network design to compare the expected performance of an instrument against practical observations. This demonstrated a method of checking whether instrument performance is within manufacturer's specifications. It also allowed instrument errors to be detected and error sources identified, irrespective of the instrument's calibration history. This reiterated the importance of network analysis, but also highlighted the effect of instrumentation error on a deformation network, where a systematic error in the instrument could be misconstrued as deformation. The method of determining performance of this instrumentation was developed by drawing upon established metrology standards, such as determining length error, and using a laser tracker along with nests that allowed measurements of different target types to provide a gold standard baseline. This work is being submitted as a full paper to the *Survey Review* journal. Further work would allow this procedure to be developed for checking instrumentation for "wear and tear" on site during the monitoring measurement process, particularly for instruments carrying out continuous automatic monitoring. This could be applied by placing reference prisms within stable areas across the network and repeatedly measuring them before, during and after a set of monitoring readings. Such a procedure would allow Network Rail to mandate instrument testing either within the monitoring contract during the tender process or within the monitoring specification document, which would allow monitoring system assurance at the individual instrument level whilst performing continuous monitoring 24 hours a day, 7 days a week.

The network design procedure is well established when predicting the performance of instruments observing to a set of targets or points. However design procedures are not as well established when measuring to different surfaces using optical non-contact techniques such as TLS. Even though networks are inherent in CRP, the black box processes currently in use do not have a comparable simulation option. Measurement performance when applying these techniques to a given surface must currently be determined experimentally in order to gain an understanding of the surface reflectivity and local geometry of the surfaces. This study used test objects in the laboratory to determine the performance of TLS and CRP when measuring to a particular surface type, to determine if these solutions fulfilled the engineering requirements. The test

surfaces, in this case railway track and masonry brick, were selected to closely match the ones found on the London Bridge Redevelopment Project site to allow validation of the laboratory testing whilst having to take into account typical construction site restrictions, for example limited lines of sight to the surface due to safety access and vehicles occluding it, as well as restricted working hours.

Plane fitting can be applied to the web of the rail to determine the noise levels from TLS and CRP when measuring to the planar surface. A sub-millimetre level of fit of 0.6mm could be achieved in the laboratory using the Leica HDS7000 laser scanner (Chapter 4, experiment 3). This was validated by achieving the same level of fit of 0.6mm from the same scanner model on a track monitoring site (Chapter 5). Agreement between data sets was excellent despite the restrictions with respect to the oblique line of sight to the track surface from platform level and longer instrument stand-off distance (approximately 15 metres), as well as time availability when working within vicinity of track.

A brick surface can be captured through TLS and CRP and modelled by applying plane fitting in the laboratory with an RMS of approximately 2mm (Chapter 4, experiment 4). These match the noise levels achieved in the laboratory by Laefer et al. (2014) when applying plane fitting to detect cracks on a masonry brick surface using TLS. The same level of plane fitting could be achieved on a very active construction site (Chapter 6) where there were restrictions in terms of gaining access to the site as well as lines of sight available to the surface due to large plant vehicles and piling equipment constantly moving.

The validation of the laboratory tests allowed a TLS monitoring survey to be applied to both of these sites, independent of the prism based monitoring (implemented by the monitoring contractors), to achieve fit for purpose solutions. Chapter 5 discussed how direct measurement of track surfaces using TLS can be used to calculate engineering parameters including track cant and twist. The method shows the flexibility of the TLS method to extract particular profiles from point cloud data which might be delivered live from an instrument, or be extracted from archival data. Due to the larger scale of the test area compared to the laboratory, the method relies upon targeting for point cloud registration where an RMS of 1mm was achieved.

A novel methodology for applying rail fitting in order to extract parameters was developed in this thesis. The overall results show that track cant and twist results from

TLS are within 1mm of those recorded by prisms attached to the sleeper of the track. Whilst comparative data was limited to a short sequence of prism data, these results not only show an agreement with the current monitoring system, but also illustrate that the same track geometry parameters can be achieved by measuring directly to the rail without needing to apply an off-set correction (see Chapter 5) or making the assumption that the sleeper and track move together. The methodology and development of this novel rail fitting process has been published in the *ISPRS Archives, Commission V, Working Group 4, 2014* as well as the proceedings from *FIG Working Week 2015, Commission 6* which are both peer-reviewed conference papers.

The novel technique for rail fitting developed in Chapter 5 is capable of complete automation:

- i. By using the minimum railway curvature radius computation to determine the longest length of straight track, plane fitting can be reliably applied to detect the web of the track.
- ii. Using the design rail geometry the remainder of the track could be extracted too, which would then be used to apply a rail fitting procedure.
- iii. Based on the design rail model, an automatic filtering technique could also be applied to remove the head of the rail recorded by TLS, which shows inaccuracies and affects the rail fitting process due to the interaction between the laser and the shiny surface
- iv. Whilst applying the plane fitting technique to the web, automatic detection and removal of artefacts could be applied using the known levels of an “optimum” fit as well as plotting the residuals in a histogram.

A comparison between the track parameters extracted from the continuous prism monitoring and the TLS survey was carried out over an area of track required to be monitored by a contractor over the duration of this study. Out of the four TLS epochs it was established that prism based data was only available for one of these epochs. This was due to poor planning of the lines of sight of the total station available to the reference prisms during the construction work taking place within the vicinity of the track. This not only shows poor network design and contingency planning from the monitoring contractor, but also highlights the lack of prism monitoring data over this period against a Network Rail requirement. The poor reliability of the prism monitoring data limited the comparison results of the TLS extraction method in this

study. It did, however, provide an archive of scanned track data that could be used for monitoring, where there was a lack of prism monitoring data.

Chapter 6 described a method of implementing a TLS survey on a deforming set of brick arches. Prior laboratory tests concluded that plane fitting was limiting the precision of the detection of deformation to around 2mm. However, comparing surface meshes between epochs allowed sub-millimetre levels of accuracy and precision to be achieved as well as reducing the level of noise in the data. Global registration between the TLS epochs was restricted due to the lack of a stable reference network outside the zone of influence for this site. This is a significant issue for industry practice for surveying and monitoring long and narrow structures such as arches and tunnels. This restriction led to calculating relative movements between TLS epochs, expressed on a site grid, to be measured with an average uncertainty of 7mm based on the ICP registration. Despite this uncertainty, the TLS study resulted in validation of the relative movement detected by the prism-based monitoring through the extraction of 2D arch profiles in CAD, as well as 3D deformation displacement maps between the TLS epochs to the millimetre level. This provided engineers with a better visual understanding of the deformation of the brick arches where a full 3D data set provided more “complete” information about the surface changes, particularly regarding the springing points and crown of the arches, compared to the discrete set of points provided by the prism-based monitoring. The process of comparing these different engineering surveying methods for monitoring the arches is published in the journal of *Applied Geomatics, Volume 7, Issue 2, 2015*.

The method of using the as-built TLS scan of the arches as the baseline epoch in Chapter 6 highlighted the value of having an archive of data that can be reassessed later if needed, particularly where unexpected movement occurs. For example if the type of movement in the arches changed, e.g. the engineers suspected some level of twist as well as settlement, variations in the TLS scan could be investigated. Therefore having a plethora of epoch measurements of the surface would allow a better understanding of the trend of the movement. In theory, prism monitoring allows this through continuous monitoring which would result in discrete measurements to a prism 24 hours a day, 7 days a week. However in this study TLS and CRP surveys were carried out at discrete and irregular intervals. This could be resolved by combining discrete and continuous surface measurement techniques to allow

“redundant” archive data at different intervals. One possibility of obtaining discrete points and continuous surface information simultaneously could include using the recently introduced combined scanning total station. Further work would require investigation of the capability and robustness of TLS, CRP and hybrid instrumentation (e.g. Leica MS50) as a method of continuous monitoring.

7.2 Further work

The majority of further work from this thesis concerns with transitioning the ideas and experimental outcomes from the thesis into industry. However there are key pieces of academic work which are also needed to understand some of the fundamental limitations of point based surface based measurements more comprehensively. These stem from biases in the instrument data and limitations in point cloud registration tools using vendor software:

1. Tests from measuring the track surface with TLS through plane fitting in the laboratory and applying rail fitting in Chapter 5 showed the presence of a systematic bias when plotting the residuals. A similar finding of a systematic bias with the same model of laser scanner was found by Al-Manasir and Lichti (2015). Therefore further work would be required to test measurements to a broader range of surfaces typical in a railway monitoring environment to understand the presence of this error in this system as well as any other TLS systems. For example measuring surfaces such as steel, concrete as well as rusty surfaces would allow a “library” of optical properties for these surfaces to be produced. This would allow a prediction of the performance of optical non-contact techniques when measuring to these surfaces, improving the design/simulation process for applying TLS. Understanding of the BRDF (bi-directional reflectance distribution function) of a surface and its influence on non-contact optical performance would be a key issue for further work.
2. Point cloud registration using vendor software was a limiting factor when carrying out the site tests in this study. The registration tools provided by vendors are very much a “black box” where the output of quality measures of the process is very limited, e.g. Leica Cyclone reports an RMS of the registration. Even with a very accurate total station survey to co-ordinate target positions in Chapter 5, the best registration RMS using the Cyclone was 1mm. The residuals of this registration are not provided in this or similar vendor

packages. For this thesis point cloud registration affects the quality of the rail fitting procedure as well as the uncertainty of applying inter-epoch registration in the arches. If the residuals of the registration were provided, similarly to the track artefact removal process through plane fitting, the areas where large residuals (e.g. due to noise) are present could be eliminated in order to optimise the quality of the registration to a sub-millimetre level. A registration process that provides residuals of the registration could be developed using the Point Cloud Library, for example, which allows a more “open access” approach to the quality measures to gain a better understanding of the point cloud.

3. Along with a bespoke registration tool, better point cloud understanding would aid with comparing each TLS epoch of the arches that was presented in Chapter 6. In this case the unstable areas were manually omitted from the inter-epoch registration when analysing deformation. Further work on global and local congruency testing from the least squares fitting outputs, described in Chapter 3, and could be applied to a point cloud where points perceived as unstable are automatically removed before inter-epoch registration is applied.

Having dealt with academic refinements based on the physics and data processing of the technology, the remainder of the suggested further work is exclusively related to the rail industry situation:

4. Based on the interviews carried out on key figures in the monitoring industry (Chapter 2) further work is required on understanding the engineer’s requirements from monitoring data. It is often the case that geotechnical engineers determine accuracy of the monitoring system based on the instrument’s capabilities and often default onto prism based methods as it is well-known. However by fully understanding the information that is essential to them: the patterns they are looking for, whether this information is required in 1, 2 or 3D, as well as the accuracy that they require could then be used to determine collaboratively between the engineer, surveyor and monitoring specialist what instrumentation is suitable for that specific site. This type of information could then be used to build up a portfolio of the movement detection requirements and recommendations of the instrumentation, leading to a best practice guide.
5. Access to Network Rail sites to carry out site testing was the largest barrier to this study. The lab work was able to provide an indication of the performance

of the instrumentation when measuring to a network of points and surfaces typical to a railway environment. However the laboratory cannot replicate the large scale test measurements required in reality. In general there are strict regulations with respect to site access and safety which affects the logistics of designing tests. Therefore a dedicated test site that is free from these restrictions would allow testing the capability of current monitoring technology. Instrumentation testing could allow inter-comparison between different systems, for example discrete and continuous point measurements. It would also allow a place for different contractors to test their instrumentation before and during their implementation for monitoring. The next stage of this study would be to test the capability and robustness of TLS and CRP for carrying out continuous monitoring of structures such as track and tunnels, i.e. 24/7 monitoring, which current prism based monitoring allows. The tests would need to consider the method of remotely communicating the surface information, processes required for analysing the point clouds, handling the large data volumes and reporting this information to the engineer/stakeholder within a timely manner to establish if it was fit for purpose. The test site would provide a realistic environment to allow all of these to be investigated. Ultimately this test site could be a competency test against emerging monitoring technology.

6. Further testing on different types of track (i.e. different design models) would allow the rail fitting method to be adopted to different rail types in the UK. The test site described above would allow testing of the typical conditions present with respect to track visibility, e.g. on sections of track where a TLS system cannot be mounted on an adjacent platform, which could be used to compare track parameters achievable at different quality levels between static TLS, kinematic TLS e.g. through trolley-based systems, as well as a train inspection car and the potential of continuous monitoring of localised areas of track using a scanning total station, e.g. Leica MS50. This would provide a best practice for determining track parameters depending on the type of track and its surrounding environment.
7. A full cost benefit analysis of the newer technologies for monitoring, such as TLS and CRP, compared to the traditional prism based methods needs to be carried out and the project lifetime costs of the instrumentation must be

addressed. For example, the thesis has shown TLS can achieve similar levels of accuracy compared to prism based monitoring when measuring surfaces of a structure or object. By removing the need for targets using these technologies, the huge cost and safety implications associated with installing and maintaining prisms can be removed. On the other hand the current cost of TLS instrumentation is higher than a total station and the number of instruments required may not be the same.

It is also important to include other factors which affect the cost benefit of monitoring. For example, during the study the issue of a false alarm (i.e. prism deliberately moved during maintenance) almost caused the stopping of the Eastbound Jubilee Line services. If stopped, the costs for partial line closure were estimated at £3million. Movement impacts on some structures can also have huge consequential costs. At London Bridge Station a movement which caused one London Underground escalator to go out of service. If movement caused the stopping of two escalators the entire station would be closed at rush hour and the penalty cost would be £½million per day. The fine for closing a station would cost £20K/minute.

Therefore the following provides an example of factors that should be considered for a cost benefit analysis:

An example of cost benefit factors to be considered
Frequency of observations
Time taken to complete measurement
Interference with observation line of sight
Interference with sensors or targets (e.g. external disturbance)
Coverage of observations (e.g. discrete or surface)
Detectability of false readings
Impact of sensor relocation (due to construction works)
Safety of observations (e.g. staff safety for manual observations)
Maintainability of sensor/target during monitoring (e.g. cleaning, instrument checks)
Data processing costs
Data processing time
Power supply costs
Communications supply costs
Flexibility in back up or replacement of sensor / target
Speed of re-setting system from fault
Flexibility to go from manual to automatic mode without losing baseline measurement
Impact of failure to detect movement (e.g. non-compliance of system, requiring to stop works)

References and bibliography

- Abbas, M. A., L. C. Luh, H. Setan, Z. Majid, A. K. Chong, A. Aspuri, K. M. Idris and M. F. M. Ariff (2014) Terrestrial Laser Scanners Pre-Processing: Registration and Georeferencing. *Jurnal Teknologi* 71(4).
- Abellan, A., M. Jaboyedoff, T. Oppikofer and J. M. Vilaplana (2009) Detection of millimetric deformation using a terrestrial laser scanner: experiment and application to a rockfall event. *Natural Hazards and Earth System Sciences* 9(2): 365-372.
- Abellan, A., J. M. Vilaplana, J. Calvet, D. Garcia-Selles and E. Asensio (2011) Rockfall monitoring by Terrestrial Laser Scanning - case study of the basaltic rock face at Castellfollit de la Roca (Catalonia, Spain). *Natural Hazards and Earth System Sciences* 11(3): 829-841.
- Alba, M., L. Barazzetti, A. Giussani, F. Roncoroni and M. Scaioni (2010) Development and Testing of a Method for Tunnel Monitoring Via Vision Metrology. *Proceedings of the ISPRS Commission V Mid-Term Symposium Close Range Image Measurement Techniques* 38(5): 17-22.
- Alba, M., L. Fregonese, F. Prandi, M. Scaioni and P. Valgoi (2006) Structural monitoring of a large dam by terrestrial laser scanning. *International Archives of Photogrammetry, Remote Sensing and Spatial Information Sciences*, 36(5):6.
- Alba, M. and M. Scaioni (2010) Automatic detection of changes and deformation in rock faces by terrestrial laser scanning. *Proceedings of the ISPRS Commission V Mid-Term Symposium 'Close Range Image Measurement Techniques* Vol. 1501:11-16.
- Allan, A. L. (2007) Principles of geospatial surveying, *Whittles Publishing*.
- Al-Manasir, K. and D. Lichti (2015) Self-calibration of a Leica HDS7000. *FIG Working Week 2015 Proceedings: From the Wisdom of the Ages to the Challenges of the Modern World*, Sofia, Bulgaria.
- Amberg Technologies (2015) Amberg Clearance GRP 5000. *Amberg Technologies*, Switzerland: <http://www.ambergtechnologies.ch/en/products/rail-surveying/grp-system-fx/grp-5000/> (URL last accessed February 2016)
- Arastounia, M. (2012) Automatic classification of LiDAR point clouds in a railway environment. MSc Dissertation, University of Twente.
- Awwad, T. M., Q. Zhu, Z. Q. Du and Y. T. Zhang (2010) An Improved Segmentation Approach for Planar Surfaces from Unstructured 3D Point Clouds. *Photogrammetric Record* 25(129): 5-23.
- Baarda, W. (1968) A testing procedure for use in geodetic networks. Delft, *Kanaalweg 4, Rijkscommissie voor Geodesie*, 1968. 1.
- Baltsavias, E. P. (1991). Multiphoto geometrically constrained matching. PhD Thesis, ETH Zurich, Switzerland.

- Barbarella, M., M. Fiani and A. Lugli (2015) Multi-temporal Terrestrial Laser Scanning Survey of a Landslide. *Modern Technologies for Landslide Monitoring and Prediction*. Springer Berlin Heidelberg: 89-121.
- Becerik-Gerber, B., F. Jazizadeh, G. Kavulya and G. Calis (2011) Assessment of target types and layouts in 3D laser scanning for registration accuracy. *Automation in Construction* 20(5): 649-658.
- Berberan, A., M. Machado and S. Batista (2007) Automatic multi total station monitoring of a tunnel. *Survey Review* 39(305): 203-211.
- Besl, P. J. and N. D. McKay (1992) A method for registration of 3-D shapes. *IEEE Transactions on pattern analysis and machine intelligence*, 14(2): 239-256.
- Binder, N. (2014) Moving London safely forward. *Leica Reporter* Heerbrugg, Switzerland 71: 18-21.
- Bird, B. (2009) Analysis of Survey Point Displacements Using Total Station Measurements, MSc Dissertation, British Columbia Institute of Technology.
- Boehm, J., S. Julier, K. Liu, Z. Jiang, M. Spagnuolo, S. Biasotti, A. Cerri, S. Pittaluga and E. Quak (2013). Iqmulus Project: Feature Extraction and Classification Toolkit (Month 12), *IQmulus Consortium*.
- Bowness, D., A. C. Lock, D. J. Richards and W. Powrie (2005) Innovative remote video monitoring of railway track displacements. *Advances in Experimental Mechanics IV* 3-4: 417-422.
- BTS (British Tunnelling Society) (2011). Monitoring Underground Construction: A best guide practice, 1st Edition, *ICE Publishing*.
- Brownjohn, J. M. W. (2007) Structural health monitoring of civil infrastructure. *Philosophical Transactions of the Royal Society of London A: Mathematical, Physical and Engineering Sciences* 365(1851): 589-622.
- Buenfield, N. R., Davies, R.D., Karimi, A., Gilberston, A. L. (2008) Intelligent monitoring of concrete structures (C661), *CIRIA*.
- Burnside, C. D. (1979) Mapping from aerial photographs, *Crosby Lockwood Staples*.
- Capra, A., E. Bertacchini, C. Castagnetti, R. Rivola and M. Dubbini (2015) Recent approaches in geodesy and geomatics for structures monitoring. *Rendiconti Lincei-Scienze Fisiche E Naturali* 26: S53-S61.
- Caspary, W. and J. M. Rüeger (2000). Concepts of network and deformation analysis, Monograph, 3rd Edition, Vol. 11, University of New South Wales.
- Caspary, W. F., W. Haen and H. Borutta (1990) Deformation Analysis by Statistical-Methods. *Technometrics* 32(1): 49-57.
- CEN (2008). Railway applications: Track. Track geometry quality - Part 1: Characterisation of track geometry, CEN. EN 13848-1:2003 +A1, *European Committee for Standardisation*, Brussels.

Chan, T. O., D. D. Lichti and D. Belton (2015) A rigorous cylinder-based self-calibration approach for terrestrial laser scanners. *ISPRS Journal of Photogrammetry and Remote Sensing* 99: 84-99.

Choudhury, M., C. Rizos and B. Harvey (2009) A survey of techniques and algorithms in deformation monitoring applications and the use of the Locata technology for such applications. *22nd International Technology Meeting of the satellite division of the US institute of navigation*. Savannah, Georgia.

Chow, J., D. Lichti and W. Teskey (2012) Accuracy assessment of the faro focus3D and Leica HDS6100 panoramic type terrestrial laser scanner through point-based and plane-based user self-calibration. In *Proceedings of the FIG Working Week: Knowing to Manage the Territory, Protect the Environment, Evaluate the Cultural Heritage*. Rome, Italy: 6-10.

Chow, J. C., A. Ebeling and W. F. Teskey (2012) Point-based and plane-based deformation monitoring of indoor environments using terrestrial laser scanners. *Journal of Applied Geodesy* 6(3-4): 193-202.

Chow, J. C. K., A. Ebeling and B. Teskey (2010) Low Cost Artificial Planar Target Measurement Techniques for Terrestrial Laser Scanning. *FIG Congress 2010, Facing the Challenges - Building the Capacity*. Sydney, Australia.

Chow, J. C. K., W. F. Teskey and J. W. Lovse (2011) In-situ Self-calibration of Terrestrial Laser Scanners and Deformation Analysis Using Both Signalized Targets and Intersection of Planes for Indoor Applications. *Joint International Symposium on Deformation Monitoring*. Hong Kong.

Clark, J. and S. Robson (2004) Accuracy of measurements made with a Cyrax 2500 laser scanner against surfaces of known colour. *Survey Review* 37(294): 626-638.

Cooper, M. A. R. (1987). Control surveys in civil engineering, *Nichols Publishing Company*. London.

Cosser, E., G. W. Roberts, X. Meng and A. H. Dodson (2003) Measuring the dynamic deformation of bridges using a total station. *Proceedings, 11th FIG Symposium on Deformation Measurements*. Santorini, Greece.

Dumalski, A. and K. Hejbudzka (2010) An Attempt at Using a Terrestrial Laser Scanner for Detecting Minimal Displacement and Objects' Deformation. *FIG Congress 2010 - Facing the Challenges - Building the Capacity*. Sydney, Australia.

Dunnicliff, J. (1993). Geotechnical instrumentation for monitoring field performance, *John Wiley & Sons*.

Ehrhart, M. and W. Lienhart (2015). Image-based dynamic deformation monitoring of civil engineering structures from long ranges. In *IS&T/SPIE Electronic Imaging* (pp. 94050J-94050J). International Society for Optics and Photonics.

Erdélyi, J., Kopáček, A., Ilkovičová, Ľ, Lipták, I. and Kajánek, P (2014). Deformation Monitoring of a Parabolic Roof Structure using TLS. *INGEO 2014 - 6th International Conference on Engineering Surveying*. Prague, Czech Republic.

- Erol, S., B. Erol and T. Ayan (2004). A general review of the deformation monitoring techniques and a case study: Analysing deformations using GPS/levelling. *In XXth ISPRS Congress* (pp12-23).
- FARO (2013). FARO Focus3D: Features, Benefits & Technical Specifications. Retrieved 13 January 2014, <http://www.faro.com/products/3d-surveying/laserscanner-faro-focus-3d/overview>
- Fonstad, M. A., J. T. Dietrich, B. C. Courville, J. L. Jensen and P. E. Carbonneau (2013) Topographic structure from motion: a new development in photogrammetric measurement. *Earth Surface Processes and Landforms* 38(4): 421-430.
- Fraser, C. S. and B. Riedel (2000) Monitoring the thermal deformation of steel beams via vision metrology. *ISPRS Journal of Photogrammetry and Remote Sensing* 55(4): 268-276.
- Fryer, J., R. Parberry and S. Robson (1992) Analysis of as-built cylindrical shapes. *Australian Journal of Geodesy, Photogrammetry and Surveying* 56: 91-109.
- Garrido-Villen, N., A. Anton-Merino, J. L. B. Valero, R. Mata and D. Raboso (2015) Atmospheric Attenuation and Scintillation Effects on the Range of EDM Instruments. *Journal of Surveying Engineering* 141(3): 05015001.
- Gassner, G. and R. Ruland (2011) Instrument tests with the new Leica AT401, (No. SLAC-PUB-14300). *SLAC National Accelerator Laboratory (SLAC)*.
- Gleeson, B. (2011) Laser Scanning on Network Rail's Thameslink Project. *Geomatic World, PV Publications*. 19: 18-23.
- Golparvar-Fard, M., J. Bohn, J. Teizer, S. Savarese and F. Pena-Mora (2011) Evaluation of image-based modeling and laser scanning accuracy for emerging automated performance monitoring techniques. *Automation in Construction* 20(8): 1143-1155.
- Gordon, S., D. Lichti, J. Franke and M. Stewart (2004) Measurement of structural deformation using terrestrial laser scanners. *1st FIG International Symposium on Engineering Surveys for Construction Works and Structural Engineering*, Nottingham, United Kingdom.
- Gordon, S., D. Lichti and M. Stewart (2001) Application of a high-resolution, ground-based laser scanner for deformation measurements. *Proceedings of 10th International FIG Symposium on Deformation Measurements*, Orange, California, USA.
- Gordon, S. J., D. Lichti, M. Stewart and J. Franke (2005) Structural deformation measurement using terrestrial laser scanners. *In Proceedings of 11th International FIG Symposium on Deformation Measurements* (p. 8).
- Gordon, S. J. and D. D. Lichti (2007) Modeling terrestrial laser scanner data for precise structural deformation measurement. *Journal of Surveying Engineering* 133(2): 72-80.
- Grafarend, E. W., F. Sanso and B. Benciolini (1985) Optimization and design of geodetic networks. *Berlin; New York: Springer-Verlag*, c1985. 1.

- Granshaw, S. (1980) Bundle adjustment methods in engineering photogrammetry. *The Photogrammetric Record* 10(56): 181-207.
- Groom, R. (2009). GEO-9 Conference Report: Busy event hosts global launch of major products and services. *Geomatics World, PV Publications* 17 (4): 18-21.
- Gruen, A. and D. Akca (2005). Least squares 3D surface and curve matching. *ISPRS Journal of Photogrammetry and Remote Sensing* 59(3): 151-174.
- Habib, A. F., D. D. Lichti, M. M. El-Badry and I. D. Datchev (2014) Optical Remote Sensing Systems for Structural Deflection Measurement and Crack Characterization. In *9th International Conference on Short and Medium Span Bridges*, Calgary, Alberta, Canada.
- Henke, K., R. Pawlowski, P. Schregle and S. Winter (2014) Use of digital image processing in the monitoring of deformations in building structures. *Journal of Civil Structural Health Monitoring* 5(2): 141-152.
- Hess, M. (2015). A metric test object informed by user requirements for better 3D recording of cultural heritage artefacts, PhD thesis, University College London.
- Hill, C. D. and K. Sippel (2002). "Modern deformation monitoring: A multi sensor approach."
- James, M. R. and S. Robson (2012) Straightforward reconstruction of 3D surfaces and topography with a camera: Accuracy and geoscience application. *Journal of Geophysical Research:Earth Surface* 117(F3).
- Jiang, R. N., D. V. Jauregui and K. R. White (2008) Close-range photogrammetry applications in bridge measurement: Literature review. *Measurement* 41(8): 823-834.
- Kahlmann, T., F. Remondino and H. Ingensand (2006) Calibration for increased accuracy of the range imaging camera swissrangertm. *Image Engineering and Vision Metrology (IEVM)* 36(3): 136-141.
- Kang, Z. Z., L. Tuo and S. Zlatanova (2012) Continuously Deformation Monitoring of Subway Tunnel Based on Terrestrial Point Clouds. *XXII ISPRS Congress, Technical Commission V* 39-B5: 199-203; *IAPRS XXXIX-B5*.
- Kersten, T., K. Mechelke, M. Lindstaedt and H. Sternberg (2008) Geometric accuracy investigations of the latest terrestrial laser scanning systems. In *Proc. Integrating Generations FIG Working Week* (pp14-19)
- Kopáčík, A., J. Erdélyi, I. Lipták, and P. Kyrinovič, (2013) Deformation of Bridge Structures using TLS. *2nd Joint International Symposium in Deformation Monitoring*, University of Nottingham, UK.
- Kuang, S. (1996) Geodetic network analysis and optimal design: concepts and applications, *Ann Arbor Press Inc*.
- Kuhlmann, H. and A. Glaser (2002) Investigation of new measurement techniques for bridge monitoring. *2nd Symposium on Geodesy for Geotechnical and Structural Engineering*, Berlin, Germany.

- Kutterer, H. and C. Hesse (2007) High Speed Laser Scanning for Near Real-Time Monitoring of Structural Deformations. In *Dynamic Planet* 130: 776-781. Springer Berlin Heidelberg.
- Kyle, S., S. Robson, D. Chapman, P. Cross, J. Iliffe and S. Oldfield (2001) Understanding Large Scale Metrology. Proceedings in *National Measurement Conference (NMC)*, Harrogate, UK.
- Laefer, D. F., L. Truong-Hong, H. Carr and M. Singh (2014) Crack detection limits in unit based masonry with terrestrial laser scanning. *NDT & E International* 62: 66-76.
- Lari, Z. and A. Habib (2014) An adaptive approach for the segmentation and extraction of planar and linear/cylindrical features from laser scanning data. *ISPRS Journal of Photogrammetry and Remote Sensing* 93: 192-212.
- Lee, Y. J. and R. H. Bassett (2006) Application of a photogrammetric technique to a model tunnel. *Tunnelling and Underground Space Technology* 21(1): 79-95.
- Leica Geosystems (2010) Leica Viva TS15 Datasheet: http://w3.leica-geosystems.com/downloads123/zz/tps/Viva%20TS15/brochures-datasheet/Leica%20Viva%20TS15%20Datasheet_en.pdf (URL accessed February 2016)
- Leica Geosystems (2012) Leica ScanStation C10. Product Specifications: http://hds.leica-geosystems.com/downloads123/hds/hds/ScanStation%20C10/brochures-datasheet/Leica_ScanStation_C10_DS_en.pdf (URL accessed February 2016)
- Leica Geosystems, (2013) Leica ScanStation P20: Product Specifications: http://w3.leica-geosystems.com/downloads123/hds/hds/ScanStation_P20/brochures-datasheet/Leica_ScanStation_P20_DAT_en.pdf (URL accessed February 2016)
- Lemy, F., S. Yong and T. Schulz (2006) A case study of monitoring tunnel wall displacement using laser scanning technology. In *Proceedings of IAEG 2006*.
- Lerma García, J. L., B. Van Genechten and M. Santana Quintero (2008) 3D Risk Mapping. Theory and Practice on Terrestrial Laser Scanning. *Training Material Based on Practical Applications, Universidad Politécnica de Valencia, Valencia*.
- Lichti, D., M. Stewart, M. Tsakiri and A. Snow (2000) Calibration and testing of a terrestrial laser scanner. *International Archives of Photogrammetry and Remote Sensing* 33(B5/2; PART 5): 485-492.
- Lichti, D. D. (2007) Error modelling, calibration and analysis of an AM-CW terrestrial laser scanner system. *ISPRS Journal of Photogrammetry and Remote Sensing* 61(5): 307-324.
- Lichti, D. D. (2010) A Review of Geometric Models and Self-Calibration Methods for Terrestrial Laser Scanners. *Boletim De Ciencias Geodesicas* 16(1): 3-19.
- Lichti, D. D., S. J. Gordon, M. P. Stewart, J. Franke and M. Tsakiri (2002) Comparison of Digital Photogrammetry and Laser Scanning. *Proceedings CIPA WG 6 International Workshop on Scanning Cultural Heritage Recording, Corfu, Greece*.

- Lindenbergh, R. and N. Pfeifer (2005) A statistical deformation analysis of two epochs of terrestrial laser data of a lock. *Proc. of Optical 3D Measurement Techniques* 2: 61-70.
- Lindenbergh, R. and P. Pietrzyk (2015) Change detection and deformation analysis using static and mobile laser scanning. *Applied Geomatics* 7(2): 65-74.
- Lindenbergh, R., L. Uchanski, A. Bucksch and R. Van Gosliga (2009) Structural monitoring of tunnels using terrestrial laser scanning. *Reports of Geodesy* 2(87): 231-239.
- Liu, C., N. Li, H. Wu and X. Meng (2013) Detection of High-Speed Railway Subsidence and Geometry Irregularity Using Terrestrial Laser Scanning. *Journal of Surveying Engineering* 140(3): 04014009.
- Luhmann, T., S. Robson, S. Kyle and J. Boehm (2014) Close-range Photogrammetry and 3D Imaging, 2nd Edition, *De Gruyter, Berlin/Boston*.
- Maas, H. G. and U. Hampel (2006) Photogrammetric techniques in civil engineering material testing and structure monitoring. *Photogrammetric Engineering and Remote Sensing* 72(1): 39-45.
- Martin, D. and G. Gatta (2006) Calibration of total stations instruments at the ESRF. In *Shaping the Change, XXIII FIG International Congress* (Vol. 39).
- McKibbins, L., Melbourne, C., Sawar, N. and C. Sicilia Gaillard, (2006). Masonry arch bridges: condition appraisal and remedial treatment (C656), *CIRIA*.
- Meng, X., C. Liu, N. Li and J. Ryding (2014) Precise determination of mini railway track with ground based laser scanning. *Survey Review* 46(336): 213-218.
- Merkle, W. J. and J. Myers (2006) Load testing and load distribution response of Missouri bridges retrofitted with various frp systems using a non-contact optical measurement system. In *Transportation Research Board 85th Annual Meeting*, Washington D.C., USA
- MicroSurvey (2014). STAR*NET software documentation. *MicroSurvey Software Inc.*
- Mikhail, E. M. and F. E. Ackermann (1976) Observations and least squares. *Dun-Donnelley*, New York.
- Monserrat, O. and M. Crosetto (2008) Deformation measurement using terrestrial laser scanning data and least squares 3D surface matching. *ISPRS Journal of Photogrammetry and Remote Sensing* 63(1): 142-154.
- Moss, J. L., W. J. McGuire and D. Page (1999) Ground deformation monitoring of a potential landslide at La Palma, Canary Islands. *Journal of Volcanology and Geothermal Research* 94(1-4): 251-265.
- Network Rail (2010) Governance for Railway Investment Projects (GRIP) - Policy Manual. NR/L1/INI/PM/GRIP/100. London, Network Rail.

- Network Rail Thameslink (2010) Inner Area Tour Presentation (provided during site induction).
- Network Rail Thameslink (2013) London Bridge Station Redevelopment Monitoring Specification - NR assets monitoring requirements. N420 COT ESP CS 000009 version 1.0.
- Nurunnabi, A., D. Belton and G. West (2012) Diagnostic-robust statistical analysis for local surface fitting in 3d point cloud data. *ISPRS Annals of the Photogrammetry, Remote Sensing and Spatial Information Sciences* 1 (2012): 3.
- Nuttens, T., A. De Wulf, L. Bral, B. De Wit, L. Carlier, M. De Ryck, C. Stal, D. Constales and H. De Backer (2010). High Resolution Terrestrial Laser Scanning for Tunnel Deformation Measurements. In *Proceedings of FIG Congress 2010: Facing the Challenges - Building the Capacity*, Sydney, Australia.
- Nuttens, T., A. De Wulf, G. DERUYTER, C. Stal, H. De Backer and K. Schotte (2012). Application of laser scanning for deformation measurements: a comparison between different types of scanning instruments. In *Proceedings of FIG Working Week 2012*.
- Nuttens, T., C. Stal, H. De Backer, K. Schotte, P. Van Bogaert and A. De Wulf (2014) Methodology for the ovalization monitoring of newly built circular train tunnels based on laser scanning: Liefkenshoek Rail Link (Belgium). *Automation in Construction* 43: 1-9.
- Olsen, M. J., F. Kuester, B. J. Chang and T. C. Hutchinson (2009) Terrestrial laser scanning-based structural damage assessment. *Journal of Computing in Civil Engineering* 24(3): 264-272.
- Oude Elberink, S., K. Khoshelham, M. Arastounia and D. Díaz Benito (2013) Rail track detection and modelling in mobile laser scanner data. *ISPRS Annals of Photogrammetry, Remote Sensing and Spatial Information Sciences* 1(2): 223-228.
- Park, H. S., H. M. Lee, H. Adeli and I. Lee (2007) A new approach for health monitoring of structures: terrestrial laser scanning. *Computer-Aided Civil and Infrastructure Engineering* 22(1): 19-30.
- Psimoulis, P. A. and S. C. Stiros (2007) Measurement of deflections and of oscillation frequencies of engineering structures using Robotic Theodolites (RTS). *Engineering Structures* 29(12): 3312-3324.
- Puente, I., H. Gonzalez-Jorge, B. Riveiro and P. Arias (2012) Deformation Monitoring of Motorway Underpasses Using Laser Scanning Data. *XXII ISPRS Congress, Technical Commission V* 39-B5: 235-238.
- Railway Group Standard, (1998). Track Standards Manual - Section 8: Track Geometry. GC/RT5017. UK, Railtrack PLC.
- Reshetyuk, Y. (2006) Calibration of terrestrial laser scanners for the purposes of geodetic engineering. In *3rd IAG Symposium on Geodesy for Geotechnical and Structural Engineering and 12th FIG Symposium on Deformation Measurements*, Baden, Austria.

- Reshetyuk, Y. (2010) Direct georeferencing with GPS in terrestrial laser scanning. *Zf V-Zeitschrift für Geodäsie, Geoinformation und Landmanagement* 135(3): 151-159.
- Reshetyuk, Y. (2010) A unified approach to self-calibration of terrestrial laser scanners. *ISPRS Journal of Photogrammetry and Remote Sensing* 65(5): 445-456.
- Richardus, P. (1977) Project surveying: general adjustment and optimization techniques with applications to engineering surveying, *Noord-Hollandse Uitgeversmaatschappij*, Amsterdam
- Rietdorf, A., F. Gielsdorf and L. Gruendig (2004) A concept for the calibration of terrestrial laser scanners. In *Proceedings FIG Working Week 2004*, pp.22-27.
- Riveiro, B., H. Gonzalez-Jorge, M. Varela and D. V. Jauregui (2013) Validation of terrestrial laser scanning and photogrammetry techniques for the measurement of vertical underclearance and beam geometry in structural inspection of bridges. *Measurement* 46(1): 784-794.
- Riveiro, B., P. Morer, P. Arias and I. de Arteaga (2011) Terrestrial laser scanning and limit analysis of masonry arch bridges. *Construction and Building Materials* 25(4): 1726-1735.
- Rusu, R. B. and S. Cousins (2011) 3D is here: Point Cloud Library (PCL). *IEEE 2001 International Conference on Robotics and Automation (ICRA)*.
- Scherer, M. and J. L. Lerma (2009) From the Conventional Total Station to the Prospective Image Assisted Photogrammetric Scanning Total Station: Comprehensive Review. *Journal of Surveying Engineering* 135(4): 173-178.
- Schnabel, R., R. Wahl and R. Klein (2007) Efficient RANSAC for Point-Cloud Shape Detection. In *Computer graphics forum*, 26 (2): 214-226, Blackwell Publishing Ltd.
- Schneider, D. (2006). Terrestrial laser scanning for area based deformation analysis of towers and water dams. In *Proceedings of 3rd IAG/12th FIG Symposium*, Baden, Austria, May.
- Schuhmacher, S. and J. Böhm (2005). Georeferencing of terrestrial laserscanner data for applications in architectural modeling. In *Proceedings of 3D-ARCH 2005: "Virtual Reconstruction and Visualization of Complex Architectures*, Venice, Italy
- Setan, H. (1997) A Flexible Analysis Procedure for Geometrical Detection of Spatial Deformation. *The Photogrammetric Record* 15(90): 841-861.
- Setan, H. and M. S. Ibrahim (2003) Procedure for deformation detection using STARNET. In *Proceedings of 11th International Symposium on Deformation Measurement*.
- Setan, H. and R. Singh (2001). Deformation analysis of a geodetic monitoring network. *Geomatica-Ottawa* 55(3): 333-346.
- Setan, H. B. (1995) Functional and stochastic models for geometrical detection of spatial deformation in engineering: a practical approach, PhD thesis, City University.

- Shafiullah, G. M., A. Gyasi-Agyei and P. Wolfs (2007) Survey of Wireless Communications Applications in the Railway Industry. In *The 2nd International Conference on Wireless Broadband and Ultra Wideband Communications, 2007. (AusWireless 2007)* pp.65-70
- Soni, A. (2011) MRes Report: The feasibility of terrestrial laser scanning for structural monitoring along the Thameslink Programme, Masters dissertation, University College London.
- Soni, A., S. Robson and B. Gleeson (2014) Extracting Rail Track Geometry from Static Terrestrial Laser Scans for Monitoring Purposes. *ISPRS International Archives of the Photogrammetry, Remote Sensing and Spatial Information Sciences*, Volume XL-5, 2014: 553-557.
- Soni, A., S. Robson and B. Gleeson (2015) Optical non-contact railway track measurement with static terrestrial laser scanning to better than 1.5mm RMS. In *FIG Working Week 2015: From Wisdom of the Ages to the Challenges of the Modern World*, Sofia, Bulgaria.
- Soni, A., S. Robson and B. Gleeson (2015) Structural monitoring for the rail industry using conventional survey, laser scanning and photogrammetry. *Applied Geomatics* 7(2): 123-138.
- Teskey, B. and B. Paul (2005) New Instrumentation and Methodology for Deformation Monitoring. *Optical 3-D Measurement Techniques VII*, Vienna 2005.
- Tsakiri, M., D. D. Lichti and N. Pfeifer (2006) Terrestrial Laser Scanning for Deformation Monitoring. *3rd AIG/12th FIG Symposium*. Baden, Germany.
- Tse, J. and J. Luk (2011) Design and Implementation of Automatic Deformation Monitoring System for the Construction of Railway Tunnel: A Case Study in West Island Line. *14th FIG Symposium on Deformation Measurement and Analysis*, Hong Kong.
- Uren, J. and W. F. Price (2010) Surveying for engineers, *5th Edition*, Palgrave Macmillan.
- Valanis, A. and M. Tsakiri (2004). Automatic Target Identification for Laser Scanners. Proceedings XX ISPRS Congress, Turkey.
- Van Gosliga, R., R. Lindenbergh and N. Pfeifer (2006). "Deformation analysis of a bored tunnel by means of terrestrial laser scanning." *Image Engineering and Vision Metrology*. ISPRS Commission 36: 167-172.
- VDE (2002). VDI 2634-1 (Association of German Engineers): Optical 3D measuring systems – Imaging systems with point-by-point probing. Practical acceptance and reverification methods for the evaluation of the accuracy of optical measuring systems. *VDI/VDE-Handbuch Messtechnik II*.
- Vezocnik, R., T. Ambrozic, O. Sterle, G. Bilban, N. Pfeifer and B. Stopar (2009) Use of Terrestrial Laser Scanning Technology for Long Term High Precision Deformation Monitoring. *Sensors* 9(12): 9873-9895.

- Vosselman, G., B. G. Gorte, G. Sithole and T. Rabbani (2004) Recognising structure in laser scanner point clouds. *International Archives of Photogrammetry, Remote Sensing and Spatial Information Sciences* 46(8): 33-38.
- Vosselman, G. V. and H.-G. Maas (2010). Airborne and Terrestrial Laser Scanning, *Whittles Publishing*.
- Wang, W., W. Zhao, L. Huang, V. Vimarlund and Z. Wang (2014) Applications of terrestrial laser scanning for tunnels: a review. *Journal of Traffic and Transportation Engineering* (English Edition) 1(5): 325-337.
- Werner, T. and D. Morris (2010) 3D Laser Scanning for Masonry Arch Bridges. In *FIG Congress 2010: Facing the Challenges - Building the Capacity*, Sydney, Australia.
- Westoby, M. J., J. Brasington, N. F. Glasser, M. J. Hambrey and J. M. Reynolds (2012) Structure-from-Motion' photogrammetry: A low-cost, effective tool for geoscience applications. *Geomorphology* 179: 300-314.
- Whiteman, T., D. Lichti and I. Chandler (2002) Measurement of deflections in concrete beams by close-range digital photogrammetry. Proceedings of the *Symposium on Geospatial Theory, Processing and Applications, ISPRS Commission IV*, Ottawa, ON, Canada.
- Whitworth, J. (2010) Real-time automated railtrack monitoring system - A470 Penloyn to Tan Lan carriage-way improvement scheme. Unpublished report provided by author.
- Woodhouse, N. G., S. Robson and J. R. Eyre (1999) Vision metrology and three dimensional visualization in structural testing and monitoring. *Photogrammetric Record* 16(94): 625-641.
- Wunderlich, T. A. (2004) Geodetic Monitoring with Prismless Polar Methods. *INGEO 2004 and FIG Regional Central and Eastern European Conference on Engineering Surveying*, Bratislava, Slovakia.
- Yang, H., X. Xu and I. Neumann (2014) The benefit of 3D laser scanning technology in the generation and calibration of FEM models for health assessment of concrete structures. *Sensors* 14(11): 21889-21904.
- Yoon, J. S., M. Sagong, J. S. Lee and K. S. Lee (2009) Feature extraction of a concrete tunnel liner from 3D laser scanning data. *NDT & E International* 42(2): 97-105.
- Zhang, W., Z. Zhang, D. Qi and Y. Liu (2014) Automatic crack detection and classification method for subway tunnel safety monitoring. *Sensors* 14(10): 19307-19328.

Appendices

Appendix A - Instrumentation specifications

The following tables provide a summary of the manufacturer specifications of the instrumentation used in this study: total stations, laser trackers, time-of-flight and phase based laser scanners.

		Total Station Model			Laser Tracker
		Leica TS15i	Leica TS30 and TM30	Leica MultiStation MS50	Leica Absolute Tracker AT401
Angular Measurement	Accuracy Hz, V	1"	0.5"	1"	0.07"
Distance Measurement	Standard prism (max) Accuracy	3.5km 1mm + 1.5ppm	3.5km 1mm + 1ppm	10km 1mm + 1.5ppm	80 m 320 m (working volume) 0.01mm
	Reflectorless (max) Accuracy	1km 2mm + 2ppm	1km 2mm + 2ppm	2km 2mm + 2ppm	Function not available

		Time-of-flight terrestrial laser scanners			
		Leica ScanStation 2	Leica ScanStation C10	Leica ScanStation P20	Leica MultiStation MS50
Release year		2007	2010	2012	2013
Accuracy of single point measurement	Position	6mm	6mm	3mm	n/a
	Distance	4mm	4mm	1mm	
	Angle (Hz/V)	12"/12"	12"/12"	8"/8"	
Range capability		300m at 90% albedo	300m at 90% albedo	120m	up to 1000m
Scan rate		Up to 50,000 points/sec	Up to 50,000 points/sec	Up to 1,000,000 points/sec	Up to 1,000 points/sec @ 300m
Laser spot size		0-50m: 4mm	0-50m: 4.5mm	2.8mm	8mm x 20mm
Weight		18.5kg	13.8kg	12.7kg	7.6kg

		Phase-based terrestrial laser scanners	
		Leica HDS7000	Faro Focus 3D 120
Release year		2010	2011
Accuracy of single point measurement	Position Distance Angle (Hz/V)	n/a n/a 26"/26"	n/a 2mm n/a
Range capability		187m	120m
Scan rate		~ 1,000,000 points/sec	Up to 1,000,000 points/sec
Laser spot size		3.5mm	3.0mm
Weight		10kg	5kg

The following provides a typical specification of a TLS system provided by the manufacturer, which includes the performance of range noise based on the surface type being scanned.

General				
Instrument type	Compact, ultra-high speed pulsed laser scanner with survey grade accuracy, range and field-of-view; integrated camera and laser plummet			
User interface	Onboard control, notebook or tablet PC, PDA			
Data storage	Integrated solid-state drive (SSD) or external USB flash drive			
Camera	Auto-adjusting, integrated high-resolution digital camera with zoom video			
System Performance				
Accuracy of single measurement	3D Position Accuracy 3 mm at 50 m; 6 mm at 100 m			
Linearity error	≤ 1 mm			
Angular accuracy	8° horizontal; 8° vertical			
Target acquisition*	2 mm standard deviation up to 50 m			
Dual-axis compensator	Selectable on/off, resolution 1°, dynamic range +/- 5°, accuracy 1.5°			
Laser Scanning and Imaging System				
Type	Ultra-high speed time-of-flight enhanced by Waveform Digitising (WFD) technology			
Wavelength	808 nm (invisible) / 658 (visible)			
Laser class	2 (in accordance with IEC 60825-1)			
Beam divergence	0.2mrad			
Beam diameter at front window	≤ 2.8 mm			
Range	Up to 120 m; 18% reflectivity (minimum range 0.4 m)			
Scan rate	Up to 1,000,000 points/s			
Range noise**	Range	Black (10%)	Gray (28%)	White (100%)
	10 m	0.8 mm rms	0.5 mm rms	0.4 mm rms
	25 m	1.0 mm rms	0.6 mm rms	0.5 mm rms
	50 m	2.8 mm rms	1.1 mm rms	0.7 mm rms
	100 m	9.0 mm rms	4.3 mm rms	1.5 mm rms
Scan time and resolution (hh:mm:ss)	7 pre-set point spacings (mm at 10 m)			
	Spacing mm	1	2	3
		Quality level	4	
	50	00:20	00:20	00:28
	25	00:33	00:33	00:53
	12.5	00:58	01:44	03:24
	6.3	01:49	03:25	06:46
	3.1	03:30	06:47	13:30
	1.6	13:33	27:04	54:07
	0.8	54:07	1:48:13	----
Field-of-View	Horizontal 360° Vertical 270°			
Aiming/Sighting	Parallax-free, integrated zoom video			
Scanning optics	Vertically rotating mirror on horizontally rotating base Up to 50 Hz with internal battery Up to 100 Hz with external power supply			
Data storage capacity	256 GB onboard solid-state drive (SSD) or external USB device			
Communications	Gigabit Ethernet or integrated Wireless LAN			
Imaging	5 megapixels per each 17° x 17° colour image; streaming video with zoom; auto-adjusts to ambient lighting			
Onboard display	Touchscreen control with stylus, full colour VGA graphic display (640 x 480 pixels)			
Level indicator	External bubble, electronic bubble in onboard software			
Data transfer	Ethernet, WLAN or USB 2.0 device			
Laser plummet	Laser class 1 (IEC 60825-1) Centering accuracy: 1.5 mm at 1.5 m Laser dot diameter: 2.5 mm at 1.5 m			

The camera system used for close-range photogrammetry in the laboratory and site testing was the Nikon D3200, with a 16mm fish-eye lens. Full specifications of the camera system can be found at: <http://imaging.nikon.com/lineup/dslr/d3200/spec.htm>

Appendix B - Notes from railway industry monitoring interviews

In order to gain perspective of the monitoring issues observed on the TLP during the early stages of this research project, specialists within the railway industry across the UK were approached and asked if they would be willing to contribute to the study through an interview. Interviewees were selected to ensure that there was feedback from all parties involved in the monitoring implementation supply chain (see organogram in Figure 2.4). When inviting them to participate, they were asked to think of monitoring related issues they had experienced on current and/or previous projects. They were also informed that this research project would be looking at exploring the potential of newer “non-contact” technologies such as laser scanning and photogrammetry as a monitoring solution.

All interviewees were asked two questions: “what do you see as the main issues with regards to monitoring in the railway industry in the UK?” and “what are your thoughts on using newer technologies, such as laser scanning or photogrammetry, for monitoring railway infrastructure?”. Handwritten notes of all the issues raised as well as their feedback of implementing newer technologies were made during the interviews.

After all the interviews had taken place, it could be seen that there were some common themes with regards to monitoring issues, for example lack of monitoring standards, cost, and lack of development of new technology and so on. The interview notes were then categorised according to these themes, which is summarised in Table 2.2. The following provides notes from interviews with five key specialists within the monitoring industry, with common themes underlined. These interviews and presence of common themes allowed a monitoring industry context to be provided to TLP, as well as for this thesis. This can be found in section 2.4.

1. Interview with survey manager at London Underground Bond Street Station Upgrade (LUL)

Lack of Monitoring Standards and approaches to specification or sense checks for approval of specs

There needs to be a standard. The BTS is a guide and not a specification. Need it to be more detailed. You sometimes get over specification from the designers.

LU/CR/NR/tunnels in general – higher level projects – same for HS2 and CR2. In particular LUL and NR need to have a standard.

There is a risk that CR2 monitoring may result in some sort of overkill. Do we need to keep a hold of this and check the monitoring specification?

Manual monitoring done in-house and automatic monitoring done by SolData.

Definition of Predicted Movement

You get a good idea from the tender on the expected movements. As the design is updated, the movement levels are updated. This DEFINES monitoring. As the design is developed it makes the scope of the monitoring better or worse.

Problems with defining the trigger levels – having to meet with the designers for specific works and levels of movement and updates etc.

In this particular LUL office Costain Laing O'Rourke Halcrow/Atkins – have them in the same office and are accessible.

There was an interim report which informs the designers of what happened with monitoring up until that point. Designers can then validate this movement and sometimes gives flexibility when looking forward (on the trigger levels etc).

Access to Railway Infrastructure for Monitoring

Working with LU requires more paperwork and requires you to be on top of it. Have to programme paperwork into the routine. It's all in their benefit and you can't stop the works if monitoring isn't ready so just get it done.

Development/Transfer of new technology and process developments to Railway Infrastructure – incentive

Fibre optics are cheap.

Processing is the expensive bit – data loggers.

Need to have the money for experimenting in parallel – probably doesn't exist at LU

You have to convince the PM to have multiple systems running for monitoring.

What would the longevity be? Does it last the project? Would need a dummy project in an ideal world. Not to mention the space, installation and maintenance of the system.

However using TLS for condition surveys. Positional condition survey.

If using Amberg Trolley – need access and scanning equipment. Would need someone to do additional monitoring. Not possible to scan in a day at LU (if daily monitoring required).

West coast mainline – Amberg trolley was used for gauging surveys. Processing and analysing costs and equipment costs. 1 day on site scanning = 2 days processing.

Predicted System performance and setup

Knowing the limitations of the system. $\pm 2\text{mm}$ with current system. Doubling on prisms to improve the accuracies etc – worth it in the long run in terms of cost.

In terms of setup of system – naming is standardised at CR ---- goes into having a monitoring standard (question 1). Need to set this from the beginning. They have the AGS format. This should be formalised with the EPP and alarm system.

Needs to be flexible.

Installation and Maintenance of Target Based Monitoring Systems

TM30s are being calibrated once a year to prevent further repair costs.

Always a communications problem with the data boxes and need to get access to logger boxes to reboot them roughly once a week. They use dial-up connection and sometimes in the tunnels

can cause delays and a jam in the network for the instruments. For tunnelling, monitoring is crucial and can't be having unreliable systems.

Currently using Geoscope which allows to switch limits on and off for movement and timescale can be changed. Currently restricted to the vertical movement but quite happy with it.

Temperature + movement has a massive link and only learn this from baseline monitoring = +/- 3mm

Data handling and reporting systems – presentation intelligence, timeliness and analysis

3D modelling from planning and BIM with monitoring = FUTURE ideas

At Crossrail they tend to meet with the contractors and look at each individual graph. At this site they don't go in with graphs unless there is a need to. All analysis is done in-house by the engineers and allows SolData to work with them to continually improve the system.

Cost vs benefit

CR monitoring is costing £100million.

All the stakeholders have to invest in monitoring. Designers need to work with Commercial team have to have money in the pot just in case there are complaints or repairs that need to be done and to cover risk generally.

Generally most buildings can take 20mm settlement. The main thing is to keep the clients happy. A condition survey could be done to prove the state of the building and how much it could potentially take in terms of movement.

If a building is going to move, it's mitigating the risk. Will it still moving if he carry on with the works? Can the area be cleared?

For the future they would hope that they would use the lessons learnt from Crossrail for HS2. Keeping the requirements realistic and what need/don't need. Have a compromise on reporting and having templates for different situations.

Looking back the JLE construction, there was hardly any automatic monitoring and very few prisms for manual monitoring. Mainly done through manual precise levelling.

2. Interview with geotechnical engineer (ground and structural monitoring expert) at Crossrail

Monitoring standards

At Crossrail there is a fairly consistent approach with monitoring.

There are Crossrail design standards (based on and incorporating Crossrail, NR and LUL standards). This is a rigid process for assessing impact. This is based on lessons learnt on previous experiences of projects at similar levels (C122 – Arup)

Designers are required to produce the expected predicted movement according to the framework design consultant (???)

When assessing the impact looking at surface, utilities and structures and the potential damage taking a very conservative approach. The most intensive analysis is then carried out to eliminate anything where possible.

Then look at the most impacted assets and work towards least impacted. Asses the trigger levels for the allowable movement. Produce RAG levels and B (emergency response).

Assessment for monitoring is carried out = minimum requirement. Typically involving levelling points or ATR monitoring. Contractors must follow these minimum requirements and can implement additional stuff if they wish.

There may be additional requirements for land owners – e.g. NR/LUL require cant calcs which have to be accounted for.

Data handling and reporting

Generally there is no problem with the instrument reading: can interpret the data through data analysis and visualisations. The problem is the size of the Crossrail project.

UCIMS was setup by the AGS (Association Geotechnical Specialists with the intention of having an industry standard so that multiple contractors can submit monitoring data error free (issues with CSV and ASCII format). Therefore it gives central contractors a way of defining what is to be done and then contractors must abide by it.

Crossrail have some initiatives for Instrumentation and Monitoring:

- 1) Cut down on instruments and carry out less monitoring. Having a focused person on data management
- 2) Lessons learnt when moving forward – better instrumentation etc.
- 3) 3rd party asset monitoring – verification of manual monitoring during engineering hours.
- 4) Covering areas already by current instruments setup for other reasons – overlap! Just overcoming the logistical problems as notice needs to be given for installation.

Newer technologies

Work shopping to carry out blue sky thinking – Quantum Black – data management company that help Formula 1 with real-time data reading.

The potential of output of data from non-contact monitoring:

?surface changes

?contour changes

Currently trialling at Liverpool Street with TLS with Cambridge Uni

Photogrammetry (potentially automatic?) is being trialled by Keith Bowers at LUL

Procurement

Procurement with the Civils for carrying out the work. This is dependent on the scale of the project, but the monitoring does tend to get tied up in this part of the process independent of which asset it is. This is because the contracts are weak and requires somebody to enforce it – but this would require financial backing. Need tighter monitoring specifications and getting contractors to deliver and not getting their money until it's done! At the tender level there needs to be more rationalising. There needs to be allowances and awareness for common sense!

On a big project you have (for example) 3 contractors working over 3 phases; they will use 3 different types of systems. Therefore need an overall contractor to oversee everything.

Reporting system (continued from above)

UCIM doesn't work (yet)! Ideally/in reality it needs to:

- Be a centralised system for ALL monitoring
- Allow for multiple users login simultaneously
- Be able to see what triggers have gone off overnight
- Be more incorporated into the GIS centralised database system using the 3D graphics (CAD) and monitoring system is incorporated into existing features + design

models. Also useful to see where construction work currently taking place in relation to the monitoring results.

There are issues with data feeding – really require something more off the shelf. It was trialled for the project but wasn't developed enough.

3. Interview with survey assurance manager at Crossrail project

Technical Data Manager (surveyor) at Crossrail (now retired).

Trialled a system for the TLS + monitoring with Steve Ramsey – which failed on accuracy requirements and repeating scans.

Very keen to have a system with GIS integration with monitoring – believes the technology is there. Improve the way in which engineers handling (the raw survey data) to get the triggers – having a global visualisation of monitoring data. For example a prism movement on one side of a building relative to a boring machine location and movements (for example). Like a live system.

Wants to bridge the gap between surveyors and engineers. This will only work if there is an established worked example.

Predicted Movement

For Jubilee Line extension Mike Black (engineer) wrote a comprehensive report on predicted movement expected. Same engineer on the Crossrail Project. There is a standard way for predicting movement when digging a hole...etc etc...for particular situations.

Lack of standards..

Need to remember what is important for railway standards in order for trains to run. Can we just run a trolley through the track at certain epochs?

..and specifications

Engineers are always designing the spec and always have a geotechnical bias. When money is awarded to a large scale project (such as Crossrail) there is a commitment/obligation made in parliament to have monitoring well established in a project.

Data Collection & Reporting

There is a gap here with the technology available and what is actually being presented. Ideally the engineers can see visually in 3D what is happening to a structure. There is a possibility of incorporating GIS into monitoring. However the engineers don't know or want this necessarily – so convincing them that there is a better way is key.

Cost

The problem is that when funding is allocated to monitoring for a large project, the budget is quite big (see before) so they just use the budget as it is there anyway. The monitoring budget goes straight to the construction contractors. This is the main problem with the money – it is spent “willy nilly”

Recommendations for improvements:

Specifications – needs to be tightened up and who is writing it. Should be collaborative between surveyor and engineer

Data Display and Visualisations – getting the surveyor to do something innovate and produce 3D models with little extra cost.

Has provided the CR monitoring specification (or an earlier draft version) for reviewing purposes only.

4. Interview with associate geotechnical engineer (produced the advanced works monitoring specification at London Bridge Station)

Lack of monitoring standards

NR + LUL always asking for more.

Other clients include Thames Water and BT

Process is planning – money assigned – site investigations – ground movement assessment – this is for 3rd parties and confirm with them.

It is important to have continuation between these processes. BT have a structural protection team. LUL have a smaller group. Network Rail has a much larger team which does change and makes it harder for continuation. Thames Water – able to build relationship up.

No standards or knowledge for movement on Shard escalators. Cost of up to 1 million pounds per escalator if was closed. Used electro-levels due to the tolerances required (and TS). No differential movement and no known global movement. Useful for lessons learnt.

NR assets. Arches – targets at crown and springing points from lessons learnt. Track – ATS – real time and tiltmeters for global movement.

3rd party of NR – dealing with these is harder than the actual client.

Access to Railway Infrastructure for Monitoring

ACCESS IS AN ISSUE

NR – clean targets every 4-6 weeks which can be a logistical nightmare

LUL – fine with access

BT – can be difficult

Data handling and reporting systems

It is a problem when the consultant is specifying the type of system required.

Should know from the beginning to ensure get what you want – essentially comes from a good specification.

If want 3D visualisations from data through online reporting system – DoE should know where they are.

In terms of analysis the specification should budget for maintenance through a PM in the office and on site. They should be the one developing it throughout the project (i.e. someone being paid for continuous maintenance).

Newer technologies doing differential movement calcs and strain damage. Total station producing X,Y,Z co-ordinate. Strain damage and calcs not always helpful for client. Moving away from global movement.

The potential of new technologies is good but who will pay for it? The main thing that the engineer is interested in is whether it can be displayed and interpreted by the engineers easily.

Cost

Example 3rd party monitoring – reduce scope. This can be hard. Engineer would claim to why this needs to be done when there is an increased risk if something were to happen. It is just a cost that you need to allow for.

Lead-time and baseline monitoring length is usually due to costs available (but not always). Baseline monitoring allows correlating movements with temperatures and redundant data confirms this. If something moves – then aware of the temperature environments. Then this changes the thresholds originally set in the monitoring specification.

As long as keep communication and can justify baseline measurements.

For Shard monitoring never went over amber threshold. Not sure what arches can tolerate. Use a generic chart for structural movement and predictions – not arches!

Newer technologies – main concerns

How accurate is it?

Does it show co-ordinate change?

Could be easier for costing.

Need to know which clients would be open to it and which assets it could be applicable to. In the spec want to see what asset could be used for this measurement? Also need to say what want in terms of output and the frequency required.

Accuracy values are right in the specification. It is up to the monitoring contractor to say if alternative methods possible. Also up to them to say if a target is not being seen. Assuming the quality and assurance is being done by them (and should tell the engineer if otherwise). This is usually stated in the monitoring specification.

Need to be careful when asking for more than the original spec. Contractors would want more money.

Inclinometers- lack of sight with surveying it. Maybe need a generic checklist for a specification? That would be a good spec!

5. Interview with monitoring specialist contractors

Lack of Monitoring Standards

10 year old specifications - tend not to have anything recent.

What kind of accuracy? Wireless? Dynamic measurement? DO NOT EXIST.

Depends on the simplicity of the job – only sometimes necessary

Definition of Predicted Movement

Action Protocol. Track – standard.

Unserviceable – all service ability driven functions. The way around that? What has happened before? What is the noise? Look at previous events? Basing on historic events and looking forward.

However for a station for re-build. 1 limit is handy. Looking at serviceability limit for a grown of an arch. Reverse engineer the limits based on the monitoring system. Think about Blackfriars and strain gauges gave a predicted movement – didn't think about tide gauges and temperature sensor.

Access to Railway Infrastructure for Monitoring

PTS and line blockages. Datum has invested people to have these skills to reduce these costs. Cutting down time on site. Plug in instead of stripping cables. Checking equipment

Development new technology

Commercial drive to make a living. Being helpful. Looking at the long term benefits. Doing a good job. And motivated

Predicted System performance and setup/Standards

From the specification you (referring to Network Rail) have a 1mm accuracy specification – not possible on track. Then architects and designers to question why 1mm? Going back to the standards?

Access to railway infrastructure Installation and Maintenance of Target Based Monitoring Systems

Using prisms to measure twist and cant – not the right thing. Not being implemented the right way.

Data handling and reporting systems – presentation intelligence, timeliness, analysis

Datum has a solution to that – the hub and server developments! In house system that is bespoke and customer relevant.

Cost

If it is 5x more expensive to fix it then repair it. Buying time for monitoring it. Manual monitoring is the most expensive. Encourage people to be innovation. False selling from monitoring contractors. This stuff is too specialist but also requires you to have generalist skills. Need a reasonably good surveyor, civil engineer, logistics co-ordinator and method of communicating. Collaboratively decide which sensor to use? How to fix it? How to read it?

Sounds a lot of money. Associate expense with what you're doing. Keeping it open on line speed. Asset value (and replacement value). Operating value (driven by line speed). NR start racking up the cost for delays and don't think about it practically.

Emphasis of importance of the monitoring will change. Is this a contract issue? Because it isn't open ended? To some extent? But at the end of the day it is required to be monitored. But then how do you ask a contractor to cost something up like that? South Hampstead project with 100mm movement...never would have thought it would have happened to that?

Non-contact feature monitoring –

Built-in measurement points or systems

Demand for cloud scanning monitoring bit. Not a real-time system.

Communications – relying on internet and GPRS. Underground – local wi-fi to bounce off until somewhere you can get signal. Best way of comms.

Power – only have battery power. Power budget. Got to operate to the power budget. Thinking about frequency of the work depending on the . Reliable piece of kit. Show a previous case study and figure out the lessons learnt. If the provision of power could be introduced by NR – there would be an increased number of sensors available.